The Role of the Secretory Pathway and Cell Surface Proteolysis in the Regulation of the Aggressiveness of Breast Cancer Cells

by

Randi Wise

B.S., Sterling College, 2013

AN ABSTRACT OF A DISSERTATION

submitted in partial fulfillment of the requirements for the degree

DOCTOR OF PHILOSOPHY

Department of Biochemistry and Molecular Biophysics
College of Arts and Sciences

KANSAS STATE UNIVERSITY
Manhattan, Kansas

2017

Abstract

Cancer cells exploit key signaling pathways in order to survive, proliferate, and metastasize. Understanding the intricacies of the aberrant signaling in cancer may provide new insight into how to therapeutically target tumor cells. The goal of my research was to explore the role of two modulators of transmembrane signaling, the secretory pathway and cell surface proteolysis, in the aggressiveness of breast cancer cells. To study the role of the secretory pathway, I focused on the family of endoplasmic reticulum (ER) chaperones. I found that several ER chaperones were upregulated in breast cancer cells grown under anchorage-independent conditions as mammospheres *versus* those grown under adherent conditions. Furthermore, certain members of the protein disulfide isomerase (PDI) family were consistently upregulated in two different cell lines at both the mRNA and protein levels. Knocking down these PDIs decreased the ability of the cells to form mammospheres. I demonstrated that the requirement for PDI chaperones in mammosphere growth is likely due to an increased flux of extracellular matrix (ECM) components through the ER. Next, I examined the role of cell surface proteolysis in modulating the aggressiveness of breast cancer cells. Cell-surface metalloproteases release soluble growth factors from cells and activate the corresponding growth factor receptors. I determined that specific metalloproteases (ADAM9 or ADAM12), modulate the activation of Epidermal Growth Factor Receptor (EGFR). I demonstrated that EGFR activation enhances the $CD44^{+}/CD24^{-}$ cell surface marker profile, which is a measure of cancer cell aggressiveness. I found that the MEK/ERK pathway, which is a downstream effector of EGFR activation, modulates the $CD44^{+}/CD24^{-}$ phenotype. When DUSP4, a negative regulator of the MEK/ERK pathway, is lost, activation of EGFR by metalloproteases no longer plays a significant role in cancer cell aggressiveness. This indicates that the ligand dependent activation of the

EGFR/MEK/ERK pathway is a critical step in DUSP4-positive aggressive breast cancer. Finally, I examined the importance of metalloproteases in the regulation of Programmed-death ligand 1 (PD-L1), a transmembrane protein expressed by some cancer cells that plays a major role in suppressing the immune system. I demonstrated that cell-surface metalloproteases have the ability to cleave PD-L1 and release its receptor-binding domain to the extracellular environment. Collectively, these data indicate that (a) ER chaperones support anchorage-independent cell growth, (b) metalloproteases are important in regulation of an aggressive phenotype through the EGFR/MEK/ERK pathway, and (c) metalloproteases cleave PD-L1, a key component of immunosuppression in cancer.

The Role of the Secretory Pathway and Cell Surface Proteolysis in the Regulation of the Aggressiveness of Breast Cancer Cells

by

Randi Wise

B.S., Sterling College, 2013

A DISSERTATION

submitted in partial fulfillment of the requirements for the degree

DOCTOR OF PHILOSOPHY

Department of Biochemistry & Molecular Biophysics
College of Arts and Sciences

KANSAS STATE UNIVERSITY
Manhattan, Kansas

2017

Approved by:

Major Professor
Anna Zolkiewska

Abstract

Cancer cells exploit key signaling pathways in order to survive, proliferate, and metastasize. Understanding the intricacies of the aberrant signaling in cancer may provide new insight into how to therapeutically target tumor cells. The goal of my research was to explore the role of two modulators of transmembrane signaling, the secretory pathway and cell surface proteolysis, in the aggressiveness of breast cancer cells. To study the role of the secretory pathway, I focused on the family of endoplasmic reticulum (ER) chaperones. I found that several ER chaperones were upregulated in breast cancer cells grown under anchorage-independent conditions as mammospheres *versus* those grown under adherent conditions. Furthermore, certain members of the protein disulfide isomerase (PDI) family were consistently upregulated in two different cell lines at both the mRNA and protein levels. Knocking down these PDIs decreased the ability of the cells to form mammospheres. I demonstrated that the requirement for PDI chaperones in mammosphere growth is likely due to an increased flux of extracellular matrix (ECM) components through the ER. Next, I examined the role of cell surface proteolysis in modulating the aggressiveness of breast cancer cells. Cell-surface metalloproteases release soluble growth factors from cells and activate the corresponding growth factor receptors. I determined that specific metalloproteases (ADAM9 or ADAM12), modulate the activation of Epidermal Growth Factor Receptor (EGFR). I demonstrated that EGFR activation enhances the $CD44^{+}/CD24^{-}$ cell surface marker profile, which is a measure of cancer cell aggressiveness. I found that the MEK/ERK pathway, which is a downstream effector of EGFR activation, modulates the $CD44^{+}/CD24^{-}$ phenotype. When DUSP4, a negative regulator of the MEK/ERK pathway, is lost, activation of EGFR by metalloproteases no longer plays a significant role in cancer cell aggressiveness. This indicates that the ligand dependent activation of the

EGFR/MEK/ERK pathway is a critical step in DUSP4-positive aggressive breast cancer. Finally, I examined the importance of metalloproteases in the regulation of Programmed-death ligand 1 (PD-L1), a transmembrane protein expressed by some cancer cells that plays a major role in suppressing the immune system. I demonstrated that cell-surface metalloproteases have the ability to cleave PD-L1 and release its receptor-binding domain to the extracellular environment. Collectively, these data indicate that (a) ER chaperones support anchorage-independent cell growth, (b) metalloproteases are important in regulation of an aggressive phenotype through the EGFR/MEK/ERK pathway, and (c) metalloproteases cleave PD-L1, a key component of immunosuppression in cancer.

Table of Contents

List of Figures

List of Tables

List of Abbreviations

ADAM	a disintegrin and metalloprotease
AEBSF	4-(2-Aminoethyl) benzenesulfonyl fluoride hydrochloride
AKT	protein kinase B
ALDH	aldehyde dehydrogenase activity
APC	allophycocyanin
APC	antigen presenting cell
AREG	amphiregulin
ATF6	activating transcription factor 6
ATP	adenosine triphosphate
BB-94	batimastat
BCA	bicinchoninic acid assay
bFGF	basic fibroblast growth factor
BiP	binding immunoglobulin protein
BTIC	breast tumor initiating cell
CAM	cell adhesion molecules
CHOP	C/EBP homologous protein
CL	claudin-low
COL3A1	collagen alpha-1(III) chain
COL6A2	collagen alpha-2(VI) chain
CQ	chloroquine
CSC	cancer stem cells
CTC	circulating tumor cells
DMEM	Dulbecco's modified Eagle medium
DMSO	dimethyl sulfoxide
DOX	doxycycline
DPBS	Dulbecco's phosphate buffered saline
DUSP4	dual specificity phosphatase 4
ECM	extracellular matrix
EDTA	ethylenediaminetetraacetic acid

EGA	European Genome-Phenome Archive
EGF	epidermal growth factor
EGFR	epidermal growth factor receptor
EIF2α	eukaryotic translation initiation factor 2A
ELISA	enzyme-linked immunosorbent assay
EMT	epithelial-to-mesenchymal transition
EpCAM	epithelial cell adhesion molecule
ER	endoplasmic reticulum
ER	estrogen receptor
ERAD	endoplasmic reticulum associated degradation
ERK	mitogen activated protein kinase
ERp44	endoplasmic reticulum protein 44
ERp57	protein disulfide isomerase A3
ERp72	protein disulfide isomerase A4
FACS	fluorescence activated cell sorting
FAK	focal adhesion kinase
FBS	fetal bovine serum
FITC	fluorescein isothiocyanate
FN1	fibronectin
GADD34	growth arrest and DNA-damage-inducible 34
GDP	guanosine diphosphate
GEO	Gene Expression Omnibus
GISTIC	Genomic Identification of Significant Targets in Cancer
GPI	glycosylphosphatidylinositol
GRP-170	170 kDa glucose-regulated protein
GRP-94	94 kDa glucose-regulated protein
GSEA	gene set enrichment analysis
GT	glycoprotein glucosyltransferase
GTP	guanosine triphosphate
HB-EGF	heparin-binding epidermal-like growth factor
HEPES	4-(2-hydroxyethyl)-1-piperazineethanesulfonic acid

HER2	human epidermal growth factor receptor
HR	hazard ratio
HRP	horseradish peroxidase
HYOU1	170 kDa glucose-regulated protein
IFN	interferon
IL-6R	interleukin-6 receptor
IRE1	endoplasmic reticulum to nucleus signaling 1
JNK	Jun N-terminal kinase
LAMB1	laminin subunit β-1
MAPK	mitogen-activated protein kinase
MEK	mitogen-activated protein kinase kinase
MEMB	mammary epithelial basal media
MHC	major histocompatibility complex
MMP	matrix metalloprotease
MMP-13	matrix metallopeptidase 13
MSL	mesenchymal stem-like
mTOR	mammalian target of rapamycin
NF-κB	nuclear factor κB
NSCLC	non-small cell lung cancer
PAM50	prediction analysis of microarray 50
PD-1	programmed cell death protein 1
PDI	protein disulfide isomerase
PD-L1	programmed death-ligand 1
PE	phycoerythrin
PERK	protein kinase R-like endoplasmic reticulum kinase
PI3K	phosphatidylinositol 3-kinase
PIP2	phosphatidylinositol–4,5–bisphosphate
PR	progesterone receptor
PTB	phosphotyrosine-binding
PTEN	phosphatase and tensin homolog
qRT-PCR	quantitative real time PCR

RAF	mitogen-activated protein kinase kinase kinase
RFS	relapse free survival
RTK	receptor tyrosine kinase
SDS	sodium dodecyl sulfate
SEM	standard error of the mean
SH2	Src homology 2
STAT3	signal transducer and activator of transcription 3
TCGA	The Cancer Genome Atlas
TCR	T cell receptor
TGF-α	transforming growth factor α
TN	triple negative
TNBC	triple negative breast cancer
TNF-α	tissue necrosis factor α
tRFP	turbo red fluorescent protein
Tris	2-Amino-2-hydroxymethyl-propane-1,3-diol
UPR	unfolded protein response
UTR	untranslated region
XBP1	X-box binding protein 1

Acknowledgements

I would like to thank numerous individuals for their contribution to my success. First, I would like to thank Dr. Anna Zolkiewska and Dr. Michal Zolkiewski for all of their support throughout my graduate studies. They were both invaluable resources as I grew as a researcher and scientist. I would not be where I am without their dialogue, guidance, and leadership. I am indebted to them for molding me into the person that I am today. I would also like to extend my thanks to all of my colleagues during my time in the Biochemistry Department at Kansas State University. Each of you holds a special place in my heart. This is especially true for all of my lab mates during the course of my studies. Drs. Sara Duhachek-Muggy and Yue Qi are not only valuable friends; they also taught me how to be a competent researcher and freely shared their knowledge and years of experience with me. Linda Alyahya and I had countless fun-filled evenings enjoying each other's company, and I will always appreciate her positive attitude and unwavering friendship. Additionally, I would like to acknowledge my family for their continued support for all of my endeavors. Finally, I cannot thank my husband, Tyler, enough. He has been a rock for myself and our son, Levi, throughout my graduate studies. When life becomes overwhelming, he is there to offer solutions and help me through it. His support and encouragement were essential to this accomplishment.

Chapter 1 - Literature Review

Cancer is a disease that is characterized by the uninhibited growth and spread of abnormal, malignant cells. Cancer cells can originate from numerous places within the body, including the skin, lungs, prostate or breast, and stomach. The main focus of the research presented in this dissertation is on breast cancer, as it is still one of the major causes of cancer death for women, second only to lung cancer [1]. It is estimated that there will be approximately 255,000 new cases of breast cancer diagnosed in 2017 [2]. While much research has been done to understand how to treat various types of breast cancer (see 'Overview of Breast Cancer' below), there is much left to do to understand the intricacies of these signaling pathways and cell to cell interactions in breast cancer cells.

Overview of Breast Cancer

Clinical Classification

Currently, the treatment plan for breast cancer patients is based on the staining for a panel of three predictive immunohistochemical markers. These markers clinically subdivide breast cancers into three general categories: (1) hormone receptor positive breast cancer (estrogen receptor [ER] or progesterone receptor [PR] positive); (2) human epidermal growth factor receptor 2 (HER2) positive, and; (3) breast cancer that is negative for all three markers (triple negative breast cancer, TNBC) [3]. Hormone-receptor positive and HER2 positive breast cancer can be treated by exploiting the tumor's dependence on these overexpressed marker(s). This is called targeted therapy [4]. If there is no expression of these markers, the tumor can only be treated by conventional methods, such as chemotherapy [5, 6]. Current research in the field has focused on the need for directed therapies, which take into account both the marker profile and specific characteristics of cancer cells. The heterogeneity and complexity of breast cancer cells

are becoming apparent, and an increased efficacy to diagnose the intricacies of these cells would help allow for the development of additional therapies.

Molecular Subtypes

In a concentrated effort to classify breast cancers based on their intrinsic properties, rather than a profile of only three markers, five molecular subtypes of breast cancer have been identified [7]. These molecular subtypes of breast cancer were determined based on a set of genes, whose expression was determined either by microarrays or RNA sequencing, and which did not appear to vary significantly within the same tumor sample, including within its metastases, but differed in various breast cancers [8]. A set of 50 of these intrinsic genes, called PAM50, has been used to classify breast cancers into four molecular subtypes, which include (1) luminal A, (2) luminal B, (3) HER2-enriched, (4) basal. The fifth subtype of breast cancer, called claudin-low, is not able to be distinguished based on solely a PAM50 test [9].

Additionally, while the molecular subtypes of breast cancer have high similarities to the predictive immunohistochemical markers widely used in diagnostics and treatment plans, there are small but significant differences between the two [10]. For example, hormone receptor positive cancers share high similarities with the Luminal A and B molecular subtypes, but interestingly only 77% of tumors that were clinically classified as ER-/HER2+ were found to be HER2-enriched. Triple negative breast cancers appeared in the basal (57%) and HER2-enriched (30%) molecular subtypes [7]. The claudin-low molecular subtype, characterized by the downregulation of genes involved in cell-cell interactions, shares some similarities to the basal subtype and is also usually clinically classified as TNBC [11]. While the benefits of using the PAM50 test are numerous, the cost, amount of tumor sample required, and data analysis prevent

this test from being used for common clinical diagnosis, even though it has potential to serve as an important prognostic marker [12].

Future Directions of the Therapies for Triple Negative Breast Cancer

For a long time, chemotherapy has been the preferred course of treatment for TNBC. In the recent years, numerous enzymes and signaling pathways have emerged as potential therapeutic targets. For example, inhibitors that target Epidermal Growth Factor Receptor (EGFR, see below) have been tested in clinical trials, but the results have been disappointing [13]. Other therapies currently in clinical trials include inhibitors that target the cell cycle, DNA damage repair, and gene transcription [13-15]. Importantly, cancer immunotherapy has been recently revolutionizing cancer treatment [16] (see 'Cancer Immunotherapy').

Cell Culture Models of Aggressiveness

Models of breast cancer cell aggressiveness are needed to identify targets for future therapy directions and drug development. Effective therapies target cancer metastases, as they are primarily the cause of cancer mortality. Accumulating evidence points to certain cancer cells linked to the formation of metastases. These cells are termed "breast tumor initiating cells (BTICs)" or "cancer stem cells (CSCs)". These cells do not undergo death caused by detachment from the extracellular matrix (termed "anoikis resistance"), enter into the bloodstream (where they are called circulating tumor cells, CTCs), and exit the bloodstream to form a metastatic colony at a distant site [17]. It is important to note that not all cancer cells found in circulation are CSCs. Cancer stem cells have often undergone epithelial-to-mesenchymal transition (EMT), escape recognition by the immune system, and are resistant to conventional treatment methods. The described assays below are commonly used techniques that serve as a surrogate measure of cancer cell aggressiveness.

Cell Migration and Invasion Assays

A common cell migration test is termed the "wound healing" or "scratch" assay. Cancer cells are plated at high density, then a pipette tip or similar tool is used to create a disruption in the cell layer. Imaging techniques are used to measure the rate that the cells are able to fill the entirety of the wound [18]. This simple assay has the benefits of being cost-effective and easy to perform. To some extent, it mimics what is seen regarding the migration of cells *in vivo*. Limitations include the lack of *in vivo* conditions and the inability to take into account the chemotaxis of cells [19].

Cell invasion techniques are used to measure the tendency of cancer cells to form invadopodia, which are protrusions from the plasma membrane that extend outwards towards the extracellular matrix. Breast cancer cells are suspended in Matrigel, a substance that mimics the 3D growth of attached cells by using components of the extracellular matrix as its base [20]. As cancer cells must degrade the extracellular matrix in order to invade the surrounding tissue and metastasize, this assay provides a snapshot into the *in vivo* growth of cancer cells more accurately than cells grown in normal tissue culture conditions [21].

Anchorage-Independent Growth

Cells that detach from the extracellular matrix normally undergo anoikis. Certain cancer cells are anoikis-resistant: they survive the detachment, proliferate, and grow to form spheroids called "mammospheres" [22]. Anchorage-independent growth can be accomplished with cells either grown in a liquid suspension that allows cell aggregation, or in an inert substance that prevents cell aggregation. The inert substance assures that all spheroids originate from a single cell and are not the result of cell aggregation. This assay was developed from a need to further

identify conditions that allow the selection of cancer stem cells, capable of forming metastatic colonies, and provides a viable option for replicating a metastatic condition *in vitro* [20, 23].

Cancer Stem Cell Markers

The cell surface expression levels of certain proteins, which can be determined by flow cytometry techniques, have been shown to serve as indicators of the aggressiveness of breast cancer cells Common cell surface markers that have been shown to correlate with the tumorigenic potential of human breast cancer cells grown in mice [24] include CD44, a cell surface glycoprotein shown to be involved in cell-cell interactions, adhesion, and migration [25]; and CD24, a cell surface protein with a glycosylphosphatidylinositol (GPI) anchor that is heavily glycosylated [26, 27]. Cancer stem cells typically express high levels of CD44 and low levels of CD24. Other proteins have been proposed as CSC markers, such as EpCAM, CD133, and CD166, but they are less commonly used. There has been much discussion about the efficacy of cell surface markers in general, as it appears that no marker combination is accurately predictive of the aggressiveness of all types of cancer cells, and these markers do not fully correlate with the tumor-forming potential of cells [28-30]. Another commonly used assay to identify tumor initiating cells detects the activity of aldehyde dehydrogenase (ALDH), which has been shown to be increased in CSCs [31, 32].

The Secretory Pathway

The secretory pathway determines how proteins are synthesized and sorted within a cell. The main components of the secretory pathway include the endoplasmic reticulum (ER) and associated proteins, including ribosomes that synthesize proteins and direct them into the ER, the Golgi complex, and vesicles that transport proteins from the ER to the Golgi, and from the Golgi to their final destination. Secretion rates control both the release of soluble proteins from those

vesicles to the extracellular compartment, and the transport of integral membrane proteins to the plasma membrane of cells. Additionally, proteins may be modified along their journey to maturation, with the help of ER chaperones [33].

Much discussion has surrounded the secretory pathway in its importance to the progression of cancer [34]. As many of the proteins necessary for enhanced tumor growth progress through this pathway, the idea of limiting the function of the secretory pathway is an attractive one [35]. The post-translational modifications that occur in the Golgi also generate a huge variety of different proteins among cancer cell secretomes [36]. Exploiting the dependence and vulnerabilities of cancer cells on the secretory pathway may prove to be a valuable strategy for development of new anti-cancer therapies.

ER Chaperones

ER chaperones are a class of proteins that reside in the ER and assist in the protein folding and assembly (or disassembly) [37]. Chaperones are also present in a cell at places other than the ER, including in the cytosol, mitochondria, and on the cell surface [38], but these enzymes do not directly influence the secretory pathway and will not be discussed here. All proteins are synthesized as a polypeptide chain, and need to be directed into their functional and active conformation. ER chaperones possess the ability to guide a terminally misfolded protein through appropriate channels in the ER membrane for degradation in the cytosol [39]. Also, the accumulation of misfolded proteins in the ER elicits the unfolded protein response (UPR). The UPR is a series of three separate pathways which provides increased compensatory mechanisms and decreases new protein synthesis [40]. With a wide variety of proteins being synthesized, numerous chaperones are necessary to accomplish this function. There are various classes of chaperones which have differing functions within the ER.

Classifications of Chaperones

The three major categories of chaperones are: (1) molecular chaperones that shield unfolded regions from other proteins, (2) lectins, which bind to and facilitate folding of glycoproteins, and (3) foldases that catalyze the various steps involved with protein folding [41, 42]. These categories of chaperones, including examples of each class, are described in detail below.

Molecular Chaperones

The family of molecular chaperones has a wide range of substrate specificities. Members of this family include HSP70-class chaperones (BiP and GRP-170) and the HSP90-class chaperone GRP-94. To prevent premature binding and protein aggregation of partially misfolded proteins, molecular chaperones bind to small hydrophobic patches of newly synthesized polypeptides [43, 44]. The HSP70-class of molecular chaperones is the best studied group of molecular chaperones. These enzymes are composed of three domains, an N-terminal ATPase domain, a substrate binding domain, and a C-terminal lid. Additionally, there is a short sequence at the very C-terminus of the protein that allows interactions with co-chaperones [42]. The ADP/ATP state of the ATPase domain facilitates binding to various substrates. When ATP is bound, the lid at the C-terminal end of the protein remains open, and there is a low affinity for peptide binding. When a substrate binds to these molecular chaperones, the ATP is hydrolyzed to ADP and the lid clamps down on the bound peptide. After ADP is exchanged for ATP, the substrate dissociates from the chaperone [43]. Co-chaperones may facilitate this exchange in various ways, including stimulating ATP hydrolysis or facilitating ADP release [37]. BiP (also named GRP-78) has been termed the “master regulator” of the ER, as it binds to the majority of proteins that traverse through the ER [37]. It also functions outside of its chaperone role by

maintaining the permeability of the ER by sealing the luminal side of the inactive translocons [43]. Additionally, BiP has been suggested to function as a positive regulator of breast cancer progression and may serve as a predictor of chemoresistance [45-48]. The HSP90-class chaperone GRP-94 is the most abundant glycoprotein in the ER and has a similar domain organization as the HSP70-class chaperones, with the C-terminal lid replaced by a dimerization domain located at the end of the protein [43]. GRP-94 possesses ATPase activity only upon dimerization [42]. The interactions between the chaperone and its clients appear to: (1) facilitate the formation of an active form of certain proteins, namely kinases, (2) help form multiprotein complexes, and (3) promote the binding of ligands to their proteins [49].

Lectins

The lectin class of ER chaperones consists of calreticulin and calnexin. As their name implies, the lectin chaperones bind to the carbohydrate-containing portion of glycosylated proteins and help facilitate their folding. These substrates include major histocompatibility complex (MHC) class I molecules [50]. Both calnexin (membrane bound) and calreticulin (soluble) contain a single carbohydrate binding domain that binds monoglucosylated glycans [51]. An additional domain, termed the P-domain, is rich in proline residues and serves to recruit an oxidoreductase (ERp57, discussed in the next section), which is involved in the formation and isomerization of disulfide bonds [43]. Additionally, this binding helps slow the rate of folding, thus increasing the overall folding efficiency. The binding of glycans to the lectin chaperones is modulated primarily by two other enzymes: glucosidase II and UDP-glucose:glycoprotein glucosyltransferase (GT) [37]. As with molecular chaperones mentioned above, protein folding appears to occur in the unbound form. However, substrate-chaperone binding helps to slow the rate of folding and minimize the formation of intermediate aggregates due to disruptive

interaction with other proteins [43]. Knockout of either calreticulin or calnexin is embryonically lethal in mice [52]. There has been little evidence connecting these lectin chaperones to the survival of cancer cells. A study by Delom, et al. showed that in tunicamycin-treated apoptosis-resistant MCF-7 cells upregulate calnexin, and escape apoptosis by a mechanism independent of its chaperone function [53].

Foldases

Perhaps the most important class of proteins related to the research presented in this dissertation is the foldases. The human PDI family consists of approximately 20 members [54]. These thiol oxidoreductases, which include ERp44, protein disulfide isomerase (PDI), ERp57, and ERp72, facilitate the oxidation, isomerization, or reduction of disulfide bonds through a conserved CXXC motif, which can vary in number between different family members [55, 56]. The two residues that lie between the cysteines in the thioredoxin-like catalytic domains play a major role in determining the redox potential of the enzyme, and its function as either as an isomerase, reductase, or oxidase [57]. The domain organization of the PDI family is depicted in Figure 1.1.

In addition to their role in disulfide bonds, certain family members, including PDI, may also function as molecular chaperones, recognizing misfolded proteins due to the presence of a hydrophobic sequence in the structure of the protein [42]. PDI family members can be found in numerous places within the cellular environment, including the ER (discussed), cytosol, nucleus, cell surface, and extracellular region [58-61]. The reason for this large number of PDI family members is unclear. There is a large degree of functional redundancy, but particular members do seem to play a more specialized role. For instance, PDI and ERp57 both exhibit broad substrate specificity, and can generally compensate for the loss of the other [62]. However, ERp57

preferentially forms a complex with calnexin and calreticulin (described above). This is due to a conserved positively charged region in the b' domain which interacts with a negatively charged region in the P-domains of the lectins [43, 63]. As such, deletion of ERp57 results in a major defect in the MHC class I proteins [64]. The PDI chaperone ERp44 has been shown to function at the ER-Golgi interface, preventing the release of non-native conformations of proteins to the Golgi [65, 66]. Depletion of ERp72 in human hepatoma cells showed minimal impact and thus suggests a narrow substrate specificity or existence of an alternative mechanism with an unidentified protein [62]. As such, even with the large degree of functional redundancy among the PDI family, there are some specialized functions associated with each family member.

The Unfolded Protein Response (UPR)

ER stress caused by the accumulation of misfolded proteins leads to the activation of the unfolded protein response (UPR) [67]. The primary goals of the UPR are to eliminate misfolded proteins and to reduce the amount of newly synthesized proteins within the ER, both which contribute to regaining homeostasis [40]. Activation of the UPR due to ER stress in solid tumors has been shown to originate from an altered metabolism, hypoxic conditions, or signals from the tumor microenvironment, which leads to an increase in ER chaperones [40, 48, 68, 69]. The UPR consists of three parallel signaling pathways: IRE1, PERK, and ATF6, shown in Figure 1.2, adapted from ref [70]. Each of these pathways uses unique mechanisms of signal transduction due to the presence of misfolded proteins. Previous studies have shown that IRE1 and/or ATF6 pathways, but not PERK alone, play a critical role in the induction of important ER chaperones during the UPR [71, 72]. However, in regard to epithelial-to-mesenchymal transition (EMT), it has been shown that the PERK branch is required for cells to invade and metastasize [73].

ATF6

The transcription factor ATF6 initially is synthesized and resides in the ER as a transmembrane protein, which contains a large luminal domain (Figure 1.2A). In the presence of high concentrations of unfolded proteins in the ER, ATF6 is transported to the Golgi complex [41]. After it reaches the Golgi, two proteases (S1P and S2P) cleave ATF6, releasing the cytoplasmic N-terminal domain, ATF6(N), from the membrane. The ATF6(N) fragment then serves as a transcription factor in the nucleus to activate UPR target genes [70]. Genes that are induced by the ATF6 branch of the UPR include various chaperones, such as BiP, GRP94, and PDI [48, 70]. It is thought that ATF6 responds to ER stress via its association with the molecular chaperone BiP. Under normal conditions, ATF6 associates with BiP in the ER. When ER stress occurs and BiP dissociates, two Golgi localization sites are exposed and ATF6 is then transported to the Golgi [40]. Additionally, the domain present in the ER (luminal side) has various disulfide bonds, possibly allowing it to sense its redox environment [70].

A recent article by Dadey, et al. described the impact of ATF6 on glioblastoma cells. Radiation treatment induced the ER stress response and downstream pathway events. Downregulation of ATF6 seemed to sensitize various glioblastoma cell lines to induce cell death by radiation therapy, though it did not appear to be a strong effect [74].

PERK

In the second branch of the UPR, a transmembrane serine/threonine kinase called PERK oligomerizes and autophosphorylates in the presence of misfolded proteins (Figure 1.2B). PERK then phosphorylates eIF2α, which inhibits its function as a translation initiation factor and as a result inhibits mRNA translation. This reduces the flux of proteins into the ER and helps alleviate ER stress. In addition to this function, a transcription factor called ATF4 is induced, as

some mRNAs are preferentially translated when eIF2 is rate-limiting. ATF4 drives the expression of CHOP, which controls genes involved in apoptosis, and GADD34, which dephosphorylates eIF2α.

Interestingly, Sequeira, et al. showed that a loss of cellular adhesion can regulate eIF2α phosphorylation in a PERK-dependent manner. Additionally, there was an increase in phosphorylation of eIF2α after blocking the function of β1-integrin [75]. As phosphorylation of eIF2α should lead to a decrease in translation and an increase in apoptotic proteins, the authors proposed that PERK activation reduces tumorigenicity. Whether this function was due to an increase in ER stress and the UPR caused by the loss of cell adhesion or by a different mechanism has not been determined.

IRE1

This is the most conserved part of the UPR, and the only branch present in both yeast and humans [40] (Figure 1.2C). In the presence of unfolded proteins, the serine/threonine kinase IRE1 dimerizes and undergoes autophosphorylation [48]. The resulting complex has two functions involved in relieving ER stress. The first is as a transmembrane kinase, which uses an unconventional mRNA splicing mechanism to create an mRNA encoding a transcription factor (XBP1) [40]. This mRNA product is then translated to the protein XBP1s, which is translocated to the nucleus and drives expression of molecular chaperones and genes involved in lipid synthesis and the ERAD (ER associated degradation) pathway [70]. The second function of the active IRE1 complex involves ribonuclease (RNase) activity facilitated by conformation changes involving its lateral oligomerization within the ER membrane.

A recent article published by Chen, et al. demonstrated that the IRE1 pathway was selectively activated in triple negative breast cancer and had an important role in the

tumorigenesis and tumor progression. In breast cancer cell line models, depletion of XBP1 inhibited tumor growth and tumor relapse and reduced the $CD44^{high}CD24^{low}$ population [76]. Additionally, the authors believe that this function of XBP1 is through the control of the transcriptional pathway of H1F1α, as chromatin immunoprecipitation showed that XBP1 and H1F1α occupy the same DNA motifs.

The Secretory Pathway and Cancer Aggressiveness

Various components of the secretory pathway have been shown to play a role in modulating cancer aggressiveness. While there are countless secreted proteins and pathway modulators that have been linked to cancer, two stand out as likely candidates and deserve further explanation. These are the PDI family of molecular chaperones and the secreted proteins involved in extracellular matrix (ECM) formation.

The protein disulfide isomerase family of molecular chaperones appears to play important roles in cancer progression (discussed below). A specific member of the family, PDI, was found to have increased levels of gene expression in multiple types of cancers including brain, kidney, and lung cancer [77]. The inhibition of PDI activity, but not a catalytically inactive mutant, was shown to sensitize melanoma cells to apoptosis caused by ER stress inducers [78]. In another study, the levels of PDI were significantly higher in axillary lymph node metastatic breast tumors than in the primary breast tumor [77]. Taken together with data showing that lower levels of PDI correlate with a better prognosis in breast cancer [79], this suggests a possible role of PDI in metastasis. While these effects of PDI in cancer have been well-documented, it is not clear if these effects are due to PDI in the endoplasmic reticulum or some other cellular location [61, 80]. PDI has also been shown to be required for the assembly of procollagen, a precursor to an important component of the extracellular matrix [81, 82]. The PDI family member ERp57 has

also been linked to various aspects of cancer signaling pathways. The mRNA expression level of ERp57 was increased in a number of invasive ductal carcinoma samples compared to normal breast tissue, and in tumors with lymph node metastases [83]. Expression of ERp57 at different cellular locations also appears to have an important role in cancer progression. Along with calreticulin, ERp57 translocates to the cell surface, where it has been shown to regulate EGFR internalization and phosphorylation in breast cancer [84, 85]. ERp57 additionally plays a role in the nucleus by facilitating the activation of STAT3 in laryngeal cancer [60]. As such, it appears that the documented role of ERp57 in cancer has little to do with its localization in the ER. ERp44 has not been thoroughly studied in regard to its effect on cancer aggressiveness, though there is some evidence that knockdown of ERp44 leads to apoptosis of various cancer cells, possibly due to a role in calcium release [86-88]. Currently, there is no literature suggesting a significant connection between ERp72 and cancer progression.

The ECM composition at both the primary tumor and secondary metastatic site has been increasingly accepted as an important modulator of the aggressiveness of cancer cells. The ECM comprises a variety of distinct compounds which include proteins, proteoglycans, glycoproteins, and polysaccharides. Signaling to and from the ECM is modulated by integrins, a family of transmembrane ECM receptors. Integrins are comprised of two noncovalently linked glycoprotein subunits called α and β. There are twenty-four α and nine β subunits of integrins, resulting in the formation of heterodimers with different binding specificities [89]. As a link between the ECM and intracellular components, integrins have been implicated in breast cancer aggressiveness. The stiffening of the ECM leads to integrin clustering, which then initiates tumorigenesis by increasing ECM rigidity [90]. Additionally, a downstream effector of a β1

integrin is focal adhesion kinase (FAK), which modulates cellular contractility and activates the mitogen-activated protein kinase (MAPK) pathway leading to cancer proliferation [89].

In addition to providing a support structure and modulating cellular adhesion, certain components of the ECM can activate cellular signaling pathways. The aforementioned compounds that constitute the ECM are normally secreted from cells through the secretory pathway. These secreted ECM components have been shown to be linked to cancer aggressiveness in a variety of ways. An abnormally large amount of deposited ECM components, including collagen I, which would increase flux through the secretory pathway, is a common ECM alteration in many tumor types and linked to a metastatic phenotype [91, 92]. This aggressiveness is thought to be due to an interaction between collagen I and β1 integrin, which leads to the destabilization of the E-cadherin/β-catenin adhesion complex and an increase in the levels of N-cadherin [93, 94]. The interactions between collagen and integrins can lead to prosurvival signals and a decrease in apoptosis (also discussed above) [95]. As expected, studies have shown a significant decrease in the aggressiveness of cancer when collagen synthesis is inhibited [91].

Cell Surface Proteolysis

While proteolysis can occur throughout the cell, the focus of this section will be on a specific class of proteolytic enzymes that catalyze the cleavage or "shedding" of membrane-bound proteins.

The ADAM Metalloproteases

Certain classes of proteases that catalyze cell surface cleavage reactions are called A Disintegrin And Metalloproteases (ADAMs). This class of metalloproteases has broad, but specialized cleavage capabilities, as the systematic deletion of individual ADAMs in mice

produce different phenotypic effects on animal survival [96]. ADAMs are transmembrane proteins with their metalloprotease domain exposed to the extracellular compartment [97]. As a result, their substrates include transmembrane ligand precursors, which are released to the extracellular space and participate in either cell autonomous or paracrine signaling [97].

The human ADAM family contains twenty members that can be classified into three major subgroups: testis-specific, hematopoietic, or globally expressed [98]. Additionally, within each group, ADAMs may be catalytically active or inactive. While it is possible that ADAMs may possess an important function unrelated to their metalloprotease activity, I will consider only catalytically active ADAMs of the globally expressed or hematopoietic subclass in regard to cancer development. Out of these ADAMs, the knockouts of ADAM10, ADAM17, ADAM19, and to some extent ADAM12, show embryonic lethality in mice [96, 98]. This indicates an important role of these proteins in cellular functions.

ADAMs are multi-domain proteins, which serve independent but complementary roles. The N-terminal region of the protein contains a signal sequence, which is followed by the pro-domain, metalloprotease domain, disintegrin domain, cysteine-rich region, EGF-like motif, transmembrane domain, and finally the cytoplasmic tail at the C-terminal end [99] (Figure 1.3). The signal sequence directs the protein to enter the secretory pathway at the ER. There, it will undergo proper folding, glycosylation, and removal of the signal peptide. To prevent premature substrate recognition and cleavage, the pro-domain serves as an auto-inhibitor of the catalytically active metalloprotease domain until its removal in the Golgi complex [97]. The consensus sequence of the catalytic site in the metalloprotease domain is “HEXGHXXGXXHD”, where “X” can be any amino acid residue [100]. A triad of histidine (H) residues binds a zinc ion and a glutamate (E) serves as the catalytic residue. After removal of the pro-domain by another

proteolytic enzyme, the mature protein is trafficked from the Golgi to the cell surface where it can serve as a protease [101]. At the cell surface, both the disintegrin and cysteine-rich regions retain the capacity to facilitate adhesion and binding of various substrates, including integrins and other cell adhesion molecules [102]. Limited research has been done on the EGF-like domain, but there are hints that it could serve to facilitate the formation of oligomers or mediate substrate specificity [103, 104]. The transmembrane domain connects the extracellular N-terminal portion of the ADAM with the intracellular C-terminal part of the protein. The cytoplasmic tail can interact discriminately with various intracellular proteins through different motifs present in that region of the protein [105].

Functional Roles and Activity of ADAMs

As cell surface metalloproteases, the commonly understood function of ADAMs is to modulate the cleavage or "shedding" of membrane-bound proteins. These proteins are usually transmembrane precursors to various ligands required for activation of cellular signaling pathways. The cleaved portion of the protein (usually a soluble ligand) is released to the ECM to function in cell signaling by binding to receptors or other signaling components [106].

A growing amount of research has focused on analyzing the ADAM degradomics, that is a collection of all substrates for catalytically active ADAMs, especially in the context of cellular diseases, such as cancer [107]. While the information obtained from these assays is almost certainly related to a direct role of an ADAM's sheddase capabilities, the possibility of direct interactions between a particular domain (e.g. disintegrin, cysteine-rich, EGF-like, or cytoplasmic domain) within the ADAM and another protein cannot be eliminated. Transmembrane signaling pathways that have been shown to be influenced by ADAMs include the TNFα, NOTCH, and EGFR pathways [97]. Additional proteins that have been linked to

metalloprotease cleavage include those that mediate cell-cell interactions, such as members of the cadherin family or CD44 [108].

EGFR Signaling

ADAM proteases play an important role in signaling through the epidermal growth factor receptor (EGFR). EGFR is a receptor tyrosine kinase that dimerizes and autophosphorylates upon ligand binding. The kinase activity induces downstream signaling cascade events leading to cell proliferation (discussed in 'Epidermal Growth Factor Receptor (EGFR) Signaling' below). A number of ligands can serve as activation signals for EGFR, including epidermal growth factor (EGF), heparin-binding EGF (HB-EGF), epiregulin, amphiregulin, betacellulin, and transforming growth factor α (TGF-α) [109]. Different ADAMs can mediate cleavage of the transmembrane precursors of these ligands, yet there is some preference with regards to the favored substrate [106]. After the cleavage of transmembrane precursors, soluble ligands are released from the cell surface, bind to EGFR receptor, and initiate intracellular signaling responses.

Other Signaling Events Regulated by ADAMs

ADAMs have been shown to regulate other important signaling pathways, including Notch and tumor necrosis factor α (TNFα) signaling. The Notch pathway is important in the regulation of cell proliferation, differentiation, and death. Notch ligands are membrane-bound ligands that interact with their receptor on neighboring cells. Endocytosis of the ligand in the ligand-expressing cell exerts a pulling force on the receptor-ligand complex and exposes the S2 cleavage site in the Notch receptor. [110]. After the cleavage of the receptor by an ADAM, specifically ADAM10 or ADAM17, another proteolytic enzyme, γ-secretase, releases the cytoplasmic domain of the receptor, which allows it to translocate to the nucleus and serve as a

transcription factor that regulates important cellular pathways [111]. Aside from receptor cleavage, ADAMs can serve as negative regulators of this pathway by cleaving the ligand (e.g., Delta-like ligand 1), which limits its ability to interact with Notch receptors [112].

TNFα signaling requires the cleavage of a transmembrane ligand precursor, which must be released from the cell surface by ADAM17 [102]. Additionally, ADAM17 modulates the shedding of its receptor, tumor necrosis factor receptor (TNFR) [98]. TNFα is a cytokine that induces a pro-inflammatory response or apoptosis [97]. When TNFα is bound to its receptor (TNFR1), the receptor forms trimers, which causes the dissociation of an inhibitory protein and initiates different intracellular signaling pathways [105].

Cell adhesion receptors are involved in both cell-cell and cell-ECM interactions. The proteins included in this category include E-cadherin, N-cadherin, and various CAMs (cell adhesion molecules; e.g. L1-CAM, V-CAM) [113]. Cleavage by ADAMs (usually ADAM10 or ADAM17) mediates ectodomain shedding and results in a decrease in cell-cell or cell-matrix interactions [97, 114]. This promotes a mesenchymal cell phenotype and promotes metastasis [115].

ADAMs and Breast Cancer

Signaling and interactions of certain ADAM metalloproteases have been linked to various types of cancers, mainly through the exploitation of the above-mentioned signaling pathways. Alluding to this is the fact that numerous ADAMs are upregulated in different cancers, including breast cancer [116]. Several ADAMs with links to breast cancer are described below.

ADAM8 has been shown to be upregulated in breast cancers and is associated with poor patient prognosis [117]. However, since ADAM8 is classified as hematopoietic and expressed in lymphocytes, this correlation may be due in part to the presence of an increased vasculature in

the tumor microenvironment. Nevertheless, ADAM8 is strongly linked to an aggressive phenotype of various types of cancer [118, 119]. Knockdown of ADAM8 was able to inhibit cell migration and invasion in MDA-MB-231 and Hs578T breast cancer cells, and was able to impede tumor growth and metastasis in mice, likely due to the diminished shedding of pro-angiogenic factors, resulting in decreased vascularization [117].

ADAM9 has been weakly linked to a breast cancer phenotype. Several studies have identified ADAM9 as an elevated protease in cancer cell lines [120]. In non-small cell lung cancer, ADAM9 overexpression correlated with tumor metastases [121]. Additionally, miR-126 was shown to regulate breast cancer cell invasion by targeting ADAM9 [122].

ADAM10 appears to play a key role in resistance to HER2-targeted therapies in HER2+ breast cancer. Initially, ADAM10 was shown to shed the ectodomain of HER2 [123]. ADAM10 was then characterized as an essential mediator of trastuzumab resistance, knockdown of ADAM10 enhanced trastuzumab response, even in trastuzumab resistant breast cancer cells [124].

ADAM12 has been shown to be upregulated in numerous breast carcinomas and breast cancer cell lines [125-128]. Additionally, ADAM12 is correlated with poor prognosis in an aggressive subtype of breast cancer [129]. Our laboratory demonstrated that high expression of ADAM12 is associated with EGFR phosphorylation in breast tumors, induction of EMT in mammary epithelial cells, and a breast tumor initiating cell phenotype in cancer cell lines [126, 129]. In this dissertation, I show that ADAM12 knockdown diminishes both EGFR phosphorylation and a CSC phenotype in SUM159PT cells (Fig 4.2b,c). Therefore, ADAM12 likely serves as a modulator of breast cancer aggressiveness through its proteolytic activity and the release of EGFR ligands.

The *ADAM15* gene appears to be frequently amplified in breast cancer, as there are five or more copies of the gene present in the majority of breast cancer cell lines. ADAM15 is associated with increased metastasis and an aggressive phenotype [130, 131]. ADAM15 has been shown to cleave E-cadherin *in vitro*, resulting in a loss of cell-cell contacts [132]. A variety of splice variants for ADAM15 have been identified, and one of the splice variants has been shown to be associated with poor prognosis in lymph node-negative breast cancer [133].

ADAM17 is the most studied metalloprotease and has regulatory implications many cell signaling pathways. As seen with other ADAMs, overexpression of this family member results in a poor prognosis among breast cancer patients [134]. In cell based assays, targeting ADAM17 with a monoclonal antibody decreased the proliferation and invasion capabilities [135]. Importantly, ADAM17 has also been shown to be essential for EGFR activation and enhanced tumor invasiveness through ligand shedding [136]. In another study, the PI3K/AKT/mTOR pathway downstream of ADAM17-mediated ligand cleavage and EGFR activation was linked to a cancer cell invasive phenotype, though the $CD44^{+}/CD24^{-}$ CSC markers were not examined [137].

In this dissertation, I present the results showing that a broad spectrum metalloprotease inhibitor limited breast cancer cell proliferation and invasion and was able to change an aggressive cell phenotype to a less aggressive phenotype (see Chapters 3 and 4). Thus, ADAM metalloproteases play important roles in breast cancer progression and there are multiple lines of evidence documenting the importance of ADAMs in regulating different breast cancer signaling pathways.

Epidermal Growth Factor Receptor (EGFR) Signaling

EGFR signaling cascades contain some of the most frequently mutated proteins in cancer. Activation of EGFR signaling has been linked to tumor growth, progression, invasion, and metastasis [138]. EGFR overexpression is associated with an overall reduced survival and a poor prognosis in patients with lung and various other types of cancer [138, 139]. Additionally, EGFR is expressed at a higher level in approximately 75% of basal-like TNBCs *versus* non-TNBCs [13]. While there was early hope for EGFR inhibitors being used as targeted treatment for TNBC, a recent study demonstrated a low response rate for a combination of chemotherapy and an EGFR inhibitor [140]. This was the case even though *in vitro* studies using basal-like breast cancer cell lines showed promising results, including a change from a mesenchymal phenotype to an epithelial phenotype in a basal breast cancer cell line (SUM149PT) grown in 3D using Matrigel in the presence of an EGFR inhibitor [13, 140-142].

EGFR itself belongs to the family of receptor tyrosine kinases (RTKs), which exist at the cell surface and dimerize upon activation. EGFR can be activated by overexpression of the receptor, which is a common occurrence in cancer, as well as ligand-independent or ligand-dependent mechanisms [143]. Ligand-independent mechanisms include those caused by radiation that cause cellular stresses and inactivate phosphatases that antagonize EGFR activity [143]. Recently it was shown that in glioblastoma, the signaling pathways triggered by EGFR overexpression or ligand-dependent EGFR activation were mutually exclusive [144]. Upon ligand binding, EGFR undergoes a conformation change that allows receptor dimerization and autophosphorylation on tyrosine residues in the kinase domain of the receptor. The phosphotyrosines provide a docking site for cytoplasmic proteins that contain Src homology 2 (SH2) and phosphotyrosine-binding (PTB) domains. As a result, the intracellular signaling

pathways are activated. The three major signaling avenues for phosphorylated EGFR are the MEK/ERK pathway, the PI3K/AKT/mTOR pathway, and the STAT pathway.

MEK/ERK Pathway

After the autophosphorylation of the tyrosine kinase domain of EGFR, Grb2 and Sos either associate directly with these phosphorylated tyrosine residues, or through association with Shc, an adaptor molecule. The interaction between these proteins facilitates a conformation change in Sos, which is then able to recruit a small GTPase Ras with bound GDP. Ras is then activated, and the GDP is exchanged for GTP [145]. There are three Ras proteins: H-Ras, K-Ras, and N-Ras. Interestingly, K-Ras is mutated in 90% of pancreatic cancers [145]. Raf is released from an autoinhibitory state by the dephosphorylation of a specific serine residue, releasing an inhibitory form of 14-3-3, a cofactor for Raf. Ras-GTP is then able to bind to Raf, which induces its partial activation. Full activation occurs when Raf dimerizes, binds to an activating form of its cofactor, and phosphorylates an activating serine residue, along with other phosporylation sites in its kinase domain [146]. Phosphorylated Raf then phosphorylates a dual specificity kinase MEK1/2. MEK1/2 then phosphorylates and activates ERK1/2. Phosphorylated ERK can act in the cytosol or is trafficked to the nucleus to activate nuclear substrates. An example of a nuclear substrate of ERK1/2 is the Ets family of transcription factors which, when phosphorylated, can activate the synthesis of various pro-survival genes [147]. Negative regulators of this pathway include the DUSP family of phosphatases which antagonize ERK by dephosphorylating the kinase [148].

Specific inhibitors of various components of the MEK/ERK pathway exist, and appear to have a strong phenotype in *in vitro* studies, as these downstream components are required for the transforming capabilities of various oncogenes [145]. Inhibition of MEK in an aggressive breast

cancer cell line (SUM149PT) sensitized cells to erlotinib treatment (an EGFR inhibitor). Conversely, constitutively active MEK conferred resistance to EGFR inhibition [138]. DUSP loss is also associated with constitutive activation of the MEK/ERK pathway, as the absence of a negative regulator can be thought of as not being able to "put on the brakes" of the MEK/ERK pathway. As such, DUSP4 has been shown to be important in the modulation of growth, invasion, and a CSC phenotype in basal breast cancers [149, 150].

PI3K/AKT/mTOR Pathway

The PI3K/AKT/mTOR pathway is important in cell growth, apoptosis resistance, and migration. It is stimulated after the tyrosine kinase domain of the activated EGFR phosphorylates adaptor proteins. These adaptor proteins then bind to PI3K (phosphatidylinositol 3-kinase). PI3K consists of a regulatory p85 subunit, whose function is to anchor the protein to the docking sites, and a catalytic p110 subunit [143]. When PI3K is recruited to the membrane via p85, the p110 subunit phosphorylates PIP2 (phosphatidylinositol–4,5–bisphosphate, a lipid substrate) to PIP3. PIP3 then helps recruit other proteins to the plasma membrane, including AKT, a serine/threonine kinase. PTEN is a lipid phosphatase that dephosphorylates PIP3 and attenuates the signal [151]. PTEN is a tumor suppressor that is commonly lost in various cancers, including TNBC. It also functions in the nucleus to increase genomic stability [152]. Further downstream events in the PI3K pathway include full activation of AKT by a complex of mTOR/Rictor, and regulation of a variety of cellular proteins, including transcription factors. AKT also phosphorylates a negative regulator of the mTOR/Raptor complex that modulates RNA translation, protein synthesis, cell growth, and autophagy [151].

The PI3K pathway has been shown to be important in nasopharyngeal carcinoma, as only EGFR and PI3K inhibitors, but not a MEK inhibitor, was able to block a side population of

cancer stem cells observed when EGF was added [153]. In clinical trials, inhibitors to both the PI3K/AKT/mTOR pathway and MEK/ERK pathways seemed to yield improved patient survival, at the expense of an increase in toxicity of the drugs [154].

STAT Pathway

The signal transducer and activator of transcription (STAT) pathway involves direct phosphorylation of STAT proteins by EGFR, followed by the interactions of two phosphorylated STAT proteins via their SH2 domains. Upon dimerization, the STAT complex translocates to the nucleus, where it facilitates the transcription of specific target genes [143]. Constitutive activation of STAT family members, especially STAT3, has been found in numerous tumors and cell lines, leading to increased proliferation and invasion [155].

Cancer Immunosuppression

Cancer immunotherapy has recently emerged as a promising area of cancer treatment options. The goal of cancer immunotherapy is to use the body's own defense system to target and fight cancer. Immunotherapy originated in the late 1800s from the observation that sometimes the presence of a fever in cancer patients would cause remission of the cancer [156]. The first attempts to treat cancer using the immune system were done by the injection of bacteria into a patient, thus inducing an infection and indirectly activating the immune system. Surprisingly, this treatment had a 10% response rate but was not widely accepted due to the resulting severe fever and a reduced cure rate [156]. At the current time, much more sophisticated cancer immunotherapy treatments have been developed, due to the enhanced understanding of cellular signaling pathways that cause aberrant activation of cancer cells. Additionally, these treatments, which target a receptor on immune cells called PD-1, have shown

promising results in clinical trials for multiple cancer types, including early phase I trials for breast cancer, eliciting an overall response rate of ~20-80% [16, 157-159].

Adaptive Immune Response

The immune system consists of two components: the innate and adaptive immune response. The innate immune system provides a nonspecific response to pathogen invasion, and it includes cells such as natural killer cells, neutrophils, and macrophages. The adaptive immune system is a specialized and acquired response to pathogen infection, and is comprised of both B cells and T cells. A specific subtype of T cells, called cytotoxic T cells, recognize and kill pathogens through pore formation in the plasma membrane and the injection of proteolytic enzymes. The ultimate immune response is initiated through the recognition of an antigen on antigen-presenting cells by the T cell receptor (TCR) on T cells [160]. Immune checkpoints, which include co-stimulatory and inhibitory molecules, are crucial for the balance of the immune recognition system and the prevention of autoimmunity. These checkpoints are also able to prevent tissue damage when the immune system is responding to a pathogenic threat. Cancer cells are able to utilize these important regulators necessary for autoimmunity to evade recognition by the immune system [161]. Very often, cancer cells prevent the immune response in cytotoxic T cells by overexpressing inhibiting ligands or receptors that regulate the effectiveness of T cells [161].

In order to elicit an immune response and become activated, T cells must recognize a particular antigen that is on the cell surface of an antigen presenting cell (APC) or a tumor cell. This signal is presented to a receptor on the surface of T cells (specifically, the TCR) through a peptide bound to the major histocompatibility complex (MHC) on the APC. This, along with another co-stimulatory signal, activates T cells (shown in Figure 1.4, from ref [161]). Once a T

cell becomes activated, the expression of an inhibitory receptor, programmed cell death protein 1 (PD-1), is induced [162]. The major function of PD-1 is to prevent autoimmune responses from T cell activity in peripheral tissues during an infection [161]. Tumors can use this fail-safe mechanism as a means of immune evasion.

In order for PD-1 to limit the activation of T cells, it has to be bound to a ligand. There are two ligands for PD-1: PD-L1 and PD-L2. These ligands are transmembrane proteins found on the surface of cancer cells, which bind to PD-1 on effector T cells, and inhibit the immune response of these cells by limiting T cell proliferation and effector functions, inducing apoptosis, and promoting an "exhausted" state [160]. Generally, PD-L1 is the ligand that is implicated in immune evasion. Tumor cells can overexpress PD-L1 by two general mechanisms. First, an innate immune resistance stems from PD-L1 overexpression that is driven by constitutive oncogenic pathway activation in the cancer cells, such as in glioblastoma [161]. Cells from these types of cancers would have an innate expression of PD-L1 due to the activation of signaling pathways that regulate PD-L1 gene expression. The pathways that are believed to be responsible for driving expression of PD-L1 are the PI3K/AKT/mTOR pathway and STAT3 signaling [163]. Alternatively, PD-L1 can be upregulated in tumors through a process called adaptive immune resistance. In this response, cancer cells use the natural processes that evolved to protect normal tissues from damage by the immune system by the secretion of cytokines from helper T cells [164]. In adaptive immune resistance, PD-L1 is induced by interferons (IFNs), specifically IFNγ [165]. There has also been evidence pointing to an immunosuppressive role of PD-L1 in other cells present in the tumor microenvironment [166]. In either case, PD-L1 expression, which can be thought of as a marker of cancer aggressiveness, allows immune escape by binding to PD-1 and inducing a change in the function of the immune cells around this tumor, resulting in T cell

exhaustion [167, 168]. Blocking the PD-1/PD-L1 interaction usually restores the immune system recognition of cancer cells [169].

Programmed Cell Death Ligand 1 (PD-L1)

As mentioned in the section above, programmed cell death ligand 1 (PD-L1) binds to programmed cell death protein 1 (PD-1) and inhibits T cell-mediated killing of cancer cells and immune evasion. Therefore, the expression of PD-L1 is necessary to inhibit T cells. Even though its presence is vitally important, it is not clear if the expression of PD-L1 can serve as an independent prognostic marker for various types of cancer, as the status of PD-L1 can correlate with poor prognosis, good prognosis, or show no correlation [170-174]. There could be multiple reasons for this, including varying cancer types, stages, and treatments received.

Structure and Domain Organization of PD-L1

PD-L1 is a transmembrane protein that possesses four independent domains. Starting from the N-terminus, these domains are an IgV-like (variable) domain at the N-terminus, IgC-like (constant) domain, transmembrane domain, and an intracellular domain (shown in Figure 1.5, from ref [160]). The immunoglobin-like domains exist on the extracellular portion of the matrix. A solved crystal structure of the murine PD-1 complexed to human PD-L1 showed interactions between the IgV domains of each protein that facilitate binding [169, 175]. It is currently not known if the C-terminal tail transmits intracellular signals. Additionally, PD-L1 can undergo various post-translational modifications including the presence of four *N*-glycosylation sites in the extracellular domain [176]. A recent report suggested that PD-L1 undergoes mono-ubiquitination at the C-terminal region of the protein [177].

PD-L1 in Circulation

There is evidence in the literature that points to the presence of a soluble form of PD-L1 (sPD-L1) that is present in the bloodstream and circulatory system. This soluble form of PD-L1 found in the serum of patients has been associated with a poor prognosis in various types of cancers, including gastric cancer [178], hepatocellular carcinoma [179], melanoma [180], and non-small cell lung cancer [181]. To my knowledge, no such studies have been performed for breast cancer. Importantly, sPD-L1 was shown to retain its ability to inhibit T cell activation to a similar extent as the membrane-bound form of PD-L1 [182]. Thus, a soluble form of PD-L1 should have functional relevance in modulating the immune responses, either due to its presence in the tumor microenvironment or in patient sera. It is not clear how sPD-L1 is generated, and several possible mechanisms have been proposed, including alternative mRNA splicing that generates a secreted PD-L1 isoform, cleavage of the transmembrane PD-L1, or the presence of transmembrane PD-L1 on exosomes or circulating tumor cells.

A recent paper by Zhou, et al. has described the presence of four naturally occurring splice variants of PD-L1 in A375 and M34 melanoma cell lines [180]. These variants lack the transmembrane domain, but retain the IgV domain, raising the possibility that these proteins may be secreted and functionally active. Additionally, another splice variant in peripheral blood mononuclear cells has been previously described, which lacks the IgV domain, and is retained in the endoplasmic reticulum [183]. Additionally, low levels of PD-L1 cleavage have been detected in fibroblasts by a secreted matrix metalloprotease, MMP-13 [184]. Lending support to this hypothesis, the ADAM family of metalloproteases have been shown to shed immune system components [185, 186]. Finally, it is probable that the soluble form of PD-L1 detected in the sera of patients is due to the presence of the membrane bound form on either exosomes [187] or circulating tumor cells [188, 189], as the transmembrane form of PD-L1 has been documented on

both exosomes and circulating tumor cells. Exosomes are ~40-100-nm vesicles that are secreted from practically all cell types, including cancer cells. They do not have any organelles in their cytosol, but are composed of a variety of proteins, mRNA, and miRNAs, depending on their cell of origin. Exosomes are thought to play critical roles in breast cancer cell communication with distant sites and niche formation [190]. Exosomes may play a function in the immune response as (1) they have been shown to have biological activity, (2) they contain a MHC complex, and (3) T cells do not normally take up exosomes, but interact with the surface molecules on them promoting downstream signaling [187]. Regardless of the source of soluble PD-L1, it appears to play an important role in cancer immunosuppression.

Main Goals of the Study

As the identities of pathway modulators that support breast cancer cell aggressiveness have not been fully understood, investigations into key signaling pathways should provide novel insight into pathway components required for an aggressive cell phenotype. In this dissertation, I aimed to study the roles of several proteins within different cellular pathways, including the secretory pathway and cell surface proteolysis, in the regulation of certain aggressive cellular phenotypes.

- I investigated the effects of endoplasmic reticulum chaperones upon the anchorage-independent growth of aggressive breast cancer cell lines. I then selected the PDI family of molecular chaperones for conducting more specific studies, as these chaperones appeared to be the most consistently upregulated during anchorage-independent growth.
- I also explored the role of metalloprotease-mediated cleavage of EGFR ligands in regulation of the $CD44^{+}/CD24^{-}$ phenotype of breast cancer cells, which is a surrogate

measure of cancer cell aggressiveness. I was able to show that this cell surface marker profile was modulated exclusively through the MEK/ERK pathway.

- Additionally, I looked at specific metalloproteases, namely ADAM9 and ADAM12, and determined that these two ADAMs are able to enhance the $CD44^{+}/CD24^{-}$ phenotype of breast cancer cells.
- Finally, I showed that matrix-metalloproteases are able to cleave an important regulator of the cancer cell immune evasion pathway, though the significance of this finding has yet to be determined, possibly through *in vivo* studies

References

1. Ban KA, Godellas CV (2014) Epidemiology of Breast Cancer. Surg Oncol Clin N Am. 23:409-422.
2. American Cancer Society (2017) Cancer Facts & Figures 2017 1-71.
3. Sandhu R, Parker JS, Jones WD, Livasy CA, Coleman WB (2010) Microarray-Based Gene Expression Profiling for Molecular Classification of Breast Cancer and Identification of New Targets for Therapy. Lab Med 41:364-372.
4. Sledge GW, Mamounas EP, Health F, Hortobagyi GN, Burstein HJ (2017) Past, Present, and Future Challenges in Breast Cancer Treatment. J Clin Oncol 32:15-19.
5. Kathryn JC, Sireesha V G, Stanley L (2012) Triple Negative Breast Cancer Cell Lines: One Tool in the Search for Better Treatment of Triple Negative Breast Cancer. Breast Dis. 32:35-48.
6. Carey L, Winer E, Viale G, Cameron D, Gianni L (2010) Triple-negative breast cancer: disease entity or title of convenience? Nat Rev Clin Oncol 7:683-692.
7. Bastien RR, Rodríguez-Lescure Á, Ebbert MT, Prat A, Munárriz B, Rowe L, et al (2012) PAM50 Breast Cancer Subtyping by RT-qPCR and Concordance with Standard Clinical Molecular Markers. BMC Med Genomics 5:44.
8. Parker JS, Mullins M, Cheang MCU, Leung S, Voduc D, Vickery T, et al (2009) Supervised risk predictor of breast cancer based on intrinsic subtypes. J Clin Oncol 27:1160-1167.
9. Prat A, Pineda E, Adamo B, Galván P, Fernández A, Gaba L, et al (2015) Clinical implications of the intrinsic molecular subtypes of breast cancer. Breast 24:S26-S35.

10. Nielsen TO, Parker JS, Leung S, Voduc D, Ebbert M, Vickery T, et al (2010) A comparison of PAM50 intrinsic subtyping with immunohistochemistry and clinical prognostic factors in tamoxifen-treated estrogen receptor-positive breast cancer. Clin Cancer Res 16:5222-5232.

11. Perou CM (2010) Molecular stratification of Triple negative breast cancer. Oncologist 15:39-48.

12. Bombard Y, Rozmovits L, Trudeau M, Leighl NB, Deal K, Marshall DA (2015) The Value of Personalizing Medicine: Medical Oncologists' Views on Gene Expression Profiling in Breast Cancer Treatment. Oncologist 20:351-356.

13. Lehmann BD, Pietenpol JA (2014) Identification and use of biomarkers in treatment strategies for triple-negative breast cancer subtypes. J Pathol 232:142-150.

14. Mayer IA, Abramson VG, Lehmann BD, Pietenpol JA (2014) New strategies for triple-negative breast cancer-deciphering the heterogeneity. Clin Cancer Res 20:782-790.

15. Tryfonidis K, Senkus E, Cardoso M, Cardoso F (2015) Management of locally advanced breast cancer - perspectives and future directions. Nat Rev Clin Oncol 12:147-162.

16. Denkert C, Liedtke C, Tutt A, von Minckwitz G (2017) Molecular alterations in triple-negative breast cancer—the road to new treatment strategies. Lancet 389:2430-2442.

17. Taddei ML, Giannoni E, Fiaschi T, Chiarugi P (2012) Anoikis: An emerging hallmark in health and diseases. J Pathol 226:380-393.

18. Justus CR, Leffler N, Ruiz-Echevarria M, Yang LV (2014) *In vitro* Cell Migration and Invasion Assays. J Vis Exp 88:1-8.

19. Liang C-C, Park AY, Guan J-L (2007) *In vitro* scratch assay: a convenient and inexpensive method for analysis of cell migration *in vitro*. Nat Protoc 2:329-333.

20. Katt ME, Placone AL, Wong AD, Xu ZS, Searson PC (2016) *In Vitro* Tumor Models: Advantages, Disadvantages, Variables, and Selecting the Right Platform. Front Bioeng Biotechnol 4.

21. Benton G, Arnaoutova I, George J, Kleinman HK, Koblinski J (2014) Matrigel: From discovery and ECM mimicry to assays and models for cancer research. Adv Drug Deliv Rev 79:3-18.

22. Manuel Iglesias J, Beloqui I, Garcia-Garcia F, Leis O, Vazquez-Martin A, Eguiara A, et al (2013) Mammosphere Formation in Breast Carcinoma Cell Lines Depends upon Expression of E-cadherin. PLoS One 8:1-12.

23. Mori S, Chang JT, Andrechek ER, Matsumura N, Baba T, Yao G, et al (2010) An Anchorage-Independent Cell Growth Signature Identifies Tumors with Metastatic Potential 28:2796-2805.

24. Al-Hajj M, Wicha M, Benito-Hernandez A, Morrison S, Clarke M (2003) Prospective identification of tumorigenic breast cancer cells. Proc Natl Acad Sci 100:3983-3988.

25. Basakran NS (2015) CD44 as a potential diagnostic tumor marker. Saudi Med J 36:273-279.

26. Honeth G, Bendahl P-O, Ringnér M, Saal LH, Gruvberger-Saal SK, Lövgren K, et al (2008) The $CD44^+/CD24^-$ phenotype is enriched in basal-like breast tumors. Breast Cancer Res 10:R53.

27. Sheridan C, Kishimoto H, Fuchs RK, Mehrotra S, Bhat-Nakshatri P, Turner CH, et al (2006) $CD44^+/CD24^-$ breast cancer cells exhibit enhanced invasive properties: an early step necessary for metastasis. Breast Cancer Res 8:59.

28. Jaggupilli A, Elkord E (2012) Significance of CD44 and CD24 as cancer stem cell markers: An enduring ambiguity. Clin Dev Immunol 2012:1-11.

29. Fillmore CM, Kuperwasser C (2008) Human breast cancer cell lines contain stem-like cells that self-renew, give rise to phenotypically diverse progeny and survive chemotherapy. Breast Cancer Res 10:R25.

30. Liu Y, Nenutil R, Appleyard MV, Murray K, Boylan M, Thompson AM, et al (2014) Lack of correlation of stem cell markers in breast cancer stem cells. Br J Cancer 110:2063-2071.

31. Marcato P, Dean CA, Giacomantonio CA, Lee PWK (2011) Aldehyde dehydrogenase its role as a cancer stem cell marker comes down to the specific isoform. Cell Cycle 10:1378-1384.

32. Ginestier C, Hur MH, Charafe-Jauffret E, Monville F, Dutcher J, Brown M, et al (2007) ALDH1 is a marker of normal and malignant human mammary stem cells and a predictor of poor clinical outcome. Cell Stem Cell 1:555-567.

33. Lodish H, Berk A, Zipursky SL, Matsudaira P, Baltimore D, Darnell J (2000) Overview of the Secretory Pathway. In: Molecular Cell Biology. 4th ed. New York: W. H. Freeman.

34. Wlodkowic D, Skommer J, McGuinness D, Hillier C, Darzynkiewicz Z (2009) ER-Golgi network– a future target for anti-cancer therapy. Leuk Res 33:1440-1447.

35. Dejeans N, Manié S, Hetz C, Bard F, Hupp T, Agostinis P, et al (2014) Addicted to secrete - novel concepts and targets in cancer therapy. Trends Mol Med 20:242-250.

36. Gill DJ, Tham KM, Chia J, Wang SC, Steentoft C, Clausen H, et al (2013) Initiation of GalNAc-type O-glycosylation in the endoplasmic reticulum promotes cancer cell invasiveness. Proc Natl Acad Sci USA 110:E3152-61.

37. Braakman I, Hebert DN (2013) Protein folding in the endoplasmic reticulum. Cold Spring Harb Perspect Biol 5:a013201.

38. Graner MW, Lillehei KO, Katsanis E (2015) Endoplasmic Reticulum Chaperones and Their Roles in the Immunogenicity of Cancer Vaccines. Front Oncol 4:1-12.

39. Needham PG, Brodsky JL (2013) How early studies on secreted and membrane protein quality control gave rise to the ER associated degradation (ERAD) pathway: The early history of ERAD. Biochim Biophys Acta - Mol Cell Res 1833:2447-2457.

40. Clarke R, Cook KL, Hu R, Facey COB, Tavassoly I, Schwartz JL, et al (2012) Endoplasmic reticulum stress, the unfolded protein response, autophagy, and the integrated regulation of breast cancer cell fate. Cancer Res 72:1321-1331.

41. Schröder M, Kaufman RJ (2005) The Mammalian Unfolded Protein Response. Annu Rev Biochem 74:739-789.

42. Buck TM, Wright CM, Brodsky JL (2007) The Activities and Function of Molecular Chaperones in the Endoplasmic Reticulum. Semin Cell Dev Biol 18:751-761.

43. Hebert DN, Molinari M (2007) In and out of the ER: protein folding, quality control, degradation, and related human diseases. Physiol Rev 87:1377-1408.

44. Flynn G, Pohl J, Flocco MT, Rothman JE (1991) Peptide-binding specificity of the molecular chaperone BiP. Lett to Nat 353:737-740.

45. Dong D, Ni M, Li J, Xiong S, Ye W, Virrey JJ, et al (2008) Critical role of the stress chaperone GRP78/BiP in tumor proliferation, survival, and tumor angiogenesis in transgene-induced mammary tumor development. Cancer Res 68:498-505.

46. Lee E, Nichols P, Spicer D, Groshen S, Yu MC, Lee AS (2006) GRP78 as a novel predictor of responsiveness to chemotherapy in breast cancer. Cancer Res 66:7849-7853.

47. Roller C, Maddalo D (2013) The molecular chaperone GRP78/BiP in the development of chemoresistance: Mechanism and possible treatment. Front Pharmacol 4:1-5.

48. Wang M, Kaufman RJ (2014) The impact of the endoplasmic reticulum protein-folding environment on cancer development. Nat Rev Cancer 14:581-597.

49. Schopf FH, Beibl MM, Buchner J (2017) The Hsp90 chaperone machinery. Nat Rev Mol Cell Biol 18:345-360.

50. Neefjes J, Jongsma MLM, Paul P, Bakke O (2011) Towards a systems understanding of MHC class I and MHC class II antigen presentation. Nat Rev Immunol 11:823-836.

51. Schrag JD, Procopio DO, Cygler M, Thomas DY, Bergeron JJM (2003) Lectin control of protein folding and sorting in the secretory pathway. Trends Biochem Sci 28:49-57.

52. Williams DB (2006) Beyond lectins: the calnexin/calreticulin chaperone system of the endoplasmic reticulum. J Cell Sci 119:615-623.

53. Delom F, Emadali A, Cocolakis E, Lebrun J-J, Nantel A, Chevet E (2007) Calnexin-dependent regulation of tunicamycin-induced apoptosis in breast carcinoma MCF-7 cells. Cell Death Differ 14:586-596.

54. Brodsky JL, Skach WR (2011) Protein folding and quality control in the endoplasmic reticulum: Recent lessons from yeast and mammalian cell systems. Curr Opin Cell Biol 23:464-475.

55. Feige MJ, Hendershot LM (2011) Disulfide bonds in ER protein folding and homeostasis. Curr Opin Cell Biol 23:167-175.

56. Galligan JJ, Petersen DR (2012) The human protein disulfide isomerase gene family. Hum Genomics 6:6.

57. Ellgaard L, Ruddock LW (2005) The human protein disulphide isomerase family: substrate interactions and functional properties. EMBO Rep 6:28-32.

58. Santana-Codina N, Carretero R, Sanz-Pamplona R, Cabrera T, Guney E, Oliva B, et al (2013) A transcriptome-proteome integrated network identifies endoplasmic reticulum thiol oxidoreductase (ERp57) as a hub that mediates bone metastasis. Mol Cell Proteomics 12:2111-2125.

59. Liao C-J, Wu T-I, Huang Y-H, Chang T-C, Wang C-S, Tsai M-M, et al (2011) Glucose-regulated protein 58 modulates cell invasiveness and serves as a prognostic marker for cervical cancer. Cancer Sci 102:2255-2263.

60. Choe MH, Min JW, Jeon HB, Cho D, Oh JS (2015) ERp57 modulates STAT3 activity in radioresistant laryngeal cancer cells and serves as a prognostic marker for laryngeal cancer. Oncotarget 6:2654-2666.

61. Wiersma VR, Michalak M, Abdullah TM, Bremer E, Eggleton P (2015) Mechanisms of translocation of ER chaperones to the cell surface and immunomodulatory roles in cancer and autoimmunity. Front Oncol 5:1-14.

62. Rutkevich LA, Cohen-Doyle MF, Brockmeier U, Williams DB (2010) Functional Relationship between Protein Disulfide Isomerase Family Members during the Oxidative Folding of Human Secretory Proteins. Mol Biol Cell 21:3093-3105.

63. Maattanen P, Kozlov G, Gehring K, Thomas DY (2006) ERp57 and PDI: multifunctional protein disulfide isomerases with similar domain architectures but differing substrate-partner associations. Biochem Cell Biol 84:881-889.

64. Garbi N, Tanaka S, Momburg F, Hämmerling GJ (2006) Impaired assembly of the major histocompatibility complex class I peptide-loading complex in mice deficient in the oxidoreductase ERp57. Nat Immunol 7:93-102.

65. Vavassori S, Cortini M, Masui S, Sannino S, Anelli T, Caserta IR, et al (2013) A pH-Regulated Quality Control Cycle for Surveillance of Secretory Protein Assembly. Mol

Cell 50:783-792.

66. Sannino S, Anelli T, Cortini M, Masui S, Degano M, Fagioli C, et al (2014) Progressive quality control of secretory proteins in the early secretory compartment by ERp44. J Cell Sci 127:4260-4269.

67. Zhao G, Lu H, Li C (2015) Proapoptotic activities of Protein Disulfide Isomerase (PDI) and PDIA3 protein, a role of the Bcl-2 protein Bak. J Biol Chem 290:8949-8963.

68. Gutiérrez T, Simmen T (2014) Endoplasmic reticulum chaperones and oxidoreductases: critical regulators of tumor cell survival and immunorecognition. Front Oncol 4:291.

69. Luo B, Lee AS (2013) The critical roles of endoplasmic reticulum chaperones and unfolded protein response in tumorigenesis and anti-cancer therapies. Oncogene 32:1-29.

70. Walter P, Ron D (2011) The Unfolded Protein Response: From Stress Pathway to Homeostatic Regulation. Science 334:1081-1086.

71. Yamamoto K, Sato T, Matsui T, Sato M, Okada T, Yoshida H, et al (2007) Transcriptional Induction of Mammalian ER Quality Control Proteins Is Mediated by Single or Combined Action of ATF6α and XBP1. Dev Cell 13:365-376.

72. Shoulders MD, Ryno LM, Genereux JC, Moresco JJ, Tu PG, Wu C, et al (2013) Stress-Independent Activation of XBP1s and/or ATF6 Reveals Three Functionally Diverse ER Proteostasis Environments. Cell Rep 3:1279-1292.

73. Feng YX, Sokol ES, Del Vecchio CA, Sanduja S, Claessen JHL, Proia TA, et al (2014) Epithelial-to-mesenchymal transition activates PERK-eIF2α and sensitizes cells to endoplasmic reticulum stress. Cancer Discov 4:702-715.

74. Dadey DYA, Kapoor V, Khudanyan A, Urano F, Kim AH, Thotala D, et al (2016) The ATF6 pathway of the ER stress response contributes to enhanced viability in glioblastoma. Oncotarget 7:2080-2092.

75. Sequeira SJ, Ranganathan AC, Adam AP, Iglesias BV., Farias EF, Aguirre-Ghiso JA (2007) Inhibition of proliferation by PERK regulates mammary acinar morphogenesis and tumor formation. PLoS One 2:e615.

76. Chen X, Iliopoulos D, Zhang Q, Tang Q, Greenblatt MB, Hatziapostolou M, et al (2014) XBP1 promotes triple-negative breast cancer by controlling the HIF1α pathway. Nature 508:103-107.

77. Xu S, Sankar S, Neamati N (2014) Protein disulfide isomerase: A promising target for cancer therapy. Drug Discov Today 19:222-240.

78. Lovat PE, Corazzari M, Armstrong JL, Martin S, Pagliarini V, Hill D, et al (2008) Increasing melanoma cell death using inhibitors of protein disulfide isomerases to abrogate survival responses to endoplasmic reticulum stress. Cancer Res 68:5363-5369.

79. van de Vijver MJ, He YD, van't Veer LJ, Dai H, Hart AAM, Voskuil DW, et al (2002) A Gene-expression signature as a predictor of survival in breast cancer. N Engl J Med 347:1999-2009.

80. Khan HA, Mutus B (2014) Protein disulfide isomerase a multifunctional protein with multiple physiological roles. Front Chem 2:1-9.

81. Benham AM (2012) The Protein Disulfide Isomerase Family: Key Players in Health and Disease. Antioxid Redox Signal 16:781-789.

82. Bateman JF, Boot-Handford RP, Lamandé SR (2009) Genetic diseases of connective tissues: cellular and extracellular effects of ECM mutations. Nat Rev Genet 10:173-183.

83. Ramos FS, Serino LTR, Carvalho CMS, Lima RS, Urban CA (2015) PDIA3 and PDIA6 gene expression as an aggressiveness marker in primary ductal breast cancer. Genet Mol Res 14:6960-6967.

84. Panaretakis T, Joza N, Modjtahedi N, Tesniere A, Vitale I, Durchschlag M, et al (2008) The co-translocation of ERp57 and calreticulin determines the immunogenicity of cell death. Cell Death Differ 15:1499-1509.

85. Gaucci E, Altieri F, Turano C, Chichiarelli S (2013) The Protein ERp57 Contributes to EGF Receptor Signaling and Internalization in MDA-MB-468 Breast Cancer Cells. J Cell Biochem 114:2461-2470.

86. Chang Y, Wu Y, Liu W, Ji G (2015) Knockdown of ERp44 leads to apoptosis via activation of ER stress in HeLa cells. Biochem Biophys Res Commun 463:606-611.

87. Cho JH, Jeon YJ, Park SM, et al (2015) Multifunctional effects of honokiol as an anti-inflammatory and anti-cancer drug in human oral squamous cancer cells and xenograft. Biomaterials 53:274-284.

88. Jin M, Wang J, Zhai K, Chang Y, Yuan Q, Ji G (2016) ERp44 inhibits human lung cancer cell migration mainly via IP3R2. Aging 8:1276-1286.

89. Kaushik S, Pickup MW, Weaver VM (2016) From transformation to metastasis: deconstructing the extracellular matrix in breast cancer. Cancer Metastatsis Rev 35:655-667.

90. Maziveyi M, Alahari SK (2015) Cell matrix adhesions in cancer: The proteins that form the glue. Oncotarget 8:48471-48487.

91. Venning FA, Wullkopf L, Erler JT (2015) Targeting ECM Disrupts Cancer Progression. Front Oncol 5:224.

92. Lu P, Weaver VM, Werb Z (2012) The extracellular matrix: A dynamic niche in cancer progression. J Cell Biol 196:395-406.

93. Koenig A, Mueller C, Hasel C, Adler G, Menke A (2006) Collagen type I induces disruption of E-cadherin-mediated cell-cell contacts and promotes proliferation of pancreatic carcinoma cells. Cancer Res 66:4662-4671.

94. Shintani Y, Hollingsworth MA, Wheelock MJ, Johnson KR (2006) Collagen I promotes metastasis in pancreatic cancer by activating c-Jun NH2-terminal kinase 1 and up-regulating N-cadherin expression. Cancer Res 66:11745-11753.

95. Aoudjit F, Vuori K (2012) Integrin Signaling in Cancer Cell Survival and Chemoresistance. Chemother Res Pract 2012:1-16.

96. Hoiruchi K, Blobel CP (2005) Studies from ADAM knockout mice. In: The ADAM Family of Proteases 29-64.

97. Murphy G (2008) The ADAMs: signalling scissors in the tumour microenvironment. Nat Rev Cancer 8:932-941.

98. Edwards DR, Handsley MM, Pennington CJ (2009) The ADAM metalloproteinases. Mol Aspects Med 29:258-289.

99. Qi Y, Duhachek-Muggy S, Lino H, Zolkiewska A (2014) Phenotypic diversity of breast cancer-related mutations in metalloproteinase-disintegrin ADAM12. PLoS One 9:e92536.

100. Goth CK, Halim A, Khetarpal SA, Rader DJ, Clausen H, Schjoldager KT-BG (2015) A systematic study of modulation of ADAM-mediated ectodomain shedding by site-specific O-glycosylation. Proc Natl Acad Sci 112:14623-14628.

101. Anzellotti AI, Farrell NP (2008). Zinc metalloproteins as medicinal targets. Chem Soc Rev 37:1629-1651.

102. Moss ML, White JM, Lambert MH (2001) TACE and other ADAM proteases as targets for drug discovery. Drug Discov Today 6:417-426.

103. Lorenzen I, Trad A, Grötzinger J (2011) Multimerisation of A disintegrin and metalloprotease protein-17 (ADAM17) is mediated by its EGF-like domain. Biochem Biophys Res Commun 415:330-336.

104. Lu D, Scully M, Kakkar V, Lu X (2010) ADAM-15 disintegrin-like domain structure and function. Toxins 2:2411-2427.

105. Blobel CP (2005) ADAMs: key components in EGFR signalling and development. Nat Rev Mol Cell Biol 6:32-43.

106. Duffy MJ, Mullooly M, O'Donovan N, Sukor S, Crown J, Pierce A, et al (2011) The ADAMs family of proteases: new biomarkers and therapeutic targets for cancer? Clin Proteomics 8:1-13.

107. Dreymueller D, Uhlig S, Ludwig A (2015) ADAM-family metalloproteinases in lung

inflammation: potential therapeutic targets. Am J Physiol - Lung Cell Mol Physiol 308:L325-L343.

108. Stamenkovic I, Yu Q (2009) Shedding light on proteolytic cleavage of CD44: the responsible sheddase and functional significance of shedding. J Invest Dermatol 129:1321-1324.

109. Seshacharyulu P, Ponnusamy M, Haridas D, Jain M, Ganti A, Batra S (2013) Targeting the EGFR signaling pathway in cancer therapy. Expert Opin Ther Targets 16:15-31.

110. Giebeler N, Zigrino P (2016) A disintegrin and metalloprotease (ADAM): Historical overview of their functions. Toxins 8:1-14.

111. Zolkiewska A (2008) ADAM proteases: Ligand processing and modulation of the Notch pathway. Cell Mol Life Sci 65:2056-2068.

112. Six E, Ndiaye D, Laabi Y, Brou C, Gupta-Rossi N, Israel A, et al (2003) The Notch ligand Delta1 is sequentially cleaved by an ADAM protease and γ-secretase. Proc Natl Acad Sci USA 100:7638-7643.

113. Ponnuchamy B, Khalil RA (2008) Role of ADAMs in endothelial cell permeability: Cadherin shedding and leukocyte rolling. Circ Res 102:1139-1142.

114. Rupp AK, Rupp C, Keller S, Brase JC, Ehehalt R, Fogel M, et al (2011) Loss of EpCAM expression in breast cancer derived serum exosomes: Role of proteolytic cleavage. Gynecol Oncol 122:437-446.

115. Ieguchi K, Tomita T, Omori T, Komatsu A, Deguchi A, Masuda J, et al (2014) ADAM12-cleaved ephrin-A1 contributes to lung metastasis. Oncogene 33:2179-2190.

116. Lendeckel U, Kohl J, Arndt M, Carl-McGrath S, Donat H, Röcken C (2005) Increased expression of ADAM family members in human breast cancer and breast cancer cell lines. J Cancer Res Clin Oncol 131:41-48.

117. Romagnoli M, Mineva ND, Polmear M, Conrad C, Srinivasan S, Loussouarn D, et al (2014) ADAM 8 expression in invasive breast cancer promotes tumor dissemination and metastasis. EMBO Mol Med 6:278-294.

118. Ishikawa N, Daigo Y, Yasui W, Inai K, Nishimura H, Tsuchiya E, et al (2004) ADAM8 as a novel serological and histochemical marker for lung cancer. Clin Cancer Res 10:8363-8370.

119. Schlomann U, Koller G, Conrad C, Ferdous T, Golfi P, Garcia AM, et al (2016) ADAM8 as a drug target in pancreatic cancer. Nat Commun 6:6175.

120. Mochizuki S, Okada Y (2007) ADAMs in cancer cell proliferation and progression. Cancer Sci 98:621-628.

121. Shintani Y, Higashiyama S, Ohta M, Hirabayashi H, Yamamota S, Yoshimasu T, et al (2004) Overexpression of ADAM9 in non-small cell lung cancer correlates with brain metastasis. Cancer Res 64:4190-4196.

122. Wang CZ, Yuan P, Li Y (2015) miR-126 regulated breast cancer cell invasion by targeting ADAM9. Int J Clin Exp Pathol 8:6547-6553.

123. Liu PCC, Liu X, Li Y, Covington M, Wynn R, Huber R, et al (2006) Identification of ADAM10 as a major source of HER2 ectodomain sheddase activity in HER2 overexpressing breast cancer cells. Cancer Biol Ther 5:657-664.

124. Feldinger K, Generali D, Kramer-Marek G, Gijsen M, Ng TB, Wong JH, et al (2014) ADAM10 mediates trastuzumab resistance and is correlated with survival in HER2 positive breast cancer. Oncotarget 5:6633-6646.

125. Kveiborg M, Frohlich C, Albrechtsen R, Tischler V, Dietrich N, Holck P, et al (2005) A role for ADAM12 in breast tumor progression and stromal cell apoptosis. Cancer Res 65:4754-4761.

126. Li H, Duhachek-Muggy S, Dubnicka S, Zolkiewska A (2013) Metalloproteinase-disintegrin ADAM12 is associated with a breast tumor-initiating cell phenotype. Breast Cancer Res Treat 139:691-703.

127. Roy R, Rodig S, Bielenberg D, Zurakowski D, Moses MA (2011) ADAM12 transmembrane and secreted isoforms promote breast tumor growth: A distinct role for ADAM12-S protein in tumor metastasis. J Biol Chem 286:20758-20768.

128. Frohlich C, Nehammer C, Albrechtsen R, Kronqvist P, Kveiborg M, Sehara-Fujisawa A, et al (2011) ADAM12 Produced by Tumor Cells Rather than Stromal Cells Accelerates Breast Tumor Progression. Mol Cancer Res 9:1449-1461.

129. Li H, Duhachek-Muggy S, Qi Y, Hong Y, Behbod F, Zolkiewska A (2012) An essential role of metalloprotease-disintegrin ADAM12 in triple-negative breast cancer. Breast Cancer Res Treat 135:759-769.

130. Kuefer R, Day KC, Kleer CG, Sabel MS, Hofer MD, Varambally S, et al (2006) ADAM15 disintegrin is associated with aggressive prostate and breast cancer disease. Neoplasia 8:319-329.

131. Hou Y, Chu M, Cai Y, Lei J, Chen Y, Zhu R, et al (2015) Antitumor and anti-angiogenic activity of the recombinant human disintegrin domain of A disintegrin and metalloproteinase 15. Mol Med Rep 12:2360-2366.

132. Najy AJ, Day KC, Day ML (2008) The ectodomain shedding of E-cadherin by ADAM15 supports ErbB receptor activation. J Biol Chem 283:18393-18401.

133. Zhong JL, Poghosyan Z, Pennington CJ, Scott X, Handsley MM, Warn A, et al (2008) Distinct Functions of Natural ADAM-15 Cytoplasmic Domain Variants in Human

Mammary Carcinoma. Mol Cancer Res 6:383-394.

134. McGowan PM, McKiernan E, Bolster F, Ryan BM, Hill ADK, McDermott CW, et al (2008) ADAM-17 predicts adverse outcome in patients with breast cancer. Ann Oncol 19:1075-1081.

135. Caiazza F, McGowan PM, Mullooly M, Murray A, Synnott N, O'Donovan N, et al (2015) Targeting ADAM-17 with an inhibitory monoclonal antibody has antitumour effects in triple-negative breast cancer cells. Br J Cancer 112:1895-1903.

136. Kenny PA, Bissell MJ (2007) Targeting TACE-dependent EGFR ligand shedding in breast cancer. J Clin Invest 117:337-345.

137. Zheng X, Jiang F, Katakowski M, Zhang ZG, Lu Q-E, Chopp M (2009) ADAM17 promotes breast cancer cell malignant phenotype through EGFR-PI3K-AKT activation. Cancer Biol Ther 6:760-769.

138. Zhang D, LaFortune TA, Krishnamurthy S, Esteva FJ, Cristofanilli M, Liu P, et al (2009) Epidermal growth factor receptor tyrosine kinase inhibitor reverses mesenchymal to epithelial phenotype and inhibits metastasis in inflammatory breast cancer. Clin Cancer Res 15:6639-6648.

139. Steelman LS, Fitzgerald T, Lertpiriyapong K, Cocco L, Follo MY, Martelli AM, et al (2016) Critical Roles of EGFR Family Members in Breast Cancer and Breast Cancer Stem Cells : Targets for Therapy. Curr Pharm Des 22:2358-2388.

140. Carey LA, Rugo HS, Marcom PK, Mayer EL, Esteva FJ, Ma CX, et al (2012) TBCRC 001: Randomized phase II study of cetuximab in combination with carboplatin in stage IV triple-negative breast cancer. J Clin Oncol 30:2615-2623.

141. Hoadley KA, Weigman VJ, Fan C, Sawyer LR, He X, Troester MA, et al (2007) EGFR associated expression profiles vary with breast tumor subtype. BMC Genomics 8:258.

142. Ueno NT, Zhang D (2011) Targeting EGFR in triple negative breast cancer. J Cancer 2:324-328.

143. Scaltriti M, Baselga J (2006) The Epidermal Growth Factor Receptor Pathway : A Model for Targeted Therapy. Clin Cancer Res 12:5268-5272.

144. Chakraborty S, Li L, Puliyappadamba VT, Guo G, Hatanpaa KJ, Mickey B, et al (2014) Constitutive and ligand-induced EGFR signalling triggers distinct and mutually exclusive downstream signalling networks. Nat Commun 5:5811.

145. Roberts P, Der C (2007) Targeting the Raf-MEK-ERK mitogen-activated protein kinase cascade for the treatment of cancer. Oncogene 26:3291-3310.

146. Lavoie H, Therrien M (2015) Regulation of RAF protein kinases in ERK signalling. Nat Rev Mol Cell Biol 16:281-298.

147. Zhang W, Liu HT (2002) MAPK signal pathways in the regulation of cell proliferation in mammalian cells. Cell Res 12:9-18.

148. Jeffrey KL, Camps M, Rommel C, Mackay CR (2007) Targeting dual-specificity phosphatases: manipulating MAP kinase signalling and immune responses. Nat Rev Drug Discov 6:391-403.

149. Balko JM, Schwarz LJ, Bhola NE, Kurupi R, Owens P, Miller TW, et al (2013) Activation of MAPK pathways due to DUSP4 loss promotes cancer stem cell-like phenotypes in basal-like breast cancer. Cancer Res 73:6346-6358.

150. Mazumdar A, Poage GM, Shepherd J, Tsimelzon A, Hartman ZC, Hollander PD, et al (2016) Analysis of phosphatases in ER-negative breast cancers identifies DUSP4 as a critical regulator of growth and invasion. Breast Cancer Res Treat 158:441-454.

151. Mayer IA, Arteaga CL (2016) The PI3K/AKT Pathway as a Target for Cancer Treatment. Annu Rev Med 67:11-28.

152. Dillon LM, Miller TW (2014) Therapeutic targeting of cancers with loss of PTEN function. Curr Drug Targets 15:65-79.

153. Ma L, Zhang G, Miao X-B, Deng X-B, Wu Y, Liu Y, et al (2013) Cancer Stem-like Cell Properties are Regulated by EGFR/AKT/β-catenin Signaling and Preferentially Inhibited by Gefitinib in Nasopharyngeal Carcinoma. FEBS J 280.

154. Shimizu T, Tolcher AW, Papadopoulos KP, Beeram M, Rasco DW, Smith LS, et al (2012) The clinical effect of the dual-targeting strategy involving PI3K/AKT/mTOR and RAS/MEK/ERK pathways in patients with advanced cancer. Clin Cancer Res 18:2316-2325.

155. Yu H, Pardoll D, Jove R (2016) STATs in cancer inflammation and immunity: a leading role for STAT3. Nat Rev Cancer 9:798-809.

156. Parish CR (2003) Cancer immunotherapy: The past, the present and the future. Immunol Cell Biol 81:106-113.

157. Gettinger S, Rizvi NA, Chow LQ, Borghaei H, Brahmer J, Ready N, et al (2016) Nivolumab Monotherapy for First-Line Treatment of Advanced Non-Small-Cell Lung Cancer. J Clin Oncol 34:2980-2987.

158. Weber JS, D'Angelo SP, Minor D, Hodi FS, Gutzmer R, Neyns B, et al (2015) Nivolumab versus chemotherapy in patients with advanced melanoma who progressed after anti-CTLA-4 treatment (CheckMate 037): A randomised, controlled, open-label, phase 3 trial. Lancet Oncol 16:375-384.

159. El-Khoueiry AB, Melero I, Crocenzi TS, Welling TH, Yau TC, Yeo W, et al (2015) Phase I/II safety and antitumor activity of nivolumab in patients with advanced hepatocellular carcinoma (HCC): CA209-040. J Clin Oncol 33.

160. Chen J, Jiang CC, Jin L, Zhang XD (2016) Regulation of PD-L1: A novel role of pro-survival signalling in cancer. Ann Oncol 27:409-416.

161. Pardoll DM (2012) The blockade of immune checkpoints in cancer immunotherapy. Nat Rev Cancer 12:252-264.

162. Li Y, Li F, Jiang F, Lv X, Zhang R, Lu A, et al (2016) A mini-review for cancer immunotherapy: Molecular understanding of PD-1/ PD-L1 pathway & translational blockade of immune checkpoints. Int J Mol Sci 17:1-23.

163. Tumeh PC, Harview CL, Yearley JH, Shintaku IP, Taylor EJM, Robert L, et al (2014) PD-1 blockade induces responses by inhibiting adaptive immune resistance. Nature 515:568-571.

164. Enwere EK, Kornaga EN, Dean M, Koulis TA, Phan T, Kalantarian M, et al (2017) Expression of PD-L1 and presence of CD8-positive T cells in pre-treatment specimens of locally advanced cervical cancer. Mod Pathol 1:1-10.

165. Sharpe AH, Wherry EJ, Ahmed R, Freeman GJ (2007) The function of programmed cell death 1 and its ligands in regulating autoimmunity and infection. Nat Immunol 8:239-245.

166. Noguchi T, Ward JP, Gubin MM, Arthur CD, Lee SH, Hundal J et al (2017) Temporally Distinct PD-L1 Expression by Tumor and Host Cells Contributes to Immune Escape. Cancer Immunol Res 5:106-117.

167. Romero D (2016) Immunotherapy: PD-1 says goodbye, TIM-3 says hello. Nat Rev Clin Oncol 13:202-203.

168. Koyama S, Akbay EA, Li YY, Herter-Sprie GS, Buczkowski KA, Richards WG, et al (2016) Adaptive resistance to therapeutic PD-1 blockade is associated with upregulation of alternative immune checkpoints. Nat Commun 7:1-9.

169. Zak KM, Kitel R, Przetocka S, Golik P, Guzik K, Musielak B, et al (2015) Structure of the Complex of Human Programmed Death 1, PD-1, and Its Ligand PD-L1. Structure 23:2341-2348.

170. Sabatier R, Finetti P, Mamessier E, Adelaide J, Chaffanet M, Ali HR, et al (2015) Prognostic and predictive value of PDL1 expression in breast cancer. Oncotarget 6:5449-5464.

171. Lin Y-M, Sung W-W, Hsieh M-J, Tsai S-C, Lai H-W, Yang S-M, et al (2015) High PD-L1 expression correlates with metastasis and poor prognosis in oral squamous cell carcinoma. PLoS One 10:1-12.

172. Baptista MZ, Sarian LO, Derchain SFM, Pinto GA, Vassallo J (2016) Prognostic significance of PD-L1 and PD-L2 in breast cancer. Hum Pathol 47:78-84.

173. Schalper KA, Velcheti V, Carvajal D, Wimberly H, Brown J, Pusztai L, et al (2014) *In*

situ tumor PD-L1 mRNA expression is associated with increased TILs and better outcome in breast carcinomas. Clin Cancer Res 20:2773-2782.

174. Schmidt LH, Kümmel A, Görlich D, Mohr M, Bröckling S, Henrik Mikesch J, et al (2015) PD-1 and PD-L1 expression in NSCLC indicate a favorable prognosis in defined subgroups. PLoS One 10:1-15.

175. Lin DY-W, Tanaka Y, Iwasaki M, Gittis AG, Su H-P, Mikami B, et al (2008) The PD-1/PD-L1 complex resembles the antigen-binding Fv domains of antibodies and T cell receptors. Proc Natl Acad Sci USA 105:3011-3016.

176. Li C-W, Lim S-O, Xia W, Lee H-H, Chan L-C, Kuo C-W, et al (2016) Glycosylation and stabilization of programmed death ligand-1 suppresses T-cell activity. Nat Commun 7:12632.

177. Horita H, Law A, Hong S, Middleton K (2017) Identifying Regulatory Posttranslational Modifications of PD-L1: A Focus on Monoubiquitinaton. Neoplasia 19:346-353.

178. Takahashi N, Iwasa S, Sasaki Y, Shoji H, Honma Y, Takashima A, et al (2016) Serum levels of soluble programmed cell death ligand 1 as a prognostic factor on the first-line treatment of metastatic or recurrent gastric cancer. J Cancer Res Clin Oncol 142:1727-1738.

179. Zeng Z, Shi F, Zhou L, Zhang M, Chen Y, Chang X, et al (2011) Upregulation of circulating PD-L1/PD-1 is associated with poor post-cryoablation prognosis in patients with HBV-related hepatocellular carcinoma PLoS One 6:e23621.

180. Zhou J, Mahoney KM, Giobbie-Hurder A, Zhao F, Lee S, Liao X, et al (2017) Soluble PD-L1 as a Biomarker in Malignant Melanoma Treated with Checkpoint Blockade. Cancer Immunol Res 5:480-492.

181. Cheng S, Zheng J, Zhu J, Xie C, Zhang X, Han X, et al (2015) PD-L1 gene polymorphism and high level of plasma soluble PD-L1 protein may be associated with non-small cell lung cancer. Int J Biol Markers 30:e364-e368.

182. Davies LC, Heldring N, Kadri N, Le Blanc K (2016) Mesenchymal Stromal Cell Secretion of Programmed Death-1 Ligands Regulates T Cell Mediated Immunosuppression. Stem Cells 1-11.

183. He XH, Xu LH, Liu Y (2005) Identification of a novel splice variant of human PD-L1 mRNA encoding an isoform-lacking Igv-like domain. Acta Pharmacol Sin 26:462-468.

184. Dezutter-Dambuyant C, Durand I, Alberti L, Bendriss-Vermare N, Valladeau-Guilemond J, Duc A, et al (2016) A novel regulation of PD-1 ligands on mesenchymal stromal cells through MMP-mediated proteolytic cleavage. OncoImmunology 5:e1091146.

185. Schlecker E, Fiegler N, Arnold A, Altevogt P, Rose-John S, Moldenhauer G, et al (2014) Metalloprotease-mediated tumor cell shedding of B7-H6, the ligand of the natural killer

cell-activating receptor NKp30. Cancer Res 74:3429-3440.

186. Möller-Hackbarth K, Dewitz C, Schweigert O, Trad A, Garbers C, Rose-John S, et al (2013) A disintegrin and metalloprotease (ADAM) 10 and ADAM17 are major sheddases of T cell immunoglobulin and mucin domain 3 (Tim-3). J Biol Chem 288:34529-34544.

187. Whiteside TL (2016) Exosomes and tumor-mediated immune suppression. J Clin Invest 126:1216-1223.

188. Mazel M, Jacot W, Pantel K, Bartkowiak K, Topart D, Cayrefourcq L, et al (2015) Frequent expression of PD-L1 on circulating breast cancer cells. Mol Oncol 9:1773-1782.

189. Wu Y, Chen M, Wu P, Chen C, Xu ZP, Gu W (2017) Increased PD-L1 Expression in Breast and Colon Cancer Stem Cells. Clin Exp Pharmacol Physiol 44:602-604.

190. Azmi AS, Bao B, Sarkar FH (2013) Exosomes in cancer development, metastasis, and drug resistance: a comprehensive review. Cancer Metastasis Rev 32:623-642.

Figure 1.1 Domain organization of the PDI family of chaperones.

This figure was created based on the following journal article:

Ellgaard L, Ruddock LW (2005) The human protein disulphide isomerase family: substrate interactions and functional properties. EMBO Rep 6:28-32

Thioredoxin-like domains are shown in green with the active site including the catalytic residues (**a** or **a'** domains). The **b'** domain (purple) is the primary binding site for proteins in their non-native conformations, though binding is not exclusive to this domain. The **b** domain (blue) functions to stabilize the structure. A linker region is shown in gray. Signal sequences are not portrayed. ERp44 lacks a second active-site cysteine residue and thus forms stable mixed disulfides mediating ER retention of its substrates.

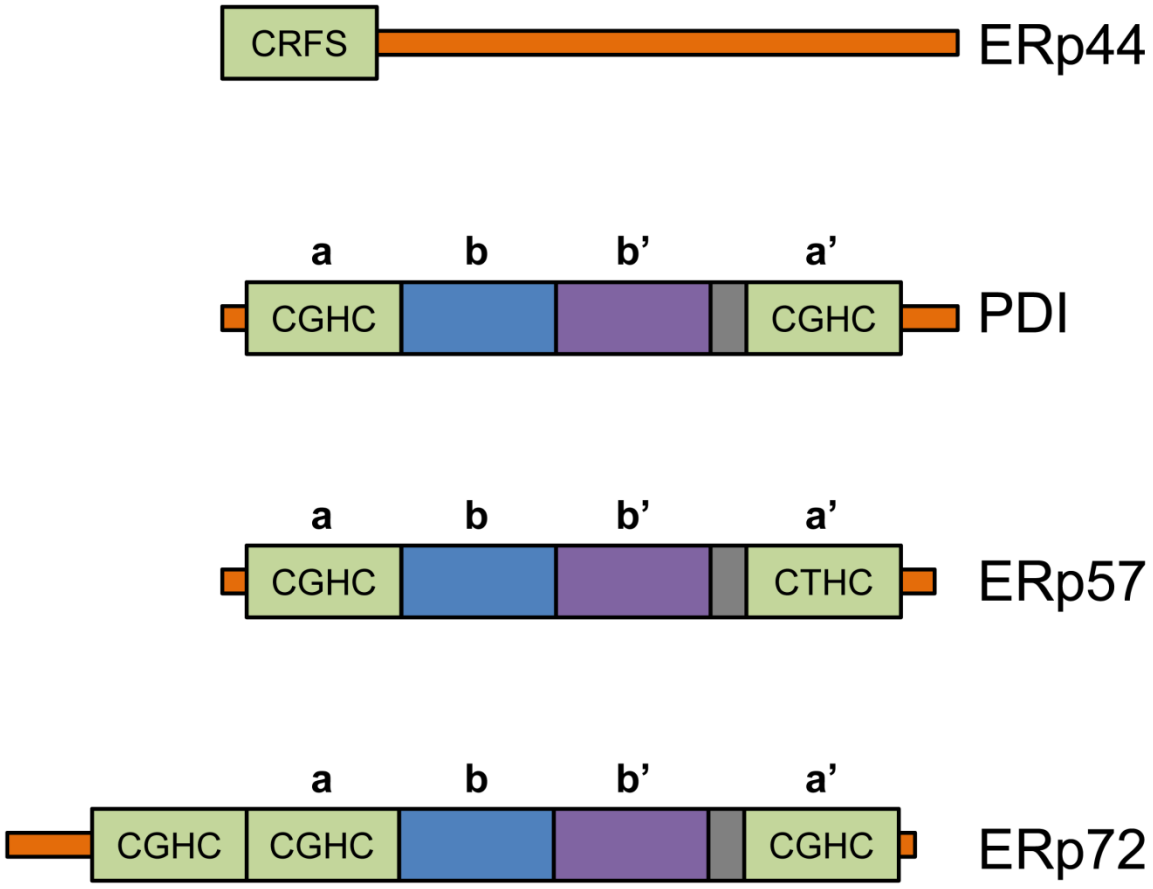

Figure 1.2 The three branches of the Unfolded Protein Response (UPR).

This figure was reproduced from the following journal article:

Walter P, Ron D (2011) The Unfolded Protein Response: From Stress Pathway to Homeostatic Regulation. Science 334:1081-1086. Reprinted with permission from AAAS.

a-c The three UPR signaling pathways sense and transmit information regarding the protein folding conditions in the ER. Each pathway utilizes a different mechanism of signal transduction that activates unique responses.

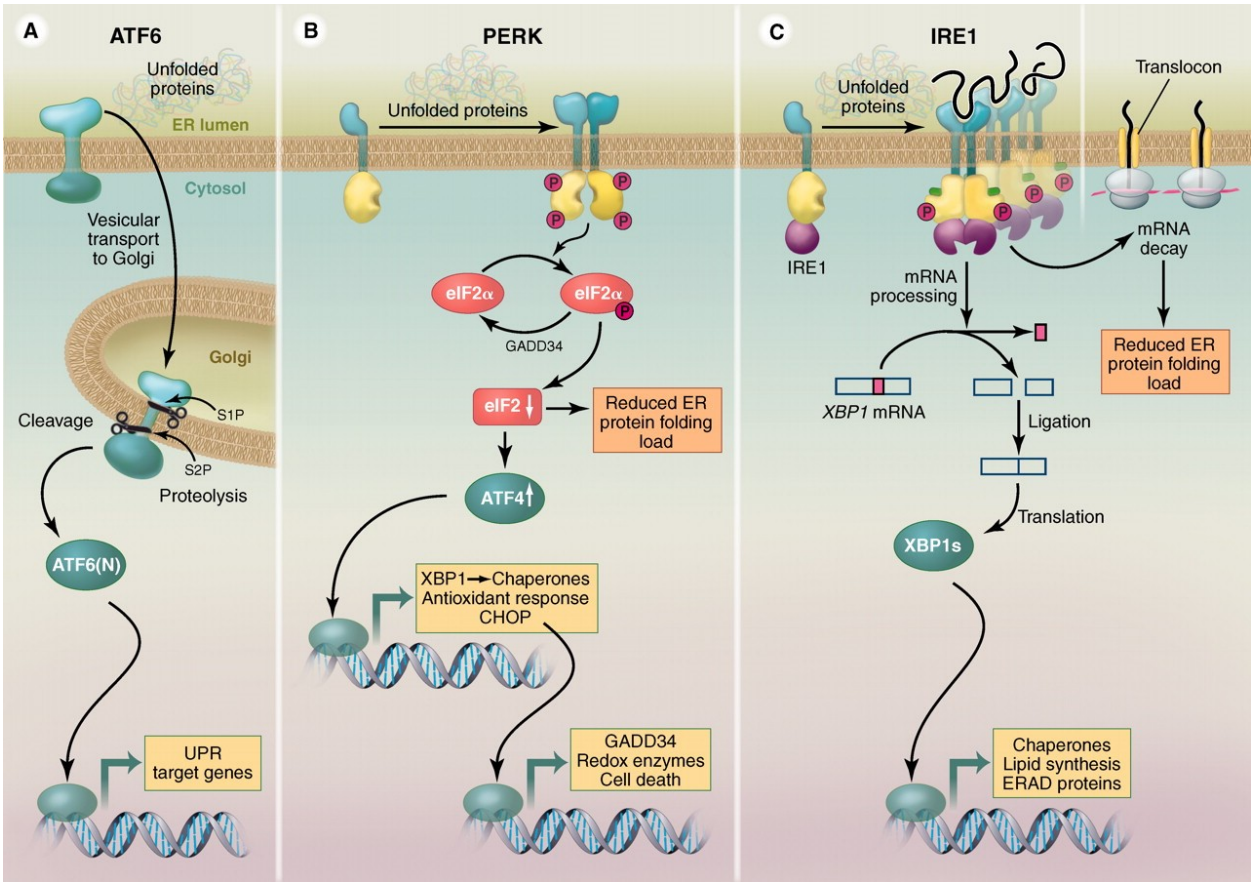

Figure 1.3 Domain organization of ADAM metalloproteases.

This figure is based on a diagram from VASGEN® (http://vasgen.co.uk).

A cartoon diagram of the domain organization of the ADAM family of metalloproteases in an auto-inhibited form is represented below. Pro, Pro-Domain; MP, Metalloprotease Domain; D, Disintegrin Domain; C, Cysteine-Rich Region; EGF-like, EGF-like motif; Cyt, Cytoplasmic tail. The black rectangle indicates the transmembrane domain.

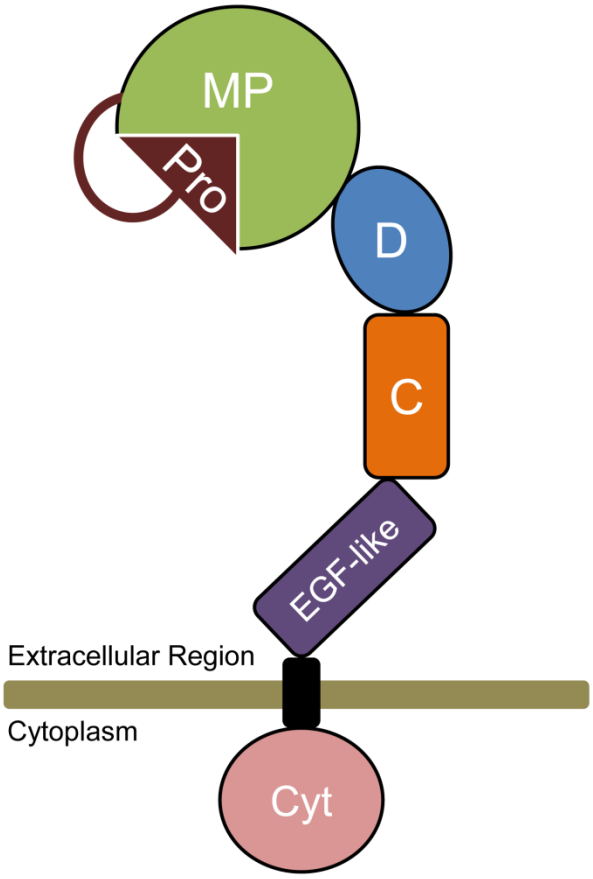

Figure 1.4 PD-L1/PD-1 signaling antagonizes T cell activation.

This figure was reproduced from the following journal article:

Pardoll D (2012) The blockade of immune checkpoints in cancer immunotherapy. Nat Rev Cancer 12:252-264. Reprinted by permission from Macmillan Publishers Ltd. Available at https://www.nature.com.

Activation of T cells in the tumor microenvironment occurs through the interaction between T-cell receptor (TCR) on the T cell and its cognate peptide presented on major histocompatibility complex (MHC) on the tumor cell. Activated T cells upregulate the expression of an immune-checkpoint receptor PD-1. Interaction of PD-1 and its ligand PD-L1 or PD-L2 expressed on the tumor cell inhibits T cell activation. PD-L1 and PD-L2 expression is either driven by oncogenic signaling pathways in tumor cells or is induced in response to pro-inflammatory signals, such as interferon γ. The function of T cell repression by PD-L1/PD-1 is to limit inflammatory responses and prevent collateral damage to tissues.

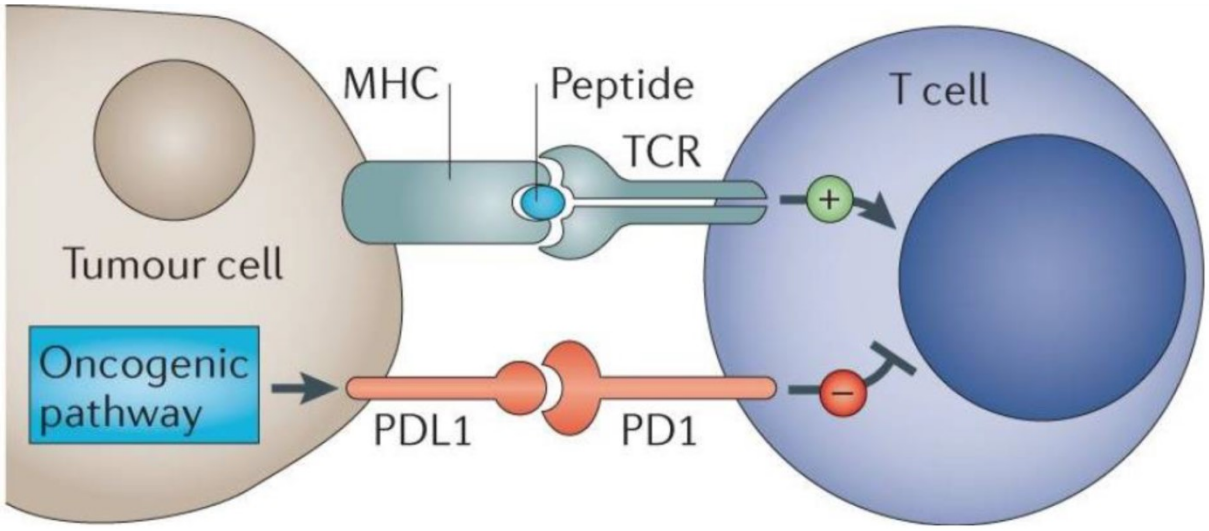

Figure 1.5 Domain organization of PD-L1.

This panel was reproduced from the following journal article by permission of Oxford University Press.

Chen J, Jiang CC, Jin L, Zhang XD (2016) Regulation of PD-L1: a novel role of pro-survival signalling in cancer. Ann Oncol 27:409-416.

The PD-L1 gene contains seven exons, of which exons 2 through 6 are translated into the PD-L1 protein. Exon 1 encodes the 5'UTR, and exon 7 encodes both a portion of the intracellular domain and the 3'UTR. The PD-L1 protein contains two extracellular IgV-like and IgC-like domains, a transmembrane domain, and a C-terminal tail. The extracellular IgV-like domain is responsible for the binding of PD-L1 to PD-1.

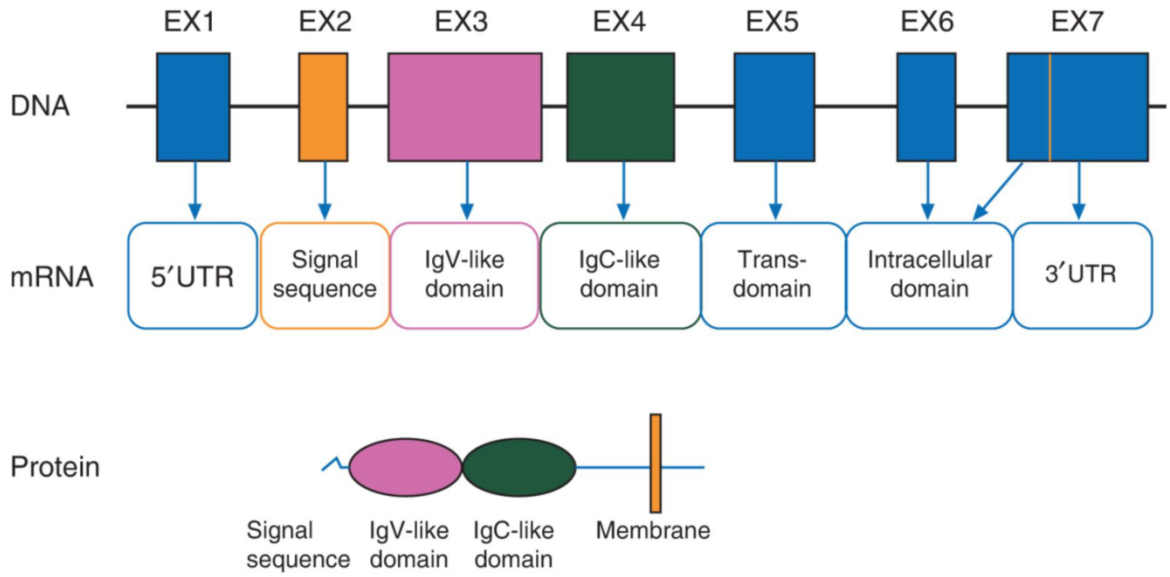

Chapter 2 - Protein disulfide isomerases in the endoplasmic reticulum promote anchorage-independent growth of breast cancer cells

This chapter has been published as the following journal article:

Wise R, Duhachek-Muggy S, Qi Y, Zolkiewski M, Zolkiewska A (2016) Protein disulfide isomerases in the endoplasmic reticulum promote anchorage-independent growth of breast cancer cells. Breast Cancer Res Treat 157: 241-252. The final publication is available at link.springer.com via https://doi.org/10.1007/s10549-016-3820-1.

Abstract

Metastatic breast cancer cells are exposed to stress of detachment from the extracellular matrix (ECM). Cultured breast cancer cells that survive this stress and are capable of anchorage-independent proliferation form mammospheres. The purpose of this study was to explore a link between mammosphere growth, ECM gene expression, and the protein quality control system in the endoplasmic reticulum (ER). We compared the mRNA and protein levels of ER folding factors in SUM159PT and MCF10DCIS.com breast cancer cells grown as mammospheres versus adherent conditions. Publicly available gene expression data for mammospheres formed by primary breast cancer cells and for circulating tumor cells (CTCs) were analyzed to assess the status of ECM/ER folding factor genes in clinically relevant samples. Knock-down of selected protein disulfide isomerase (PDI) family members was performed to examine their roles in SUM159PT mammosphere growth. We found that cells grown as mammospheres had elevated

expression of ECM genes and ER folding quality control genes. CTC gene expression data for an index patient indicated that upregulation of ECM and ER folding factor genes occurred at the time of acquired therapy resistance and disease progression. Knock-down of PDI, ERp44, or ERp57, three members of the PDI family with elevated protein levels in mammospheres, in SUM159PT cells partially inhibited the mammosphere growth. Thus, breast cancer cell survival and growth under detachment conditions require enhanced assistance of the ER protein folding machinery. Targeting ER folding factors, in particular members of the PDI family, may improve the therapeutic outcomes in metastatic breast cancer.

Keywords

Breast cancer, Anoikis, Mammospheres, Endoplasmic reticulum, Extracellular matrix

Introduction

Metastatic breast cancer is initiated by circulating tumor cells (CTCs) that originate from the primary tumor and spread in the body through the blood circulatory system [1, 2]. Early detection and potential targeting of CTCs are of great importance in the effective treatment of metastatic breast cancer [3–5]. CTCs exist as single cells with increased features of epithelial-to-mesenchymal transition (EMT) or as small clusters of 2–50 cells with partial EMT [6, 7]. CTCs are detached from the extracellular matrix (ECM) and, in the case of non-clustered CTCs, they are also devoid of cell–cell interactions typical for epithelial cells. Loss of cell-ECM or cell–cell interactions among a majority of cancer cells induces anoikis, a form of apoptotic cell death [8–10]. To acquire a metastatic potential, CTCs must develop resistance to anoikis [11–13]. The adaptive processes that help CTCs evade anoikis include EMT [14, 15], metabolic changes and antioxidant activity [16–18], activation of receptor tyrosine kinases [19–22], activation of the

NF-κB pathway [23, 24], activation of YAP/TAZ transcription coactivators [25, 26], or increased autophagy [27–30].

ECM is a key component of the local tumor microenvironment and has a major impact on each of the classical hallmarks of cancer [31, 32]. Since ECM deprivation is the primary trigger of anoikis, stimulated secretion of ECM protein components by detached cells, followed by engagement of their integrin receptors should provide prosurvival signals and promote anchorage-independent growth. However, whether increased expression of ECM genes is a general feature of anoikis-resistant breast cancer cells is currently unknown. Also, a specific role of the secretory protein folding machinery during anchorage-independent growth of breast cancer cells has not been established.

Efficient folding of secreted proteins within the endoplasmic reticulum (ER) depends on the function of a complex protein folding machinery that consists of three classes of proteins: molecular chaperones (e.g., the HSP70 class chaperones BiP and GRP-170, and the HSP90-class chaperone GRP-94), foldases (e.g., disulfide isomerases PDI, ERp57, ERp72, and ERp44), and lectins (e.g., calreticulin and calnexin) [33, 34]. ER stress associated with the accumulation of misfolded proteins leads to activation of the unfolded protein response (UPR), which comprises three parallel signaling pathways: PERK, IRE1, and ATF6 [34]. In solid tumors, including breast cancers, an altered metabolism, hypoxic conditions, or signals from the tumor microenvironment, have been shown to induce ER stress, activate the UPR, and lead to increased expression of the ER chaperones [35–38]. Significantly less is known about the status of the UPR and the role of the ER folding machinery during the stage of cancer dissemination via CTCs and the detachment from ECM.

In this study, we found that breast cancer cells grown as mammospheres had elevated expression of a number of ECM genes and ER folding quality control genes. Analysis of a publicly available gene expression data for CTCs in an index patient revealed that upregulation of ECM genes, as well as genes encoding ER folding factors, but not cytoplasmic chaperones, occurred at the time of acquired therapy resistance and disease progression. Despite the elevated expression of ECM and ER folding quality genes during anchorage-independent growth, we did not detect a robust activation of UPR, as only the PERK branch of the UPR, but not IRE1 or ATF6, was activated in mammospheres. An inducible knock-down of PDI, ERp44, or ERp57, three different members of the protein disulfide isomerase family, resulted in reduced mammosphere formation by SUM159PT cells. Collectively, these results suggest that the anchorage-independent growth of breast cancer cells in vitro and anoikis resistance of CTCs in vivo may be associated with an increased flux of secretory proteins through the ER and require an enhanced assistance of the ER folding machinery.

Materials and Methods

Data Mining

mRNA expression data for ECM and ER quality control genes in attached cells and mammospheres formed by primary tumor cells, described in [39], were retrieved from Gene Expression Omnibus (GEO) using the accession number GSE7515. mRNA levels of ECM genes and chaperones in CTCs from a breast cancer patient, described in [6], were retrieved from GEO using the accession number GSE41245.

Additional methods are described in Appendix A.

Results

To investigate the significance of the ECM and ER protein folding machinery during anchorage-independent growth of breast cancer cells, we compared expression levels of several representative ECM genes, ER chaperones, PDI family members, and lectins in cells grown under two different conditions: without cell-ECM or cell-cell interactions and under normal adherent conditions. For the former conditions, single-cell suspensions were plated into ultra-low attachment plates and were incubated in serum-free media (to eliminate the effect of ECM proteins present in the serum). The media were supplemented with essential growth factors and methylcellulose (to prevent cell aggregation). Under these conditions, cells that are anoikis-resistant and survive the initial stress associated with depletion of ECM and cell-cell contacts may proliferate and, over the course of 8–12 days, form mammospheres. Typical mammospheres are composed of ~100–200 cells and reach ~50–100 μm in size [40]. For adherent conditions, cells were plated in tissue culture-treated plates and were incubated with full media containing serum. We utilized two different breast cancer cell lines, SUM159PT and MCF10DCIS.com. The SUM159PT cell line was originally developed from a primary tumor in a patient with estrogen receptor-negative, progesterone receptor-negative, and HER2-negative anaplastic carcinoma of the breast [41]. SUM159PT cells are highly invasive and tumorigenic [42]. The MCF10DCIS.com cell line was derived from a tumor originating from xenografting premalignant MCF10AT cells into severe combined immunodeficient mice [43]. MCF10DCIS.com cells are estrogen receptor/progesterone receptor/HER2 negative, and they form comedo-type ductal carcinoma in situ after injection into mouse mammary glands [42]. Both SUM159PT cells and MCF10DCIS.com cells form mammospheres with a relatively high efficiency (Fig. 2.1a; [44]).

First, using qRT-PCR, we determined that expression levels of several ECM genes: collagen alpha-1(III) chain (*COL3A1*), collagen alpha-2(VI) chain (*COL6A2*), laminin subunit β-1 (*LAMB1*), and fibronectin (*FN1*) were ~5–1,600-fold higher in mammospheres than in adherent SUM159PT and MCF10DCIS.com cells (Fig. 2.1b), although the extent of upregulation of the ECM transcripts differed between the two cell lines. Second, our analysis of a publicly available gene expression dataset obtained for primary cells isolated from breast tumors (GSE7515, available at http://www.ncbi.nlm.nih.gov/geo/) [39] revealed that expression of *COL3A1*, *COL6A2*, *LAMB1*, and *FN1* (Fig. 2.1c) and many other ECM genes (Appendix A: Supplementary Table 3) was significantly higher in mammospheres grown in suspension than in bulk tumors. Among 87 genes encoding collagens, common glycoproteins, and proteoglycans [45] that were differentially expressed between mammospheres and adherent conditions, expression of 57 genes was significantly upregulated in mammospheres (Appendix A: Supplementary Table 3). These results suggested that an increased expression of ECM genes might be a general feature of breast cancer cells grown as mammospheres, which in turn might lead to an increased demand for upregulation of the ER folding machinery.

To begin testing this hypothesis, we compared expression levels of selected ER chaperones and folding factors in cells grown as mammospheres versus adherent conditions. The investigated ER chaperones included BiP, GRP-94, and GRP-170; the foldase/PDI family was represented by PDI, ERp44, ERp57, and ERp72; and the tested lectins were calnexin and calreticulin. Using qRT-PCR, we determined that mRNA levels of *PDI*, *ERp44*, and *ERp57* were significantly higher in mammospheres than in adherent SUM159PT and MCF10DCIS.com cells (Fig. 2.1d). In the lectin family, *Calnexin* mRNA was significantly higher in mammospheres than in adherent SUM159PT cells, but this effect was not replicated in MCF10DCIS.com cells.

Among molecular chaperones, *GRP-94* mRNA was elevated in mammospheres formed by MCF10DCIS.com cells, but not in SUM159PT cells. Furthermore, mRNA expression levels of several ER folding factors were significantly elevated in mammospheres formed by primary breast cancer cells, as compared to bulk tumors (Fig. 2.1e) [39]. To extend our in vitro analysis into breast tumors in vivo and to determine whether our findings might have a translational relevance, we examined a publicly available dataset containing gene expression profiles of CTCs from an index breast cancer patient undergoing anti-cancer treatment (GSE41245, available at http://www.ncbi.nlm. nih.gov/geo/) [6]. This patient was diagnosed with estrogen receptor-positive/progesterone receptor-positive lobular carcinoma and was treated for 7 months with inhibitors targeting phosphatidylinositol 3-kinase (PI3K) and MAP kinase kinase (MEK). Initially, the patient responded well to the treatment regimen. Three serial blood specimens were obtained during this time period, CTCs were captured from blood using a microfluidic chip, and RNA sequencing (RNA-seq) was performed to analyze the global gene expression during this initial treatment (Fig. 2.1f, columns 1–3, designated as ‘‘R’’). After 7 months, the patient showed disease progression (Fig. 2.1f, column 4, ‘‘P’’), which was accompanied by an increase in CTCs and the appearance of multicellular CTC clusters. After the treatment regimen was switched to adriamycin chemotherapy, the patient showed a transient response (Fig. 2.1f, column 5, ‘‘R’’). Blood samples from 10 healthy donors were used as controls (Fig. 2.1f, columns 6–15).

As noted previously [6], the expression levels of many ECM genes, including *COL3A1*, *COL6A2*, *LAMB1*, and *FN1*, were strongly upregulated in CTCs at the time of disease progression and an acquired resistance to PI3Kand MEK-targeted therapy (Fig. 2.1f). Strikingly, the expression levels of several ER folding factors, including *ERp57* (gene name *PDIA3*), *PDI* (*P4HB*), *BiP* (*HSPA5*), *GRP-94* (*HSP90B1*), and *GRP-170* (*HYOU1*) also surged at the same

time point (Fig. 2.1f). In contrast, the expression levels of cytoplasmic chaperones such as *HSP70* (*HSPA1A* and *HSPA1B*), *HSP90* (*HSP90AA1*), and *HSP110* (*HSPH1*) did not increase during the time of disease progression (Fig. 2.1f). These data underscore essential differences between the expression patterns of the ER protein folding factors versus those in the cytoplasm in CTCs, corroborate our results obtained for mammospheres, and highlight an important role of the ER folding machinery in CTCs during breast cancer progression.

Importantly, a trend of increased expression of the ER folding machinery during anchorage-independent growth of breast cancer cells was also detected at the protein level. We observed that the abundance of PDI, ERp44, ERp57, calnexin, and calreticulin was higher in mammospheres than in adherent cells for both cell lines (Fig. 2.2). We concluded that the members of the ER folding machinery that were the most consistently upregulated at both the mRNA and protein levels upon the anchorage-independent growth of SUM159PT and MCF10DCIS.com cells were PDI, ERp44, and ERp57, and these three proteins became the focus of our subsequent investigations.

We asked whether elevated mRNA and protein levels of PDI, ERp44, and ERp57 might be associated with the activation of the UPR in mammospheres. Using Western blot analysis of total cell lysates, we observed that the mobility of PERK was reduced in lysates prepared from SUM159PT or MCF10DCIS.com mammospheres, as compared to adherent cells (Fig. 2.3a), suggesting that PERK might have been phosphorylated and activated during anchorage-independent growth. Moreover, Western blot analysis of phosphorylated eIF2α, a downstream effector of PERK, revealed an increase of p-eIF2α in mammospheres versus adherent cells in both SUM159PT and MCF10DCIS.com cell lines (Fig. 2.3a). In contrast, we did not detect *XBP1* mRNA splicing (a downstream effector of IRE1; Fig. 2.3b) or activation of an ATF6

reporter (Fig. 2.3c) in mammospheres. Both *XBP1* mRNA splicing and the ATF6 reporter were strongly upregulated by tunicamycin, a well-known UPR inducer, validating our assays (Fig. 2.3b, c). These results indicated a lack of robust UPR during anchorage-independent growth of SUM159PT and MCF10DCIS.com cells.

Next, we asked whether PDI, ERp44, and ERp57 might actively support the anchorage-independent cell growth and mammosphere formation. We established a stable knockdown of PDI, ERp44, or ERp57 in SUM159PT cells using a doxycycline-inducible TRIPZ lentiviral shRNA vector [46]. This vector produces tightly regulated induction of shRNA expression together with turbo red fluorescent protein (tRFP) in the presence of doxycycline (Fig. 2.4a). SUM159PT cells stably transduced with the vector containing one of two different shRNAs (#1 and #2) targeting PDI, ERp44, or ERp57, or a non-targeting shControl, were selected with puromycin. Upon treatment of cells for 4 days with 1 μg/ml of doxycycline, the levels of PDI, ERp44, or ERp57 were reduced by at least 90% in adherent SUM159PT cells (Fig. 2.4b).Induction of shRNA expression in mammospheres could be readily monitored by visualizing the induction of tRFP (Fig. 2.4c, Appendix A: Supplementary Fig. 1). Western blotting confirmed that PDI, ERp44, and ERp57 knock-downs were maintained in SUM159PT cells grown as mammospheres (Fig. 2.4d). Importantly, a loss of expression of any one of these three members of the PDI family was not compensated for by an increased expression of the other two investigated family members (Fig. 2.4d).

We determined that PDI, ERp44, or ERp57 knock-down did not have significant effects on the growth of SUM159PT cells under adherent conditions (Fig. 2.5a). However, in contrast to adherent cells, the established knock-downs significantly impaired the growth of SUM159PT mammospheres. The total volume of mammospheres formed by shPDI, shERp44, or shERp57

cells after 10 days of culture in the presence of doxycycline was significantly lower than the volume of mammospheres formed by the same cells in the absence of doxycycline (Fig. 2.5b). Doxycycline treatment did not affect the volume of mammospheres formed by shControl cells. In our calculations, we included all spheres with diameter >15 μm. This size cut-off was lower than typically used during mammosphere counting (50 μm, [47]) to account for a broad range of spheres, containing both rapidly and slowly proliferating cells.

We next determined whether the reduction in total mammosphere volumes after PDI, ERp44, or ERp57 knock-down was due to a decreased likelihood of sphere formation (i.e., mammosphere numbers) or to a slower sphere growth (i.e., mammosphere size). First, we observed that while the total numbers of mammospheres were not significantly changed after shPDI, shERp44, or shERp57 knock-down, there was a statistically significant decrease in the numbers of large spheres (>50 μm) formed by shPDI, shERp44, or shERp57 cells in the presence of doxycycline (Fig. 2.6a). Second, when shRNA-expressing, doxycycline-treated mammospheres were directly visualized by tRFP fluorescence, the mean diameter of shPDI-, shERp44-, or shERp57-expressing spheres was significantly lower than the mean diameter of shControl spheres, indicating an impact on the growth of these spheres (Fig. 2.6b). Altogether these results suggest that the three tested PDI family members do not impact the formation of mammospheres, but they play important roles in promoting anchorage-independent growth of SUM159PT cells.

Discussion

The propensity for anchorage-independent growth is a common feature of transformed cells in solid tumors. Anchorage-independent growth requires that cells not only survive under detachment conditions, but that they also actively proliferate under the stress associated with

matrix deprivation. The mammosphere assay, which measures anchorage-independent proliferation at clonal cell densities in serum-free media in the presence of well-defined growth factors, is well suited for evaluating the capacity of cells to survive and divide without exogenous ECM support. Mammosphere formation has been also associated with the presence of mammary stem cells and cancer stem-like cells, as these cell populations have increased anoikis resistance [40]. In the current study, mammospheres were formed by claudin-low SUM159PT cells, which have low levels of claudins, an important component of tight junctions. As such, it is likely that these mammospheres were held together by certain adhesion proteins that are upregulated in mesenchymal cells, such as N-cadherin, or interactions between integrins and ECM secreted from the mammospheres. Our results obtained for two different breast cancer cell lines, as well as the results obtained by others for primary breast tumor cells [39], indicate that mammosphere formation and growth are associated with upregulation of ECM gene expression, and this effect correlates with an increased expression of several ER folding factors, in particular those from the PDI family (see Figs. 2.1d, e, 2.2). Exosome secretion and uptake may contribute to the phenotype observed, but it is unlikely that the effects of knockdown of the ER folding factors are directly due to a change in the exosome composition of mammosphere cells

The human PDI family consists of more than 20 members, which differ in the domain arrangement and their abilities to oxidize, reduce, or isomerize disulfide bonds in proteins [33, 48]. While there is a large degree of functional redundancy between PDIs, some family members play more specialized functions [49–52]. Our results indicate that among the oxidoreductases, PDI, ERp44, and ERp57 are consistently elevated in mammospheres, suggesting a broad but specialized activation of the PDI family during anchorage-independent growth of breast cancer cells. Furthermore, downregulation of expression of PDI, ERp44, or ERp57 in SUM159PT cells

partially inhibits mammosphere growth (see Figs. 2.5, 2.6), suggesting that each of these PDI family members plays an important and non-redundant role during anchorage-independent cell proliferation. What mechanisms are responsible for the observed elevated levels of selected ER folding factors during mammosphere growth (see Figs. 2.1d, e, 2.2)? One possible explanation might be that an increased secretion of ECM proteins leads to ER stress, activation of the UPR, and transcriptional upregulation of ER folding factors. However, this scenario is not readily reconciled with our data, which indicate that only the PERK branch of the UPR, but not IRE1 or ATF6, was activated in mammospheres (see Fig. 2.3). Previous studies demonstrated that ATF6 and/or IRE1, but not PERK alone play a critical role in the induction of major ER chaperones during the UPR [53–55]. Thus, the lack of IRE1 or ATF6 activation (see Fig. 2.3) argues against a robust UPR in mammospheres and cannot account for the observed increased mRNA and protein levels shown in Figs. 2.1d, 2.2. Another explanation for the elevated mRNA and protein levels of selected ER folding factors in mammospheres might be a gradual selection of cells with high expression levels of those genes during anchorage-independent growth. Such cells would have a selective advantage in responding to dramatically increased demands for efficient folding of ECM proteins and an increased likelihood of survival. As such, it would be beneficial to compare the expression of various folding factors discussed in this paper for larger spheres and smaller spheres, rather than analyzing all mammosphere sizes together. It is possible that larger spheres could have a selective advantage for growth, possibly due to the increased presence of these folding factors compared to smaller spheres.

EMT is a key regulator of breast tumor progression, as it promotes anoikis resistance, expansion of cancer stem cell subpopulations, metastatic potential, drug resistance, and disease recurrence [14, 56–59]. The EMT gene signature of human mammary epithelial cells (HMLE)

partially overlaps with the ECM signature [60], and the hallmark EMT gene set at MolSigDB (http://www.broadinstitute.org/gsea/msigdb/) contains many genes of secreted proteins. Not surprisingly, a recent study demonstrated that HMLE cells induced to undergo EMT synthesize and secrete large quantities of ECM proteins [61]. Consistent with their increased secretory output and a higher ER load, HMLE EMT cells were more sensitive to perturbations of the ER function. For example, downregulation of BiP expression, a major ER chaperone of the HSP70 family, in HMLE EMT, but not the parental cells, decreased cell survival and caused a significant reduction of cell growth [61].

Our results suggest that the functions of PDIs, and possibly other components of the ER quality control system, in detached cells extend beyond their role in supporting the secretory phenotype of EMT. Firstly, the two breast cancer lines used in our study, MCF10DCIS.com and SUM159PT, are of the basal/claudin-low subtype [62, 63] and they already express phenotypic and molecular features associated with EMT. Yet, these cells further upregulate expression (or select for elevated expression) of ER folding factors upon anchorage-independent growth. Secondly, a knock-down of PDI, ERp44, or ERp57 does not affect the proliferation of attached cells in 2D, but it impairs the anchorage-independent growth of mammospheres. Thus, PDI, ERp44, ERp57, and possibly other PDI family members, help resolve the demand for enhanced ER folding capacity during anchorage-independent growth of cancer cells.

Additional insight into the role of ER folding factors in breast cancer progression, as well as validation of our in vitro results, comes from our analysis of the gene expression profiling of CTCs present in the bloodstream of an index breast cancer patient at different time points during the disease progression (see Fig. 2.1f; [6]). In this patient with metastatic breast cancer, disease progression correlated with upregulation of a number of ER folding factors. While the original

report highlighted the upregulation of many EMT genes at the time point of disease progression, the gene set enrichment analysis (GSEA) identified the ECM module as the most significantly enriched among the 170 genes upregulated at that time point [6]. The disease progression was accompanied not only by an increased number of CTCs, but also by the appearance of multicellular CTC clusters [6]. The presence of CTC clusters might have been facilitated, in part, by increased production of ECM proteins, increased proliferation of single CTCs, or both. While it is generally believed that CTCs are quiescent and reside at the G0 phase of the cell cycle [64–66], CTCs may actually represent a more heterogeneous population with regard to the degree of proliferation [67]. Intriguingly, the mRNA levels of Ki-67 and cyclin D3, an important regulator of the G1/S transition during the cell cycle, also increase in CTCs at the time of disease progression in the patient dataset shown in Fig. 2.1f, together with ECM genes and ER folding factors [6]. We propose, therefore, that the disease progression in this patient might have marked an exit of CTCs from quiescence and initiation of their proliferation. However, more studies involving larger patient populations, with serial isolations of CTCs, are needed to further validate the apparent correlation between increased expression of ECM and ER quality control genes, disease progression, and enhanced CTC proliferation. Furthermore, to directly test a role of ER quality control genes in metastasis, the mammosphere-based model of anoikis resistance utilized in the current study should be extended into in vivo approaches, such as experimental metastasis assay employing mouse tail vein injection of breast cancer cells with downregulated expression of ER quality control genes. Given the critical role of CTCs in breast cancer metastasis, better understanding of the mechanisms controlling anoikis resistance of cultured cancer cells and CTC survival in vivo should remain a high priority in the field.

Acknowledgements

This work was supported by NIH grant R01CA172222 to AZ and Innovative Research Award from Terry C. Johnson Center for Basic Cancer Research at KSU to MZ. This is contribution 15-424-J from Kansas Agricultural Experiment Station.

Disclosure of potential conflict of interest

The authors declare no conflicts of interest.

References

1. Joosse SA, Gorges TM, Pantel K (2015) Biology, detection, and clinical implications of circulating tumor cells. EMBO Mol Med 7:1-11. doi:10.15252/emmm.201303698

2. Yu M, Stott S, Toner M, Maheswaran S, Haber DA (2011) Circulating tumor cells: approaches to isolation and characterization. J Cell Biol 192:373-382. doi:10.1083/jcb.201010021

3. McInnes LM, Jacobson N, Redfern A, Dowling A, Thompson EW, Saunders CM (2015) Clinical implications of circulating tumor cells of breast cancer patients: role of epithelial-mesenchymal plasticity. Front Oncol 5:42. doi:10.3389/fonc.2015.00042

4. Yap TA, Lorente D, Omlin A, Olmos D, de Bono JS (2014) Circulating tumor cells: a multifunctional biomarker. Clin Cancer Res 20:2553-2568. doi:10.1158/1078-0432.CCR-13-2664

5. Haber DA, Velculescu VE (2014) Blood-based analyses of cancer: circulating tumor cells and circulating tumor DNA. Cancer Discov 4:650-661. doi:10.1158/2159-8290.CD-13-1014

6. Yu M, Bardia A, Wittner BS, Stott SL, Smas ME, Ting DT, Isakoff SJ, Ciciliano JC, Wells MN, Shah AM, Concannon KF, Donaldson MC, Sequist LV, Brachtel E, Sgroi D, Baselga J, Ramaswamy S, Toner M, Haber DA, Maheswaran S (2013) Circulating breast tumor cells exhibit dynamic changes in epithelial and mesenchymal composition. Science 339:580-584. doi:10.1126/science.1228522

7. Aceto N, Bardia A, Miyamoto DT, Donaldson MC, Wittner BS, Spencer JA, Yu M, Pely A, Engstrom A, Zhu H, Brannigan BW, Kapur R, Stott SL, Shioda T, Ramaswamy S, Ting DT, Lin CP, Toner M, Haber DA, Maheswaran S (2014) Circulating tumor cell clusters are oligoclonal precursors of breast cancer metastasis. Cell 158:1110-1122. doi:10.1016/j.cell.2014.07.013

8. Buchheit CL, Weigel KJ, Schafer ZT (2014) Cancer cell survival during detachment from the ECM: multiple barriers to tumour progression. Nature Rev Cancer 14:632-641. doi:10.1038/nrc3789

9. Reginato MJ, Mills KR, Paulus JK, Lynch DK, Sgroi DC, Debnath J, Muthuswamy SK, Brugge JS (2003) Integrins and EGFR coordinately regulate the pro-apoptotic protein Bim to prevent anoikis. Nat Cell Biol 5:733-740. doi:10.1038/ncb1026

10. Buchheit CL, Rayavarapu RR, Schafer ZT (2012) The regulation of cancer cell death and metabolism by extracellular matrix attachment. Semin Cell Dev Biol 23:402-411. doi:10.1016/j.semcdb.2012.04.007

11. Nagaprashantha LD, Vatsyayan R, Lelsani PC, Awasthi S, Singhal SS (2011) The sensors and regulators of cell-matrix surveillance in anoikis resistance of tumors. Int J Cancer 128:743-752. doi:10.1002/ijc.25725

12. Taddei ML, Giannoni E, Fiaschi T, Chiarugi P (2012) Anoikis: an emerging hallmark in health and diseases. J Pathol 226:380-393. doi:10.1002/path.3000

13. Horbinski C, Mojesky C, Kyprianou N (2010) Live free or die: tales of homeless (cells) in cancer. Am J Pathol 177:1044-1052. doi:10.2353/ajpath.2010.091270

14. Frisch SM, Schaller M, Cieply B (2013) Mechanisms that link the oncogenic epithelial-mesenchymal transition to suppression of anoikis. J Cell Sci 126:21-29. doi:10.1242/jcs.120907

15. Thiery JP, Lim CT (2013) Tumor dissemination: an EMT affair. Cancer Cell 23:272-273. doi:10.1016/j.ccr.2013.03.004

16. Schafer ZT, Grassian AR, Song L, Jiang Z, Gerhart-Hines Z, Irie HY, Gao S, Puigserver P, Brugge JS (2009) Antioxidant and oncogene rescue of metabolic defects caused by loss of matrix attachment. Nature 461:109-113. doi:10.1038/nature08268

17. Grassian AR, Metallo CM, Coloff JL, Stephanopoulos G, Brugge JS (2011) Erk regulation of pyruvate dehydrogenase flux through PDK4 modulates cell proliferation. Genes Dev 25:1716-1733. doi:10.1101/gad.16771811

18. Grassian AR, Coloff JL, Brugge JS (2011) Extracellular matrix regulation of metabolism and implications for tumorigenesis. Cold Spring Harbor Symp Quantit Biol 76:313-324. doi:10.1101/sqb.2011.76.010967

19. Whelan KA, Schwab LP, Karakashev SV, Franchetti L, Johannes GJ, Seagroves TN, Reginato MJ (2013) The oncogene HER2/neu (ERBB2) requires the hypoxia-inducible factor HIF-1 for mammary tumor growth and anoikis resistance. J Biol Chem 288:15865-15877. doi:10.1074/jbc.M112.426999

20. Douma S, Van Laar T, Zevenhoven J, Meuwissen R, Van Garderen E, Peeper DS (2004) Suppression of anoikis and induction of metastasis by the neurotrophic receptor TrkB. Nature 430:1034-1039. doi:10.1038/nature02765

21. Grassian AR, Schafer ZT, Brugge JS (2011) ErbB2 stabilizes epidermal growth factor receptor (EGFR) expression via Erk and Sprouty2 in extracellular matrix-detached cells. J Biol Chem 286:79-90. doi:10.1074/jbc.M110.169821

22. Muthuswamy SK, Li D, Lelievre S, Bissell MJ, Brugge JS (2001) ErbB2, but not ErbB1, reinitiates proliferation and induces luminal repopulation in epithelial acini. Nat Cell Biol 3:785-792. doi:10.1038/ncb0901-785

23. Toruner M, Fernandez-Zapico M, Sha JJ, Pham L, Urrutia R, Egan LJ (2006) Antianoikis effect of nuclear factor-kappaB through up-regulated expression of osteoprotegerin, BCL-2, and IAP-1. J Biol Chem 281:8686-8696. doi:10.1074/jbc.M512178200

24. Park SH, Riley P, Frisch SM (2013) Regulation of anoikis by deleted in breast cancer-1 (DBC1) through NF-kappaB. Apoptosis 18:949-962. doi:10.1007/s10495-013-0847-1

25. Vigneron AM, Ludwig RL, Vousden KH (2010) Cytoplasmic ASPP1 inhibits apoptosis through the control of YAP. Genes Dev 24:2430-2439. doi:10.1101/gad.1954310

26. Zhao B, Li L, Wang L, Wang CY, Yu J, Guan KL (2012) Cell detachment activates the Hippo pathway via cytoskeleton reorganization to induce anoikis. Genes Dev 26:54-68. doi:10.1101/gad.173435.111

27. Kenific CM, Debnath J (2015) Cellular and metabolic functions for autophagy in cancer cells. Trends Cell Biol 25:37-45. doi:10.1016/j.tcb.2014.09.001

28. Avivar-Valderas A, Salas E, Bobrovnikova-Marjon E, Diehl JA, Nagi C, Debnath J, Aguirre-Ghiso JA (2011) PERK integrates autophagy and oxidative stress responses to promote survival during extracellular matrix detachment. Mol Cell Biol 31:3616-3629. doi:10.1128/MCB.05164-11

29. Avivar-Valderas A, Bobrovnikova-Marjon E, Alan Diehl J, Bardeesy N, Debnath J, Aguirre-Ghiso JA (2013) Regulation of autophagy during ECM detachment is linked to a selective inhibition of mTORC1 by PERK. Oncogene 32:4932-4940. doi:10.1038/onc.2012.512

30. Debnath J (2008) Detachment-induced autophagy during anoikis and lumen formation in epithelial acini. Autophagy 4:351-353

31. Lu P, Weaver VM, Werb Z (2012) The extracellular matrix: a dynamic niche in cancer progression. J Cell Biol 196:395-406. doi:10.1083/jcb.201102147

32. Pickup MW, Mouw JK, Weaver VM (2014) The extracellular matrix modulates the hallmarks of cancer. EMBO Rep 15:1243-1253. doi:10.15252/embr.201439246

33. Rutkevich LA, Williams DB (2011) Participation of lectin chaperones and thiol oxidoreductases in protein folding within the endoplasmic reticulum. Curr Opin Cell Biol 23:157-166. doi:10.1016/j.ceb.2010.10.011

34. Schroder M, Kaufman RJ (2005) The mammalian unfolded protein response. Annu Rev Biochem 74:739-789. doi:10.1146/annurev.biochem.73.011303.074134

35. Wang M, Kaufman RJ (2014) The impact of the endoplasmic reticulum protein-folding environment on cancer development. Nature Rev Cancer 14:581-597. doi:10.1038/nrc3800

36. Gutierrez T, Simmen T (2014) Endoplasmic reticulum chaperones and oxidoreductases: critical regulators of tumor cell survival and immunorecognition. Front Oncol 4:291. doi:10.3389/fonc.2014.00291

37. Luo B, Lee AS (2013) The critical roles of endoplasmic reticulum chaperones and unfolded protein response in tumorigenesis and anticancer therapies. Oncogene 32:805-818. doi:10.1038/onc.2012.130

38. Clarke R, Cook KL, Hu R, Facey CO, Tavassoly I, Schwartz JL, Baumann WT, Tyson JJ, Xuan J, Wang Y, Warri A, Shajahan AN (2012) Endoplasmic reticulum stress, the unfolded protein response, autophagy, and the integrated regulation of breast cancer cell fate. Cancer Res 72:1321-1331. doi:10.1158/0008-5472.CAN-11-3213

39. Creighton CJ, Li X, Landis M, Dixon JM, Neumeister VM, Sjolund A, Rimm DL, Wong H, Rodriguez A, Herschkowitz JI, Fan C, Zhang X, He X, Pavlick A, Gutierrez MC, Renshaw L, Larionov AA, Faratian D, Hilsenbeck SG, Perou CM, Lewis MT, Rosen JM, Chang JC (2009) Residual breast cancers after conventional therapy display mesenchymal as well as tumor-initiating features. Proc Natl Acad Sci USA 106:13820-13825. doi:0905718106 [pii]10.1073/pnas.0905718106

40. Dontu G, Abdallah WM, Foley JM, Jackson KW, Clarke MF, Kawamura MJ, Wicha MS (2003) In vitro propagation and transcriptional profiling of human mammary stem/progenitor cells. Genes Dev 17:1253-1270. doi:10.1101/gad.106180317/10/1253 [pii]

41. Flanagan L, Van Weelden K, Ammerman C, Ethier SP, Welsh J (1999) SUM-159PT cells: a novel estrogen independent human breast cancer model system. Breast Cancer Res Treat 58:193-204

42. Barnabas N, Cohen D (2013) Phenotypic and molecular characterization of MCF10DCIS and SUM breast cancer cell lines. Int J Breast Cancer 2013:872743. doi:10.1155/2013/872743

43. Miller FR, Santner SJ, Tait L, Dawson PJ (2000) MCF10DCIS.com xenograft model of human comedo ductal carcinoma *in situ*. J Natl Cancer Inst 92:1185-1186

44. Li H, Duhachek-Muggy S, Dubnicka S, Zolkiewska A (2013) Metalloproteinase-disintegrin ADAM12 is associated with a breast tumor-initiating cell phenotype. Breast Cancer Res Treat 139:691-703. doi:10.1007/s10549-013-2602-2

45. Hynes RO, Naba A (2012) Overview of the matrisome--an inventory of extracellular matrix constituents and functions. Cold Spring Harb Perspect Biol 4:a004903. doi:10.1101/cshperspect.a004903

46. Silva JM, Li MZ, Chang K, Ge W, Golding MC, Rickles RJ, Siolas D, Hu G, Paddison PJ, Schlabach MR, Sheth N, Bradshaw J, Burchard J, Kulkarni A, Cavet G, Sachidanandam R, McCombie WR, Cleary MA, Elledge SJ, Hannon GJ (2005) Second-generation shRNA libraries covering the mouse and human genomes. Nat Genet 37:1281-1288. doi:10.1038/ng1650

47. Shaw FL, Harrison H, Spence K, Ablett MP, Simoes BM, Farnie G, Clarke RB (2012) A detailed mammosphere assay protocol for the quantification of breast stem cell activity. J Mammary Gland Biol Neoplasia 17:111-117. doi:10.1007/s10911-012-9255-3

48. Feige MJ, Hendershot LM (2011) Disulfide bonds in ER protein folding and homeostasis. Curr Opin Cell Biol 23:167-175. doi:10.1016/j.ceb.2010.10.012

49. Solda T, Garbi N, Hammerling GJ, Molinari M (2006) Consequences of ERp57 deletion on oxidative folding of obligate and facultative clients of the calnexin cycle. J Biol Chem 281:6219-6226. doi:10.1074/jbc.M513595200

50. Rutkevich LA, Cohen-Doyle MF, Brockmeier U, Williams DB (2010) Functional relationship between protein disulfide isomerase family members during the oxidative folding of human secretory proteins. Mol Biol Cell 21:3093-3105. doi:10.1091/mbc.E10-04-0356

51. Anelli T, Sannino S, Sitia R (2015) Proteostasis and "redoxtasis" in the secretory pathway: Tales of tails from ERp44 and immunoglobulins. Free Radic Biol Med 83:323-330. doi:10.1016/j.freeradbiomed.2015.02.020

52. Sannino S, Anelli T, Cortini M, Masui S, Degano M, Fagioli C, Inaba K, Sitia R (2014) Progressive quality control of secretory proteins in the early secretory compartment by ERp44. J Cell Sci 127:4260-4269. doi:10.1242/jcs.153239

53. Yamamoto K, Sato T, Matsui T, Sato M, Okada T, Yoshida H, Harada A, Mori K (2007) Transcriptional induction of mammalian ER quality control proteins is mediated by single or combined action of ATF6alpha and XBP1. Dev Cell 13:365-376. doi:10.1016/j.devcel.2007.07.018

54. Shoulders MD, Ryno LM, Genereux JC, Moresco JJ, Tu PG, Wu C, Yates JR, Su AI, Kelly JW, Wiseman RL (2013) Stress-independent activation of XBP1s and/or ATF6 reveals three functionally diverse ER proteostasis environments. Cell Rep 3:1279-1292. doi:10.1016/j.celrep.2013.03.024

55. Lu PD, Jousse C, Marciniak SJ, Zhang Y, Novoa I, Scheuner D, Kaufman RJ, Ron D, Harding HP (2004) Cytoprotection by pre-emptive conditional phosphorylation of translation initiation factor 2. EMBO J 23:169-179. doi:10.1038/sj.emboj.7600030

56. Brabletz T (2012) To differentiate or not--routes towards metastasis. Nature Rev Cancer 12:425-436. doi:10.1038/nrc3265

57. De Craene B, Berx G (2013) Regulatory networks defining EMT during cancer initiation and progression. Nature Rev Cancer 13:97-110. doi:10.1038/nrc3447

58. Polyak K, Weinberg RA (2009) Transitions between epithelial and mesenchymal states: acquisition of malignant and stem cell traits. Nature Rev Cancer 9:265-273. doi:10.1038/nrc2620

59. Creighton CJ, Chang JC, Rosen JM (2010) Epithelial-mesenchymal transition (EMT) in tumor-initiating cells and its clinical implications in breast cancer. J Mamm Gland Biology Neoplasia 15:253-260. doi:10.1007/s10911-010-9173-1

60. Taube JH, Herschkowitz JI, Komurov K, Zhou AY, Gupta S, Yang J, Hartwell K, Onder TT, Gupta PB, Evans KW, Hollier BG, Ram PT, Lander ES, Rosen JM, Weinberg RA, Mani SA (2010) Core epithelial-to-mesenchymal transition interactome gene-expression signature is associated with claudin-low and metaplastic breast cancer subtypes. Proc Natl Acad Sci USA 107:15449-15454. doi:10.1073/pnas.1004900107

61. Feng YX, Sokol ES, Del Vecchio CA, Sanduja S, Claessen JH, Proia TA, Jin DX, Reinhardt F, Ploegh HL, Wang Q, Gupta PB (2014) Epithelial-to-mesenchymal transition activates PERK-eIF2alpha and sensitizes cells to endoplasmic reticulum stress. Cancer Discov 4:702-715. doi:10.1158/2159-8290.CD-13-0945

62. Behbod F, Kittrell FS, LaMarca H, Edwards D, Kerbawy S, Heestand JC, Young E, Mukhopadhyay P, Yeh HW, Allred DC, Hu M, Polyak K, Rosen JM, Medina D (2009) An intraductal human-in-mouse transplantation model mimics the subtypes of ductal carcinoma in situ. Breast Cancer Res 11:R66. doi:bcr2358 [pii]10.1186/bcr2358

63. Prat A, Karginova O, Parker JS, Fan C, He X, Bixby L, Harrell JC, Roman E, Adamo B, Troester M, Perou CM (2013) Characterization of cell lines derived from breast cancers and normal mammary tissues for the study of the intrinsic molecular subtypes. Breast Cancer Res Treat 142:237-255. doi:10.1007/s10549-013-2743-3

64. Giancotti FG (2013) Mechanisms governing metastatic dormancy and reactivation. Cell 155:750-764. doi:10.1016/j.cell.2013.10.029

65. Sosa MS, Bragado P, Aguirre-Ghiso JA (2014) Mechanisms of disseminated cancer cell dormancy: an awakening field. Nature Rev Cancer 14:611-622. doi:10.1038/nrc3793

66. Muller V, Stahmann N, Riethdorf S, Rau T, Zabel T, Goetz A, Janicke F, Pantel K (2005) Circulating tumor cells in breast cancer: correlation to bone marrow micrometastases, heterogeneous response to systemic therapy and low proliferative activity. Clin Cancer Res 11:3678-3685. doi:10.1158/1078-0432.CCR-04-2469

67. Aurilio G, Sciandivasci A, Munzone E, Sandri MT, Zorzino L, Cassatella MC, Verri E, Rocca MC, Nole F (2012) Prognostic value of circulating tumor cells in primary and metastatic breast cancer. Expert Rev Anticancer Ther 12:203-214. doi:10.1586/era.11.208

Figure 2.1 Elevated Expression of ECM and ER quality control genes in mammospheres.

a Representative images of SUM159PT and MCF10DCIS.com cells grown under adherent conditions (ADH) or in suspension as mammospheres for 10 days (MMS). **b** mRNA ratios of selected ECM genes in mammospheres (MMS) versus adherent (ADH) SUM159PT and MCF10DCIS.com cells were evaluated by qRT-PCR; *ACTIN* was used as a normalization control. The results represent the mean values from at least two independent experiments, ±S.E.M. *Asterisks* indicate mRNA fold changes significantly greater than 1 (*$P < 0.05$, one sample *t* test). **c** mRNA expression levels of selected ECM genes in primary breast tumor cells isolated from 11 breast cancer patients, grown as mammospheres (*M*) or adherent cultures (*A*), based on [39]. The results of microarray profiling were retrieved from Gene Expression Omnibus (GEO) using the accession number GSE7515. Downloaded data were $\log_2$-transformed and mean-centered. **d** mRNA levels of selected ER folding factors in SUM159PT and MCF10DCIS.com cells were quantified by qRT-PCR; *ACTIN* was used as normalization control. The average fold change of each mRNA in MMS versus ADH cells ±S.E.M was calculated based on three (SUM159PT) or two (MCF10DCIS.com) independent experiments. *Asterisks* indicate mRNA fold changes significantly greater than 1 (*$P < 0.05$, one sample *t* test). **e** Comparison of the mRNA expression levels of selected ER folding factors in mammospheres (*M*) and adherent cultures (*A*) of primary breast cancer cells. The data were retrieved and processed as in (c). **f** Elevated expression of ECM genes coincides with upregulated expression of the ER folding machinery genes in circulating tumor cells (CTCs). mRNA expression levels of ECM genes, ER chaperones/foldases/lectins, and selected cytoplasmic chaperones in CTCs from a breast cancer patient (columns 1–5) and identically processed blood specimens from 10 healthy donors (columns 6–15), based on [6]. The index breast cancer patient was sampled at five time points during treatment. At points 1, 2, and 3, there was a response (*R*) to a targeted therapy. Time point 4 corresponds to the therapy resistance and disease progression (*P*). After switching to chemotherapy, a response was observed at time point 5. The expression data were retrieved from GEO:GSE41245. Gene names are on the *right*, gene name aliases are provided in *parentheses*. The expression values for each gene were normalized between 0 and 1, with the minimal value out of the 15 column values set as 0 and the maximal value set as 1.

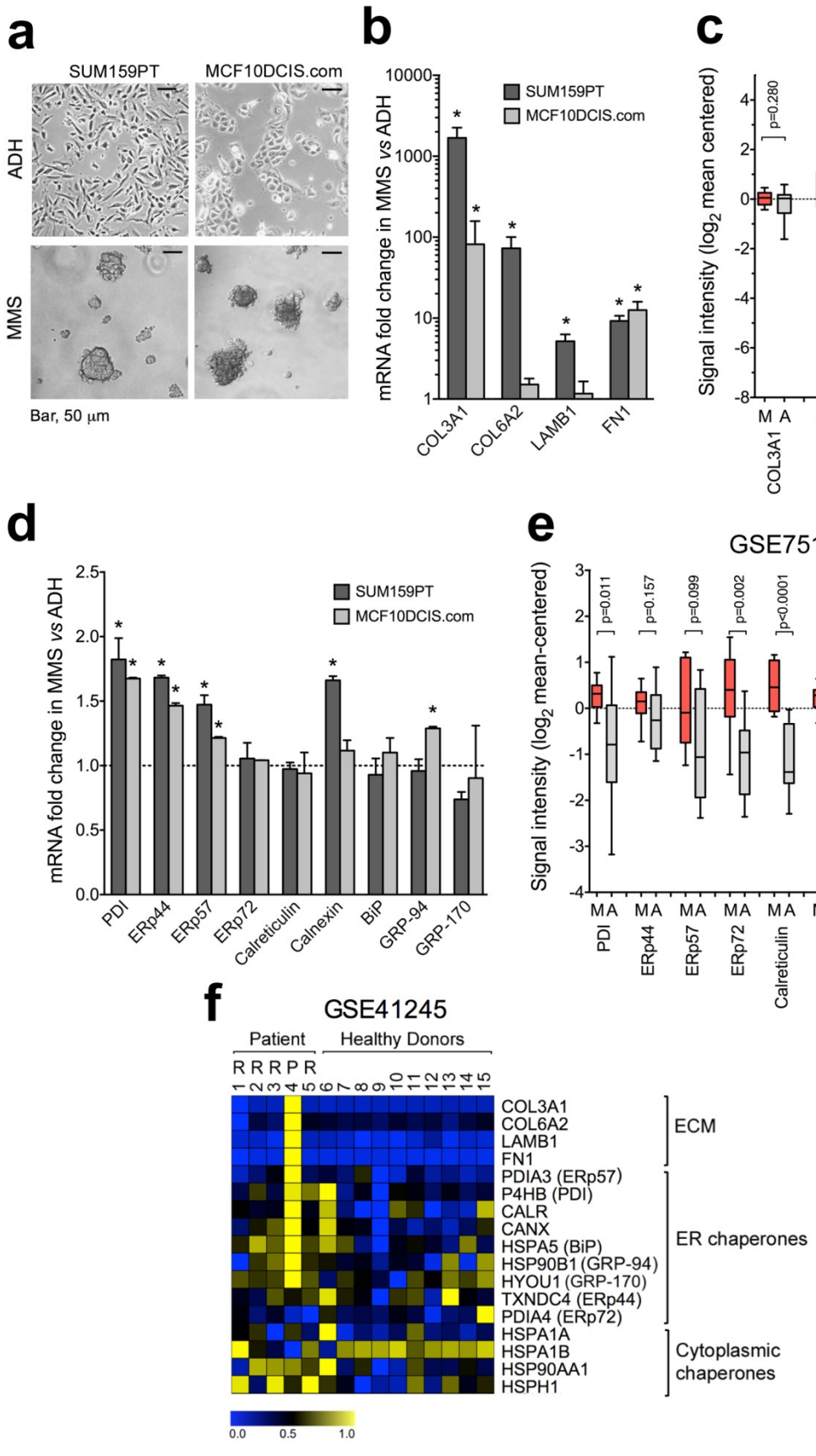
a
SUM159PT
MCF10DCIS.com
ADH
MMS
Bar, 50 μm
b
mRNA fold change in MMS vs ADH
SUM159PT
MCF10DCIS.com
COL3A1
COL6A2
LAMB1
FN1
c
GSE7515
Signal intensity (log2 mean centered)
p=0.280
p=0.001
p<0.0001
p<0.0001
M A
d
mRNA fold change in MMS vs ADH
SUM159PT
MCF10DCIS.com
PDI
ERp44
ERp57
ERp72
Calreticulin
Calnexin
BiP
GRP-94
GRP-170
e
GSE7515
Signal intensity (log2 mean-centered)
p=0.011
p=0.157
p=0.099
p=0.002
p<0.0001
p=0.006
p=0.001
p=0.226
p=0.254
M A
f
GSE41245
Patient
Healthy Donors
R R R P R
1 2 3 4 5 6 7 8 9 10 11 12 13 14 15
COL3A1
COL6A2
LAMB1
FN1
ECM
PDIA3 (ERp57)
P4HB (PDI)
CALR
CANX
HSPA5 (BiP)
HSP90B1 (GRP-94)
HYOU1 (GRP-170)
TXNDC4 (ERp44)
PDIA4 (ERp72)
ER chaperones
HSPA1A
HSPA1B
HSP90AA1
HSPH1
Cytoplasmic chaperones
0.0
0.5
1.0

Figure 2.2 Comparison of the protein levels of selected ER folding factors in mammospheres versus adherent cells.

SUM159PT (**a**) or MCF10DCIS.com (**b**) cell lysates were analyzed by Western blotting using antibodies specific for the following ER folding factors: PDI, 57 kDa; ERp44, 44 kDa, ERp57, 57 kDa; ERp72, 72 kDa; Calreticulin, 48 kDa; Calnexin, 80 kDa, BiP, 78 kDa, GRP-94, 94 kDa, GRP-170, 170 kDa. Tubulin is a gel-loading control. **a** The following ER proteins were analyzed in the same gel and share the same loading control: PDI and GRP-170; ERp44 and Calnexin. **b** The following ER proteins were analyzed in the same gel and share the same loading control: ERp57 and GRP-170; ERp44, Calreticulin, Calnexin, and BiP; PDI and ERp72. Band intensities from three independent experiments were quantified using ImageJ. The average fold change in the ER folding factor levels in mammospheres versus adherent cells ±S.E.M is indicated in each panel.

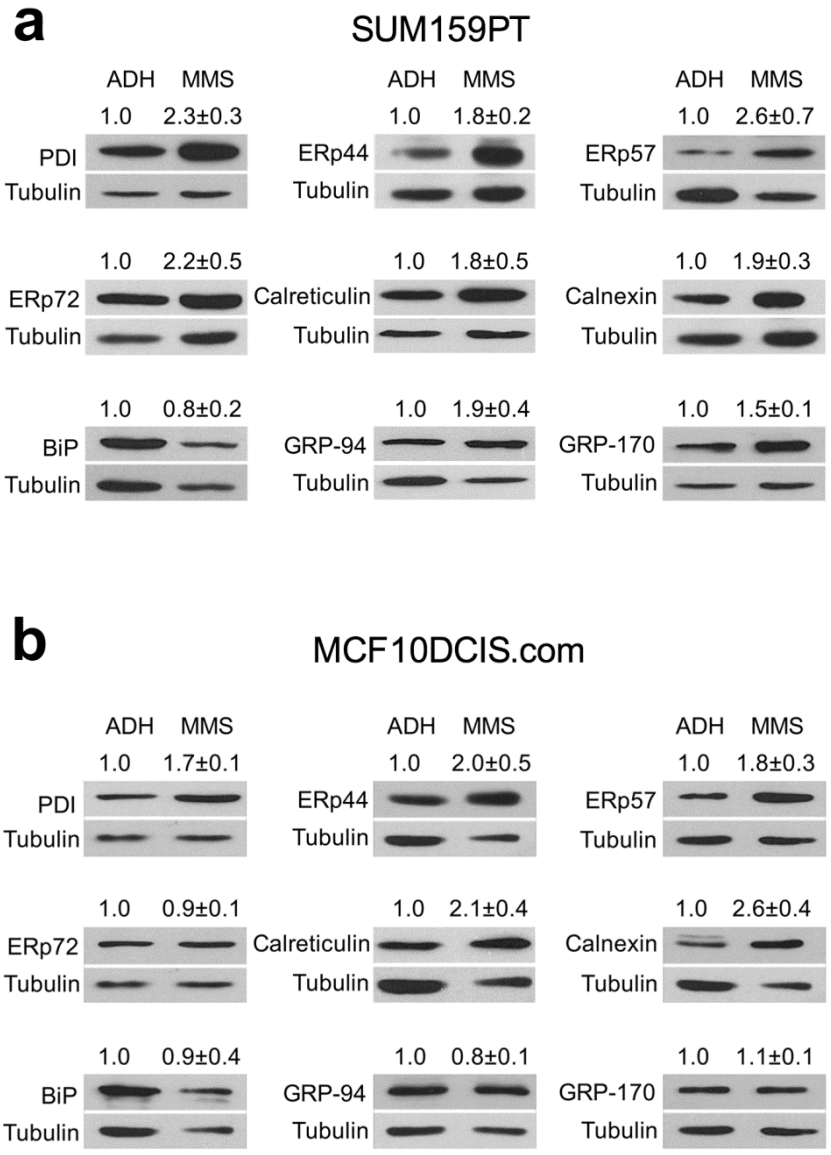

Figure 2.3 Evaluation of the three branches of the unfolded protein response in mammospheres (MMS) and adherent (ADH) SUM159PT and MCF10DCIS.com cells.

a Activation of the PERK branch of the UPR was assessed based on a change in mobility of PERK in immunoblots and the extent of phosphorylation of eIFα (p-eIF2α). **b** The status of the IRE1 branch of the UPR was evaluated by measuring the extent of splicing of *XBP1* mRNA by semi-quantitative PCR. "u XBP1" and "s XBP1" indicate the un-spliced and spliced forms of *XBP1* mRNA, respectively. **c** The status of the ATF6 branch of the UPR was probed using an ATF6 reporter. Cells were co-transfected with ATF6-firefly luciferase reporter and control *Renilla* luciferase plasmids, and the relative luciferase activity was determined using a dual luciferase assay. Tunicamycin (Tun) was used as a positive control for the ER stress-mediated activation of IRE1 and ATF6. Mammospheres were grown for 10 days in experiments shown in panels **a** and **b**, and for 3 days in panel **c**.

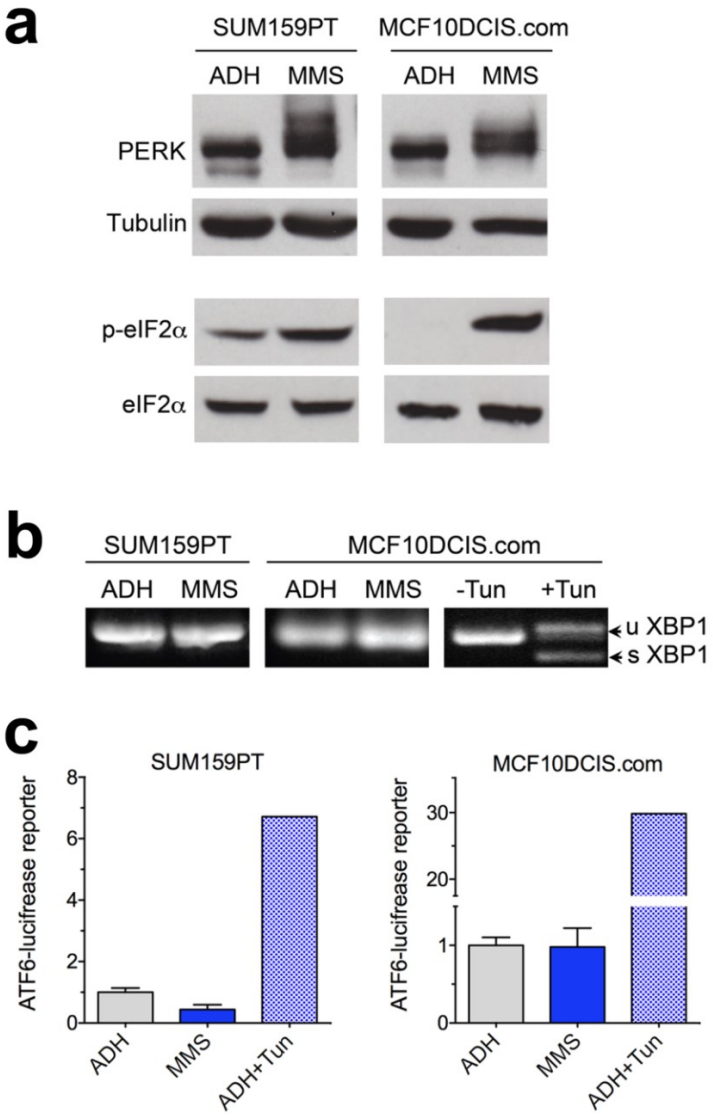

Figure 2.4 PDI, ERp44, or ERp57 knock-down in SUM159PT cells.

a Diagram of the doxycycline-inducible lentiviral shRNA construct (TRIPZ) targeting PDI, ERp44, or ERp57, or a construct harboring a non-targeting shRNA (shControl). *5'-LTR* 5'-long terminal repeat, *TRE* tetracycline-inducible promoter, *tRFP* turbo red fluorescent protein, *miR30-5'* and *shERp57/shPDI/shERp44* micro-RNA-30 adapted shRNA targeting ERp57/PDI/ERp44, *Ubc* human ubiquitin C promoter, *rtTA3* reverse tetracycline-transactivator 3, *IRES* internal ribosomal entry site, *Puro* puromycin resistance gene, *3'-LTR* 3'-long terminal repeat. **b** PDI, ERp44, or ERp57 knock-down in adherent SUM159PT cells. Cells were stably transduced with two different shRNA constructs targeting PDI, ERp44, or ERp57, or with shControl. Cells were incubated for 4 days without or with 1 μg/ml doxycycline (Dox), and the levels of indicated proteins in total cell lysates were evaluated by Western blotting; tubulin is a gel-loading control. **c** Monitoring doxycycline-inducible shRNA expression in mammospheres based on the RFP fluorescence. SUM159PT-shControl cells were pre-incubated for 4 days without or with doxycycline and were further grown for 10 days in mammosphere media in the absence or presence of doxycycline. Representative phase contrast and fluorescent images are shown. Analogous levels of RFP fluorescence were obtained for shPDI, shERp44, or shERp57-expressing cells (see Appendix A: Supplementary Fig. 1). **d** PDI, ERp44, or ERp57 knock-down is maintained in SUM159PT cells grown as mammospheres and is not compensated for by other members of the PDI family.

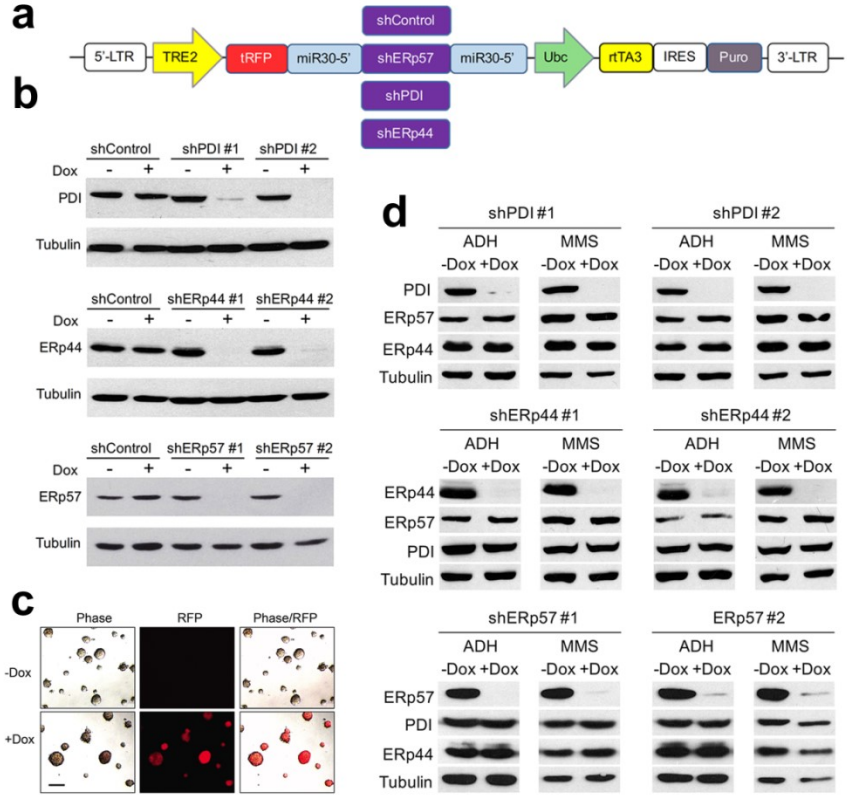

Figure 2.5 The effect of PDI, ERp44, or ERp57 knock-down on cell growth under adherent versus mammosphere conditions.

a PDI, ERp44, or ERp57 knock-down does not have a significant effect on the growth rate of adherent cells. SUM159PT cells stably transduced with two different shRNA constructs targeting PDI, ERp44, or ERp57, or with a construct harboring a non-targeting shRNA (shControl) were seeded into 96-well plates at the density of 3000 cells/well and incubated under adherent conditions in the absence or presence of 1 μg/ml doxycycline (Dox). Cell viability at the indicated times was measured using the CellTiter Glo assay. The results (arbitrary units, a.u.) are shown as means from 3 determinations, ±S.E.M. **b** PDI, ERp44, or ERp57 knock-down reduces the growth of cells under mammosphere conditions. Each cell type was seeded into 4 wells of a 24-well plate. After 10 days, spheres were visualized by phase contrast imaging, counted using ImageJ, and the total sphere volume was estimated as described in Methods. The results are shown as mean values obtained from 3 independent experiments. * $P < 0.05$.

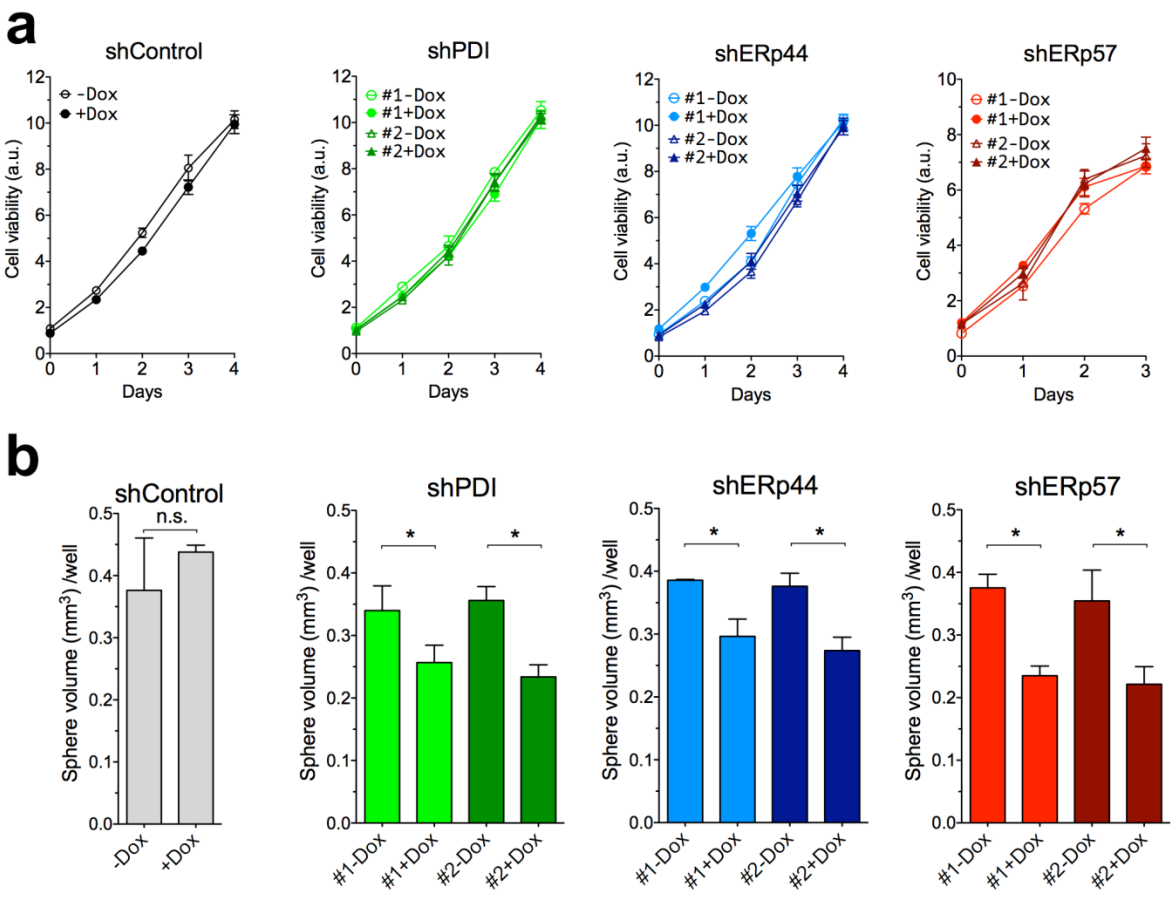

Figure 2.6 The effect of PDI, ERp44, or ERp57 knock-down on mammosphere formation and size.

a The number of spheres in the absence or presence of doxycycline. Each cell type was seeded into 4 wells of a 24-well plate. After 10 days, spheres were visualized by phase contrast imaging and counted using ImageJ, as described in Methods. The numbers of mammospheres with diameters >50 μm are indicated by *solid color bars*. The numbers of mammospheres with diameters <50 μm and >15 μm are shown with *white bars*. The results are shown as mean values obtained from 3 independent experiments. * $P < 0.05$; ** $P < 0.01$. **b** Size distribution of RFP-positive spheres. RFP-positive spheres formed in the presence of doxycycline were visualized by fluorescence microscopy. Sphere diameters were determined using ImageJ. For each cell type, a *box*-and-*whisker plot* of the diameters of 100 randomly selected spheres formed under identical conditions is shown. **** $P < 0.0001$

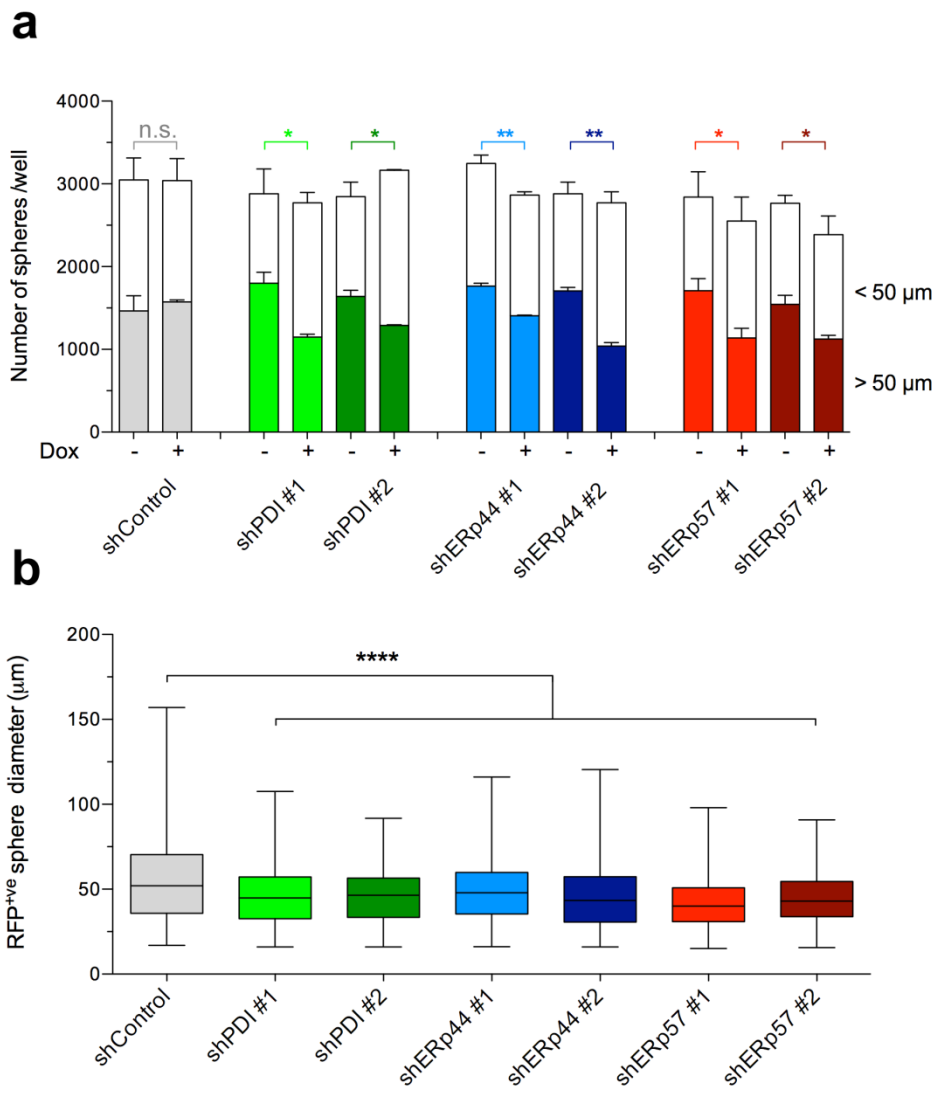

Chapter 3 - Metalloprotease-dependent activation of EGFR modulates the $CD44^+/CD24^-$ populations in triple negative breast cancer cells through the MEK/ERK pathway

This chapter has been published as the following journal article:

Wise R, Zolkiewska A (2017) Metalloprotease-dependent activation of EGFR modulates $CD44^+/CD24^-$ populations in triple negative breast cancer cells through the MEK/ERK pathway. Breast Cancer Res Treat 1-13. The final publication is available at link.springer.com via https://doi.org/10.1007/s10549-017-4440-0.

Abstract

Purpose: The $CD44^+/CD24^-$ cell phenotype is enriched in triple negative breast cancers (TNBCs), is associated with tumor invasive properties, and serves as a cell surface marker profile of breast cancer stem-like cells. Activation of Epidermal Growth Factor Receptor (EGFR) promotes the $CD44^+/CD24^-$ phenotype, but the specific signaling pathway downstream of EGFR responsible for this effect is not clear. The purpose of this study was to determine the role of the MEK/ERK pathway in the expansion of $CD44^+/CD24^-$ populations in TNBC cells in response to EGFR activation.

Methods: Representative TNBC cell lines SUM159PT (claudin-low) and SUM149PT (basal) were used to evaluate cell surface expression of CD44 and CD24 by flow cytometry in response to EGFR and MEK inhibition or activation. EGFR and ERK phosphorylation levels were analyzed by Western blotting. The relationship between EGFR phosphorylation and MEK activation score in basal and claudin-low tumors from the TCGA database was examined.

Results: Inhibition of ERK activation with selumetinib, a MEK1/2 inhibitor, blocked EGF-induced expansion of $CD44^+/CD24^-$ populations. Sustained activation of ERK by overexpression of constitutively active MEK1 was sufficient to expand $CD44^+/CD24^-$ populations in cells in which EGFR activity was blocked by either erlotinib, an EGFR kinase inhibitor, or BB-94, a metalloprotease inhibitor that prevents generation of soluble EGFR ligands. In basal and claudin-low tumors from the TCGA database, there was a positive correlation between EGFR_pY1068 and MEK activation score in tumors without genomic loss of *DUSP4*, a negative regulator of ERK, but not in tumors harboring *DUSP4* deletion.

Conclusion: Our results demonstrate that ERK activation is a key event in EGFR-dependent regulation of $CD44^+/CD24^-$ populations. Furthermore, our findings highlight the role of ligand-mediated EGFR signaling in the control of MEK/ERK pathway output in TNBC tumors without *DUSP4* loss.

Keywords

Breast cancer; Epidermal growth factor receptor, Mitogen-activated protein kinase pathway, CD44, CD24, Cancer stem cells, Metalloproteases

Abbreviations

TNBC, triple negative breast cancer; EGF, epidermal growth factor; EGFR, epidermal growth factor receptor; HER2, human epidermal growth factor receptor 2; ER, estrogen receptor; PR, progesterone receptor; MEK, mitogen-activated protein kinase kinase; MAPK, mitogen-activated protein kinase; ERK, extracellular signal-regulated kinase; JNK; Jun N-terminal kinase; DUSP4, dual specificity phosphatase 4; EMT, epithelial-to-mesenchymal transition; CSCs, cancer stem cells; FACS, fluorescence-activated cell sorting; PE, phycoerythrin; APC, Allophycocyanin;

GEO, Gene Expression Omnibus; TCGA, The Cancer Genome Atlas; GISTIC, Genomic Identification of Significant Targets in Cancer

Introduction

Epidermal Growth Factor Receptor (EGFR) is frequently overexpressed in triple negative breast cancers (TNBCs, negative for expression of estrogen receptor (ER) and progesterone receptor (PR), and lacking amplification of the human epidermal growth factor receptor-2 (*HER2*) gene), and its overexpression is associated with poor clinical outcomes [1-3]. EGFR and its downstream signaling pathways regulate many aspects of cell behavior associated with tumor growth and progression, including cell proliferation, survival, epithelial-to-mesenchymal transition (EMT), migration, invasion, and drug resistance [4-13].

The $CD44^{+}/CD24^{-}$ cell surface marker profile is associated with basal-like breast tumors [14], which are largely represented by triple-negative tumors [15], EMT [16], enhanced invasiveness [17], and stem-like properties of breast cancer cells [18]. Recently, it has been reported that inhibition of EGFR signaling in SUM159PT and MDA-MB-231 TNBC cell lines using Cetuximab, an anti-EGFR blocking monoclonal antibody, reduced $CD44^{+}/CD24^{-/low}$ and $Aldefluor^{+}$ cell populations, decreased mammosphere formation, and partially inhibited tumor growth in vivo in mouse xenograft models [19]. These results indicated that inhibition of EGFR signaling reduced cancer stem cell (CSC) populations and suggested that anti-EGFR therapies, in combination with chemotherapy, may be more effective in eliminating CSCs compared to chemotherapy alone in some TNBC patients. It was further postulated that the reduction of CSC populations by Cetuximab was mediated through inhibition of autophagy [19]. However, while EGFR may regulate autophagy in a context-dependent manner, most of the published reports indicate that EGFR tyrosine kinase activity inhibits autophagy [13, 20-23]. Therefore, inhibition

of EGFR activity with Cetuximab should lead to activation, rather than inhibition, of autophagy, and the mechanism by which EGFR would control CSC populations is not clear.

Importantly, the CSC phenotype in basal and claudin-low breast cancers was reported to be promoted by activation of two mitogen-activated protein kinase (MAPK) pathways: the extracellular signal-regulated kinase (ERK) pathway and the Jun N-terminal kinase (JNK) pathway [24]. Specifically, activation of these pathways due to genomic loss of dual specificity phosphatase 4 (DUSP4), a negative regulator of ERK1/2 and JNK1/2, expanded CSC populations in several TNBC cell lines. Conversely, enforced expression of DUSP4 in BT549 and SUM159PT cell lines reduced $CD44^+/CD24^-$ populations [24]. Since ERK1 and ERK2 are downstream effectors of mitogen-activated protein kinase kinases 1 and 2 (MEK1/2) [25], which in turn are regulated by EGFR, our first goal was to determine whether EGFR activity controls the $CD44^+/CD24^-$ phenotype through the MEK/ERK pathway.

The second goal of this study was to examine the role of metalloproteases in regulation of the $CD44^+/CD24^-$ phenotype and the MEK/ERK pathway output in TNBC. ADAM metalloproteases release soluble ligands for EGFR, namely EGF, heparin-binding EGF (HB-EGF), amphiregulin, epiregulin, transforming growth factor α (TGF-α), or betacellulin, and act as upstream regulators of EGFR [26, 27]. Ligand-dependent activation of EGFR represents the critical first step of the transcriptional programs regulated by the MEK/ERK pathway, provided that the tumors lack genetic alterations in pathway components that would render the pathway constitutively active. While activating mutations in the EGFR/RAS/RAF/MEK/ERK pathway are rare in breast cancer, approximately 50% of TNBCs are characterized by hemi- or homozygous deletion of the *DUSP4* gene, which leads to aberrant pathway activation [24, 28, 29]. Thus, TNBCs harboring *DUSP4* genomic loss should be less dependent on EGFR

activation. However, in the remaining ~50% of TNBCs without *DUSP4* copy loss, efficient MEK/ERK pathway activation might require the function of metalloproteases, generation of soluble EGFR ligands, and ligand-dependent EGFR activation.

Here, we show that ERK1/2 activation is necessary for EGFR-induced expansion of $CD44^+/CD24^-$ populations. Furthermore, we show that sustained activation of ERK1/2 by overexpression of constitutively active MEK1 is sufficient to expand $CD44^+/CD24^-$ populations in cells in which EGFR activity is blocked by either erlotinib, an EGFR kinase inhibitor, or BB-94, a metalloprotease inhibitor that prevents generation of soluble EGFR ligands. These results indicate that ERK1/2 plays an essential role in ligand-dependent EGFR signaling, which promotes the $CD44^+/CD24^-$ marker profile. Moreover, in basal and claudin-low tumors from the TCGA database, there is a positive correlation between EGFR_pY1068 and MEK1/2 activation score in tumors without *DUSP4* loss, but not in tumors harboring *DUSP4* loss. This further highlights the role of ligand-mediated EGFR signaling in regulation of the MEK/ERK pathway in TNBC tumors without *DUSP4* loss. The results of our investigations may help identify biomarkers to help predict which TNBC patients are most likely to respond to EGFR inhibitors.

Methods

Reagents and antibodies

Antibodies for immunoblotting included anti-EGFR_pY1068 (#D7A5), anti-total EGFR (#D38B1), anti-ERK1/2_pT202/Y204 (#D13.14.4E), anti-total ERK1/2 (#137F5), and anti-MEK1/2 (#D1A5), all from Cell Signaling Technology. The apparent molecular weight of EGFR detected by anti-total EGFR antibody is ~170 kDa. The phosphorylated EGFR detected with anti-EGFR pY1068 antibody migrates at a slightly slower rate (~172-175 kDa band in Western blots). These apparent molecular weights are significantly higher than the predicted molecular

weight of EGFR (134 kDa) due to extensive protein glycosylation. Antibodies for flow cytometry, PE-conjugated anti-CD24 (#ML5) and APC-conjugated anti-CD44 (#IM7), were from BD Biosciences and Affymetrix eBioscience, respectively.

Calculation of EGFR and MEK activation scores

The top 100 genes whose expression was most significantly changed upon stable expression of EGFR or constitutively active MEK in MCF-7 cells, compared to control MCF-7 cells adapted for long-term estrogen-independent growth [30], were retrieved from Gene Expression Omnibus (GEO, http://www.ncbi.nlm.nih.gov/geo/), using accession number GSE3542. Expression values for these EGFR- or MEK-regulated genes in $CD44^+/CD24^-$ and $CD44^-/CD24^+$ subpopulations of MCF10A cells [31] were then extracted from GEO using accession number GSE15192. The EGFR and MEK scores were calculated as:

$$s = \sum_i w_i x_i / \sum_i |w_i|$$

where w is the weight +1 or –1, depending on whether the gene was upregulated or downregulated in the signature, and x is the normalized gene expression level.

TCGA data mining

Expression values for MEK-regulated genes (mRNA expression z-scores, measured by Agilent microarrays) and the EGFR phosphorylation status at Y992, Y1068, and Y1173 (protein expression z-scores, measured by reverse-phase protein arrays) were retrieved from The Cancer Genome Atlas (TCGA) (Nature 2012 dataset) [32] via the cBioPortal for Cancer Genomics (http://www.cbioportal.org/public-portal/) [33, 34]. The *DUSP4* copy number status was determined by the Genomic Identification of Significant Targets in Cancer (GISTIC) algorithm. GISTIC copy numbers "-2" (a deep loss) and "-1" (a shallow loss) for *DUSP4* were considered homozygous and heterozygous deletions of *DUSP4*, respectively. Tumors for which *DUSP4*

GISTIC copy numbers were ≥ 0 were assumed not to harbor *DUSP4* deletion. Pearson *r* correlation coefficient and two-tailed P values were calculated using GraphPad Prism 6.0 software.

Cell culture, retroviral transduction, generation of stable cell lines, and immunoblotting were performed as previously described [35-37]. Additional experimental details are provided in Appendix B: Supplementary Methods.

Results

It has been previously shown that the transcriptional signature of activation of the MEK pathway is positively correlated with the CD44:CD24 mRNA ratio in the NCI-Integrative Cancer Biology Program-50 (ICBP50) panel of breast cancer cell lines [24] and in mammosphere cultures derived from primary breast tumors [24, 38]. Here, we examined the EGFR and MEK pathway activation scores in flow cytometry-sorted subpopulations of MCF10A cells expressing the $CD44^+/CD24^-$ or $CD44^-/CD24^+$ marker profile [31] (data were retrieved from GEO:GSE15192). To calculate the EGFR and MEK activation scores, we used the top 100 genes whose expression was most significantly changed upon stable expression of ligand-activatable EGFR or constitutively active MEK in MCF-7 cells [30]. We determined that the $CD44^+/CD24^-$ subpopulation had significantly higher EGFR and MEK activation scores than the $CD44^-/CD24^+$ subpopulation (Fig. 3.1a).

To study a potential cause-and-effect relationship between EGFR activation and cell surface expression of CD44 and CD24, and the role of MEK1/2 in this process, we utilized two representative TNBC cell lines, SUM159PT and SUM149PT, corresponding to the claudin-low and basal molecular subtypes of breast cancer, respectively [39]. We first examined the activation status of EGFR and its downstream effector ERK1/2 in these two cell lines in response

to erlotinib, a specific inhibitor of EGFR tyrosine kinase activity, and to EGF, an activating ligand. Treatment for 72 h with 1 μM erlotinib caused a decrease in EGFR phosphorylation at Y1068, one of the major autophosphorylation sites in EGFR, in both cell lines. Stimulation for 48 h with 20 ng/ml EGF increased the EGFR phosphorylation signal and decreased the amount of total EGFR, leading to higher pEGFR/EGFR ratios (Fig. 3.1b), which is consistent with enhanced turnover of activated EGFR [40, 41]. Of note, in SUM159PT treated with EGF, two bands were observed for total EGFR, most likely corresponding to EGFR phosphorylated on multiple tyrosine residues and unphosphorylated (or weakly phosphorylated) EGFR. Without exogenous EGF typically only one band was detected. Importantly, the extent of ERK1/2 phosphorylation decreased after erlotinib treatment and increased in the presence of EGF in both cell lines (Fig. 3.1b). This is notable, because SUM159PT cells, but not SUM149PT cells, contain an activating G12D mutation in the *HRAS* gene [42]. One of the reasons why ERK1/2 phosphorylation in SUM159PT cells was still modulated by EGFR could be the fact that the G12D mutation is heterozygous and approximately half of the HRAS protein, plus other members of the RAS family, are wild-type and amenable to regulation by external signals. Based on the results shown in Fig. 3.1b, we concluded that at the basal level, EGFR and ERK1/2 were partially active in both SUM159PT and SUM149PT cells, and they were further stimulated by adding EGF.

As reported previously, we found that the sizes of $CD44^+/CD24^-$ populations in SUM159PT and SUM149PT cells were very different [43, 44], and amounted to ~90-95% for SUM159PT cells and ~5-10% for SUM149PT cells (Fig. 3.1c and e, respectively). Inhibition of the basal activation levels of EGFR with erlotinib decreased $CD44^+/CD24^-$ populations in both SUM159PT and SUM149PT cells. Histogram analysis of the flow cytometry data showed a

modest, but reproducible increase of CD24 expression in erlotinib-treated SUM159PT cells (Fig. 3.1d) and a clear increase of the CD24 staining in erlotinib-treated SUM149PT cells (Fig. 3.1f). Erlotinib did not have any effect on CD44 levels in SUM159PT cells, but it decreased CD44 expression in SUM149PT cells (Fig. 3.1d and f, respectively). These results agreed with a recently reported effect of Cetuximab on the $CD44^+/CD24^-$ population in MDA-MB-231 cells [19]. EGF treatment caused a small increase of $CD44^+/CD24^-$ populations in SUM159PT and SUM149PT cells (Fig. 3.1c and e, respectively), and these effects were statistically significant (see Figs. 3.2c and 3.3c for statistical analyses).

To determine the role of the MEK pathway in maintaining $CD44^+/CD24^-$ populations, cells were treated for 72 h with selumenitib, a MEK1/2 inhibitor. Selumenitib dose response in SUM159PT cells established that the lowest concentration of the inhibitor that entirely blocked MEK1/2-mediated phosphorylation of ERK1/2 in response to sustained EGFR activation was 75 μM (Fig. 3.2a). Treatment of SUM159PT cells with 75 μM selumetinib did not significantly affect cell viability (results not shown), but it dramatically decreased the $CD44^+/CD24^-$ population, and this effect was not rescued by 48 h incubation with 20 ng/ml EGF (Fig. 3.2b, c). In SUM149PT cells, the lowest effective concentration of selumenitib was determined to be 10 μM (Fig. 3.3a), and this concentration had negligible effect on cell viability (not shown). Treatment of SUM149PT cells with 10 μM selumetinib entirely eliminated the $CD44^+/CD24^-$ population and, as in SUM159PT cells, this effect was not rescued by 48 h incubation with 20 ng/ml EGF (Fig. 3.3b, c). Thus, MEK1/2 activity is required for EGF-induced expansion of $CD44^+/CD24^-$ populations.

To examine whether activation of the MEK/ERK pathway in the absence of an active EGFR is sufficient to expand $CD44^+/CD24^-$ populations, we established cells with stable

overexpression of a constitutively active phosphomimetic mutant of human MEK1 (MEK1-DD) [45], wild-type human MEK1 bearing an N-terminal HA-tag (HA-MEK1-WT) [46], or empty vector (EV). Overexpression of MEK1-DD or HA-MEK1-WT in SUM159PT cells was confirmed by Western blotting using anti-MEK1/2 or anti-HA-tag antibodies (Fig. 3.4a). The basal phosphorylation level of ERK1/2 in MEK1-DD-expressing SUM159PT cells was elevated and similar to the level of ERK1/2 phosphorylation in EGF-treated cells, validating constitutive activation of MEK1-DD (Fig. 3.4b). Importantly, while inhibition of EGFR with erlotinib diminished $CD44^+/CD24^-$ populations in EV- and HA-MEK1-WT-expressing SUM159PT cells, erlotinib did not have any effect on the $CD44^+/CD24^-$ marker profile in MEK1-DD-expressing cells (Fig. 3.4c, d).

Similar results were obtained for SUM149PT cells with stable overexpression of EV, MEK1-DD, or HA-MEK1-WT (Fig. 3.5a). The basal phosphorylation level of ERK1/2 in MEK1-DD-expressing SUM149PT cells was higher than it was in EV- or HA-MEK1-WT-expressing cells and, in contrast to EV or HA-MEK1-WT cells, it was not inhibited by erlotinib (Fig. 3.5b), confirming the constitutive activation of MEK1-DD. Furthermore, while treatment of EV- or HA-MEK1-WT-expressing SUM149PT cells with erlotinib diminished $CD44^+/CD24^-$ population, overexpression of MEK1-DD blocked the effect of erlotinib on the $CD44^+/CD24^-$ population (Fig. 3.5c, d). Collectively, the results in Figs. 3.4 and 3.5 indicted that constitutive activation of the MEK/ERK pathway in the absence of an active EGFR was sufficient to expand $CD44^+/CD24^-$ populations in SUM159PT and SUM149PT cells.

Partial activation of EGFR in SUM159PT and SUM149PT cells in the absence of the exogenously added EGF, which was also observed previously in our lab in SUM159PT cells in serum-free media [37], suggested that EGFR might have been activated by endogenously

expressed ligands. All EGFR ligands are synthesized as transmembrane precursors that need to be converted to biologically active, soluble molecules via cleavage by ADAM metalloproteases [26, 27]. This raised a possibility that ADAMs may be involved in regulation of the $CD44^+/CD24^-$ marker profile. This hypothesis was tested here by treatment of cells with batimastat (BB-94), a broad-spectrum metalloprotease inhibitor. BB-94 did not have a noticeable effect on cell viability or proliferation rates at the concentrations up to 30 μM (results not shown). A 48 h incubation of SUM159PT, SUM149PT, or MCF10A, a non-tumorigenic mammary epithelial cell line, with 10 μM BB-94 significantly decreased the amount of soluble amphiregulin, an EGFR ligand highly expressed in all three cell lines, in the media (Fig. 3.6a). Consequently, the basal phosphorylation level of EGFR was significantly reduced after BB-94 treatment (Fig. 3.6b). The effect of BB-94 was eliminated after 30 min stimulation with exogenous EGF (Fig. 3.6b), which was consistent with the fact that metalloproteases act as upstream regulators of ligand availability and EGFR activation.

In addition to its effect on EGFR phosphorylation, a 72-h incubation of SUM159PT cells with 10 μM BB-94 significantly inhibited the basal phosphorylation level of ERK1/2 (Fig. 3.7a). Importantly, $CD44^+/CD24^-$ population was diminished after BB-94 treatment of EV- of HA-MEK1-WT-expressing SUM159PT cells, but not of cells expressing the constitutively active MEK1-DD (Fig. 3.7b, c). Similarly, BB-94-treated SUM149PT cells exhibited decreased levels of EGFR and ERK1/2 phosphorylation after 72-h treatment with 10 μM BB-94 (Fig. 3.8a), and BB-94 treatment reduced $CD44^+/CD24^-$ populations in EV- and HA-MEK1-DD-expressing SUM149PT cells, but not in MEK1-DD-expressing cells (Fig. 3.8b, c). Thus, inhibition of metalloproteases, which are upstream modulators of EGFR signaling, with BB-94 exerted a similar effect to direct inhibition of EGFR tyrosine kinase activity with erlotinib.

While ligand-mediated activation of EGFR and the resulting activation of the MEK/ERK pathway may be important in some TNBCs, in other breast tumors in which ERK1/2 is hyperactive due to genomic loss of DUSP4, the status of EGFR activation should be less relevant for the MEK/ERK pathway output. To examine the relationship between EGFR activation, a transcriptional signature associated with MEK/ERK activation, and *DUSP4* copy number alterations, we analyzed gene expression data for basal and claudin-low tumors (which are predominantly triple-negative) from the TCGA database [32]. EGFR phosphorylation status was available for three Tyr residues, Y992, Y1068, and Y1173, in 72 tumors. EGFR phosphorylation at Y1068 facilitates the binding of an adaptor protein GRB2 and activation of the RAS/RAF/MEK/ERK pathway, while phosphorylated Y992 and Y1173 are the major binding sites for PLCγ and SHP1 phosphatase, leading to the activation of PKC and receptor dephosphorylation, respectively [47, 48]. The MEK activation score in the 72 basal and claudin-low tumors was calculated based on the expression levels of top 100 MEK-regulated genes [30]. *DUSP4* copy number data were generated by the GISTIC algorithm (see Methods).

There was a significant positive correlation (Pearson $r = 0.375$, $P = 0.029$) between EGFR_pY1068 and MEK activation score in tumors without *DUSP4* deletion, but not in tumors harboring a heterozygous or homozygous deletion of *DUSP4* (Table 3.1). EGFR_pY992 and EGFR_pY1173 were not significantly correlated with MEK activation in any tumor group. These results are consistent with the notion that metalloprotease-dependent ligand-mediated EGFR signaling plays an important role in regulation of the MEK/ERK pathway in TNBC tumors without *DUSP4* loss.

Discussion

While a tumor-promoting role of EGFR signaling in TNBC has been well established, the results of EGFR-targeted therapies for TNBC, either as a monotherapy or in combination with cisplatin, [49], carboplatin [50], or Ixabepilone [51], have been disappointing. One of the reasons is the lack of specific markers predicting which patients are most likely to respond to anti-EGFR therapies [1, 2, 52-55]. Recent studies demonstrating that EGFR inhibitors reduce CSC populations in TNBC tumors [19] further highlight the importance of EGFR in the pathology of triple-negative disease and underscore the need for better markers guiding patient selection for anti-EGFR therapies. Understanding the mechanism by which EGFR activation controls CSCs is needed to maximize the clinical benefit of EGFR inhibitors in the treatment of TNBCs.

Here, we show that the MEK/ERK pathway is a key component of the signaling cascade downstream of the activated EGFR that regulates the $CD44^+/CD24^-$ phenotype in SUM159PT and SUM149PT cells. MEK1/2 inhibition reduced $CD44^+/CD24^-$ populations in both cell lines, and this effect was not rescued by activation of EGFR with exogenously added EGF. In contrast, overexpression of constitutively active MEK1 was sufficient to increase $CD44^+/CD24^-$ populations, and this effect was not blocked by EGFR inhibition with erlotinib. Furthermore, we showed that inhibition of cell surface metalloproteases that generate soluble, bioactive ligands for EGFR diminished $CD44^+/CD24^-$ populations, and metalloprotease inhibition with BB-94 was as effective as inhibition of tyrosine kinase activity of EGFR with erlotinib. Also, BB-94-mediated reduction of $CD44^+/CD24^-$ populations was entirely blocked by overexpression of constitutively active MEK1. Collectively, these results demonstrate that MEK/ERK activity is both necessary and sufficient for EGFR-mediated regulation of $CD44^+/CD24^-$ populations.

Our results corroborate previous studies demonstrating an important role of MEK/ERK in regulation of CSCs in breast tumors. As reported by Balko et al., activation of MAPK pathways due to DUSP4 knockdown increased mammosphere formation in MDA-MB-231 cells, and overexpression of DUSP4 in SUM159PT cells decreased mammosphere formation, reduced the $CD44^{+}/CD24^{-}$ compartment, and impeded tumor growth in a mouse xenograft model [24]. Furthermore, pharmacological inhibition of MEK1/2 reduced mammosphere numbers in MDA-MB-231, BT549, and SUM159PT cell cultures and decreased the $CD44^{+}/CD24^{-}$ population in MDA-MB-231 cells [24]. MEK1/2 inhibition also reduced anchorage-independent cell growth of MDA-MB-231 and SUM149PT cell lines, reversed EMT in 3D culture system, inhibited ALDH1 activity, and prevented lung metastasis in a MDA-MB-231 xenograft model [11].

While EGFR is one of the main upstream regulators the MEK/ERK pathway, and while EGFR inhibition, similarly to MEK1/2 inhibition, reduces the numbers of breast cancer cells with the stem-like phenotype [10, 19, 56], direct involvement of MEK/ERK in the EGFR-mediated control of breast CSCs has not been demonstrated before. Instead, it has been proposed that EGFR inhibition reduces CSC population in breast cancer through inhibition of autophagy [19]. This notion is supported by the observations that chloroquine, a lysotropic agent that inhibits a late step of autophagy, or knock-down of autophagy-specific genes diminished the CSC populations in TNBC cell lines [57-59]. The universally positive role of autophagy in CSC maintenance is, however, at odds with a report demonstrating that autophagy deficiency stabilizes the transcription factor TWIST1, promotes EMT in vitro, and tumor growth and metastasis using a A431 squamous cell carcinoma xenograft mouse model [60, 61]. Most importantly, in several cancer cell types, including breast cancer, EGFR activation suppresses autophagy [13, 20, 21]. Thus, EGFR inhibition should lead to an increase, rather than a decrease,

in autophagy [22, 23], and the role of autophagy in EGFR-mediated regulation of breast CSCs needs further clarification.

The MEK/ERK pathway is hyperactivated in ~50% of TNBCs due to genomic loss of *DUSP4*, a negative regulator of ERK1/2. Since activating mutations in the MEK/ERK pathway components upstream of ERK1/2 are rare in breast cancer, it might be postulated that TNBCs without *DUSP4* loss should rely on ligand-dependent EGFR activation to generate a sizeable ERK pathway output. Indeed, our analysis of gene expression and phosphoproteomics data from the TCGA database shows a significant positive correlation between EGFR phosphorylation at Y1068 and MEK activation score in basal and claudin-low breast cancers without *DUSP4* loss, but not in basal and claudin-low breast cancers harboring *DUSP4* loss. Thus, in the absence of *DUSP4* loss, ligand-dependent metalloprotease-mediated activation of EGFR plays an essential role in regulating the MEK/ERK pathway output. Therefore, the efficacy of EGFR inhibitors should be greater in TNBCs containing an intact *DUSP4* gene than in DUSP4-deficient TNBCs.

In summary, our results underscore the central role of the MEK/ERK signaling pathway in regulation of breast CSCs. A large body of evidence demonstrates an important role of the MEK/ERK signaling pathway in other aspects of breast cancer pathology as well. For example, inhibition of the MEK1/2 activity in estrogen receptor α (ERα)-negative breast cancer cell lines using a pharmacological inhibitor U0126 resulted in re-expression of ERα [30, 62]. More recently, increased activation of MEK/ERK in tumor cells was shown to be associated with reduced numbers of tumor-infiltrating lymphocytes in TNBC, leading to immune evasion [63]. Thus, targeting the MEK/ERK pathway may offer multiple benefits in DUSP4-deficient TNBC, whereas EGFR inhibitors should be more efficient in DUSP4-positive TNBC. Additionally, in

DUSP4-positive TNBC, a combination of both EGFR inhibitors and metalloprotease inhibitors may serve as a valuable therapeutic treatment.

Acknowledgments

This work was supported by NIH grant R01CA172222 to AZ. This is contribution 17-394-J from Kansas Agricultural Experiment Station. I would like to acknowledge Dr. Anna Zolkiewska for performing the Western blotting experiments shown in Figure 3.6b.

Disclosure of potential conflict of interest

The authors declare no conflicts of interest.

References

1. Masuda H, Zhang D, Bartholomeusz C, Doihara H, Hortobagyi GN, Ueno NT (2012) Role of epidermal growth factor receptor in breast cancer. Breast Cancer Res Treat 136:331-345.

2. Williams CB, Soloff AC, Ethier SP, Yeh ES (2015) Perspectives on epidermal growth factor receptor regulation in triple-negative breast cancer: Ligand-mediated mechanisms of receptor regulation and potential for clinical targeting. Adv Cancer Res 127:253-281.

3. Hsu JL, Hung MC (2016) The role of HER2, EGFR, and other receptor tyrosine kinases in breast cancer. Cancer Metastasis Rev 35:575-588.

4. Verbeek BS, Adriaansen-Slot SS, Vroom TM, Beckers T, Rijksen G (1998) Overexpression of EGFR and c-erbB2 causes enhanced cell migration in human breast cancer cells and NIH3T3 fibroblasts. FEBS Lett 425:145-150.

5. Mukhopadhyay P, Lakshmanan I, Ponnusamy MP, Chakraborty S, Jain M, Pai P, et al (2013) MUC4 overexpression augments cell migration and metastasis through EGFR family proteins in triple negative breast cancer cells. PLoS One 8:e54455.

6. Maretzky T, Evers A, Zhou W, Swendeman SL, Wong PM, Rafii S, et al (2011) Migration of growth factor-stimulated epithelial and endothelial cells depends on EGFR transactivation by ADAM17. Nat Commun 2:229.

7. Reginato MJ, Mills KR, Paulus JK, Lynch DK, Sgroi DC, Debnath J, et al (2003) Integrins and EGFR coordinately regulate the pro-apoptotic protein Bim to prevent anoikis. Nat Cell Biol 5:733-740.

8. Ahmed N, Maines-Bandiera S, Quinn MA, Unger WG, Dedhar S, Auersperg N (2006) Molecular pathways regulating EGF-induced epithelio-mesenchymal transition in human ovarian surface epithelium. Am J Physiol Cell Physiol 290:C1532-1542.

9. Lo HW, Hsu SC, Xia W, Cao X, Shih JY, Wei Y, et al (2007) Epidermal growth factor receptor cooperates with signal transducer and activator of transcription 3 to induce epithelial-mesenchymal transition in cancer cells via up-regulation of TWIST gene expression. Cancer Res 67:9066-9076.

10. Zhang D, LaFortune TA, Krishnamurthy S, Esteva FJ, Cristofanilli M, Liu P, et al (2009) Epidermal growth factor receptor tyrosine kinase inhibitor reverses mesenchymal to epithelial phenotype and inhibits metastasis in inflammatory breast cancer. Clin Cancer Res 15:6639-6648.

11. Bartholomeusz C, Xie X, Pitner MK, Kondo K, Dadbin A, Lee J, et al (2015) MEK inhibitor Selumetinib (AZD6244; ARRY-142886) prevents lung metastasis in a triple-negative breast cancer xenograft model. Mol Cancer Ther 14:2773-2781.

12. Wang M, Kern AM, Hulskotter M, Greninger P, Singh A, Pan Y, et al (2014) EGFR-mediated chromatin condensation protects KRAS-mutant cancer cells against ionizing radiation. Cancer Res 74:2825-2834.

13. Wei Y, Zou Z, Becker N, Anderson M, Sumpter R, Xiao G, et al (2013) EGFR-mediated Beclin 1 phosphorylation in autophagy suppression, tumor progression, and tumor chemoresistance. Cell 154:1269-1284.

14. Honeth G, Bendahl PO, Ringner M, Saal LH, Gruvberger-Saal SK, Lovgren K, et al (2008) The CD44+/CD24- phenotype is enriched in basal-like breast tumors. Breast Cancer Res 10:R53.

15. Prat A, Adamo B, Cheang MC, Anders CK, Carey LA, Perou CM (2013) Molecular characterization of basal-like and non-basal-like triple-negative breast cancer. Oncologist 18:123-133.

16. Blick T, Hugo H, Widodo E, Waltham M, Pinto C, Mani SA, et al (2010) Epithelial mesenchymal transition traits in human breast cancer cell lines parallel the CD44hi/CD24lo/- stem cell phenotype in human breast cancer. J Mammary Gland Biol Neoplasia 15:235-252.

17. Sheridan C, Kishimoto H, Fuchs RK, Mehrotra S, Bhat-Nakshatri P, Turner CH, et al (2006) CD44+/CD24- breast cancer cells exhibit enhanced invasive properties: an early step necessary for metastasis. Breast Cancer Res 8:R59.

18. Al-Hajj M, Wicha MS, Benito-Hernandez A, Morrison SJ, Clarke MF (2003) Prospective identification of tumorigenic breast cancer cells. Proc Natl Acad Sci USA 100:3983-3988.

19. Tanei T, Choi DS, Rodriguez AA, Liang DH, Dobrolecki L, Ghosh M, et al (2016) Antitumor activity of Cetuximab in combination with Ixabepilone on triple negative breast cancer stem cells. Breast Cancer Res 18:6.

20. Henson E, Chen Y, Gibson S (2017) EGFR family members' regulation of autophagy is at a crossroads of cell survival and death in cancer. Cancers (Basel) 9:27.

21. Chen Y, Henson ES, Xiao W, Huang D, McMillan-Ward EM, Israels SJ, et al (2016) Tyrosine kinase receptor EGFR regulates the switch in cancer cells between cell survival and cell death induced by autophagy in hypoxia. Autophagy 12:1029-1046.

22. Fung C, Chen X, Grandis JR, Duvvuri U (2012) EGFR tyrosine kinase inhibition induces autophagy in cancer cells. Cancer Biol Ther 13:1417-1424.

23. Li X, Fan Z (2010) The epidermal growth factor receptor antibody cetuximab induces autophagy in cancer cells by downregulating HIF-1□ and Bcl-2 and activating the beclin 1/hVps34 complex. Cancer Res 70:5942-5952.

24. Balko JM, Schwarz LJ, Bhola NE, Kurupi R, Owens P, Miller TW, et al (2013) Activation of MAPK pathways due to DUSP4 loss promotes cancer stem cell-like phenotypes in basal-like breast cancer. Cancer Res 73:6346-6358.

25. Morrison DK (2012) MAP kinase pathways. Cold Spring Harb Perspect Biol 4:a011254.

26. Blobel CP (2005) ADAMs: key components in EGFR signalling and development. Nature Rev Mol Cell Biol 6:32-43.

27. Kataoka H (2009) EGFR ligands and their signaling scissors, ADAMs, as new molecular targets for anticancer treatments. J Dermatol Sci 56:148-153.

28. Giltnane JM, Balko JM (2014) Rationale for targeting the Ras/MAPK pathway in triple-negative breast cancer. Discov Med 17:275-283.

29. Mazumdar A, Poage GM, Shepherd J, Tsimelzon A, Hartman ZC, Den Hollander P, et al (2016) Analysis of phosphatases in ER-negative breast cancers identifies DUSP4 as a critical regulator of growth and invasion. Breast Cancer Res Treat 158:441-454.

30. Creighton CJ, Hilger AM, Murthy S, Rae JM, Chinnaiyan AM, El-Ashry D (2006) Activation of mitogen-activated protein kinase in estrogen receptor □-positive breast cancer cells in vitro induces an in vivo molecular phenotype of estrogen receptor □-negative human breast tumors. Cancer Res 66:3903-3911.

31. Bhat-Nakshatri P, Appaiah H, Ballas C, Pick-Franke P, Goulet R, Jr., Badve S, et al (2010) SLUG/SNAI2 and tumor necrosis factor generate breast cells with CD44+/CD24- phenotype. BMC Cancer 10:411.

32. The Cancer Genome Atlas Network (2012) Comprehensive molecular portraits of human breast tumours. Nature 490:61-70.

33. Gao J, Aksoy BA, Dogrusoz U, Dresdner G, Gross B, Sumer SO, et al (2013) Integrative analysis of complex cancer genomics and clinical profiles using the cBioPortal. Sci Signal 6:pl1.

34. Cerami E, Gao J, Dogrusoz U, Gross BE, Sumer SO, Aksoy BA, et al (2012) The cBio cancer genomics portal: an open platform for exploring multidimensional cancer genomics data. Cancer Discov 2:401-404.

35. Li H, Duhachek-Muggy S, Qi Y, Hong Y, Behbod F, Zolkiewska A (2012) An essential role of metalloprotease-disintegrin ADAM12 in triple-negative breast cancer. Breast Cancer Res Treat 135:759-769.

36. Li H, Duhachek-Muggy S, Dubnicka S, Zolkiewska A (2013) Metalloproteinase-disintegrin ADAM12 is associated with a breast tumor-initiating cell phenotype. Breast Cancer Res Treat 139:691-703.

37. Duhachek-Muggy S, Qi Y, Wise R, Alyahya L, Li H, Hodge J, et al (2017) Metalloprotease-disintegrin ADAM12 actively promotes the stem cell-like phenotype in claudin-low breast cancer. Mol Cancer 16:32.

38. Creighton CJ, Li X, Landis M, Dixon JM, Neumeister VM, Sjolund A, et al (2009) Residual breast cancers after conventional therapy display mesenchymal as well as tumor-initiating features. Proc Natl Acad Sci USA 106:13820-13825.

39. Prat A, Parker JS, Karginova O, Fan C, Livasy C, Herschkowitz JI, et al (2010) Phenotypic and molecular characterization of the claudin-low intrinsic subtype of breast cancer. Breast Cancer Res 12:R68.

40. Haglund K, Dikic I (2012) The role of ubiquitylation in receptor endocytosis and endosomal sorting. J Cell Sci 125:265-275.

41. Sorkin A, Goh LK (2009) Endocytosis and intracellular trafficking of ErbBs. Exp Cell Res 315:683-396.

42. Hollestelle A, Elstrodt F, Nagel JH, Kallemeijn WW, Schutte M (2007) Phosphatidylinositol-3-OH kinase or RAS pathway mutations in human breast cancer cell lines. Mol Cancer Res 5:195-201.

43. Fillmore CM, Kuperwasser C (2008) Human breast cancer cell lines contain stem-like cells that self-renew, give rise to phenotypically diverse progeny and survive chemotherapy. Breast Cancer Res 10:R25.

44. Keller PJ, Arendt LM, Skibinski A, Logvinenko T, Klebba I, Dong S, et al (2011) Defining the cellular precursors to human breast cancer. Proc Natl Acad Sci USA 109:2772–2777.

45. Boehm JS, Zhao JJ, Yao J, Kim SY, Firestein R, Dunn IF, et al (2007) Integrative genomic approaches identify IKBKE as a breast cancer oncogene. Cell 129:1065-1079.

46. Brady DC, Crowe MS, Turski ML, Hobbs GA, Yao X, Chaikuad A, et al (2014) Copper is required for oncogenic BRAF signalling and tumorigenesis. Nature 509:492-496.

47. Nyati MK, Morgan MA, Feng FY, Lawrence TS (2006) Integration of EGFR inhibitors with radiochemotherapy. Nat Rev Cancer 6:876-885.

48. Shostak K, Chariot A (2015) EGFR and NF-κB: partners in cancer. Trends Mol Med 21:385-93.

49. Baselga J, Gomez P, Greil R, Braga S, Climent MA, Wardley AM, et al (2013) Randomized phase II study of the anti-epidermal growth factor receptor monoclonal antibody cetuximab with cisplatin versus cisplatin alone in patients with metastatic triple-negative breast cancer. J Clin Oncol 31:2586-2592.

50. Carey LA, Rugo HS, Marcom PK, Mayer EL, Esteva FJ, Ma CX, et al (2012) TBCRC 001: randomized phase II study of cetuximab in combination with carboplatin in stage IV triple-negative breast cancer. J Clin Oncol 30:2615-2623.

51. Tredan O, Campone M, Jassem J, Vyzula R, Coudert B, Pacilio C, et al (2015) Ixabepilone alone or with cetuximab as first-line treatment for advanced/metastatic triple-negative breast cancer. Clin Breast Cancer 15:8-15.

52. Ueno NT, Zhang D (2011) Targeting EGFR in triple negative breast cancer. J Cancer 2:324-328.

53. Costa R, Shah AN, Santa-Maria CA, Cruz MR, Mahalingam D, Carneiro BA, et al (2017) Targeting Epidermal Growth Factor Receptor in triple negative breast cancer: New discoveries and practical insights for drug development. Cancer Treat Rev 53:111-119.

54. Nakai K, Hung MC, Yamaguchi H (2016) A perspective on anti-EGFR therapies targeting triple-negative breast cancer. Am J Cancer Res 6:1609-1623.

55. Fleisher B, Clarke C, Ait-Oudhia S (2016) Current advances in biomarkers for targeted therapy in triple-negative breast cancer. Breast Cancer 8:183-197.

56. Farnie G, Clarke RB, Spence K, Pinnock N, Brennan K, Anderson NG, et al (2007) Novel cell culture technique for primary ductal carcinoma in situ: role of Notch and epidermal growth factor receptor signaling pathways. J Natl Cancer Inst 99:616-627.

57. Cufi S, Vazquez-Martin A, Oliveras-Ferraros C, Martin-Castillo B, Vellon L, Menendez JA (2011) Autophagy positively regulates the CD44(+) CD24(-/low) breast cancer stem-like phenotype. Cell Cycle 10:3871-3885.

58. Choi DS, Blanco E, Kim YS, Rodriguez AA, Zhao H, Huang TH, et al (2014) Chloroquine eliminates cancer stem cells through deregulation of Jak2 and DNMT1. Stem Cells 32:2309-2323.

59. Liang DH, Choi DS, Ensor JE, Kaipparettu BA, Bass BL, Chang JC (2016) The autophagy inhibitor chloroquine targets cancer stem cells in triple negative breast cancer by inducing mitochondrial damage and impairing DNA break repair. Cancer Lett 376:249-258.

60. Qiang L, Zhao B, Ming M, Wang N, He TC, Hwang S, et al (2014) Regulation of cell proliferation and migration by p62 through stabilization of Twist1. Proc Natl Acad Sci USA 111:9241-9246.

61. Qiang L, He YY (2014) Autophagy deficiency stabilizes TWIST1 to promote epithelial-mesenchymal transition. Autophagy 10:1864-1865.

62. Bayliss J, Hilger A, Vishnu P, Diehl K, El-Ashry D (2007) Reversal of the estrogen receptor negative phenotype in breast cancer and restoration of antiestrogen response. Clin Cancer Res 13:7029-36.

63. Loi S, Dushyanthen S, Beavis PA, Salgado R, Denkert C, Savas P, et al (2016) RAS/MAPK activation is associated with reduced tumor-infiltrating lymphocytes in triple-negative breast cancer: Therapeutic cooperation between MEK and PD-1/PD-L1 immune checkpoint inhibitors. Clin Cancer Res 22:1499-1509.

Figure 3.1 EGFR signaling modulates the CD44^{+}/CD24^{-} marker profile in representative TNBC cells.

a EGFR and MEK pathway activation scores in CD44^{-}/CD24^{+} and CD44^{+}/CD24^{-} subpopulations of MCF10A cells. Microarray gene expression data for these two cell populations were retrieved from GEO:GSE15192, and EGFR and MEK scores were calculated based on Ref. [30], as described in Methods. Results are shown as means from 4 determinations, ± S.E.M. **b** Response of SUM159PT and SUM149PT cells to sustained EGFR inhibition or activation. Cells were treated for 72 h with DMSO alone, 1 μM erlotinib, an EGFR inhibitor, dissolved in DMSO, or for 48 h with 20 ng/ml EGF and DMSO. The extent of EGFR phosphorylation at Y1068 and ERK1/2 phosphorylation at T202/Y204, total EGFR, and total ERK1/2 were analyzed by Western blotting. Tubulin is a gel-loading control. **c**-**f** Effect of EGFR inhibition or activation on the CD44 and CD24 markers. SUM159PT and SUM149PT cells were treated as in (panel **b**), stained with anti-CD24-PE and anti-CD44-APC antibodies, and analyzed by flow cytometry. Quadrant markers were set based on control antibody staining. Results of a representative experiment (n = 5) are shown as dot plots (**c** and **e**) or histogram analyses (**d** and **f**).

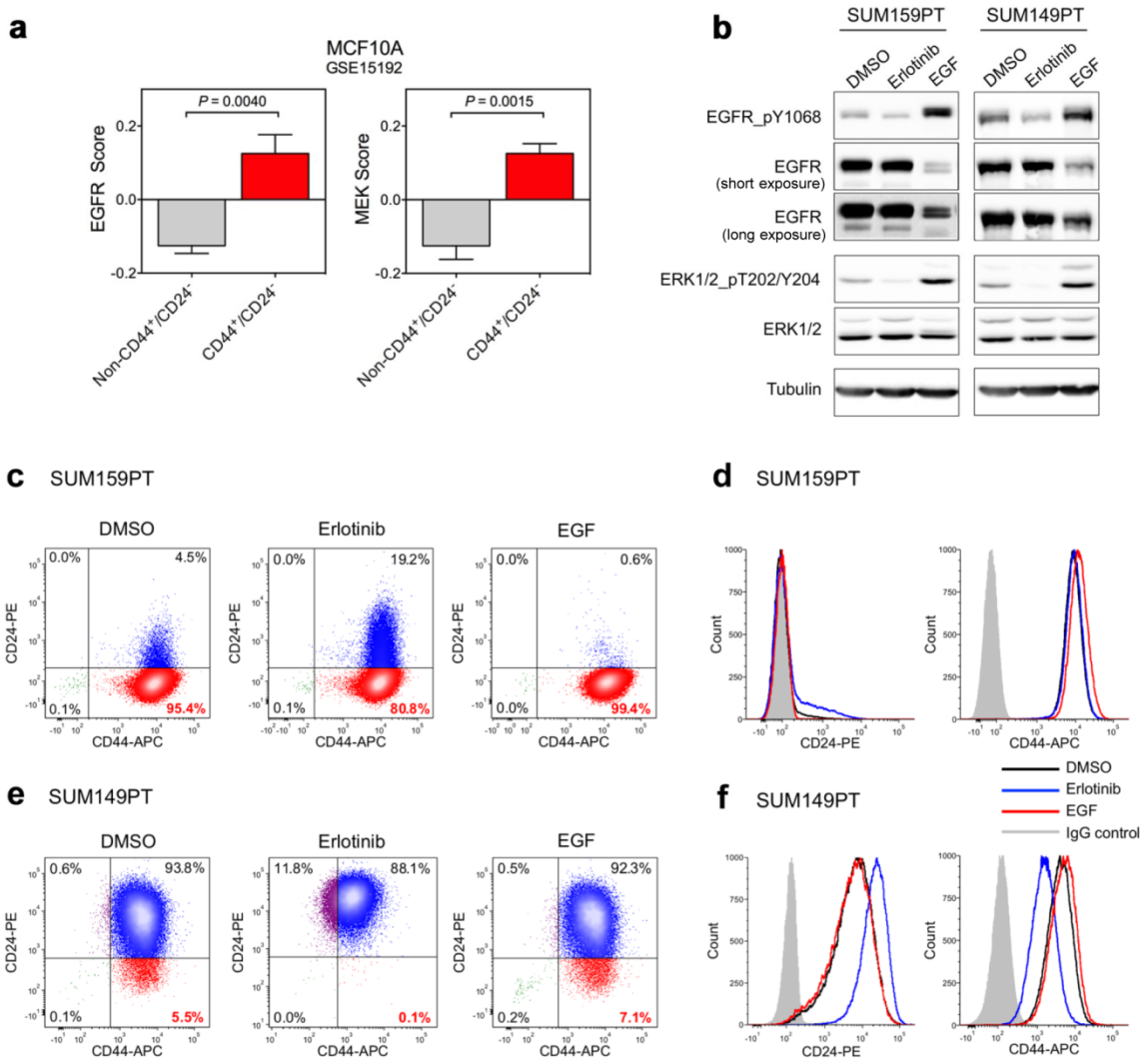

Figure 3.2 MEK1/2 inhibition blocks the effect of EGF on the CD44^{+}/CD24^{-} marker profile in SUM159PT cells.

a Dose response of selumetinib, a MEK1/2 inhibitor, on the extent of ERK1/2 phosphorylation. Cells were treated with either DMSO or indicated concentrations of selumetinib. Twenty-four hours later, 20 ng/ml EGF or vehicle alone was added for an additional 48 h. Cells were analyzed by Western blotting using anti-phospho-ERK1/2 and anti-total ERK1/2 antibodies; β1-integrin is a gel-loading control. **b** Cells were treated for 24 h with DMSO or 75 μM selumetinib, and then for an additional 48 h with or without 20 ng/ml EGF. Cells were stained with anti-CD24-PE and anti-CD44-APC antibodies and analyzed by flow cytometry. **c** Percentages of CD44^{+}/CD24^{-} cells are shown as mean values ± S.E.M. from three independent experiments. * $P < 0.05$; *** $P < 0.001$.

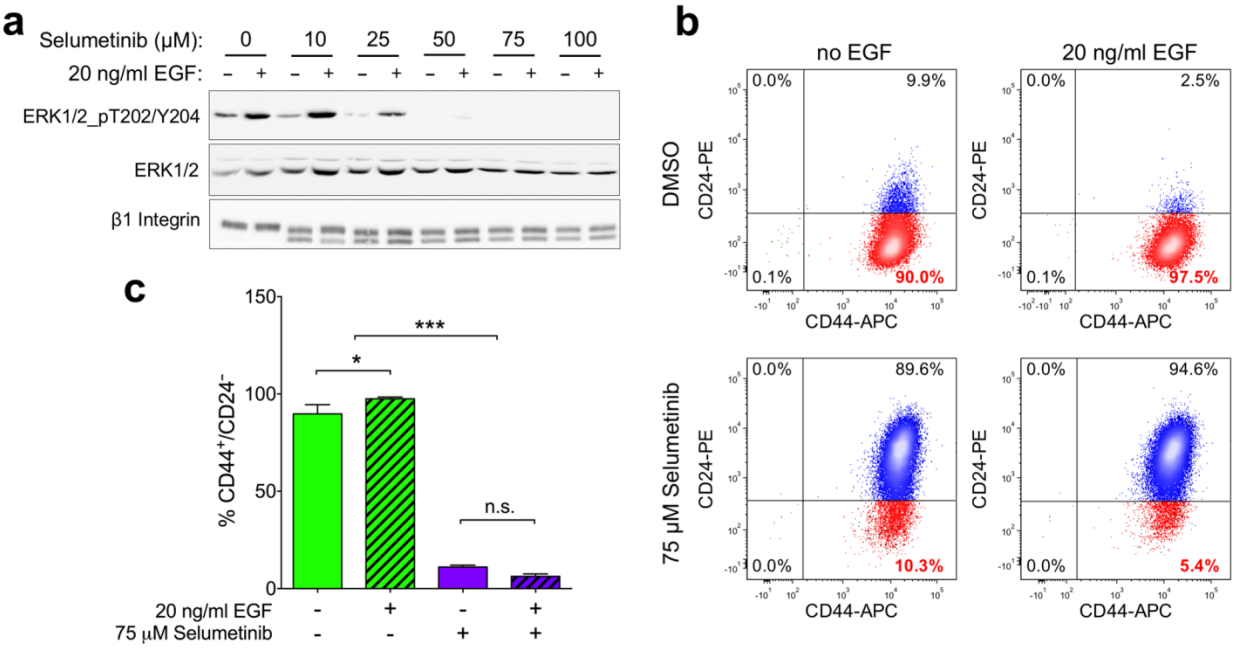

Figure 3.3 MEK1/2 inhibition blocks the effect of EGF on the $CD44^{+}/CD24^{-}$ marker profile in SUM149PT cells.

a Dose response of selumetinib, a MEK1/2 inhibitor, on the extent of ERK1/2 phosphorylation. Cells were treated with either DMSO or indicated concentrations of selumetinib. Twenty-four hours later, 20 ng/ml EGF or vehicle alone was added for an additional 48 h. Cells were analyzed by Western blotting using anti-phospho-ERK1/2 and anti-total ERK1/2 antibodies; β1-integrin is a gel-loading control. **b** Cells were treated for 24 h with DMSO or 10 μM selumetinib, and then for an additional 48 h with or without 20 ng/ml EGF. Cells were stained with anti-CD24-PE and anti-CD44-APC antibodies and analyzed by flow cytometry. **c** Percentages of $CD44^{+}/CD24^{-}$ cells are shown as mean values ± S.E.M. from three independent experiments. * $P < 0.05$; ** $P < 0.01$.

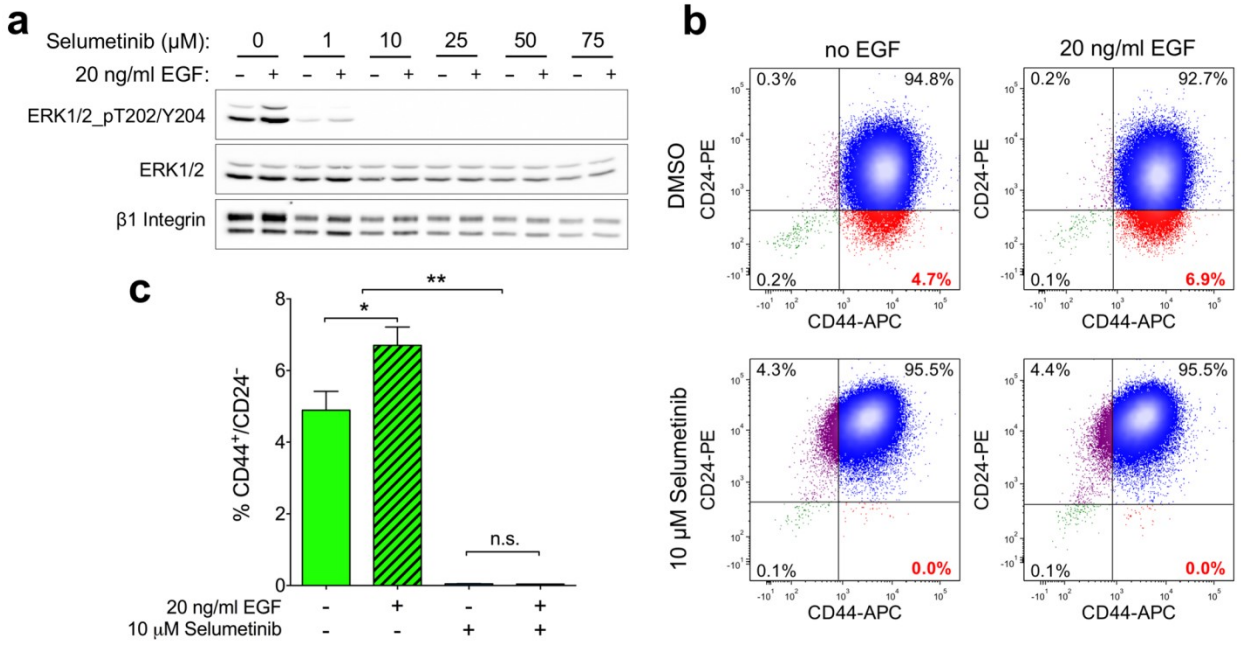

Figure 3.4 Constitutively active MEK1 blocks the effect of erlotinib on CD44^{+}/CD24^{-} population in SUM159PT cells.

a Confirmation of MEK1 overexpression. Cells stably transduced with empty vector (EV), constitutively active MEK1 (MEK1-DD), or wild-type HA-tagged MEK1 (HA-MEK1-WT) were analyzed by Western blotting using anti-MEK1 and anti-HA tag antibodies; β1-integrin is a gel-loading control. **b** Verification of constitutive activation of MEK1-DD. Cells expressing EV, MEK1-DD, or HA-MEK1-WT were incubated for 30 min with or without 20 ng/ml EGF and analyzed by Western blotting using anti-phospho-ERK1/2 and anti-total ERK1/2 antibodies. **c** Effect of MEK1-DD on the CD44^{+}/CD24^{-} marker profile. EV, MEK1-DD, or HA-MEK1-WT cells were treated with either DMSO or 1 μM erlotinib for 72 h, stained with anti-CD24-PE and anti-CD44-APC antibodies, and analyzed by flow cytometry. **d** Percentages of CD44^{+}/CD24^{-} cells are shown as mean values ± S.E.M. from two independent experiments. * $P < 0.05$; ** $P < 0.01$.

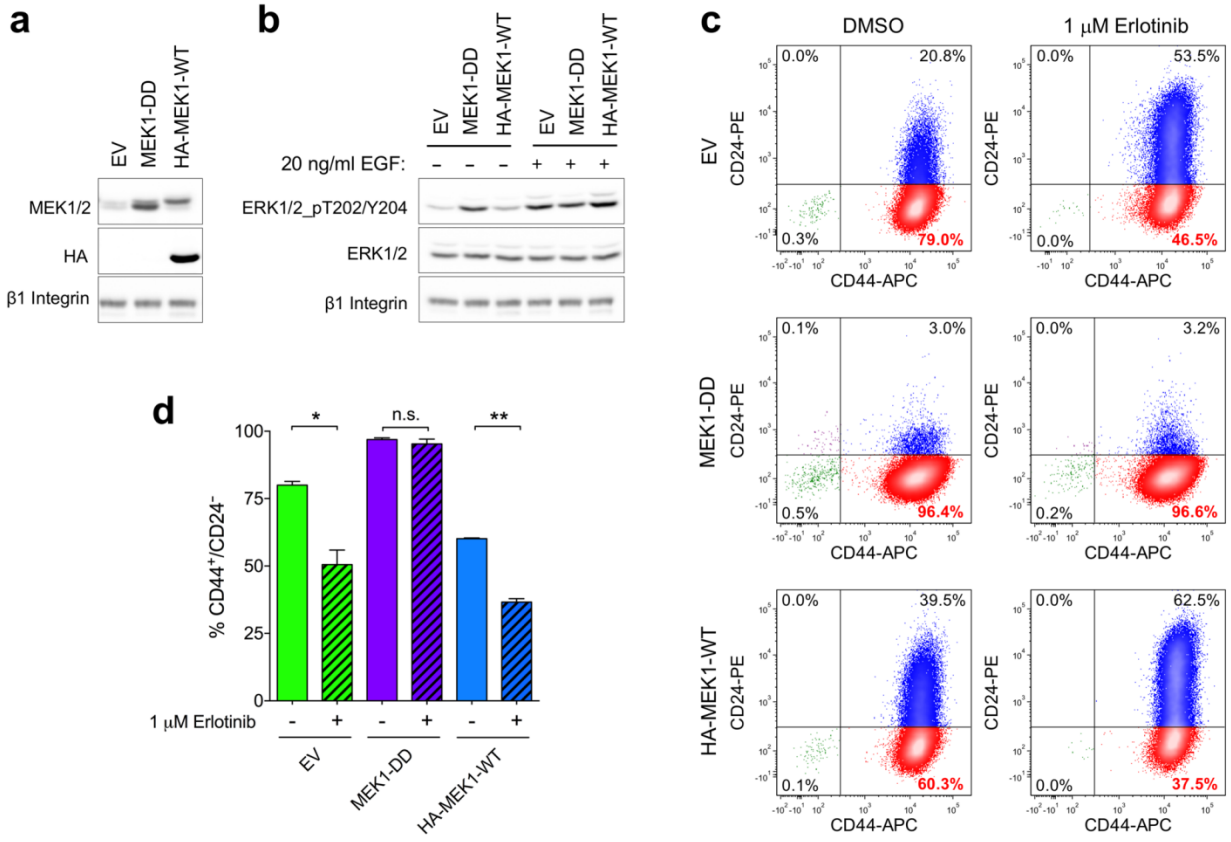

Figure 3.5 Constitutively active MEK1 blocks the effect of erlotinib on CD44^{+}/CD24^{-} population in SUM149PT cells.

a Confirmation of MEK1 overexpression. SUM149PT cells stably transduced with empty vector (EV), constitutively active MEK1 (MEK1-DD), or wild-type HA-tagged MEK1 (HA-MEK1-WT), were analyzed by Western blotting using anti-MEK1/2 and anti-HA tag antibodies; β1-integrin is a gel-loading control. **b** Verification of constitutive activation of MEK1-DD. Cells expressing EV, MEK1-DD, or HA-MEK1-WT were incubated for 24 h with DMSO or 1 μM erlotinib and analyzed by Western blotting using anti-phospho-ERK1/2 and anti-total ERK1/2 antibodies. **c** Effect of MEK1-DD on the CD44^{+}/CD24^{-} marker profile. EV, MEK1-DD, or HA-MEK1-WT cells were treated with either DMSO or 1 μM erlotinib for 72 h, stained with anti-CD24-PE and anti-CD44-APC antibodies, and analyzed by flow cytometry. **d** Percentages of CD44^{+}/CD24^{-} cells are shown as mean values ± S.E.M. from two independent experiments. * $P < 0.05$; *** $P < 0.001$.

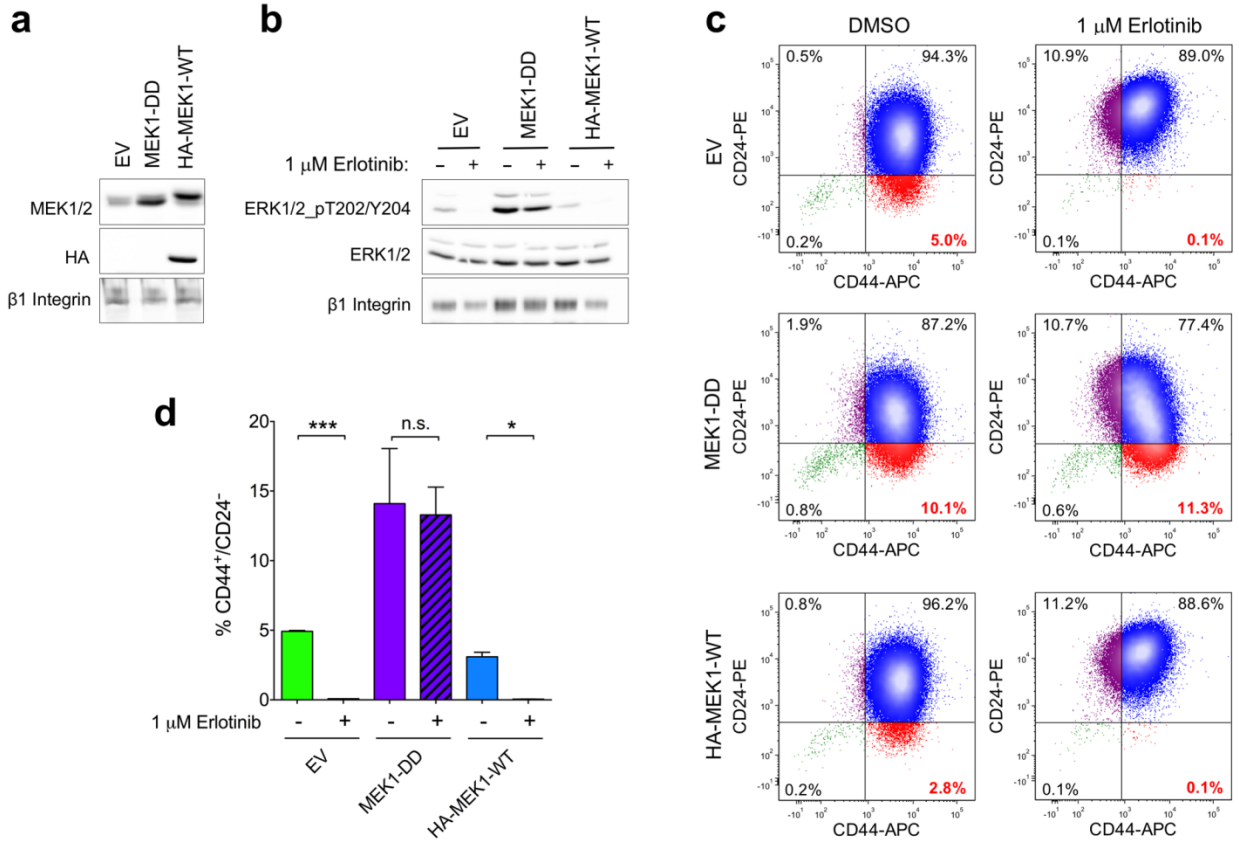

Figure 3.6 Metalloprotease inhibitor batimastat (BB-94) decreases the amount of soluble amphiregulin (AREG) released from cells to the media and reduces the basal activation level of EGFR.

SUM159PT, SUM149PT, or MCF10A cells were incubated for 48 h with DMSO or 10 μM BB-94. **a** The amount of soluble AREG in conditioned media was measured using ELISA. Shown are the mean values ± S.E.M. from three independent measurements; *** $P < 0.001$, **** $P < 0.0001$. **b** DMSO- or BB-94-treated cells were incubated for 30 min with or without 20 ng/ml EGF and analyzed by Western blotting using anti-phospho-EGFR or anti-total EGFR antibody; tubulin is a gel loading control.

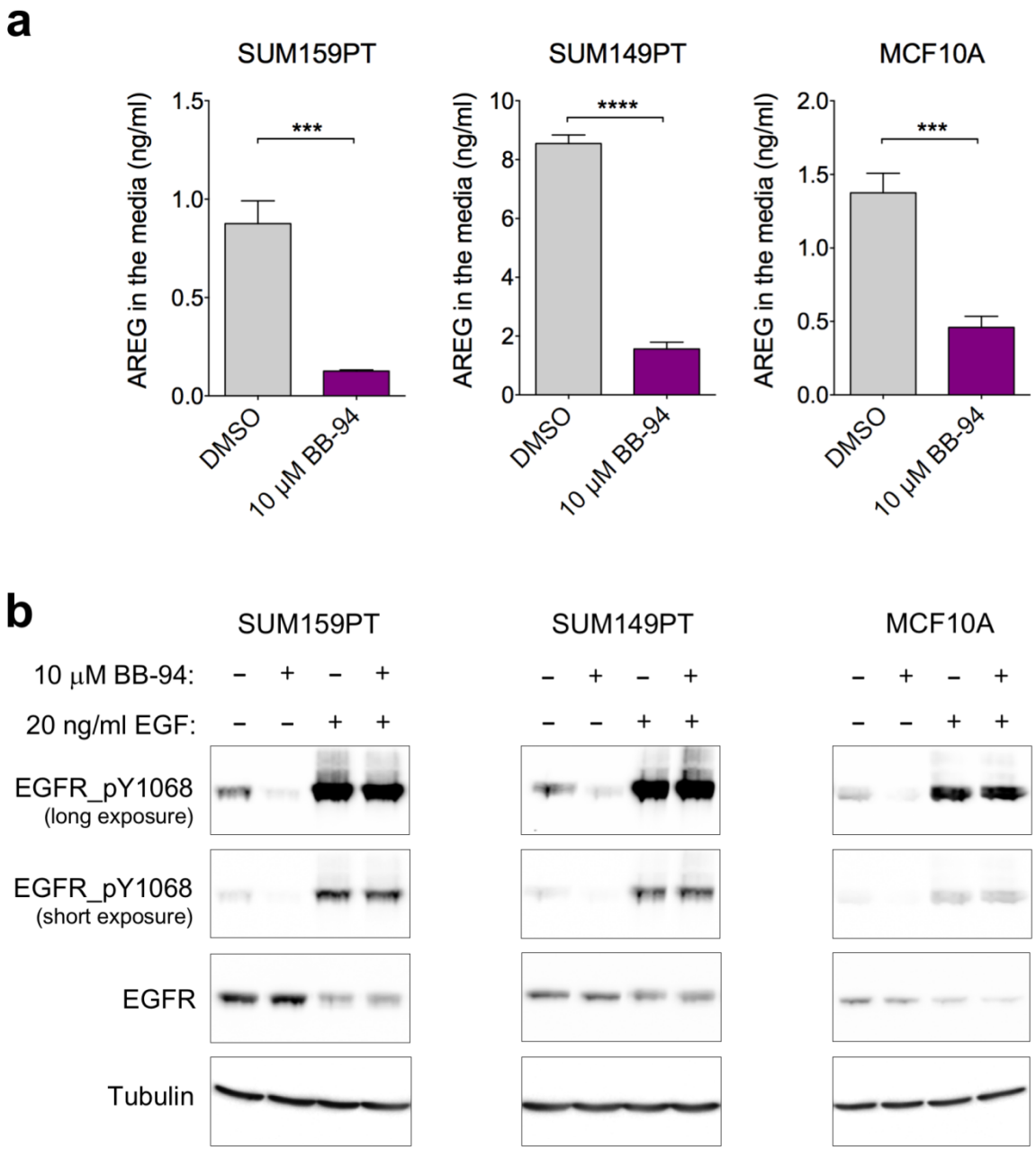

Figure 3.7 Metalloprotease inhibitor batimastat (BB-94) reduces $CD44^+/CD24^-$ population in SUM159PT cells, and this effect is blocked by the presence of constitutively active MEK1.

a Effect of 72-h treatment with BB-94 on the basal activation levels of EGFR and ERK1/2. Cells were analyzed by Western blotting using anti-phospho-EGFR, anti-total EGFR, anti-phospho-ERK1/2, or anti-total ERK1/2 antibody. **b** Effect of BB-94 on the $CD44^+/CD24^-$ marker profile, in the absence or presence of constitutively active MEK1. SUM159PT cells with stable expression of EV, MEK1-DD, or HA-MEK1-WT were treated as in (panel **a**), stained with anti-CD24-PE and anti-CD44-APC antibodies, and analyzed by flow cytometry. **c** Percentages of $CD44^+/CD24^-$ cells are shown as mean values ± S.E.M. from two independent experiments. * $P < 0.05$; ** $P < 0.01$.

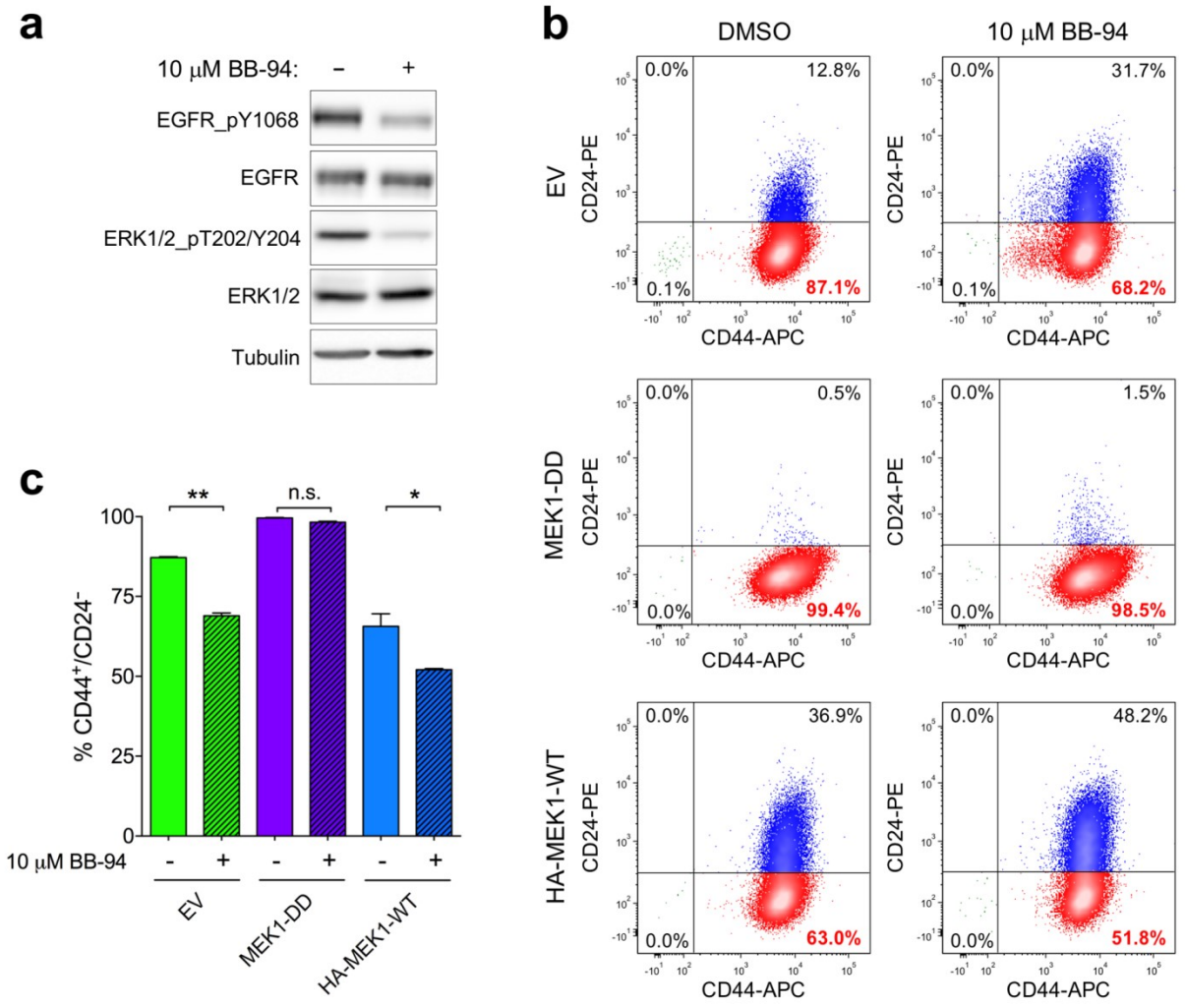

Figure 3.8 Metalloprotease inhibitor batimastat (BB-94) reduces $CD44^+/CD24^-$ population in SUM149PT cells, and this effect is blocked by the presence of constitutively active MEK1.

a Effect of 72-h treatment with BB-94 on the basal activation levels of EGFR and ERK1/2. Cells were analyzed by Western blotting using anti-phospho-EGFR, anti-total EGFR, anti-phospho-ERK1/2, or anti-total ERK1/2 antibody. **b** Effect of BB-94 on the $CD44^+/CD24^-$ marker profile, in the absence or presence of constitutively active MEK1. SUM149PT cells with stable expression of EV, MEK1-DD, or HA-MEK1-WT were treated as in (panel **a**), stained with anti-CD24-PE and anti-CD44-APC antibodies, and analyzed by flow cytometry. **c** Percentages of $CD44^+/CD24^-$ cells are shown as mean values ± S.E.M. from two independent experiments. ** $P < 0.01$; *** $P < 0.001$.

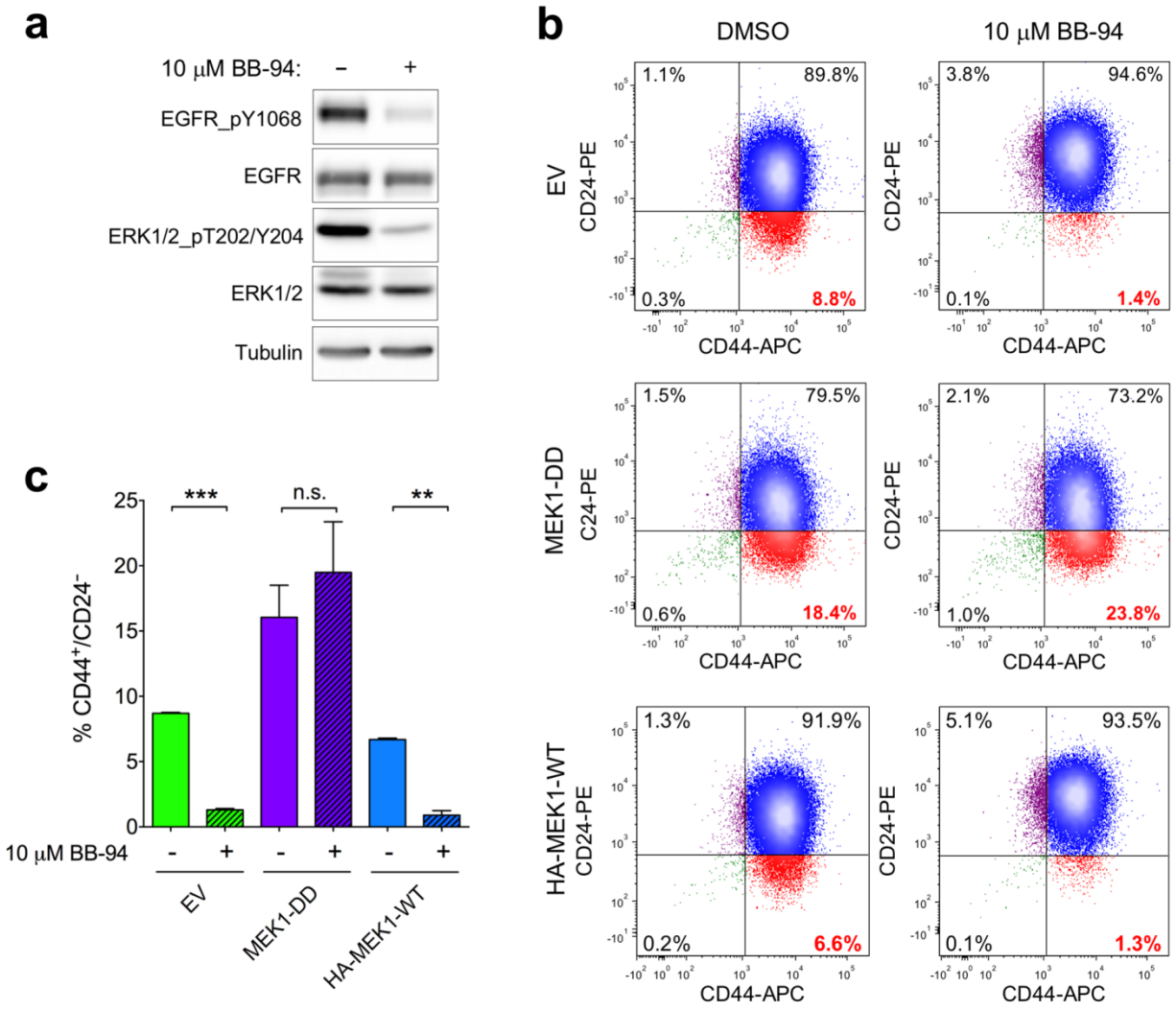

Table 3.1 Relationship between EGFR phosphorylation at Y992, Y1068, or Y1173, and MEK1/2 activation score in breast tumors from the TCGA database.

Pearson correlation coefficients and two-tailed *P* values are shown for all basal and claudin-low (CL) tumors, and for basal and CL tumors without or with *DUSP4* copy loss

Significant correlation ($P < 0.05$) is shown in bold.

MEK activation score	EGFR_pY992	EGFR_pY1068	EGFR_pY1173
All Basal and CL tumors, n=72	*r* = 0.114 *P* = 0.342	*r* = 0.190 *P* = 0.110	*r* = 0.062 *P* = 0.605
Basal and CL tumors without *DUSP4* deletion, n=34	*r* = 0.301 *P* = 0.084	***r* = 0.375** ***P* = 0.029**	*r* = 0.103 *P* = 0.563
Basal and CL tumors with hom. or het. deletion of *DUSP4*, n=38	*r* = -0.004 *P* = 0.979	*r* = 0.105 *P* = 0.531	*r* = 0.035 *P* = 0.832

Chapter 4 - Disintegrin-metalloproteases ADAM12 and ADAM9 promote the $CD44^+/CD24^-$ phenotype in the claudin-low breast cancer cell line SUM159PT through modulation of EGFR signaling

Certain parts of this chapter have been published as part of the following journal article:

Duhachek-Muggy S, Qi Y, Wise R, Alyahya L, Li H, Hodge J, Zolkiewska A (2017) Metalloprotease-disintegrin ADAM12 actively promotes the stem cell-like phenotype in claudin-low breast cancer. Mol Cancer 16:32.

Abstract

Disintegrin-metalloproteases ADAM12 and ADAM9 are upregulated and associated with an increased aggressiveness of breast cancers. ADAM12 has been more thoroughly studied and is linked to chemoresistance and epithelial to mesenchymal transition (EMT). These traits are commonly associated with a cancer stem cell-like (CSC) profile. The purpose of this study was to address the specific role that these ADAMs play in regard to modulation of the CSC phenotype in breast cancer cells. We first examined three publically available datasets and found a positive correlation between ADAM12 and an increased aggressiveness of breast cancer. Next, knockdown of ADAM12 led to a decrease in the phosphorylation of epidermal growth factor receptor (EGFR) at tyrosine 1068, and an increase in the CSC marker CD24, which was rescued upon addition of exogenous EGF, a ligand for EGFR activation. This suggested that the enhanced aggressiveness of cancers with high ADAM12 was due to the metalloprotease activity of the protein, namely the cleavage of EGFR ligand. Thus, we attempted to determine if upregulation of ADAM12 elicited a complementary effect to downregulation, but we were not

able to demonstrate this outcome. Next, we set out to determine if this effect on the CSC phenotype was specific to ADAM12. Knockdown of ADAM9 elicited a similar effect on EGFR phosphorylation and CD24 expression as ADAM12 downregulation. Therefore, we concluded that both ADAM12 and ADAM9 support the CSC phenotype is SUM159PT breast cancer cells through modulation of the EGFR pathway.

Introduction

Members of the ADAM family of cell surface metalloproteases catalyze cell context-dependent cleavage of transmembrane receptors, growth factor precursors, or adhesion molecules [1, 2]. ADAM substrates include many cancer-related proteins, such as Notch receptors and their ligands [3], epidermal growth factor receptor (EGFR) ligands [4, 5], interleukin-6 receptor (IL-6R) [6], tumor necrosis factor (TNF) and its receptors [7], E-cadherin [8], and CD44 [9]. Because ADAMs are often aberrantly expressed or misregulated in human cancers, they may contribute to tumor progression, metastasis, or therapy resistance [10, 11, 12].

Among twelve catalytically active human ADAMs [2], certain ADAMs have been shown to be upregulated in breast cancers, including ADAM 9, 12, and 17 [13]. Between these three ADAMs, both ADAM 9 and 12 are alternatively spliced and each have a transcript that encodes a longer, transmembrane isoform and a shorter, secreted isoform of the protein. However, ADAM17 is not alternatively spliced and only has a transmembrane isoform (information from UniProt). We chose to initially look at ADAM12 due to a number of reasons. First, the transmembrane isoform of ADAM12 (ADAM12-L) is highly overexpressed compared to normal mammary epithelium [14, 15]. Second, high levels of *ADAM12* transcript variant 1, which encode for the transmembrane isoform of ADAM12 (ADAM12-L) are associated with poor prognosis and decreased metastasis-free survival times in estrogen receptor (ER)-negative,

progesterone receptor (PR)-negative, and human epidermal growth factor receptor 2 (HER2)-negative (triple negative) early stage breast cancers without systemic treatment, but not in HER2-positive or ER-positive tumors [16, 17]. Finally, ADAM12-L expression is induced during epithelial-to-mesenchymal transition (EMT) in mammary epithelial cells [18] and appears to be upregulated in the claudin-low intrinsic subtype of breast cancer [19], which harbors molecular signatures of EMT.

Although claudin-low tumors amount to only ~5-10% of all breast cancers, they are clinically relevant as they are often triple negative and poorly differentiated, have elevated activities of important cellular pathways, including the EGFR pathway [20, 21, 22]. Importantly, the gene expression signatures of claudin-low tumors show a significant similarity to the signature of $CD44^{+}/CD24^{-}$ mammosphere-forming cells [21, 23], suggesting an enrichment in cancer stem cell (CSC)-like or tumor-initiating cell features. Breast CSCs are thought to be largely responsible for tumor maintenance, treatment resistance, and disease recurrence [24, 25, 26].

Our previous analysis of two clinical datasets showed that elevated expression of ADAM12 mRNA is predictive of resistance to neoadjuvant chemotherapy in ER-negative breast cancer, independent of age, tumor size, grade, and the lymph node status [19]. These observations raise a possibility that ADAM12 may serve as a marker or a therapeutic target in CSCs in ER-negative or triple-negative breast cancer (TNBC).

The goal of the current study was to assess a possible contribution of ADAM12 to the CSC phenotype of SUM159PT cells. SUM159PT is a claudin-low TNBC cell line isolated from a primary tumor of a patient with anaplastic carcinoma of the breast. Other TNBC cell lines often originate from invasive ductal carcinomas, but the exact cell types of origin of TNBC still

remains controversial. By analyzing gene expression data in various cell lines, tumor samples, and patient outcomes, and by investigating the effect of ADAM12 knockdown or overexpression on the phosphorylation status of EGFR and the CSC marker profile, we were able to determine that ADAM12 supports the CSC phenotype of SUM159PT cells. Additionally, we were able to show that this effect of ADAM12 is mostly likely not exclusive to ADAM12, as knockdown of ADAM9 had similar effect on the phosphorylation of EGFR and on the $CD44^{+}/CD24^{-}$ marker profile. Thus, we conclude that ADAMs are important modifiers of the CSC phenotype in claudin-low TNBC through the EGFR pathway, and a potential target in CSC-directed therapies.

Methods

Reagents and antibodies

SMARTpool ADAM12 siRNA (M-005118-01), SMARTpool ADAM9 siRNA (L-004504-00), and DharmaFECT1 transfection reagent were from GE Dharmacon. As a negative control, siGENOME non-targeting siRNA pool (D-001206-13) or ON-TARGETplus non-targeting siRNA pool (D-001810-10, GE Dharmacon) was used. Human recombinant EGF was from Life Technologies. Antibodies used for flow cytometry were: PE-conjugated anti-CD24 (clone ML5) and IgG2aκ isotype control (clone G155-178, both from BD Biosciences), APC-conjugated anti-CD24 (clone eBioSN3 (SN3 A5-2H10)) and IgG1κ isotype control (clone P3.6.2.8.1, both from Affymetrix eBioscience), APC or FITC-conjugated anti-CD44 (clone IM7) and IgG2bκ isotype control (clone eB149/10H5, both from Affymetrix eBioscience), anti-ADAM12 (clone 632525) and IgG1 isotype control (clone 11711, both from R&D Systems). APC-conjugated secondary anti-mouse IgG1 antibodies were from Jackson ImmunoResearch. For Western blotting, the following antibodies were used: rabbit monoclonal anti-pY1068 EGFR (clone D7A5), anti-total EGFR (clone D38B1), anti-pT202/Y204 ERK1/2 (clone D13.14.4E),

and anti-ERK1/2 (clone 137F5) all from Cell Signaling Technology, and rabbit polyclonal anti-ADAM12 antibody (Ab#3394) raised against the cytoplasmic tail of human ADAM12 [17].

Cell culture

The SUM159PT cell line was purchased from Asterand and HEK293T cells were from Thermo Scientific. The cell line was authenticated by the original supplier using the short tandem repeat (STR) analysis and has been passaged for fewer than 6 months after culture initiation from an early passage number. SUM159PT cells were cultured in Ham's F-12 medium supplemented with 5% fetal bovine serum (FBS), 10 mM HEPES, 5 μg/ml insulin, and 1 μg/ml hydrocortisone. HEK293T cells were cultured in DMEM medium containing 10% FBS, 6 mM glutamine, and 1 mM pyruvate. Cells were maintained at 37°C under humidified atmosphere containing 5% CO_2.

Lentiviral infection and generation of an inducible overexpression system

Lentiviruses were produced by transfecting HEK293T cells with pInducer20-ADAM12 Wild-type or E351Q, a catalytically inactive mutant, pMD2.G, and psPAX2 (Addgene, plasmids 12259 and 12260, respectively) using Mirus TransIT transfection reagent (Mirus). Conditioned media containing viral particles were harvested 48 h after transfection, supplemented with 5 μg/ml polybrene (Sigma), and added onto SUM159PT cells at ~20% confluence. Selection of stably transduced cells started 48 h after infection using 500 μg/ml neomycin and continued for 14 days.

Data mining

Calculation of the CSC, and EGFR gene expression signature scores

Genes (355 different genes corresponding to 493 individual transcripts) significantly upregulated or downregulated in $CD44^+/CD24^-$ subpopulations of primary breast cancer cells

and in cancer mammospheres [23] were used to calculate the CSC signature scores. Expression values for these CSC-related genes in 51 different breast cancer cell lines were retrieved from Gene Expression Omnibus (GEO, http://www.ncbi.nlm.nih.gov/geo/), using accession number GSE69017. The top 250 genes whose expression was most significantly changed upon stable expression of EGFR in MCF7 cells [28] were used to calculate EGFR-responsive gene signature scores. Expression values for these EGFR-regulated genes were retrieved from GEO, using accession number GSE3542. The expression values for ADAM12 or CSC- and EGFR-related genes in breast invasive carcinomas were extracted from TCGA (Cell 2015 dataset) [29] via the cBioPortal (http://www.cbioportal.org/public-portal/). The signature scores were then calculated for all tumors for which gene expression values were available (a total of 421 tumors) as:

$$s = \sum_i w_i x_i / \sum_i |w_i|$$

where w is the weight +1 or –1, depending on whether the gene was upregulated or downregulated in the signature, and x is the normalized gene expression level.

Survival Analysis

The effect of ADAM12 expression on relapse-free survival rates of breast cancer patients was assessed using the Kaplan-Meier Plotter (http://kmplot.com/analysis/). This online tool uses manually curated database containing gene expression data and relapse free and overall survival information downloaded from GEO, the European Genome-Phenome Archive (EGA), and TCGA [30]. The parameters were set as follows: Affymetrix probeset: 202952_s_at (as this probeset is specific for ADAM12 transcript variant 1, encoding ADAM12-L); Auto select best cutoff: On; Use array quality control: Remove redundant samples, Exclude outlier arrays; Check proportional hazards assumption: On; Restrict analysis to subtypes: All, or ER-negative (derive

ER status from gene expression data: On), PR-negative, HER2-negative, or Mesenchymal stem-like; Restrict analysis to selected cohorts: none; Database release: 2017; Datasets: all.

Immunoblotting

Immunoblotting was performed as described [17, 19], with some modifications. Lysis buffer was supplemented with phosphatase inhibitors (50 mM NaF, 2 mM Na_3VO_4, and 10 mM $Na_4P_2O_7$). Total cell lysates were directly analyzed by Western blotting. Nitrocellulose membranes were incubated with primary monoclonal antibodies and HRP-conjugated secondary antibodies, followed by signal detection using SuperSignal West Pico chemiluminescence detection kit (Pierce) and Azure c500 digital imaging system. Band intensities were quantified using the ImageJ analysis software.

Flow cytometry

CD24 and CD44 staining: Three days after transfection (for knockdown) or two days after addition of 2 μg/ml doxycycline (for overexpression), cells were stained with PE- or APC-conjugated anti-CD24 and APC- or FITC-conjugated anti-CD44 antibodies, or their respective isotype antibody controls, and analyzed by flow cytometry. **ADAM12 staining**: Cells were incubated with anti-ADAM12 antibody or mouse IgG1 isotype control antibody, washed and incubated with APC-conjugated anti-mouse IgG antibody. Cells were analyzed with a BD FACSCalibur cytometer or a LSR Fortessa X20 instrument. Data were analyzed with FCS Express 4 or 6 (DeNovo Software).

Results

ADAM12 expression in breast cancer cell lines and tumor samples is correlated with increased aggressiveness and a poor patient prognosis

In order to further investigate the importance of ADAM12, we examined its mRNA levels in a larger pool of 51 breast cancer cell lines [27] (Fig. 4.1a) and patient samples from the TCGA database (Fig. 4.1b). To have an objective indication of the aggressiveness of these cell lines or tumor samples, a cancer stem cell (CSC) signature score was determined based on the genes whose expression was most significantly changed in $CD44^{+}/CD24^{-}$ populations and in mammosphere-forming cells, as reported by Creighton et al. [23] and described in Methods. As shown in Fig. 4.1a, there was a significant positive correlation between CSC scores and *ADAM12* mRNA levels (P = 1.4E-07), indicating that breast cancer cell lines which had higher stem cell characteristics also had increased levels of *ADAM12*. Cell lines emphasized in red in Fig. 4.1a indicate various representative intrinsic molecular subtypes of breast cancer, including claudin-low (SUM159PT, Hs578T, SUM1315MO2, and BT549), basal (SUM102PT and SUM149PT), and luminal (MCF-7 and SUM225CWN) [20]. Additionally, in tumor samples retrieved from the Cell 2015 breast cancer dataset of the TCGA database there was also a significant positive correlation between *ADAM12* mRNA and the CSC score (P = 4.8E-13, Fig. 4.1b). Furthermore, the relapse-free survival (RFS) analysis demonstrated that high expression of the *ADAM12* gene was correlated with poor prognosis in 196 patients with TNBC and, most importantly, in 59 patients with the mesenchymal stem-like (MSL) subtype of TNBC, but not in a general breast cancer patient population (Fig. 4.1c, assessed by the Kaplan-Meier Plotter online tool, ref. [30]). Notably, the MSL subtype shares many features with the claudin-low subtype of breast cancer, including high expression of EMT- and CSC-related genes [31]. Overall, these

data indicate that an increased expression of *ADAM12* mRNA is correlated with a more aggressive subtype of breast cancer.

ADAM12 supports the CSC phenotype via modulation of the EGFR pathway

In order to investigate the role of ADAM12 in the modulation of the CSC phenotype, we used a pool of four siRNAs that effectively eliminated the cell surface expression of ADAM12 compared to a control pool, as measured by flow cytometry (Fig. 4.2a). As ADAMs have been shown to influence EGFR by cleavage of its ligands [1, 10] and based on previous evidence from our lab, including RNA sequencing results, we decided to test a hypothesis that ADAM12 influences the CSC phenotype by facilitating the cleavage of EGFR ligands and modifying the EGFR signaling pathway. First, we examined the effect of ADAM12 knockdown on the basal activation level of EGFR. We observed that transfection of SUM159PT cells with pooled ADAM12 siRNAs decreased the level of EGFR phosphorylation at Y1068 by ~55% (Fig. 4.2b). This result supported a model in which ADAM12 sustained the basal level of activation of EGFR by mediating the release of endogenous EGF-like ligands. To further explore the ADAM12-mediated effect on CSC features and the role of EGFR in this process, cells were transfected with either siADAM12 or a non-targeting control, treated for two days with exogenous EGF, and the cell surface expression of CD44/CD24 markers was evaluated by flow cytometry. First, we observed that knockdown of ADAM12 substantially decreased the population of $CD44^+/CD24^-$ cells. Additionally, while treatment with exogenous EGF increased the pool of $CD44^+/CD24^-$ cells, ADAM12 knockdown did not have any effect on CD44 or CD24 expression in the presence of EGF (Fig. 4.2c). These results suggested that downregulation of EGFR activation by ADAM12 knockdown was required for a reduction of CSC-containing $CD44^+/CD24^-$ cell population. To further validate our results, we explored the relationships

between *ADAM12* expression and the EGFR-responsive gene signature scores in 421 tumors from the TCGA database. The EGFR scores were calculated based on the gene expression profiling of MCF-7 breast cancer cells overexpressing EGFR [28]. We observed positive correlations between *ADAM12* expression and the EGFR score ($P = 3.2E-13$, Fig. 4.2d). Importantly, *ADAM12* expression itself was not significantly changed by manipulations of EGFR in MCF-7 cells [28].

Overexpression of ADAM12 does not increase the population of cells expressing a CSC phenotype

To determine whether overexpression of ADAM12 elicited a complementary effect to what was observed with knockdown, we used a doxycycline (dox)-inducible overexpression system. Wild-type ADAM12 or a catalytically inactive mutant, E351Q, was cloned into a pInducer20 vector and stably transduced into SUM159PT cells. Treatment for 48 hours with 2 μg/ml doxycycline significantly increased the amount both the nascent, full length protein (top band) and the processed active form of ADAM12 which lacks the prodomain (bottom band) (Fig. 4.3a). Additionally, we confirmed that the overexpressed ADAM12 was present on the cell surface, where it is involved in ectodomain shedding. When doxycycline was added, the amount of ADAM12 present at the cell surface significantly increased in both the wild-type ADAM12 and the E351Q mutant (Fig. 4.3b). Additionally, the difference between isotype control and non-induced ADAM12 samples reflect the endogenous levels of ADAM12 present in these cells. It is important to note that the presence of the E351Q mutation did not significantly alter the amount of the processed form of ADAM12 (Fig. 4.3a) and the amount of ADAM12 at the cell surface (Fig. 4.3b). After confirming induction of ADAM12 expression by doxycycline, we tested if overexpression of ADAM12 resulted in a decrease in the CSC marker, CD24. Unfortunately, we

did not see a significant change in CD24 (Fig. 4.3c) or CD44 (data not shown) between –Dox and +Dox samples in SUM159PT cells overexpressing either wild-type or E351Q ADAM12. A reason could be that the maximum amount of EGFR signaling due to ligand cleavage has already been established with the endogenous levels of ADAM12.

ADAM9 elicits similar effects as ADAM12 on the CSC populations

As our hypothesis states that the resulting effect on the CSC populations was the result of EGFR activation due ligand cleavage, we next asked if another disintegrin-metalloprotease could elicit the same effect on the $CD44^{+}/CD24^{-}$ populations as ADAM12. We chose to examine ADAM9, as its expression is high in SUM159PT cells (based on RNA sequencing results, data not shown). As shown in Fig. 4.4a, ADAM12 and ADAM9 sequences are fairly dissimilar (~40% identical), but there are certain important residues that are conserved, including those residues that are responsible for the catalytic activity of ADAMs. There are certain transmembrane ligand precursors that both ADAM12 and ADAM9 have been shown to cleave, including HB-EGF and Delta-like ligand-1 [2]. However, there are also substrates that are specific to each individual ADAM. Due to the differences in their protein sequences, it is conceivable that ADAM12 could influence the CSC populations through EGFR by cleavage of a specific ligand that may not be cleaved by other ADAMs. Therefore, we first looked at the change in phosphorylation status of Y1068 of EGFR in cells transfected with either a control siRNA or ADAM9-targeting siRNAs. We found that knockdown of ADAM9 reduced the phosphorylation level of EGFR at Y1068 to approximately the same extent as ADAM12 knockdown (Fig.4.4b). Additionally, the phosphorylation of ERK, a downstream target of EGFR signaling, was attenuated compared to the control (Fig.4.4b). Since ADAM9 knockdown elicited an identical effect on the phosphorylation of EGFR as ADAM12 knockdown, we asked if the

$CD44^+/CD24^-$ populations would be similarly affected. As expected, the cell surface expression of CD24 increased upon ADAM9 knockdown, while CD44 expression was unchanged (Fig. 4.4c).

Based on our results, we propose a model where ADAMs contribute to the activation of EGFR by releasing EGF-like ligands from the cell surface, and ultimately to the expansion of CSC populations.

Discussion

The EGFR pathway activation has been frequently observed in claudin-low TNBCs and cell lines bearing CSC-like features [21], and several reports indicated that EGFR is a positive regulator of CSCs. For example, stimulation of the EGFR pathway promoted mammosphere formation by normal breast stem cells and by ductal carcinoma in situ (DCIS)-derived epithelial cells [48]. Recently, it has been reported that cetuximab, a monoclonal anti-EGFR antibody, reduced mammosphere formation and CSC populations in breast cancer cells in vitro and potentiated the effect of Ixabepilone, a new generation microtubule-stabilizing agent, in treating orthotopic TNBC xenografts [32]. Furthermore, in A431 epidermoid cancer cells, treatment with cetuximab upregulated the expression of the epithelial markers E-cadherin and occludin, downregulated the epithelial transcriptional repressors Zeb, Snail, and Slug, and reduced the $CD44^+/CD24^-$ phenotype [33]. EGFR activation also promoted acquisition of CSC properties in head and neck squamous cell carcinoma [34, 35] and in nasopharyngeal carcinoma [36], pointing to a more general function of EGFR in CSC biology.

The postulated mechanisms by which EGFR promotes the CSC features in TNBC cells include the activation of MEK/ERK signaling [37], which is also supported by the change in ERK phosphorylation in Fig. 4.4b, the STAT3 pathway [22], and/or autophagy [32]. For

example, blocking ERK activation in claudin-low cell lines by MEK inhibitors or by forced expression of DUSP4, dual specificity phosphatase-4 that is a negative regulator of ERK, has been shown to reduce the $CD44^{+}/CD24^{-}$ populations in vitro and to diminish tumor initiating populations in vivo [37]. STAT3, which is another downstream effector of EGFR, has been recently reported to be preferentially activated in tumor-initiating cells/CSCs in claudin-low breast cancer [22], raising a possibility that it might, at least partially, mediate the downstream effects of EGFR on CSC properties of claudin-low cells.

EGFR is activated by soluble ligands that are synthesized as transmembrane precursors and need to be released from the cell surface by ADAM proteases [5, 38]. In many cell types and tissues, ADAM17 or ADAM10 act as dedicated and robust EGFR ligand "sheddases" [1, 10]. Likewise, it has been postulated that ADAM17 is the main ADAM responsible for EGFR ligand cleavage and activation of EGFR in breast cancer [39, 40, 41]. However, other ADAMs, including ADAM9 and ADAM12, may mediate the release of soluble EGFR ligands as well. For example, ADAM12 was shown to act as a sheddase for heparin-binding EGF-like growth factor (HB-EGF) during cardiac hypertrophy [42] and under hypoxia in head and neck, lung, and pancreatic cancer cells, leading to the formation of invadopodia and increasing cancer cell invasion [43]. ADAM9 has been proposed to cleave proHB-EGF [44], however Weskamp, et al. found that there was no difference in HB-EGF secretion between mice lacking ADAM9 or wild-type mice [45]. Whether ADAM9/12 activate EGFR in breast cancer cells and, in particular, whether ADAM9 or ADAM12-mediated EGFR activation promotes the acquisition of the breast CSC phenotype, has not been sufficiently explored.

In this report, we have identified ADAM9 and ADAM12 as modifiers of both the EGFR activation and the $CD44^{+}/CD24^{-}$ marker profile in SUM159PT cells. Using publically available

datasets, we show that ADAM12 mRNA levels were the highest in claudin-low cell lines and a general population of breast tumors that displayed an increases CSC score. Also, in a dataset of 196 TNBCs and 59 MSL TNBCs, high ADAM12 expression was associated with decreased metastasis-free survival times. Additionally, our previous analysis of two clinical datasets showed that high expression of ADAM12 was predictive of resistance to neoadjuvant chemotherapy in ER-negative breast cancer [19]. This is fully consistent with ADAM12 being an EMT- and CSC-related gene, as both EMT and CSCs contribute to drug resistance [46, 47]. To further validate and test these important correlations, down-regulation of both ADAM9 and ADAM12 decreased the basal activation levels of EGFR and reduced the CSC phenotype in vitro. An increased level of ADAM12 mRNA was correlated to a higher EGFR activation score in 421 breast invasive cancers, while ADAM12 mRNA itself was not significantly changed by induction of EGFR, indicating a causal relationship between high ADAM12 and increased EGFR activity. However, overexpression of ADAM12 was not able to decrease the overall amount of CD24 present at the cell surface, as the amount of CD24 in cells overexpressing an inducible wild-type form of ADAM12 was the same as those with an inactivating mutation (E351Q). Nevertheless, this result alone does not disqualify ADAM12 as a potential regulator of EGFR signaling by release of ligands, as the amount of transmembrane precursors might be a limiting factor. Thus, maximum cleavage levels of ligands responsible for EGFR activation may have already been established due to the endogenous amount of ADAMs, and further tests exploring the relationship between the CSC phenotype and ADAM12 are warranted. Additionally, future tests confirming the lack of cell apoptosis in ADAM12-overexpressing cells should be done by using dyes that allow visualization of apoptotic cells, such as Annexin V.

Current treatments of TNBC rely mainly on chemotherapy, as there are no targeted therapies specifically approved for this type of breast cancer [48]. EGFR is expressed in 60-70% of TNBCs [49, 50], raising an early hope for EGFR-targeted therapies in TNBC. Two completed clinical trials investigated the therapeutic potential of cetuximab, as a single agent or in addition to cisplatin chemotherapy, in unselected TNBC patients with metastatic disease [51, 52]. While the results have been disappointing and there was no significant effect on progression-free or overall patient survival, it is becoming clear that EGFR expression alone does not necessarily indicate tumor cell dependence on EGFR signaling and further molecular stratifications and patient selections are needed in future trials [48, 53, 54]. We propose that ADAMs, especially ADAM12, may be an important biomarker in identifying TNBCs with over-activation of the EGFR pathway and may help select patients that would better respond to EGFR inhibitors. In addition, further detailed studies of ADAM12-mediated regulation of the EGFR pathway should establish whether ADAM12 itself may be a suitable target for CSC-like populations in claudin-low TNBC.

Acknowledgements

This work was supported by NIH grant R01CA172222 to Dr. Anna Zolkiewska. This is contribution 16-371-J from Kansas Agricultural Experiment Station. I would like to acknowledge Dr. Anna Zolkiewska who performed the data mining presented in Figure 4.1c, and Dr. Yue Qi who performed the confirmation of ADAM12 knockdown experiment shown in Figure 4.2a. Figures 4.1 and 4.2 were taken from the larger publication referenced at the beginning of this chapter. All experiments for the figures in this chapter (besides Figure 4.1c and 4.2a, as mentioned above) were performed by Randi Wise.

References

1. Jones JC, Rustagi S, Dempsey PJ (2016) ADAM proteases and gastrointestinal function. Annu Rev Physiol 78:243-76.

2. Edwards DR, Handsley MM, Pennington CJ (2008) The ADAM metalloproteinases. Mol Aspects Med 29:258-89.

3. van Tetering G, van Diest P, Verlaan I, van der Wall E, Kopan R, Vooijs M (2009) Metalloprotease ADAM10 is required for Notch1 site 2 cleavage. J Biol Chem 284:31018-27.

4. Blobel CP (2005) ADAMs: key components in EGFR signalling and development. Nature Rev Mol Cell Biol 6:32-43.

5. Kataoka H (2009) EGFR ligands and their signaling scissors, ADAMs, as new molecular targets for anticancer treatments. J Dermatol Sci 56:148-53.

6. Schaper F, Rose-John S (2015) Interleukin-6: Biology, signaling and strategies of blockade. Cytokine Growth Factor Rev 26:475-87.

7. Maney SK, McIlwain DR, Polz R, Pandyra AA, Sundaram B, Wolff D, et al (2015) Deletions in the cytoplasmic domain of iRhom1 and iRhom2 promote shedding of the TNF receptor by the protease ADAM17. Sci Signal 8:ra109.

8. Maretzky T, Reiss K, Ludwig A, Buchholz J, Scholz F, Proksch E, et al (2005) ADAM10 mediates E-cadherin shedding and regulates epithelial cell-cell adhesion, migration, and β-catenin translocation. Proc Natl Acad Sci USA 102:9182-7.

9. Hartmann M, Parra LM, Ruschel A, Bohme S, Li Y, Morrison H, et al (2015) Tumor suppressor NF2 blocks cellular migration by inhibiting ectodomain cleavage of CD44. Mol Cancer Res 13:879-90.

10. Mullooly M, McGowan P, Crown J, Duffy MJ (2016) The ADAMs family of proteases as targets for the treatment of cancer. Cancer Biol Ther 17:870-80.

11. Lopez-Otin C, Hunter T (2010). The regulatory crosstalk between kinases and proteases in cancer. Nat Rev Cancer 10:278-92.

12. Murphy G (2008) The ADAMs: signalling scissors in the tumour microenvironment. Nature Rev Cancer 8:929-41.

13. Lendeckel U, Kohl J, Arndt M, Carl-McGrath S, Donat H, Röcken C (2005) Increased expression of ADAM family members in human breast cancer and breast cancer cell lines. J Cancer Res Clin Oncol 131:41-48.

14. Kveiborg M, Frohlich C, Albrechtsen R, Tischler V, Dietrich N, Holck P, et al (2005) A role for ADAM12 in breast tumor progression and stromal cell apoptosis. Cancer Res 65:4754-61.

15. Bertucci F, Finetti P, Cervera N, Charafe-Jauffret E, Mamessier E, Adelaide J, et al (2006) Gene expression profiling shows medullary breast cancer is a subgroup of basal breast cancers. Cancer Res 66:4636-44.

16. Wang Y, Klijn JG, Zhang Y, Sieuwerts AM, Look MP, Yang F, et al (2005) Gene-expression profiles to predict distant metastasis of lymph-node-negative primary breast cancer. Lancet 365:671-9.

17. Li H, Duhachek-Muggy S, Qi Y, Hong Y, Behbod F, Zolkiewska A (2012) An essential role of metalloprotease-disintegrin ADAM12 in triple-negative breast cancer. Breast Cancer Res Treat 135:759-69.

18. Ruff M, Leyme A, Le Cann F, Bonnier D, Le Seyec J, Chesnel F, et al (2015) The Disintegrin and metalloprotease ADAM12 is associated with TGF-β-induced epithelial to mesenchymal transition. PLoS One 10:e0139179.

19. Li H, Duhachek-Muggy S, Dubnicka S, Zolkiewska A (2013) Metalloproteinase-disintegrin ADAM12 is associated with a breast tumor-initiating cell phenotype. Breast Cancer Res Treat 139:691-703.

20. Prat A, Parker JS, Karginova O, Fan C, Livasy C, Herschkowitz JI, et al (2010) Phenotypic and molecular characterization of the claudin-low intrinsic subtype of breast cancer. Breast Cancer Res 12:R68.

21. Sabatier R, Finetti P, Guille A, Adelaide J, Chaffanet M, Viens P, et al (2014) Claudin-low breast cancers: Clinical, pathological, molecular and prognostic characterization. Mol Cancer 13:228.

22. Wei W, Tweardy DJ, Zhang M, Zhang X, Landua J, Petrovic I, et al (2014) STAT3 signaling is activated preferentially in tumor-initiating cells in claudin-low models of human breast cancer. Stem Cells 32:2571-82.

23. Creighton CJ, Li X, Landis M, Dixon JM, Neumeister VM, Sjolund A, et al (2009) Residual breast cancers after conventional therapy display mesenchymal as well as tumor-initiating features. Proc Natl Acad Sci USA 106:13820-5.

24. Wei W, Lewis MT (2015) Identifying and targeting tumor-initiating cells in the treatment of breast cancer. Endocr Relat Cancer 22:R135-55.

25. Colak S, Medema JP (2014) Cancer stem cells-important players in tumor therapy resistance. FEBS J 281:4779-91.

26. Visvader JE, Lindeman GJ (2012) Cancer stem cells: current status and evolving complexities. Cell Stem Cell 10:717-28.

27. Neve RM, Chin K, Fridlyand J, Yeh J, Baehner FL, Fevr T, et al (2006) A collection of breast cancer cell lines for the study of functionally distinct cancer subtypes. Cancer Cell 10:515-27.

28. Creighton CJ, Hilger AM, Murthy S, Rae JM, Chinnaiyan AM, El-Ashry D (2006) Activation of mitogen-activated protein kinase in estrogen receptor α-positive breast cancer cells in vitro induces an in vivo molecular phenotype of estrogen receptor α-negative human breast tumors. Cancer Res 66:3903-11.

29. Ciriello G, Gatza ML, Beck AH, Wilkerson MD, Rhie SK, Pastore A, et al (2015) Comprehensive molecular portraits of invasive lobular breast cancer. Cell 163:506-19.

30. Gyorffy B, Lanczky A, Eklund AC, Denkert C, Budczies J, Li Q, et al (2010) An online survival analysis tool to rapidly assess the effect of 22,277 genes on breast cancer prognosis using microarray data of 1,809 patients. Breast Cancer Res Treat 123:725-31.

31. Lehmann BD, Pietenpol JA (2014) Identification and use of biomarkers in treatment strategies for triple-negative breast cancer subtypes. J Pathol 232:142-50.

32. Tanei T, Choi DS, Rodriguez AA, Liang DH, Dobrolecki L, Ghosh M, et al (2016) Antitumor activity of Cetuximab in combination with Ixabepilone on triple negative breast cancer stem cells. Breast Cancer Res 18:6.

33. Oliveras-Ferraros C, Vazquez-Martin A, Cufi S, Queralt B, Baez L, Guardeno R, et al (2011) Stem cell property epithelial-to-mesenchymal transition is a core transcriptional network for predicting cetuximab (Erbitux) efficacy in KRAS wild-type tumor cells. J Cell Biochem 112:10-29.

34. Abhold EL, Kiang A, Rahimy E, Kuo SZ, Wang-Rodriguez J, Lopez JP, et al (2012) EGFR kinase promotes acquisition of stem cell-like properties: a potential therapeutic target in head and neck squamous cell carcinoma stem cells. PLoS One 7:e32459.

35. Leong HS, Chong FT, Sew PH, Lau DP, Wong BH, Teh BT, et al (2014) Targeting cancer stem cell plasticity through modulation of epidermal growth factor and insulin-like growth factor receptor signaling in head and neck squamous cell cancer. Stem Cells Transl Med 3:1055-65.

36. Ma L, Zhang G, Miao XB, Deng XB, Wu Y, Liu Y, et al (2013) Cancer stem-like cell properties are regulated by EGFR/AKT/β-catenin signaling and preferentially inhibited by gefitinib in nasopharyngeal carcinoma. FEBS J 280:2027-41.

37. Balko JM, Schwarz LJ, Bhola NE, Kurupi R, Owens P, Miller TW, et al (2013) Activation of MAPK pathways due to DUSP4 loss promotes cancer stem cell-like phenotypes in basal-like breast cancer. Cancer Res 73:6346-58.

38. Blobel CP (2005) ADAMs: key components in EGFR signalling and development. Nat Rev Mol Cell Biol 6:32-43.

39. Kenny PA, Bissell MJ (2007) Targeting TACE-dependent EGFR ligand shedding in breast cancer. J Clin Invest 117:337-45.

40. Kenny PA (2007) TACE: a new target in epidermal growth factor receptor dependent tumors. Differentiation 75:800-8.

41. Giricz O, Calvo V, Peterson EA, Abouzeid CM, Kenny PA (2013) TACE-dependent TGFα shedding drives triple-negative breast cancer cell invasion. Int J Cancer 133:2587-95.

42. Asakura M, Kitakaze M, Takashima S, Liao Y, Ishikura F, Yoshinaka T, et al (2002) Cardiac hypertrophy is inhibited by antagonism of ADAM12 processing of HB-EGF: metalloproteinase inhibitors as a new therapy. Nat Med 8:35-40.

43. Diaz B, Yuen A, Iizuka S, Higashiyama S, Courtneidge SA (2013) Notch increases the shedding of HB-EGF by ADAM12 to potentiate invadopodia formation in hypoxia. J Cell Biol 201:279-92.

44. Izumi Y, Hirata M, Hasuwa H, Iwamoto R, Umata T, et al (1998) A metalloprotease-disintegrin, MDC9/meltrin-y/ADAM9 and PKC0 are involved in TPA-induced ectodomain shedding of membrane-anchored heparin-binding EGF-like growth factor. EMBO J 17:7260-7272.

45. Weskamp G, Cai H, Brodie T, Higashyama S, Manova K, et al (2002) Mice lacking the metalloprotease-disintegrin MDC9 (ADAM9) have no evident major abnormalities during development or adult life. Mol Cel Biol 22:1537-1544.

46. Singh A, Settleman J (2010) EMT, cancer stem cells and drug resistance: an emerging axis of evil in the war on cancer. Oncogene 29:4741-51.

47. Nistico P, Bissell MJ, Radisky DC (2012) Epithelial-mesenchymal transition: general principles and pathological relevance with special emphasis on the role of matrix metalloproteinases. Cold Spring Harb Perspect Biol 4.

48. Turner NC, Reis-Filho JS (2013) Tackling the diversity of triple-negative breast cancer. Clin Cancer Res. 2013;19:6380-8.

49. Corkery B, Crown J, Clynes M, O'Donovan N (2009) Epidermal growth factor receptor as a potential therapeutic target in triple-negative breast cancer. Ann Oncol 20:862-7.

50. Hoadley KA, Weigman VJ, Fan C, Sawyer LR, He X, Troester MA, et al (2007) EGFR associated expression profiles vary with breast tumor subtype. BMC Genomics 8:258.

51. Carey LA, Rugo HS, Marcom PK, Mayer EL, Esteva FJ, Ma CX, et al (2012) TBCRC 001: randomized phase II study of cetuximab in combination with carboplatin in stage IV triple-negative breast cancer. J Clin Oncol 30:2615-23.

52. Baselga J, Gomez P, Greil R, Braga S, Climent MA, Wardley AM, et al (2013) Randomized phase II study of the anti-epidermal growth factor receptor monoclonal

antibody cetuximab with cisplatin versus cisplatin alone in patients with metastatic triple-negative breast cancer. J Clin Oncol 31:2586-92.

53. Williams CB, Soloff AC, Ethier SP, Yeh ES (2015) Perspectives on epidermal growth factor receptor regulation in triple-negative breast cancer: Ligand-mediated mechanisms of receptor regulation and potential for clinical targeting. Adv Cancer Res 127:253-81.

54. Masuda H, Zhang D, Bartholomeusz C, Doihara H, Hortobagyi GN, Ueno NT (2012) Role of epidermal growth factor receptor in breast cancer. Breast Cancer Res Treat 136:331-45.

Figure 4.1 ADAM12 is associated with a CSC signature and poor patient prognosis.

a CSC signature score versus ADAM12 mRNA expression in 51 breast cancer cell lines. The CSC signature scores were calculated based on ref. [23] and microarray expression data retrieved from GEO:GSE69017, as described in Methods. **b** CSC signature score versus ADAM12 mRNA expression in 421 breast invasive carcinomas from the TCGA database (Cell 2015 dataset). The CSC signature scores were calculated based on ref. [23], as described in Methods. **c** Relapse-free (RFS) rates for breast cancer patients stratified by ADAM12 expression levels were estimated using Kaplan-Meier Plotter (http://kmplot.com/analysis/) [30]. Shown are all tumors, triple-negative (TN) tumors, or tumors classified as mesenchymal stem-like (MSL). Hazard ratio (HR), 95% confidence interval, P-values, and number of patients are also included.

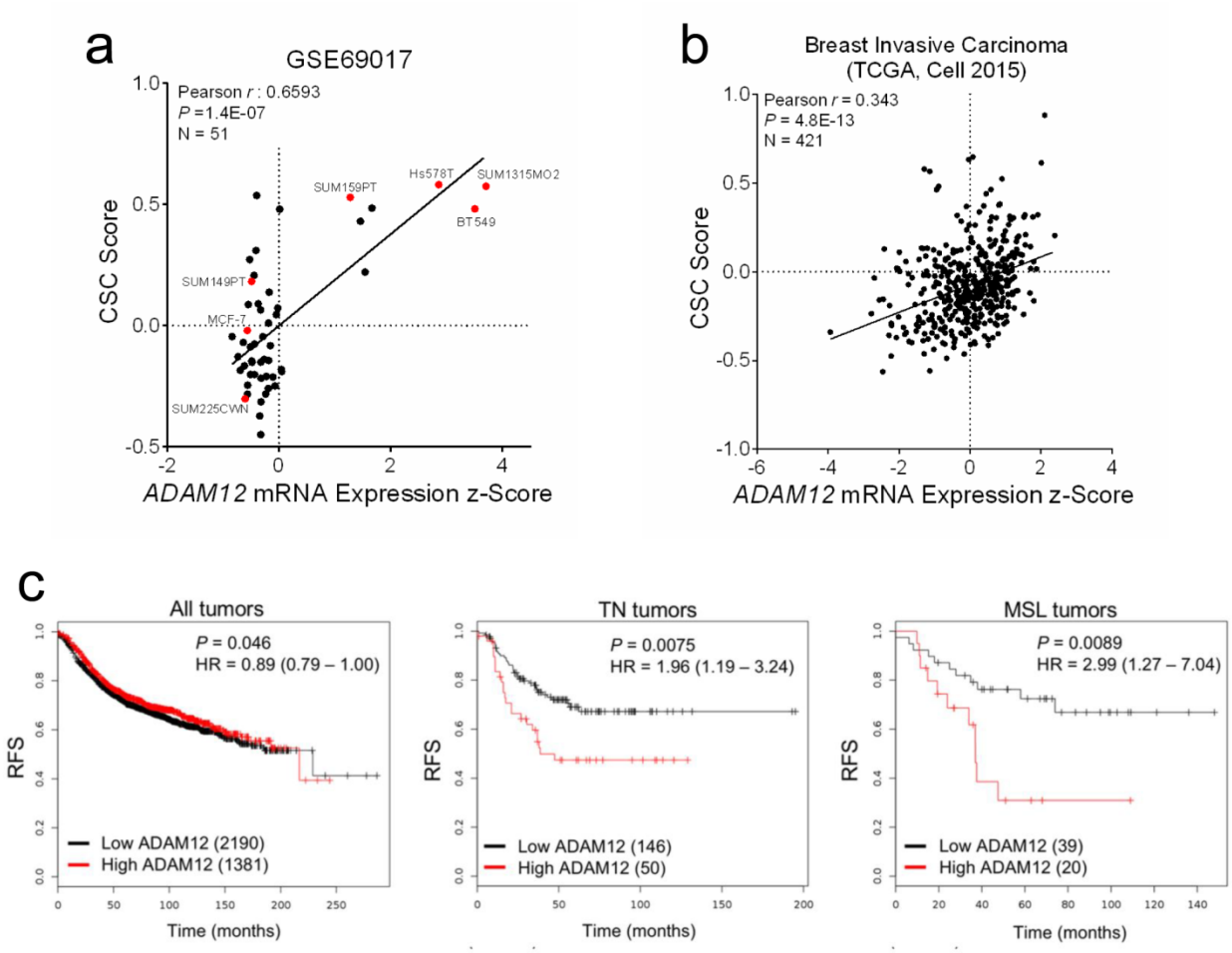

Figure 4.2 ADAM12 supports the CSC phenotype via modulation of the EGFR pathway.

a SUM159PT cells were transfected with a pool of four siRNAs targeting ADAM12 or a pool of control siRNAs. Cell surface expression of ADAM12 was evaluated by flow cytometry to confirm the knockdown. **b** SUM159PT cells were transfected with a pool of four control siRNAs (siControl) or a pool of four ADAM12 siRNAs (siADAM12) and analyzed three days later by Western blotting. **c** Activation of EGFR by exogenous EGF bypasses the effect of ADAM12 knockdown on the reduction of $CD44^{hi}/CD24^{-/lo}$ cell population. SUM159PT cells were transfected with a pool of four control siRNAs (siControl) or a pool of four ADAM12 siRNAs (siADAM12). After 24 h, cells were incubated with or without 20 ng/ml EGF in complete media for an additional 48 h and analyzed for CD44 and CD24 expression. **d** EGFR responsive gene signature score versus ADAM12mRNA expression in 421 breast invasive carcinomas from the TCGA database (Cell 2015 dataset). EGFR signature scores were calculated based on ref. [28].

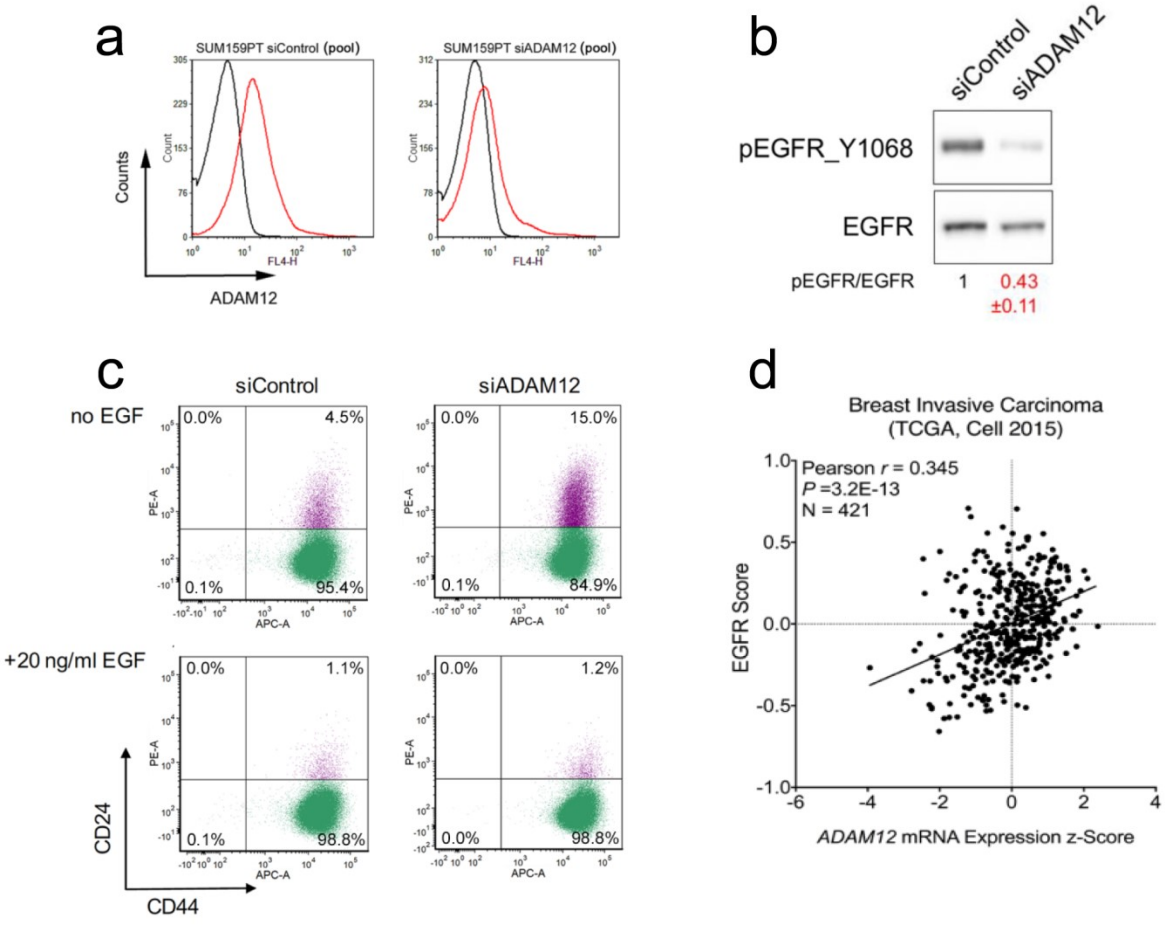

Figure 4.3 Inducible overexpression of ADAM12 does not appear to enhance the CSC phenotype in SUM159PT cells.

SUM159PT stably overexpressing either wild-type ADAM12 or a catalytically inactive mutant (E351Q) were treated for 48 h with 2 µg/ml doxycycline. **a** The levels of ADAM12 protein were determined by Western blotting. ERK1/2 is a gel loading control. The two bands represent the full-length form of ADAM12 (top) or the processed form lacking the N-terminal pro-domain (bottom). **b, c** The cell surface expression of either ADAM12 (**b**) or CD24, a CSC marker (**c**) was determined by flow cytometry.

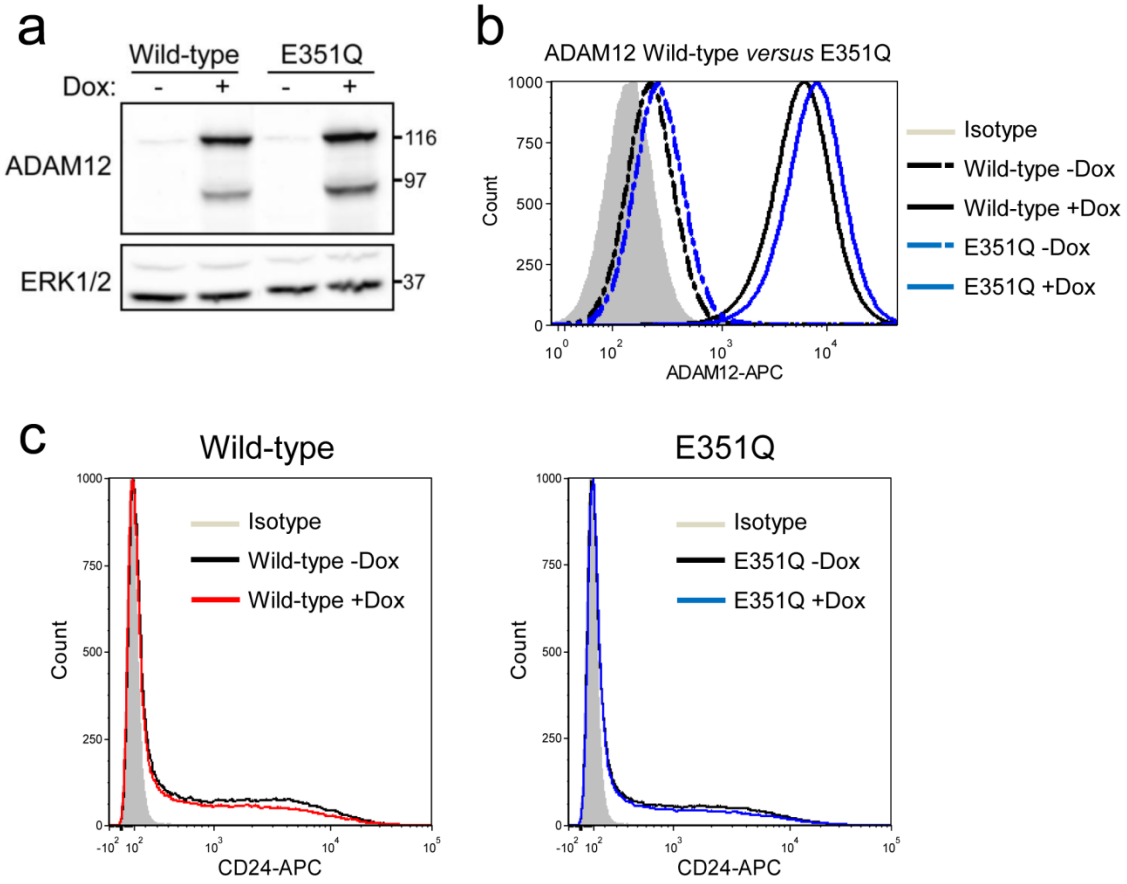

Figure 4.4 Various ADAMs may influence the CSC phenotype via modulation of the EGFR pathway.

a Amino acid sequence alignment of human ADAM9 and human ADAM12. Specific protein domains are denoted by different colors. **b, c** SUM159PT cells were transfected with a pool of four ADAM9 siRNAs (siADAM9) and analyzed three days later by either Western blotting (**b**) or flow cytometry for CD44 and CD24 expression (**c**).

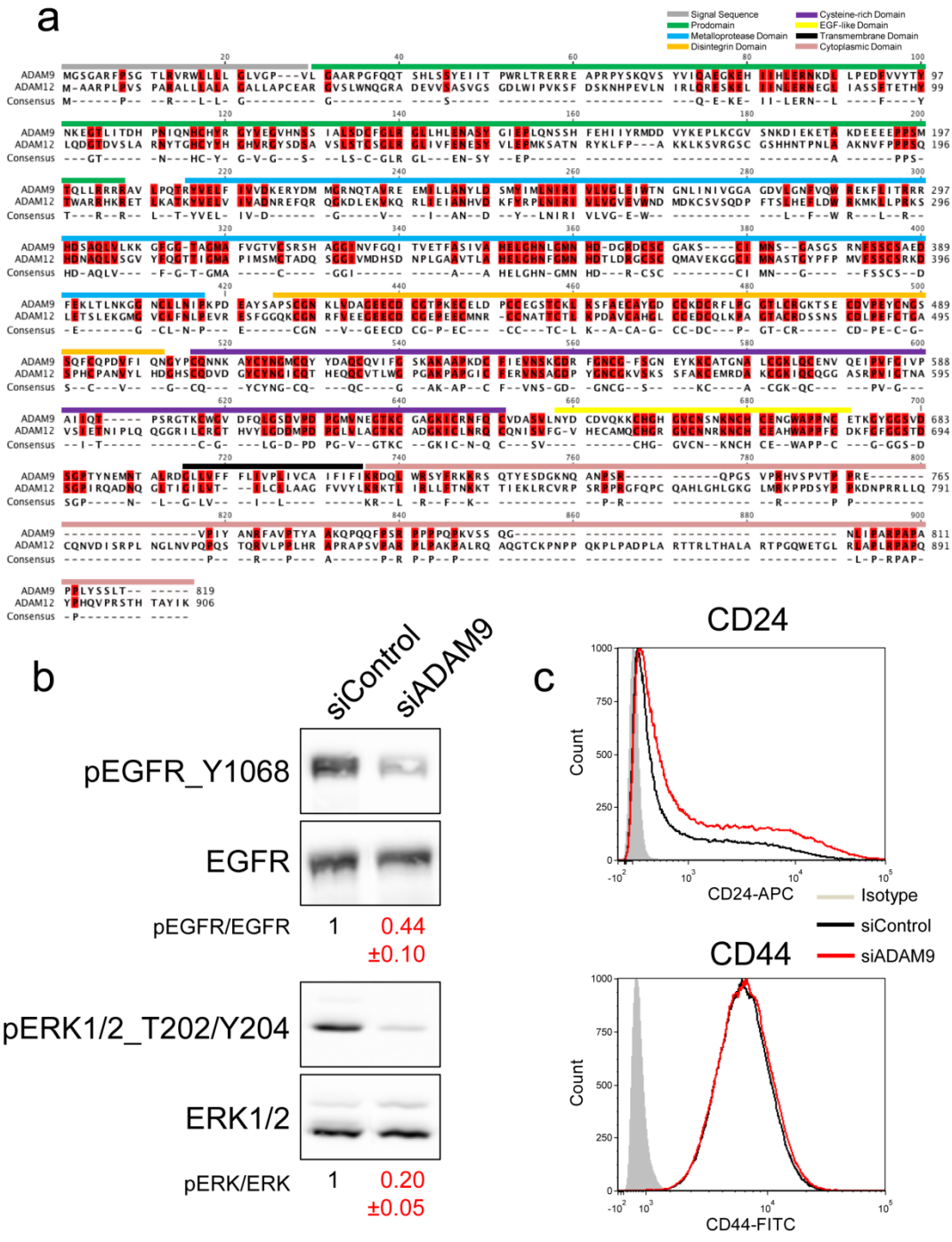

Chapter 5 - Matrix metalloprotease-mediated cleavage of programmed death-ligand 1 (PD-L1)

Abstract

Programmed death-ligand 1 (PD-L1) has emerged as a promising target for cancer immunotherapy. PD-L1 has been shown to be highly expressed on various cancer cells and within the tumor microenvironment. This allows tumor cells to evade recognition by the immune system, as PD-L1 binds to the PD-1 receptor on T-cells and suppresses the immune response. However, it is not clear which patients will respond to anti-PD-L1/PD-1 therapies, as high levels of PD-L1 have not been conclusively shown to be correlated with poor patient outcome. The goal of this study was to assess a possible role of matrix metalloproteases in the regulation of PD-L1 by its cleavage. Here, we show that batimastat (BB-94), a metalloprotease inhibitor, decreases the amount of PD-L1 in cell culture media, as determined by an ELISA assay. This effect is not due to the presence of cellular debris, as a longer and shorter centrifugation prior to the ELISA assay produced similar amounts of PD-L1 in the media. Use of a cell line stably overexpressing PD-L1 revealed that inhibition of metalloproteases decreased the amount of PD-L1 in conditioned cell culture media, without decreasing the total amount of PD-L1 in cells. Importantly, an antibody to the C-terminus of PD-L1 detected a fragment of the protein. These results suggest that PD-L1 undergoes metalloprotease-mediated cleavage in breast cancer cells. This novel mode of regulation of PD-L1 may be biologically significant, as the soluble extracellular fragment should retain its receptor binding properties. Further studies are warranted to confirm the functionality and relevance of the released extracellular domain of PD-L1.

Introduction

The interaction between programmed cell death-1 (PD-1) receptor and its ligand PD-L1 has recently emerged as a promising target for immunotherapy in aggressive cancers. Currently, there are at least five drugs targeting either PD-1 or PD-L1 in clinical trials (information from clinicaltrials.gov). T cells are activated upon the recognition of an antigen, either on antigen presenting cells (APCs) or tumor cells, by the T cell receptor (TCR) on T-cells. Activation of T cells leads to induction of PD-1 expression. Interaction between PD-1 on T cells and its ligand PD-L1 (or PD-L2) on tumor cells inhibits T cell activation, as a result of the recruitment of phosphatases that dephosphorylate key signaling components downstream of TCR. Thus, induction of PD-1 in activated T cells acts as a negative feedback loop to limit immune response [1, 2].

PD-L1 expression in tumor cells is either driven by oncogenic signaling pathways in tumor cells or is induced in response to pro-inflammatory signals, such as interferons [3]. PD-L1 is particularly upregulated in aggressive types of breast cancer, but is not expressed in normal breast epithelial tissue [4-8]. Despite the strong support for an immunosuppressive role of PD-L1 in cancer progression, there is currently no consensus whether PD-L1 itself may serve as a prognostic factor in breast cancer [6, 8-10] nor a reason as to why some patients respond to PD-1/PD-L1 therapies while others do not [3].

PD-L1 is a single-pass type I transmembrane protein that contains two immunoglobin domains in its extracellular region. There are also four N-glycosylation sites present in the extracellular domain of the protein [11]. The cytoplasmic tail of the molecule contains approximately 30 amino acids and includes potential ubiquitination sites [12]. The part of the

protein that facilitates its binding to PD-1, and thus accounts for its immunosuppressive activity, is its extracellular variable immunoglobin (IgV) domain [13].

Recently, there has been evidence in the literature pointing to a soluble form of PD-L1 (sPD-L1) that retains its immunosuppressive activity and inhibits T cell function [14-15]. Additionally, the levels of soluble PD-L1 have been shown to be associated with a poor prognosis in various types of cancer [14, 16, 17]. However, the origin of this soluble form remains unclear. Alternative splicing variants lacking the transmembrane domain have recently been detected for PD-L1, though the effects of these variants on T cell inhibition have not been thoroughly studied [18, 19]. Also, the transmembrane full-length PD-L1 was found on circulating tumor cells [20] or exosomes [21] and it seemed to inhibit the immune response. Finally, some reports have suggested metalloprotease-mediated cleavage of PD-L1, which could result in the release of the extracellular domain, though no assays testing for the presence of a soluble extracellular domain or a cleaved transmembrane/cytoplasmic fragment were performed [22].

The goal of this study was to examine the cleavage of PD-L1 by matrix metalloproteases in breast cancer. By comparing the levels of PD-L1 in the media before and after treatment with a metalloprotease inhibitor, and by utilizing an overexpression system to detect a C-terminal cleavage fragment of PD-L1 by immunoblotting, we were able to determine that PD-L1 is indeed cleaved by matrix metalloproteases. However, the amount of cleaved PD-L1 was very low, and further studies are needed to determine whether the low levels of soluble PD-L1 generated by metalloprotease-mediated cleavage have a significant impact on immunosuppression in the tumor microenvironment

Methods

Reagents and Antibodies

Batimastat (BB-94) and MG-132 were from EMD Millipore, chloroquine (CQ) was from R&D Systems. Antibodies included the DYKDDDDK Tag Antibody (clone 5A8E5) from GenScript, anti-PD-L1 (clone E1L3N), anti-HYOU1 (Catalog #13452), and anti-ERK1/2 (clone 137F5) from Cell Signaling Technology. The Human/Cynomolgus Monkey PD-L1/B7-H1 Quantikine ELISA Kit (Catalog #DB7H10) was purchased from R&D Systems. The PD-L1 pcDNA3.1$^+$/C-(K)DYK vector plasmid (Clone ID OHu22144) was from GenScript.

Cell Culture

Both the SUM149PT and SUM159PT cell lines (Asterand) were cultured in Ham's F-12 medium supplemented with 5% fetal bovine serum (FBS), 10 mM HEPES, 5 μg/ml insulin, and 1 μg/ml hydrocortisone and maintained at 37°C under humidified atmosphere containing 5% CO_2.

Generation of cells stably overexpressing PD-L1

Cells stably overexpressing the PD-L1 pcDNA3.1$^+$/C-(K)DYK vector plasmid were produced by transfecting 1 μg of plasmid into an early passage of SUM159PT cells using HP XtremeGene (Roche) at a 1:2 plasmid to reagent ratio. After two days, the media containing the transfection complex were removed and selection was started using 500 μg/ml G418 and continued for two weeks.

ELISA assay

Cells were seeded into 6-well plates at approximately $8x10^5$ cells/well. After 24 hours, cells were transferred to medium containing 1% FBS, with all other supplements included. After two days, conditioned media from three wells under the same conditions were combined, loaded

into 10-kDa cut-off concentrators, and centrifuged for ~10 min at 2,000 rpm. After concentration, the final volume of the media remaining in each concentrator was measured, and the level of sPD-L1 was determined by ELISA using a PD-L1 quantikine ELISA Kit (R&D), according to the manufacturer's protocol. For each condition, 100 µl of concentrated media/well in a 96-well plate were used, and the measurements were performed in triplicates. In parallel, the cells remaining in 6-well plates were lysed and the amount of total cellular protein was quantified using a BCA reagent (Pierce). At the end of each ELISA assay, the measured values of sPD-L1 were corrected for the media concentration factor and the amount of cellular protein.

Immunoblotting

After incubation with respective treatments (100 µM chloroquine or 10 µM MG-132 for 4 hours; 10 µM batimastat for 72 hours), cells were treated with lysis buffer (50 mM Tris-HCl pH 7.4, 150 mM NaCl, 1% Triton-X-100, 0.5% sodium deoxycholate, 0.1% sodium dodecylsulfate (SDS), 5 mM EDTA, 1 mM 4-(2-Aminoethyl) benzenesulfonyl fluoride hydrochloride (AEBSF), 5 µg/ml pepstatin, 5 µg/ml leupeptin, 5 µg/ml aprotinin, 10 mM 1,10-phenanthroline, 50 mM NaF, 2 mM Na_3VO_4, and 10 mM $Na_4P_2O_7$). After collection and centrifugation of the lysates, the supernatants were mixed at a 2:1 ratio with 3xSDS sample buffer, and heated at 95°C for 5 minutes. Total cell lysates were resolved by SDS-PAGE in either 12% or 18% polyacrylamide gels, followed by transfer to a nitrocellulose membrane. Nitrocellulose membranes were blocked in 5% milk with 0.3% Tween-20 in DPBS, incubated with primary antibodies overnight, and then for one hour with HRP-conjugated secondary antibodies, followed by signal detection using SuperSignal West Pico or Femto chemiluminescence detection kit (Pierce) and Azure c500 digital imaging system.

Results

Inhibition of metalloproteases decreases the amount of soluble PD-L1 in cell culture media

Previously, it has been reported that SUM159PT cells express high levels of PD-L1, while SUM149PT cells have low to no detectable PD-L1 present [8, 23]. Therefore, we set out to determine if inhibition of metalloproteases in SUM159PT cells would decrease the amount of soluble PD-L1 present in the media, with SUM149PT cells serving as a negative control. A commercially available ELISA kit was used to measure the amount of soluble PD-L1 in the media, as described in Methods. Importantly, the readings from ELISA assays were normalized to the amount of protein present in cell lysates and the concentration factors. This is to accurately determine the levels of PD-L1 in the media so that a direct comparison could be made between various treatments and cell lines.

We found that treatment of SUM159PT cells with the broad range metalloprotease inhibitor BB-94 significantly decreased the amount of PD-L1 found in the media from approximately 4 to 2.5 pg/ml (Fig. 5.1). Furthermore, as expected, we found that BB-94 treatment did not influence PD-L1 levels in the media of SUM149PT cells. As the levels of soluble PD-L1 measured for SUM149PT cells were similar to those obtained for SUM159PT cells treated with BB-94, it is likely that that the lower detection limit of the assay was reached.

Overexpression of PD-L1 in SUM159PT cells increases the levels of PD-L1 in cell culture supernatants

Since inhibition of metalloproteases was able to influence the amount of PD-L1 in the cell culture supernatants, this suggested the occurrence of a PD-L1 cleavage event. We set out to confirm this hypothesis by stably transfecting a tagged PD-L1 overexpression vector into

SUM159PT cells (PD-L1 OE). We confirmed the overexpression of PD-L1 by Western blotting using two antibodies: an antibody recognizing the DYKDDDDK tag and a PD-L1-specfiifc antibody (Fig. 5.2a). The amount of PD-L1 protein in stably transfected cells was significantly higher than that found in the parental cell line. Additionally, we detected multiple bands of various molecular weights in the immunoblots. These additional bands likely corresponded to differently glycosylated forms of PD-L1 [11]. Next, we set out to determine if cells stably overexpressing PD-L1 would have higher levels of PD-L1 in the cell culture supernatant than the parental cells. Indeed, we saw that the level of soluble PD-L1 in the media of PD-L1 OE cells was approximately 3.5 times higher than the level observed for the parental cell line (Fig. 5.2b). Importantly, this increased level of soluble PD-L1 was likely not merely a reflection of the amount of cellular PD-L1, as a longer centrifugation to eliminate cellular debris resulted in similar levels of PD-L1 in the media (Fig. 5.2b).

PD-L1 is likely cleaved by matrix metalloproteases

Next, we set out to show that the amount of PD-L1 in the media of cells stably overexpressing PD-L1 could also be reduced in the presence of BB-94. Indeed, the levels of soluble PD-L1 produced by cells with PD-L1 overexpression were decreased after inhibition of metalloproteases (Fig. 5.3a). As observed previously (Fig. 5.1), the amount of PD-L1 in the supernatant of the parental cell line was also affected by BB-94 treatment.

As a final confirmation of the cleavage of PD-L1 by metalloproteases, we aimed to detect a C-terminal cell-associated fragment of PD-L1 by Western blotting. To maximize the probability of detection of this fragment, we treated the cells for four hours with either a lysosomal inhibitor (chloroquine) or a proteasomal inhibitor (MG-132) to prevent a possible degradation of the fragment. Additionally, the cell lysates were resolved in a high percentage

(18%) polyacrylamide gel to allow for the separation and detections of bands with a low molecular weight. The top portion of the nitrocellulose membrane was used to confirm the overexpression of PD-L1, and the lower portion was analyzed for a cleavage fragment. Using the PD-L1-specific antibody, which recognizes the C-terminal region of the protein, we were able to detect the presence of an ~14 kDa band in the lower region of the membrane after treatment with chloroquine (Fig. 5.3c). We were not able to detect a similar ~14-kDa fragment of PD-L1 using the anti-DYKDDDDK tag antibody (results not shown), most likely due to a lower sensitivity of the antibody.

The size of the ~14-kDa fragment suggested that the cleavage occurred in the extracellular, membrane-proximal region of PD-L1. The predicted mass of the transmembrane domain and the cytoplasmic tail of PD-L1, plus the C-terminal tag, is ~4.5 kDa. A recent report suggested that PD-L1 undergoes mono-ubiquitination [12], and increased stability of the PD-L1 fragment after chloroquine treatment is indeed consistent with its mono-ubiquitination. Since the size of ubiquitin is ~8.5 kDa, an extracellular cleavage at a membrane-proximal site would bring the total predicted weight of the fragment to 13 kDa.

Discussion

While the importance of PD-L1 as a target in the treatment of various types of cancer, including NSCLC (Non-Small Cell Lung Cancer) [24], melanoma [25], and hepatocellular carcinoma [26], has been well established, the lack of the ability to predict which patients will respond to anti-PD-L1 therapy represents a major hurdle within the field [27]. The expression of PD-L1 alone does not appear to serve as a good predictive marker of response to anti-PD-1/PD-L1 therapies. While some studies have suggested that the presence of PD-L1 on cancer cells may serve as a positive predictive marker [28, 29], other evidence has suggested that the expression

of PD-L1 in the entire tumor microenvironment needs to be taken into account when deciding the appropriate therapies [30]. As such, the relationship between PD-L1 expression and tumor regression after anti-PD-L1/PD-1 treatment is not straightforward.

Here, we show that the metalloprotease inhibitor BB-94 decreased the amount of soluble PD-L1 found in the media of SUM159PT cells, which express detectable levels of PD-L1. Additionally, constitutive overexpression of PD-L1 in these cells resulted in an increased amount of PD-L1 in the media, and BB-94 decreased the amount of soluble PD-L1 produced by PD-L1 overexpressing cells. Finally, we were able to detect an ~14 kDa C-terminal fragment of PD-L1 that remained cell-bound after the cleavage. The presence of this fragment is consistent with the notion that the cleavage occurred at a membrane-proximal region and generated a soluble N-terminal fragment that most likely retained the ability to bind to the PD-1 receptor. It has to be pointed out, however, that the amount of soluble PD-L1 that we detected, compared to the full-length form, was very low and the biological significance of PD-L1 cleavage is not clear at this moment.

While our work identifies a new mechanism of regulation of PD-L1, there are still many questions that need to be answered. First, the functionality of the cleaved form of PD-L1 must be addressed. It is possible that the cleaved PD-L1 might diffuse from cancer cells to immune cells and thus act over a longer distance, potentiating the immunosuppressive effect of tumor cell. It is also possible that cleaved PD-L1 is a less potent ligand for PD-1 than transmembrane PD-L1, and thus PD-L1 cleavage would diminish its immunosuppressive function. Second, the exact location of the cleavage site in PD-L1 should be determined. Third, further studies should be done to identify the specific metalloprotease(s) responsible for the catalysis and the mechanism of the cleavage reaction. Fourth, a possible relationship between PD-L1 cleavage and patient

response to anti-PD-L1 therapy should be explored. Given the critical role of PD-L1/PD-1 interaction in regulating immune responses and clinical significance of this interaction in cancer, metalloprotease-mediated cleavage and regulation of PD-L1 should be investigated in more detail.

References

1. Pardoll DM (2012) The blockade of immune checkpoints in cancer immunotherapy. Nat Rev Cancer 12:252-264.

2. Sharpe AH, Wherry EJ, Ahmed R, Freeman GJ (2007) The function of programmed cell death 1 and its ligands in regulating autoimmunity and infection. Nat Immunol 8:239-245.

3. Tumeh PC, Harview CL, Yearley JH, Shintaku IP, Taylor EJM, Robert L, et al (2014) PD-1 blockade induces responses by inhibiting adaptive immune resistance. Nature 515:568-571.

4. Thompson E, Taube JM, Elwood H, Sharma R, Meeker A, Nassar Warzecha H, et al (2016) The immune microenvironment of breast ductal carcinoma in situ. Mod Pathol 29:249-258.

5. Ghebeh H, Mohammed S, Al-Omair A, Qattan A, Lehe C, Al-Qudaihi G, et al (2006) The B7-H1 (PD-L1) T lymphocyte-inhibitory molecule is expressed in breast cancer patients with infiltrating ductal carcinoma: Correlation with important high-risk prognostic factors. Neoplasia 8:190-198.

6. Baptista MZ, Sarian LO, Derchain SFM, Pinto GA, Vassallo J (2016) Prognostic significance of PD-L1 and PD-L2 in breast cancer. Hum Pathol 47:78-84.

7. Ali HR, Glont SE, Blows FM, Provenzano E, Dawson SJ, Liu B, et al (2015) PD-L1 protein expression in breast cancer is rare, enriched in basal-like tumours and associated with infiltrating lymphocytes. Ann Oncol 26:1488-1493.

8. Sabatier R, Finetti P, Mamessier E, Adelaide J, Chaffanet M, Raza Ali H, et al (2015) Prognostic and predictive value of PDL1 expression in breast cancer. Oncotarget 6:5449-5464.

9. Muenst S, Schaerli AR, Gao F, Däster S, Trella E, Droeser RA, et al (2014) Expression of programmed death ligand 1 (PD-L1) is associated with poor prognosis in human breast cancer. Breast Cancer Res Treat 146:15-24.

10. Li X, Wetherilt CS, Krishnamurti U, Yang J, Ma Y, Styblo TM, et al (2016) Stromal PD-L1 expression is associated with better disease-free survival in triple-negative breast cancer. Am J Clin Pathol 146:496-502.

11. Li C-W, Lim S-O, Xia W, Lee H-H, Chan L-C, Kuo C-W, et al (2016) Glycosylation and stabilization of programmed death ligand-1 suppresses T-cell activity. Nat Commun 7:12632.

12. Horita H, Law A, Hong S, Middleton K (2017) Identifying Regulatory Posttranslational Modifications of PD-L1: A Focus on Monoubiquitinaton. Neoplasia 19:346-353.

13. Lin DY-W, Tanaka Y, Iwasaki M, Gittis AG, Su H-P, Mikami B, et al (2008) The PD-1/PD-L1 complex resembles the antigen-binding Fv domains of antibodies and T cell receptors. Proc Natl Acad Sci USA 105:3011-3016.

14. Frigola X, Inman BA, Lohse CM, Krco CJ, Cheville JC, Thompson RH, et al (2011) Identification of a soluble form of B7-H1 that retains immunosuppressive activity and is associated with aggressive renal cell carcinoma. Clin Cancer Res 17:1915-1923.

15. Davies LC, Heldring N, Kadri N, Le Blanc K (2016) Mesenchymal Stromal Cell Secretion of Programmed Death-1 Ligands Regulates T Cell Mediated Immunosuppression. Stem Cells 1-11.

16. Takahashi N, Iwasa S, Sasaki Y, Shoji H, Honma Y, Takashima A, et al (2016) Serum levels of soluble programmed cell death ligand 1 as a prognostic factor on the first-line treatment of metastatic or recurrent gastric cancer. J Cancer Res Clin Oncol 142:1727-1738.

17. Zeng Z, Shi F, Zhou L, Zhang M-N, Chen Y, Chang X-J, et al (2011) Upregulation of circulating PD-L1/PD-1 is associated with poor post-cryoablation prognosis in patients with HBV-related hepatocellular carcinoma. PLoS One 6:e23621.

18. Zhou J, Mahoney KM, Giobbie-Hurder A, Zhao F, Lee S, Liao X, et al (2017) Soluble PD-L1 as a Biomarker in Malignant Melanoma Treated with Checkpoint Blockade. Cancer Immunol Res 6:480-492.

19. He XH, Xu LH, Liu Y (2005) Identification of a novel splice variant of human PD-L1 mRNA encoding an isoform-lacking IgV-like domain. Acta Pharmacol Sin 26:462-468.

20. Mazel M, Jacot W, Pantel K, Bartkowiak K, Topart D, Cayrefourcq L, et al (2015) Frequent expression of PD-L1 on circulating breast cancer cells. Mol Oncol 9:1773-1782.

21. Whiteside TL (2016) Exosomes and tumor-mediated immune suppression. J Clin Invest 126:1216-1223.

22. Dezutter-Dambuyant C, Durand I, Alberti L, Bendriss-Vermare N, Valladeau-Guilemond J, Duc A, et al (2016) A novel regulation of PD-1 ligands on mesenchymal stromal cells through MMP-mediated proteolytic cleavage. OncoImmunology 5:e1091146.

23. Heskamp S, Hobo W, Molkenboer-Kuenen JDM, Olive D, Oyen WJG, Dolstra H, et al (2015) Noninvasive imaging of tumor PD-L1 expression using radiolabeled anti-PD-L1 antibodies. Cancer Res 75:2928-2936.

24. Gettinger S, Rizvi NA, Chow LQ, Borghaei H, Brahmer J, Ready N, et al (2016) Nivolumab Monotherapy for First-Line Treatment of Advanced Non-Small-Cell Lung Cancer. J Clin Oncol 34:2980-2987.

25. Weber JS, D'Angelo SP, Minor D, Hodi FS, Gutzmer R, Neyns B, et al (2015) Nivolumab versus chemotherapy in patients with advanced melanoma who progressed after anti-CTLA-4 treatment (CheckMate 037): A randomised, controlled, open-label, phase 3 trial. Lancet Oncol 16:375-384.

26. El-Khoueiry AB, Melero I, Crocenzi TS, Welling TH, Yau TC, Yeo W, et al (2015) Phase I/II safety and antitumor activity of nivolumab in patients with advanced hepatocellular carcinoma (HCC): CA209-040. J Clin Oncol 33.

27. Romano E, Romero P (2015) The therapeutic promise of disrupting the PD-1/PD-L1 immune checkpoint in cancer: unleashing the CD8 T cell mediated anti-tumor activity results in significant, unprecedented clinical efficacy in various solid tumors. J Immunother Cancer 3:15.

28. Schmidt LH, Kümmel A, Görlich D, Mohr M, Bröckling S, Henrik Mikesch J, et al (2015) PD-1 and PD-L1 expression in NSCLC indicate a favorable prognosis in defined subgroups. PLoS One 10:1-15.

29. Schalper KA, Velcheti V, Carvajal D, Wimberly H, Brown J, Pusztai L, et al (2014) *In situ* tumor PD-L1 mRNA expression is associated with increased TILs and better outcome in breast carcinomas. Clin Cancer Res 20:2773-2782.

30. Noguchi T, Ward JP, Gubin MM, Arthur CD, Lee SH, Hundal J, et al (2017) Temporally Distinct PD-L1 Expression by Tumor and Host Cells Contributes to Immune Escape. Cancer Immunol Res 5:106-117.

Figure 5.1 Treatment with BB-94 reduces the amount of soluble PD-L1 in the media in cells with detectable levels of endogenous PD-L1.

SUM159PT and SUM149PT cells were treated for 48 hours with 10 μM BB-94 in media containing 1% FBS. The media were collected and evaluated by an ELISA assay for the presence of PD-L1. *, $P<0.05$

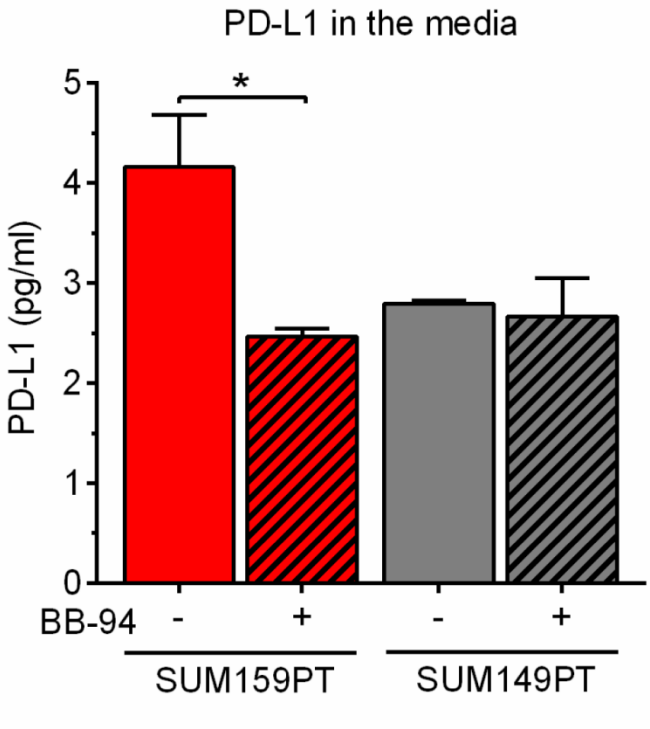

Figure 5.2 SUM159PT cells overexpressing PD-L1 release substantially more PD-L1 into the media.

a SUM159PT cells were stably transfected with a vector encoding PD-L1 containing a C-terminal DYKDDDDK tag. Shown are Western blots of total cell lysates using anti-DYKDDDDK tag or anti-PD-L1 antibodies in the parental *versus* PD-L1-overexpressing SUM159PT cells. A non-specific band and HYOU1 serve as loading controls. **b** PD-L1-overexpressing cells release more soluble PD-L1 into the media. Parental or PD-L1-overexpressing SUM159PT cells were incubated in the presence of 1% FBS for 48 h. The media were spun at 2000xg for either 3 minutes or 30 minutes to eliminate any cellular debris, then treated and assayed as described in Methods. ****, $P<0.0001$

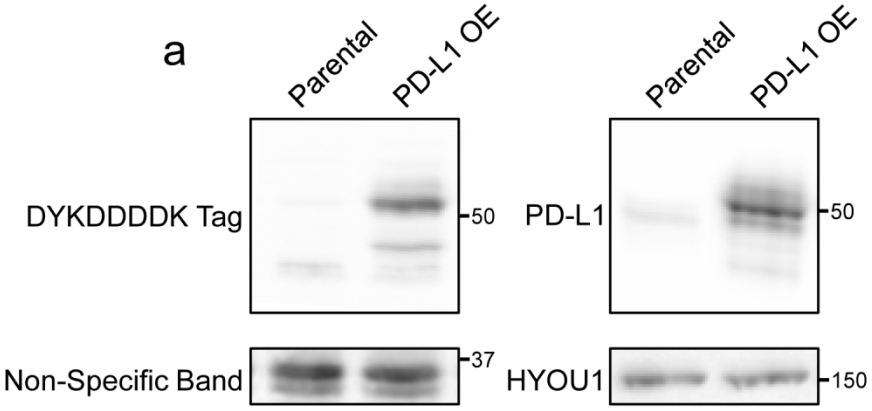

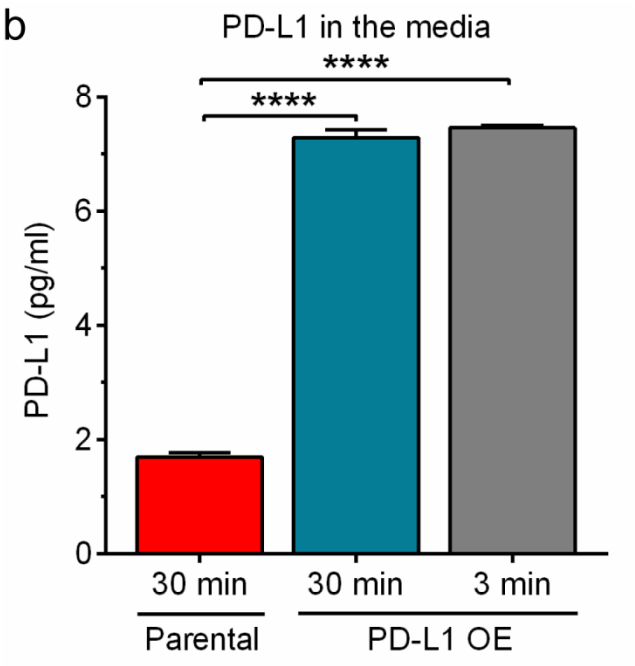

Figure 5.3 The presence of soluble PD-L1 in the media is likely due to the cleavage by matrix metalloproteases.

a Parental or PD-L1 OE SUM159PT cells were treated for 48 hours with 10 μM BB-94 in media containing 1% serum. The media were collected and evaluated by an ELISA assay for the presence of soluble PD-L1. *, $P<0.05$; **, $P<0.01$. **b** Total cell lysates were collected from parental or PD-L1 OE SUM159PT cells treated with either DMSO or 10 μM BB-94 for three days. Lysates were then analyzed by Western Blotting to determine the level of cellular PD-L1. **c** Cells were treated for four hours with either DMSO, chloroquine, or MG-132 and collected. Total lysates were analyzed for a C-terminal PD-L1 cleavage fragment by Western blotting using SuperSignal West Femto Maximum Sensitivity Substrate (bottom). The full length PD-L1 present in the lysates was visualized using SuperSignal West Pico Substrate (top).

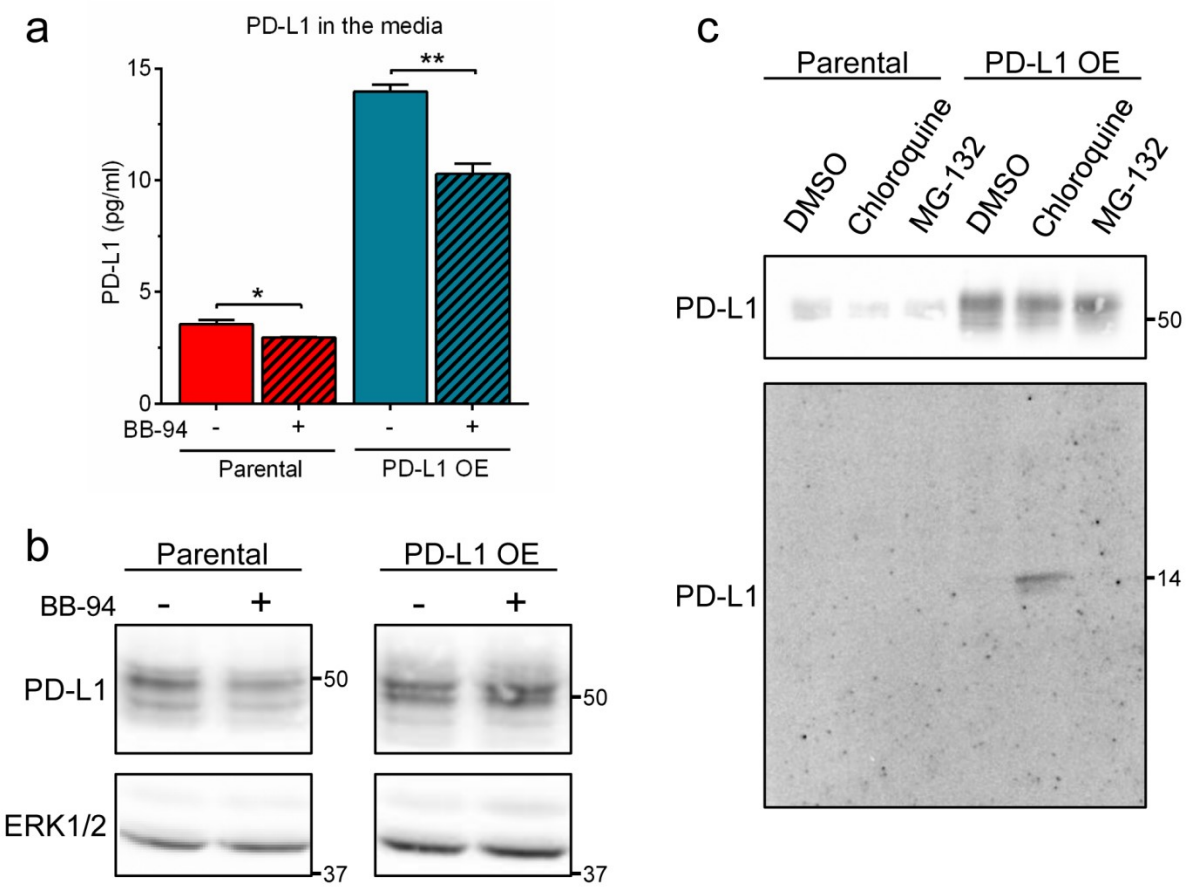

Chapter 6 - Final Conclusions

I have shown in this dissertation that removal of certain types of ER chaperones can have a detrimental effect on the anchorage-independent growth of breast cancer cells. I have also demonstrated that cell surface metalloproteases, including ADAM9 and ADAM12, modulate the expression of two cancer stem cell (CSC) markers through the MEK/ERK pathway. Finally, I showed that cell surface metalloproteases are involved in the cleavage of PD-L1, an important modulator of the immune response. Together, these data indicate that the proper function of the secretory pathway, in particular an intact protein folding quality control in the ER and an efficient growth factor signaling response, are important in sustaining metastatic properties of triple negative breast cancer (TNBC) cells.

In Chapter 2, I showed that certain protein disulfide isomerases (PDIs) in the ER are able to influence the anchorage independent growth of breast cancer cells. The PDI family of molecular chaperones is responsible for the formation of disulfide bonds in newly synthesized proteins [1]. They can also play a role in the isomerization of these bonds in misfolded proteins [2], thus helping to alleviate ER stress caused by the accumulation of misfolded proteins. These PDIs were initially identified by analyzing protein and mRNA expression of a panel of ER chaperones in adherent cells or cells grown in suspension as mammospheres. Surprisingly, assays to determine the amount of ER stress only indicated that one branch of the unfolded protein response (UPR) was increased in mammospheres. It is possible that cells that adapted to the growth under suspension condition reached a new “steady state”, in which a certain balance was achieved between modulation of the stress response and upregulation of certain chaperones. Additionally, upregulation of various extracellular matrix (ECM) components was also observed in mammospheres, indicating that the increase in expression of the PDI family members may be

related to managing an increased flux of ECM through the ER, rather than relieving a stress caused by accumulation of misfolded proteins.

In summary, it is feasible that the anchorage independent growth of breast cancer cells is affected by the availability of secreted ECM components. Indeed, recent studies have shown that the production of ECM components is essential for extravasation and metastasis [3-5]. A possible explanation for the increased survival of extravasated tumor cells could be that secretion of ECM components engages the integrin receptors at the cell surface, causing activation of pro-survival signaling pathways [6, 7]. Thus, addressing the role of PDIs in this process may provide a treatment target for metastatic cancer cells by limiting the secretion of these important ECM components. Inhibitors for PDI are available and have been shown to affect the viability of multiple myeloma and ovarian cancer cells, however there are no previous or ongoing clinical trials examining the efficacy of this inhibition in breast cancer [8, 9]. Use of PDI inhibitors, along with traditional chemotherapy, may serve as a way to target metastatic breast cancer cells at a vulnerable point in their journey.

In Chapter 3, I demonstrated that a CSC phenotype ($CD44^+/CD24^-$) of TNBC cells is modulated by metalloprotease-mediated epidermal growth factor receptor (EGFR) signaling through the MEK/ERK pathway. Both the EGFR pathway and the downstream MEK/ERK signaling have been separately shown to be important in maintaining the $CD44^+/CD24^-$ phenotype [10, 11]. However, there is currently no consensus on whether these signals act together to promote the CSC phenotype. It has been shown that EGFR signaling influences the $CD44^{+/}CD24^-$ phenotype in TNBC, but that effect was suggested to be mediated through regulation of autophagy [11]. Conversely, Balko et al., showed that the MEK/ERK pathway was important in modulating the CSC phenotype, and it was suggested the pathway activation was

achieved through the loss of a negative regulator of ERK, DUSP4 [10]. As such, we were able to show that in cells without DUSP4 loss, CD44/CD24 marker profile is also regulated by MEK, and activation of the MEK/ERK pathway is an obligatory step in EGFR-mediated regulation of the CSC phenotype.

Inhibition of MEK in SUM159PT cells with 75 μM selumetinib, even in the presence of sustained EGFR activation caused by exogenously added EGF, was able to decrease the $CD44^+/CD24^-$ population. While 75 μM selumetinib seemed rather high to use, but we determined that this was the lowest concentration that completely blocked phosphorylation of ERK upon sustained EGFR activation. When a lower concentration (10 μM) of selumetinib was used in SUM159PT cells, we observed an incomplete inhibition of ERK phosphorylation and thus only a partial response to EGF treatment. SUM149PT cells required 10 μM selumetinib for complete inhibition of MEK upon sustained EGFR activation, and this concentration of selumetinib effectively decreased the $CD44^+/CD24^-$ population in the presence of exogenous EGF. A complementary approach with constitutive MEK activity resulted in an increase of the $CD44^+/CD24^-$ populations, and this effect was not resolved upon EGFR inhibition.

While the $CD44^+/CD24^-$ marker profile has been shown to be a characteristic feature of breast CSCs, the presence of $CD44^+/CD24^-$ cells does not necessarily mean that those cells are cancer stem cells. Thus, in order to determine if manipulation of MEK activity can indeed affect the CSC population, additional assays, such as mammosphere formation or *in vivo* tumor growth studies, should be used. It has been shown in the literature and we have observed (data not shown) that selumetinib completely inhibits mammosphere formation [10, 12]. This would lend support to the hypothesis that a CSC phenotype is modulated exclusively through the MEK/ERK pathway. However, rescue experiments involving exogenous EGF and complementary

approaches involving constitutively active MEK along with EGFR inhibition would provide strong support to the idea that the MEK/ERK pathway plays a central role in regulating CSCs downstream of EGFR in TNBC cells.

In Chapter 4, I determined that specific disintegrin and metalloproteases had the capacity to influence the $CD44^{+}/CD24^{-}$ marker profile through EGFR signaling. We initially examined the role of ADAM12 in maintaining the CSC phenotype since high expression of ADAM12 has been shown to predict the resistance to neoadjuvant chemotherapy in ER-negative breast cancer, independent of age, tumor size, grade, and the lymph node status [13]. Additionally, data mining suggested a link between ADAM12, cancer stem cells, and poor patient prognosis (see Fig. 4.1). As expected, siRNA-mediated knockdown of ADAM12 decreased the $CD44^{+}/CD24^{-}$ population, and this effect was eliminated by adding exogenous EGF to the culture media. These results suggest that ADAM12 works upstream of EGFR, most likely by cleaving transmembrane precursors of EGF or EGF-like ligands and generating soluble, biologically active growth factors. A complementary approach was attempted by creating cell lines stably overexpressing an inducible form of wild-type ADAM12 or its catalytically inactive mutant, E351Q. Unfortunately, we were not able to observe a significant difference in the cell surface level of CD24 marker after ADAM12 overexpression. One reason could be that the maximum level of EGFR ligand cleavage had been already achieved by the endogenous ADAM12, and further upregulation of ADAM12 was not able to increase the concentration of soluble EGF or to upregulate EGFR. Alternatively, ADAM12 might influence the levels of CD24 directly, possibly by its cleavage. Thus, knockdown of ADAM12 would result in the increase of CD24 protein at the cell surface, but overexpression may not necessarily have an effect, as the amount of CD24 is already low in SUM159PT cells. However, this scenario is rather unlikely, as there is

no evidence in the literature for such a metalloprotease-mediated cleavage of CD24, while other CSC markers, including EpCAM and CD44 have been shown to be cleaved by metalloproteases [14, 15].

Finally in Chapter 5, I examined the role of metalloproteases in the cleavage of PD-L1, a transmembrane protein upregulated in many cancers and a ligand for PD-1, and inhibitory checkpoint molecule expressed on different immune cells, including cytotoxic T cells that kill cancer cells. Treatment with a metalloprotease inhibitor (BB-94), decreased the amount of soluble PD-L1 in the media, as measured by an ELISA assay. Additionally, we were able to detect the presence of a cleavage fragment of PD-L1 by immunoblotting. The molecular weight of this fragment was ~14 kDa.

There have been multiple pieces of evidence in the literature suggesting the presence of a form of PD-L1 found outside of the primary tumor site which correlates with a poor patient prognosis [16-19]. However, the source of this fragment remains unclear. Likely explanations then include cleavage of the transmembrane form of PD-L1 [20], the presence of PD-L1 on exosomes [21] or circulating tumor cells [22], or alternative *PD-L1* mRNA splicing leading to the synthesis of a secreted form of PD-L1 protein [23]. While we cannot entirely eliminate exosomes or circulating tumor cells as probably sources of PD-L1 *in vivo*, which may be a confounding factor in the PD-L1 study, our evidence suggests that the transmembrane PD-L1 protein is cleaved by metalloproteases and a large portion of the extracellular domain of PD-L1 is released to the media (Fig. 5.2b). Although we were not able to conclusively show that PD-L1 detected by the ELISA assay was not derived from exosomes, partial inhibition of the ELISA signals by BB-94 and the presence of a ~14-kDa C-terminal fragment of PD-L1 detected by Western blotting seem to point to the metalloprotease-mediated cleavage of the transmembrane

PD-L1 as a mechanism of release of a soluble form of the protein. More studies are needed to confirm that (1) the abundance of the low-molecular weight PD-L1 fragment is decreased after metalloprotease inhibition, and (2) that the released extracellular domain of PD-L1 would retain its ability to elicit an inhibitory effect on PD-1-expressing immune cells. Additionally, these results should be verified through use of other cell lines and *in vivo* studies.

The implications of the soluble form of PD-L1 being linked to metalloprotease cleavage are significant. Interest in cancer immunotherapy has spiked in recent years, with the development of promising treatment options. Unfortunately, there has not yet been a way to predict which patients will respond to this type of therapy. The propensity of PD-L1 to being cleaved, at least in certain circumstances, might provide additional therapy options or help predict patient response.

Considering all of the accumulated data, I believe that targeting the secretory pathway provides a viable approach for treatment of metastatic triple negative breast cancer. However, there are still numerous obstacles in succeeding with such an approach. For example, EGFR and MEK inhibitors have shown limited success in clinical trials, despite very strong preclinical data implicating these pathways in the pathology of breast cancer [24-26]. The targets that I believe hold the most promise are further inquiries into small molecule inhibitors for PDI family members, as they have had positive results in various *in vivo* mouse models [8, 27], and also addressing the issue of PD-L1 cleavage as a possible marker for efficacy of treatment.

References

1. Galligan JJ, Petersen DR (2012) The human protein disulfide isomerase gene family. Hum Genomics 6:6.

2. Grek C, Townsend DM (2014) Protein Disulfide Isomerase Superfamily in Disease and the Regulation of Apoptosis. Endoplasmic Reticulum Stress Dis 1:4-17.

3. Singleton PA (2014) Hyaluronan Regulation of Endothelial Barrier Function in Cancer. Adv Cancer Res 123:191-209.

4. Ivanova IA, Vermeulen JF, Ercan C, Houthuijzen JM, Saig FA, Vlug EJ, et al (2013) FER kinase promotes breast cancer metastasis by regulating α6- and β1-integrin-dependent cell adhesion and anoikis resistance. Oncogene 32:5582-5592.

5. Venning FA, Wullkopf L, Erler JT (2015) Targeting ECM Disrupts Cancer Progression. Front Oncol 5:224.

6. Weber GF, Bjerke MA, DeSimone DW (2011) Integrins and cadherins join forces to form adhesive networks. J Cell Sci 124:1183-1193.

7. Oellerich T, Oellerich MF, Engelke M, Münch S, Mohr S, Nimz M, et al (2013) β_2 integrin-derived signals induce cell survival and proliferation of AML blasts by activating a Syk/STAT signaling axis. Blood 121:3889-3899.

8. Xu S, Butkevich A, Yamada R, Zhou Y, Debnath B, Duncan R, et al (2012) Discovery of an orally active small-molecule irreversible inhibitor of protein disulfide isomerase for ovarian cancer treatment. Proc Natl Acad Sci 108:16348-16353.

9. Vatolin S, Phillips JG, Jha BK, Govindgari S, Hu J, Grabowski D, et al (2016) Novel protein disulfide isomerase inhibitor with anticancer activity in multiple myeloma. Cancer Res 76:3340-3350.

10. Balko JM, Schwarz LJ, Bhola NE, Kurupi R, Owens P, Miller TW, et al (2013) Activation of MAPK pathways due to DUSP4 loss promotes cancer stem cell-like phenotypes in basal-like breast cancer. Cancer Res 73:6346-6358.

11. Tanei T, Choi DS, Rodriguez AA, Liang DH, Dobrolecki L, Ghosh M, et al (2016) Antitumor activity of Cetuximab in combination with Ixabepilone on triple negative breast cancer stem cells. Breast Cancer Res 18:6.

12. Bhat-Nakshatri P, Goswami CP, Badve S, Sledge GW, Nakshatri H (2013) Identification of FDA-approved drugs targeting breast cancer stem cells along with biomarkers of sensitivity. Sci Rep 3:2530.

13. Li H, Duhachek-Muggy S, Dubnicka S, Zolkiewska A (2013) Metalloproteinase-disintegrin ADAM12 is associated with a breast tumor-initiating cell phenotype. Breast Cancer Res Treat 139:691-703.

14. Rupp AK, Rupp C, Keller S Brase JC, Ehehalt R, Fogel M, et al (2011) Loss of EpCAM expression in breast cancer derived serum exosomes: Role of proteolytic cleavage. Gynecol Oncol 122:437-446.

15. Stamenkovic I, Yu Q (2009) Shedding light on proteolytic cleavage of CD44: the responsible sheddase and functional significance of shedding. J Invest Dermatol 129:1321-1324.

16. Fest T, Rossille D, Gressier M, Maucort-Boulch D, Damotte D, Pangault C, et al (2013) Blood soluble PD-L1 protein in aggressive diffuse large B-cell lymphoma impacts patient's overall survival. Blood 122:361.

17. Cheng S, Zheng J, Zhu J, Xie C, Zhang X, Han X, et al (2015) PD-L1 gene polymorphism and high level of plasma soluble PD-L1 protein may be associated with non-small cell lung cancer. Int J Biol Markers 30:e364-e368.

18. Zeng Z, Shi F, Zhou L, Zhang M, Chen Y, Chang X, et al (2011) Upregulation of circulating PD-L1/PD-1 is associated with poor post-cryoablation prognosis in patients with HBV-related hepatocellular carcinoma PLoS One 6:e23621.

19. Takahashi N, Iwasa S, Sasaki Y, Shoji H, Honma Y, Takashima A, et al (2016) Serum levels of soluble programmed cell death ligand 1 as a prognostic factor on the first-line treatment of metastatic or recurrent gastric cancer. J Cancer Res Clin Oncol 142:1727-1738.

20. Dezutter-Dambuyant C, Durand I, Alberti L, Bendriss-Vermare N, Valladeau-Guilemond J, Duc A, et al (2016) A novel regulation of PD-1 ligands on mesenchymal stromal cells through MMP-mediated proteolytic cleavage. OncoImmunology 5:e1091146.

21. Whiteside TL (2016) Exosomes and tumor-mediated immune suppression. J Clin Invest 126:1216-1223.

22. Mazel M, Jacot W, Pantel K, Bartkowiak K, Topart D, Cayrefourcq L, et al (2015) Frequent expression of PD-L1 on circulating breast cancer cells. Mol Oncol 9:1773-1782.

23. Zhou J, Mahoney KM, Giobbie-Hurder A, Zhao F, Lee S, Liao X, et al (2017) Soluble PD-L1 as a Biomarker in Malignant Melanoma Treated with Checkpoint Blockade. Cancer Immunol Res 5:480-492.

24. Carey LA, Rugo HS, Marcom PK, Mayer EL, Esteva FJ, Ma CX, et al (2012) TBCRC 001: Randomized phase II study of cetuximab in combination with carboplatin in stage IV triple-negative breast cancer J Clin Oncol. 30:2615-2623.

25. Wang D, Boerner SA, Winkler JD, LoRusso PM (2007) Clinical experience of MEK inhibitors in cancer therapy. Biochim Biophys Acta - Mol Cell Res 1773:1248-1255.

26. Shimizu T, Tolcher AW, Papadopoulos KP, Beeram M, Rasco DW, Smith LS, et al (2012) The clinical effect of the dual-targeting strategy involving PI3K/AKT/mTOR and

RAS/MEK/ERK pathways in patients with advanced cancer. Clin Cancer Res 18:2316-2325.

27. Kaplan A, Gaschler MM, Dunn DE, Colligan R, Brown LM, Palmer III AG, et al (2015) Small molecule-induced oxidation of protein disulfide isomerase is neuroprotective. Proc Natl Acad Sci 112:E2245-E2252.

Appendix A - Supplementary Materials for Chapter 2

Supplementary Methods

Cell culture

SUM159PT and MCF10DCIS.com cell lines were obtained from Asterand (Detroit, MI). SUM159PT cells were cultured in Ham's F-12 medium supplemented with 5% fetal bovine serum (FBS), 10 mM HEPES, 5 µg/ml insulin, and 1 µg/ml hydrocortisone. MCF10DCIS.com cells were cultured in Dulbecco's modified Eagle's medium (DMEM)/F12 nutrient mixture (1:1) supplemented with 5% horse serum (HS) and 29 mM sodium bicarbonate. Cells were maintained at 37°C under humidified atmosphere containing 5% carbon dioxide. For initial mammosphere assays (levels of protein and mRNA expression), mammosphere media were prepared using Mammary Epithelial Basal Media (MEBM, Lonza, Walkersville, MD), supplemented with 20 ng/ml hEGF, 20 ng/ml bFGF, 1% B27 (Life Technologies, Grand Island, NY), 4 µg/ml heparin, and 1% penicillin/streptomycin. For mammosphere assays using stable cell lines, MammoCult Human Medium Kit (MammoCult Medium containing proliferation supplements, 4 µg/ml of heparin, and 0.48 µg/ml of hydrocortisone; STEMCELL Technologies, Vancouver, BC) was used. Cell number and viability were measured with CellTiter-Glo luminescent cell viability assay (Promega, Madison, WI), according to the manufacturer's instructions. Luminescence was measured with BioTek Synergy H1MD microplate reader.

Mammosphere growth and count

Cells were detached with DPBS containing 0.25% (w/v) trypsin and 5 mM EDTA. Single cell suspensions in mammosphere media were prepared at the densities of 5 x 10^3 cells/ml in 1% methylcellulose, and plated in quadruplicates into wells of 24-well ultra-low attachment plates (Corning), at 5,000 cells/well. After 10 days, cells were analyzed using a phase contrast or

fluorescence microscope under 4x or 10x magnification. At least 5 images were collected per well. The number and diameter of spheres in each picture were determined using ImageJ. In ImageJ, greyscale images were turned into binary images using the Triangle Auto Threshold feature, followed by the Analyze Particles command.

qRT-PCR analysis

Total RNA was extracted using the Qiagen RNeasy kit and was subjected to on-column digestion with deoxyribonuclease I (Qiagen). One microgram of the total RNA was reverse transcribed using the SuperScript III First Strand Synthesis system (Invitrogen) and oligo(dT) primers. Real time quantitative PCR (qRT-PCR) was performed in a 96 well plate using 15 µl volumes in each well on a CFX96 cycler. The final reaction mixture contained 7.5 µl iQ SYBRgreen Supermix, 6 µl diluted cDNA (1:100 for *ACTIN* analysis and 1:10 or 1:100 for other genes) and 0.5 µM primers. qRT-PCR primers for *BiP* and *ERp44* were purchased from Qiagen. qRT-PCR primers for *CALR*, *CANX*, *COL3A1*, *FN1*, *GRP-170*, *LAMB1*, *LOXL2*, and *PDI* were purchased from RealTimePrimers.com (Elkins Park, PA). Primers for *ERp57*, *ERp72*, *GRP-94*, and *ACTIN* were purchased from IDT (Coralville, IA). Sequences of all primers (except those purchased from Qiagen) are provided in Appendix A: Supplementary Table 1. The PCR conditions were: 95°C, 10 s; 60°C, 15 s; 72°C, 30 s. At the conclusion of each run, a melt curve analysis was performed to ensure that a single product had been synthesized. The relative expression of each sample, normalized to *ACTIN*, was calculated using the $2^{-\Delta\Delta Ct}$ method.

Western blotting

Adherent cells were detached using DPBS with 0.25% (w/v) trypsin and 5 mM EDTA, followed by centrifugation. Cells grown as mammospheres were collected by diluting methylcellulose-containing media 3-fold with DBPS, followed by centrifugation. Cell pellets

were treated with lysis buffer (50 mM Tris-HCl pH 7.4, 150 mM NaCl, 1% Triton X-100, 0.5% sodium deoxycholate, 0.1% sodium dodecylsulfate (SDS), 5 mM EDTA, 1 mM 4-(2-Aminoethyl) benzenesulfonyl fluoride hydrochloride (AEBSF), 5 µg/ml pepstatin, 5 µg/ml leupeptin, 5 µg/ml aprotinin, 10 mM 1,10-phenanthroline, 50 mM NaF, 2 mM Na_3VO_4, and 10 mM $Na_4P_2O_7$) and rocked at 4°C for 45 minutes. Cell lysates were then centrifuged for 15 minutes at 13,000 rpm at 4°C. Supernatants were mixed 2:1 with 3xSDS sample buffer, heated at 95^{o}C for 5 min, and resolved by SDS-PAGE in 8% or 10% polyacrylamide gels, followed by protein transfer to nitrocellulose membranes. Membranes were blocked in 5% milk and 0.3% Tween-20 in DPBS, incubated with primary antibodies, and then with horseradish peroxidase-conjugated anti-rabbit or anti-mouse IgG secondary antibodies. Sources and dilutions of the primary antibodies are provided in Appendix A: Supplementary Table 2. Signal detection was performed using SuperSignal West Pico Chemiluminescent Substrate (Pierce). The three following methods were used interchangeably to estimate protein concentration in cell lysates. (1) Protein concentration was measured with a bicinchoninic acid assay (BCA) analysis that is compatible with the detergents in the lysis buffer before a reducing agent was added. (2) Total cell lysates were run in an 8% gel, stained with Coomassie blue, and total protein levels were normalized. (3) Tubulin was used as a gel loading control to normalize Western blot signals.

The protein levels for each ER folding factor shown in Figure 2.2 were quantified using ImageJ and normalized to Tubulin. The calculated values for ADH cells were then set to “1” by dividing both the ADH and MMS number by the value of ADH cells. The average fold change in MMS ±S.E.M is indicated.

Evaluation of the unfolded protein response (UPR)

IRE1: *XBP1* mRNA splicing was used as a measure of IRE1 activation. cDNA was prepared as described above. Semi-quantitative PCR was performed using 1 µl of cDNA as a template and 0.5 µl Bio-XACT short DNA polymerase. PCR conditions were as follows: 95°C, 5 min; 72°C, polymerase added; 40 cycles of 95°C, 30 s; 55°C, 30; 72°C, 20 seconds. PCR products were resolved in a 2% agarose gel and visualized under UV light.

PERK: Total PERK was detected by Western blotting, as described above. The activation status of PERK was assessed based on changes in PERK mobility. In addition, phosphorylation status of eIF2α, a PERK substrate, was determined by Western blotting. Phospho-eIF2α- and total eIF2α-specific antibodies were incubated with the duplicate membranes.

ATF6: SUM159PT and MCF10DCIS.com cells were co-transfected with an ATF6-luciferase reporter (Addgene plasmid #11976) and a *Renilla* luciferase control plasmid pRL-TK (Promega, Madison, WI) using X-tremeGENE HP DNA transfection reagent (Roche, Indianapolis, IN). After one day, cells were detached using trypsin/EDTA in DPBS, suspended in mammosphere medium, and incubated in ultra-low attachment plates for 2 days. As a positive control for UPR activation, adherent cells were incubated for 8 h with 500 ng/ml of tunicamycin. Cells were then washed with DPBS, lysed using 1x Passive Lysis Buffer (Promega), and the lysates were analyzed for firefly and *Renilla* luciferase activities using the Dual Luciferase Reporter Assay System (Promega).

shRNA-mediated knock-down of PDI, ERp44, and ERp57

Human TRIPZ inducible lentiviral shRNA clones targeting ERp57 (V3THS_321786 through V3THS_321791), PDI (V2THS_53945, V3THS_350984, and V3THS_350989), or ERp44 (V2THS_162210, V3THS_395781, V3THS_395782, and V3THS_395784) were

purchased from GE Healthcare Dharmacon (Lafayette, CO). After initial testing of the effects of these shRNAs, the following clones showed the most potent ERp57, PDI, or ERp44 knock-down and were selected for mammosphere assay studies:

for ERp57 knock-down: V3THS_321786 (referred to as shERp57 #1) and V3THS_321788 (referred to as shERp57 #2),

for PDI knock-down: V3THS_350989 (referred to as shPDI #1) and V3THS_350984 (referred to as shPDI #2),

for ERp44 knock-down: V2THS_162210 (referred to as shERp44 #1) and V3THS_395781 (referred to as shERp44 #2).

To produce lentiviral particles, 5 µg of plasmids, along with 5 µg of pMD2.G and 5 µg of psPAX2 (Addgene plasmids #12259 and #12260, respectively), were transfected into HEK293T cells in 100-mm plates, using *Trans*IT-293 reagent (Mirus, Madison, WI). After 2 days, the conditioned media were collected, supplied with 8 µg/ml polybrene (Sigma), and applied to SUM159PT cells. Stably transduced cells were selected after growing cells for 10 days in the presence of 2 µg/ml puromycin.

Data mining

mRNA expression data for selected ECM genes in attached cells and in mammospheres formed by primary tumor cells isolated from 11 breast cancer patients, described in [40], were retrieved from Gene Expression Omnibus (GEO) using the accession number GSE7515. When several probe sets mapped to a single gene, the probe set with the broadest range of changes in signal intensities was used. The following Affymetrix Human Genome U133 Plus 2.0 Array probe sets were used: 201852_x_at for *COL3A1*, 209156_s_at for *COL6A2*, 211651_s_at for *LAMB1*, 214702_at for *FN1*, 200654_at for *PDI*, 6 208959_s_at for *ERp44*, 208612_at for

ERp57, 211048_s_at for *ERp72*, 214315_x_at for *CALR*, 208852_s_at for *CANX*, 230031_at for *BiP*, 200599_s_at for *GRP-94*, and 200825_s_at for *GRP-170*. mRNA expression levels of ECM genes, ER chaperones/foldases/lectins, and selected cytoplasmic chaperones in CTCs from a breast cancer patient and identically processed blood specimens from healthy donors, described in [6], were retrieved from GEO using the accession number GSE41245.

Statistics

Student *t* test analyses were performed using the GraphPad Prism 6.0 software. The number of times each experiment was independently replicated is indicated in the legends for each figure.

Table A.1 Primer Sequences

Primer sequences.

Gene Name	Forward Primer	Reverse Primer
ACTIN	5'-TTG CCG ACA GGA TGC AGA A-3'	5'-GCC GAT CCA CAC GGA GTA CT-3'
CALR	5'-TGG TGC AGT TCA CGG TGA AA-3'	5'-ATC AGC ACG TTC TTG CCC TT-3'
CANX	5'-GAT GAC TGG GAT GAA GAT GC-3'	5'-TCA CAT CTA GGG TTG GCA AT-3'
COL3A1	5'-AGC TAC GGC AAT CCT GAA CT-3'	5'-GGG CCT TCT TTA CAT TTC CA-3'
COL6A2	5'-GCT TGC CCT TCT GTC CAT-3'	5'-TTG GAT TCC CAG GAC CCA-3'
ERp57	5'-TCG TCC TTC ACA TCT CAC TAA C-3'	5'-TCC TTG CCC TGT ATC AAA TCT T-3'
ERp72	5'-CGC GAG TTT GTC ACT GCT TTC-3'	5'-CGT CCT TCT TGG GGT CCA TC-3'
FN1	5'-AGT GGG AGA CCT CGA GAA GA-3'	5'-ACT GTG ACA GCA GGA GCA TC-3'
GRP-94	5'-GGC CAG TTT GGT GTC GGT TTC-3'	5'-CGT TCC CCG TCC TAG AGT GTT TCC-3'
GRP-170	5'-CTC AGT CGG TGC AGA AAC TT-3'	5'-CTG CTC CTC TGT GGA CAC TT-3'
LAMB1	5'-GGA CCA AGA TGT CCT GAG TG-3'	5'-TGC TGT CCA AAT CAG CAC TA-3'
PDI	5'-TTG GGA TCA CTT CCA ACA GT-3'	5'-ACA CTC TTG GGC AAG AAC AG-3'
XBP1	5'-TTA CGA GAG AAA ACT CAT GGC C-3'	5'-GGG TCC AAG TTG TCC AGA ATG C-3'

Table A.2 Antibody Information

Antibodies used for Western Blotting.

Antibody	Species	Clone	Company	Antibody dilution
PDI	Rabbit	C81H6	Cell Signaling	1:5,000
ERp57	Rabbit	G117	Cell Signaling	1:2,000
ERp44	Rabbit	D17A6	Cell Signaling	1:2,000
ERp72	Rabbit	D70D12	Cell Signaling	1:2,000
Calreticulin	Rabbit	D3E6	Cell Signaling	1:5,000
Calnexin	Rabbit	C5C9	Cell Signaling	1:5,000
BiP	Rabbit	C50B12	Cell Signaling	1:1,000
GRP-94	Rabbit	polyclonal	Cell Signaling	1:2,000
GRP-170	Rabbit	polyclonal	Cell Signaling	1:5,000
eIF2α	Mouse	L57A5	Cell Signaling	1:2,000
p-eIF2α	Rabbit	D9G8	Cell Signaling	1:2,000
PERK	Rabbit	D11A8	Cell Signaling	1:2,000
α-Tubulin	Mouse	DM 1A	Sigma	1:100,000

Table A.3 Fold change (FC) of ECM mRNA levels in primary breast tumor cells grown as mammospheres (MMS) versus adherent cultures (ADH), based on ref. [40]

The results of microarray profiling were retrieved from Gene Expression Omnibus (GEO) using the accession number GSE7515, and were analyzed using the GEO2R web tool. The list of ECM genes was based on ref. [46] and included a total of 159 genes encoding collagens, commonly expressed glycoproteins, and proteoglycans. All microarray probes for which there was a statistically significant difference between mRNA levels under MMS vs ADH conditions ($P < 0.05$) are listed.

ID	Gene symbol	Gene title	logFC	*P* Value
Transcripts increased in MMS vs ADH conditions				
201261_x_at	*BGN*	biglycan	1.8840867	6.55E-06
213905_x_at	*BGN*	biglycan	1.1690174	1.24E-04
201262_s_at	*BGN*	biglycan	0.808383	1.93E-02
241986_at	*BMPER*	BMP binding endothelial regulator	3.6547122	1.85E-04
211343_s_at	*COL13A1*	collagen, type XIII, alpha 1	0.8373444	2.89E-02
208535_x_at	*COL13A1*	collagen, type XIII, alpha 1	0.7818679	3.48E-02
211809_x_at	*COL13A1*	collagen, type XIII, alpha 1	0.7379633	3.53E-02
204345_at	*COL16A1*	collagen, type XVI, alpha 1	1.287784	7.36E-04
209082_s_at	*COL18A1*	collagen, type XVIII, alpha 1	1.9273103	8.84E-06
209081_s_at	*COL18A1*	collagen, type XVIII, alpha 1	0.9776373	2.53E-03
1556499_s_at	*COL1A1*	collagen, type I, alpha 1	0.4721902	3.80E-02
229218_at	*COL1A2*	collagen, type I, alpha 2	1.6520319	2.00E-03
233894_x_at	*COL26A1*	collagen, type XXVI, alpha 1	1.4021222	2.65E-03
232458_at	*COL3A1*	collagen, type III, alpha 1	2.2811335	3.57E-04
211981_at	*COL4A1*	collagen, type IV, alpha 1	2.0815585	1.52E-07
211980_at	*COL4A1*	collagen, type IV, alpha 1	0.9394771	7.95E-04
211966_at	*COL4A2*	collagen, type IV, alpha 2	2.1522486	3.07E-04
211964_at	*COL4A2*	collagen, type IV, alpha 2	1.72077	1.75E-06
52255_s_at	*COL5A3*	collagen, type V, alpha 3	1.7739192	3.46E-05
212091_s_at	*COL6A1*	collagen, type VI, alpha 1	2.9337361	5.06E-08
212937_s_at	*COL6A1*	collagen, type VI, alpha 1	2.4173068	7.67E-05
212940_at	*COL6A1*	collagen, type VI, alpha 1	1.2494855	5.13E-03
216904_at	*COL6A1*	collagen, type VI, alpha 1	0.9894224	3.09E-02
213428_s_at	*COL6A1*	collagen, type VI, alpha 1	0.9744415	8.06E-05
212938_at	*COL6A1*	collagen, type VI, alpha 1	0.6627956	3.12E-02
214200_s_at	*COL6A1*	collagen, type VI, alpha 1	0.5220333	4.87E-02
209156_s_at	*COL6A2*	collagen, type VI, alpha 2	2.9719407	6.64E-05
213290_at	*COL6A2*	collagen, type VI, alpha 2	1.5985244	4.45E-07
201438_at	*COL6A3*	collagen, type VI, alpha 3	0.8708146	2.11E-03
204136_at	*COL7A1*	collagen, type VII, alpha 1	1.4218442	3.39E-03
214587_at	*COL8A1*	collagen, type VIII, alpha 1	1.0552437	3.04E-02
201289_at	*CYR61*	cysteine-rich, angiogenic inducer, 61	1.0131338	2.17E-02
211896_s_at	*DCN*	decorin	1.4367061	7.14E-05
201893_x_at	*DCN*	decorin	0.7397362	2.72E-03
211813_x_at	*DCN*	decorin	0.7334676	3.79E-03
209356_x_at	*EFEMP2*	EGF containing fibulin-like extracellular matrix protein 2	1.5393125	2.20E-04
206580_s_at	*EFEMP2*	EGF containing fibulin-like extracellular matrix protein 2	1.2724703	9.49E-05

204163_at	*EMILIN1*	elastin microfibril interfacer 1	3.0265138	4.13E-06
201787_at	*FBLN1*	fibulin 1	1.748646	8.86E-04
203088_at	*FBLN5*	fibulin 5	2.3557215	4.72E-06
202709_at	*FMOD*	fibromodulin	0.9705793	1.74E-02
214702_at	*FN1*	fibronectin 1	3.4996038	1.62E-08
214701_s_at	*FN1*	fibronectin 1	2.7604533	1.55E-06
1558199_at	*FN1*	fibronectin 1	2.750312	1.15E-05
212464_s_at	*FN1*	fibronectin 1	0.7189934	1.08E-03
211719_x_at	*FN1*	fibronectin 1	0.5724163	4.11E-03
216442_x_at	*FN1*	fibronectin 1	0.5103918	1.04E-02
210495_x_at	*FN1*	fibronectin 1	0.4465527	2.16E-02
226145_s_at	*FRAS1*	Fraser extracellular matrix complex subunit 1	3.246866	1.23E-05
231511_at	*FRAS1*	Fraser extracellular matrix complex subunit 1	2.4457747	3.75E-05
220910_at	*FRAS1*	Fraser extracellular matrix complex subunit 1	1.0210387	3.32E-03
243935_at	*FRAS1*	Fraser extracellular matrix complex subunit 1	0.9514786	8.95E-03
230360_at	*GLDN*	gliomedin	1.6868541	8.48E-08
235932_x_at	*HMCN2*	hemicentin 2	1.4706042	8.25E-04
202718_at	*IGFBP2*	insulin-like growth factor binding protein 2	3.0917799	3.85E-04
212143_s_at	*IGFBP3*	insulin-like growth factor binding protein 3	2.5246437	6.88E-04
210095_s_at	*IGFBP3*	insulin-like growth factor binding protein 3	2.2133822	4.45E-05
201508_at	*IGFBP4*	insulin-like growth factor binding protein 4	1.4607473	9.15E-03
203851_at	*IGFBP6*	insulin-like growth factor binding protein 6	2.3504271	4.40E-04
1556956_at	*KCP*	kielin/chordin-like protein	0.5549207	1.50E-02
227048_at	*LAMA1*	laminin, alpha 1	4.1692477	2.04E-13
222346_at	*LAMA1*	laminin, alpha 1	0.7656439	9.71E-03
213519_s_at	*LAMA2*	laminin, alpha 2	3.7477541	1.96E-08
205116_at	*LAMA2*	laminin, alpha 2	3.5850035	2.41E-08
216840_s_at	*LAMA2*	laminin, alpha 2	3.4187191	2.39E-08
202202_s_at	*LAMA4*	laminin, alpha 4	0.6929484	7.08E-03
211651_s_at	*LAMB1*	laminin, beta 1	1.7512033	4.58E-04
201505_at	*LAMB1*	laminin, beta 1	1.284595	7.36E-05
200770_s_at	*LAMC1*	laminin, gamma 1 (formerly LAMB2)	2.8592079	2.89E-09
200771_at	*LAMC1*	laminin, gamma 1 (formerly LAMB2)	1.4180136	4.76E-07
219407_s_at	*LAMC3*	laminin, gamma 3	1.3171169	3.20E-05
202728_s_at	*LTBP1*	latent transforming growth factor beta binding protein 1	1.8249971	6.58E-04
202729_s_at	*LTBP1*	latent transforming growth factor beta binding protein 1	1.4477771	1.04E-04
204682_at	*LTBP2*	latent transforming growth factor beta binding protein 2	2.195264	4.22E-08
223690_at	*LTBP2*	latent transforming growth factor beta binding protein 2	1.8749915	5.56E-06
227308_x_at	*LTBP3*	latent transforming growth factor beta binding protein 3	1.3944989	7.19E-03
204442_x_at	*LTBP4*	latent transforming growth factor beta binding protein 4	0.8672504	3.99E-02
212713_at	*MFAP4*	microfibrillar-associated protein 4	4.8153832	7.84E-13
202008_s_at	*NID1*	nidogen 1	3.1821103	8.22E-07
202007_at	*NID1*	nidogen 1	2.0671352	3.23E-09
1561082_at	*NID1*	nidogen 1	0.735286	3.83E-02
234496_x_at	*NYX*	nyctalopin	0.9207693	7.57E-03
210809_s_at	*POSTN*	periostin, osteoblast specific factor	0.6051061	1.53E-02
37022_at	*PRELP*	proline/arginine-rich end leucine-rich repeat protein	0.8179513	1.70E-03
206007_at	*PRG4*	proteoglycan 4	4.4457865	1.02E-07
200795_at	*SPARCL1*	SPARC-like 1 (hevin)	0.8216131	6.49E-03
202363_at	*SPOCK1*	sparc/osteonectin, cwcv and kazal-like domains proteoglycan	2.359399	7.61E-06
206433_s_at	*SPOCK3*	sparc/osteonectin, cwcv and kazal-like domains proteoglycan	1.0384485	1.10E-02
204955_at	*SRPX*	sushi-repeat containing protein, X-linked	2.9188631	2.29E-10

235086_at	*THBS1*	thrombospondin 1	1.3581552	4.18E-03
204776_at	*THBS4*	thrombospondin 4	2.0942114	1.36E-02
201645_at	*TNC*	tenascin C	2.1161124	6.05E-05
216005_at	*TNC*	tenascin C	1.6059901	4.91E-02
205792_at	*WISP2*	WNT1 inducible signaling pathway protein 2	2.5650045	8.52E-04
Transcripts decreased in MMS vs ADH conditions				
224396_s_at	*ASPN*	asporin	-1.3569421	1.20E-02
219087_at	*ASPN*	asporin	-2.3310187	1.54E-03
1557123_a_at	*CHADL*	chondroadherin-like	-0.8149395	1.46E-02
217428_s_at	*COL10A1*	collagen, type X, alpha 1	-2.3256179	9.80E-05
205941_s_at	*COL10A1*	collagen, type X, alpha 1	-3.3395995	5.20E-05
204320_at	*COL11A1*	collagen, type XI, alpha 1	-3.2797425	1.51E-05
37892_at	*COL11A1*	collagen, type XI, alpha 1	-3.4292707	1.52E-05
229271_x_at	*COL11A1*	collagen, type XI, alpha 1	-3.8392898	2.96E-06
231766_s_at	*COL12A1*	collagen, type XII, alpha 1	-1.7801331	8.64E-04
222073_at	*COL4A3*	collagen, type IV, alpha 3 (Goodpasture antigen)	-1.4273535	1.77E-02
219625_s_at	*COL4A3BP*	collagen, type IV, alpha 3 (Goodpasture antigen) binding protein	-0.7223745	4.14E-02
214602_at	*COL4A4*	collagen, type IV, alpha 4	-1.7213324	4.90E-05
229779_at	*COL4A4*	collagen, type IV, alpha 4	-2.0144422	5.28E-04
230867_at	*COL6A6*	collagen, type VI, alpha 6	-2.3075859	2.84E-04
221900_at	*COL8A2*	collagen, type VIII, alpha 2	-1.6611548	1.78E-03
204724_s_at	*COL9A3*	collagen, type IX, alpha 3	-2.0346983	8.15E-03
242288_s_at	*EMILIN2*	elastin microfibril interfacer 2	-0.9349382	4.49E-02
206439_at	*EPYC*	epiphycan	-3.2278649	1.27E-05
208394_x_at	*ESM1*	endothelial cell-specific molecule 1	-2.1087111	9.29E-04
235318_at	*FBN1*	fibrillin 1	-0.8470442	4.69E-02
205523_at	*HAPLN1*	hyaluronan and proteoglycan link protein 1	-1.6054828	1.48E-03
236028_at	*IBSP*	integrin-binding sialoprotein	-2.1972623	2.09E-04
227760_at	*IGFBPL1*	insulin-like growth factor binding protein-like 1	-0.986781	1.98E-02
236058_at	*KDF1*	keratinocyte differentiation factor 1	-2.1903326	6.80E-04
1568879_a_at	*LAMA3*	laminin, alpha 3	-0.9580444	2.81E-02
206091_at	*MATN3*	matrilin 3	-2.7858924	1.79E-04
205612_at	*MMRN1*	multimerin 1	-2.6559986	1.92E-06
219091_s_at	*MMRN2*	multimerin 2	-1.9522186	2.25E-06
236262_at	*MMRN2*	multimerin 2	-3.7741921	5.51E-12
225911_at	*NPNT*	nephronectin	-5.2099233	4.14E-09
218730_s_at	*OGN*	osteoglycin	-1.3269545	2.00E-02
205908_s_at	*OMD*	osteomodulin	-2.4904004	8.49E-05
205907_s_at	*OMD*	osteomodulin	-2.7981966	2.71E-05
202524_s_at	*SPOCK2*	sparc/osteonectin, cwcv and kazal-like domains proteoglycan	-2.3692505	8.56E-06
201859_at	*SRGN*	serglycin	-1.1046993	3.75E-03
201858_s_at	*SRGN*	serglycin	-2.151962	5.15E-03
204619_s_at	*VCAN*	versican	-1.4856827	1.92E-03
210861_s_at	*WISP3*	WNT1 inducible signaling pathway protein 3	-0.6905031	4.33E-02
Transcripts with inconsistent data of fold change in MMS vs ADH conditions				
228421_s_at	*EFEMP1*	EGF containing fibulin-like extracellular matrix protein 1	0.5546393	1.58E-02
201843_s_at	*EFEMP1*	EGF containing fibulin-like extracellular matrix protein 1	-1.3188921	7.30E-03

Figure A.1 Monitoring of doxycycline-inducible shRNA expression in mammospheres based on the RFP fluorescence.

SUM159PT-shControl cells or SUM159PT cells stably expressing one of the two different doxycycline-inducible shRNA targeting ERp57, PDI, or ERp44, were pre-incubated for 4 days without or with Dox and were further grown for 10 days in the mammosphere media in the absence or presence of Dox. Representative fluorescent (RFP) and phase contrast images are shown.

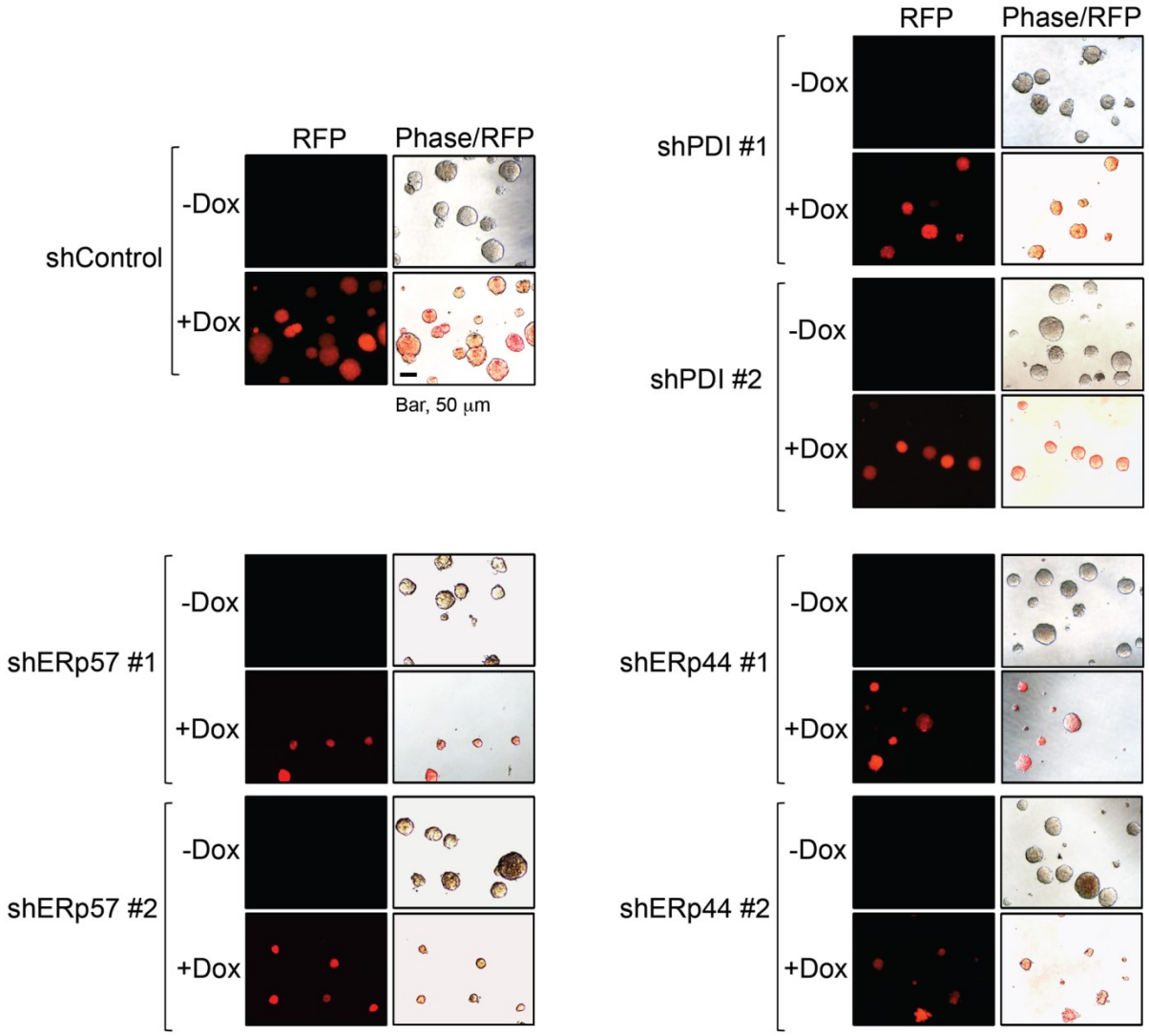

Appendix B - Supplementary Materials for Chapter 3

Supplementary Methods

Reagents and antibodies

Antibodies for immunoblotting included anti-EGFR_pY1068 (clone D7A5), anti-total EGFR (clone D38B1), anti-ERK1/2_pT202/Y204 (clone D13.14.4E), anti-total ERK1/2 (clone 137F5), and anti-MEK1/2 (clone D1A5), all from Cell Signaling Technology. Anti-HA epitope tag antibody (clone 16B12) was from BioLegend, anti-α-Tubulin antibody (clone DM1A) was from Sigma, and anti-β1-integrin (clone 18) was from BD Biosciences. For flow cytometry, PE-conjugated anti-CD24 (clone ML5) and IgG2aκ isotype control (clone G155-178) were purchased from BD Biosciences. APC-conjugated anti-CD44 (clone IM7) and IgG2bκ isotype control (clone eB149/10H5) were from Affymetrix eBioscience. Reagents included erlotinib (Cell Signaling Technology), human recombinant epidermal growth factor (EGF) (Life Technologies), and selumetinib (Selleck Chemicals). Plasmids were obtained from Addgene: pBabe-puro (#1764, "EV") was a gift from Hartmut Land, Jay Morgenstern, and Bob Weinberg [1], pBabe-puro-MEK-DD (#15268, "MEK1-DD") was a gift from William Hahn [2], pBabe-puro-HA-MEK1 (#53195, "HA-MEK1-WT") was a gift from Christopher Counter [3].

Cell culture

SUM149PT and SUM159PT breast cancer cell lines (Asterand) were cultured in Ham's F-12 medium supplemented with 5% fetal bovine serum (FBS), 10 mM HEPES, 5 μg/ml insulin, and 1 μg/ml hydrocortisone. Human MCF10A mammary epithelial cells (ATCC) were cultured in DMEM/F12 (1:1) supplemented with 5 % horse serum, 0.5 μg/ml hydrocortisone, 20 ng/ml human EGF, 10 μg/ml insulin, 100 ng/ml cholera toxin, and 1 % penicillin/streptomycin. Phoenix amphotropic (Ampho) cells (a gift of G. P. Nolan, Stanford University) were cultured in

DMEM media containing 10% FBS. Cells were maintained at 37°C under humidified atmosphere containing 5% CO_2.

Retroviral transduction and generation of stable cell lines

Phoenix Ampho cells grown in 100-mm plates and supplemented with 25 μM chloroquine were transfected with 15 μg plasmid DNA using calcium phosphate precipitation method. After 48 h, media containing retroviral particles were collected, centrifuged, and applied to SUM159PT or SUM149PT, along with 5 μg/ml polybrene. Twenty-four hours after infection, media were replaced and, after an additional 24 h, stably transduced cells were selected using 2 μg/ml puromycin.

Flow cytometry

Cells were treated for 24 h with erlotinib, selumetinib, or DMSO, then 20 ng/ml EGF or vehicle alone was added for an additional 48 h. Culture media containing fresh additives were changed daily. Seventy-two hours after treatment, cells were analyzed by flow cytometry. After blocking for 20 min with either 5% FC block (BD Biosciences #564219) or 5% donkey serum, cells were stained for 30 minutes with PE-conjugated anti-CD24 and APC-conjugated anti-CD44 antibodies or their respective isotype antibody controls, and then evaluated on a BD LSR Fortessa X20 instrument. Data were analyzed with FCS Express 6 (DeNovo) software.

Immunoblotting

Immunoblotting was performed as previously described [4-6]. Lysis buffer was supplemented with phosphatase inhibitors (50 mM NaF, 2 mM Na_3VO_4, and 10 mM $Na_4P_2O_7$). Nitrocellulose membranes were incubated with primary monoclonal antibodies and HRP-conjugated secondary antibodies, followed by signal detection using SuperSignal West Pico or

West Femto chemiluminescence detection kit (Pierce) and Azure c500 digital imaging system. Band intensities were quantified using ImageJ software.

ELISA assay

Cells were incubated for 48 h in culture media containing 1% FBS, in the presence of 10 μM BB-94 or DMSO. Conditioned media were then harvested, centrifuged for 10 min at 3,000 rpm to remove debris, and the amount of soluble amphiregulin was determined by ELISA using human amphiregulin Quantikine ELISA kit (R&D Systems) and Synergy H1 microplate reader (BioTek).

Calculation of EGFR and MEK activation scores

The top 100 genes whose expression was most significantly changed upon stable expression of ligand-activatable EGFR or constitutively active MEK in MCF-7 cells, compared to control MCF-7 cells adapted for long-term estrogen-independent growth [7], were retrieved from Gene Expression Omnibus (GEO, http://www.ncbi.nlm.nih.gov/geo/), using accession number GSE3542. The expression values for these EGFR- or MEK-regulated genes in $CD44^+/CD24^-$ and $CD44^-/CD24^+$ subpopulations of MCF10A cells [8] were then extracted from GEO using accession number GSE15192. The EGFR and MEK scores were calculated as:

$$s = \sum_i w_i x_i / \sum_i |w_i|$$

where w is the weight +1 or –1, depending on whether the gene was upregulated or downregulated in the signature, and x is the normalized gene expression level.

TCGA data mining

Expression values for MEK-regulated genes (mRNA expression z-scores, measured by Agilent microarrays) and the EGFR phosphorylation status at Y992, Y1068, and Y1173 (protein expression z-scores, measured by reverse-phase protein arrays) for basal and claudin-low tumors

were retrieved from The Cancer Genome Atlas (TCGA) (Nature 2012 dataset) [9] via the cBioPortal for Cancer Genomics (http://www.cbioportal.org/public-portal/) [10,11]. The *DUSP4* copy number status was determined by the Genomic Identification of Significant Targets in Cancer (GISTIC) algorithm. GISTIC copy numbers "-2" (a deep loss) and "-1" (a shallow loss) for *DUSP4* were considered homozygous and heterozygous deletions of *DUSP4*, respectively. Tumors for which *DUSP4* GISTIC copy numbers were ≥ 0 were assumed not to harbor *DUSP4* deletion. Pearson *r* correlation coefficient and two-tailed *P* values were calculated using GraphPad Prism 6.0 software.

References

1. Morgenstern JP, Land H (1990) Advanced mammalian gene transfer: high titre retroviral vectors with multiple drug selection markers and a complementary helper-free packaging cell line. Nucleic Acids Res 18:3587-3596.

2. Boehm JS, Zhao JJ, Yao J, Kim SY, Firestein R, Dunn IF, et al (2007) Integrative genomic approaches identify IKBKE as a breast cancer oncogene. Cell 129:1065-1079.

3. Brady DC, Crowe MS, Turski ML, Hobbs GA, Yao X, Chaikuad A, et al (2014) Copper is required for oncogenic BRAF signalling and tumorigenesis. Nature 509:492-496.

4. Duhachek-Muggy S, Qi Y, Wise R, Alyahya L, Li H, Hodge J, et al (2017) Metalloprotease-disintegrin ADAM12 actively promotes the stem cell-like phenotype in claudin-low breast cancer. Mol Cancer 16:32.

5. Li H, Duhachek-Muggy S, Qi Y, Hong Y, Behbod F, Zolkiewska A (2012) An essential role of metalloprotease-disintegrin ADAM12 in triple-negative breast cancer. Breast Cancer Res Treat 135:759-769.

6. Li H, Duhachek-Muggy S, Dubnicka S, Zolkiewska A (2013) Metalloproteinase-disintegrin ADAM12 is associated with a breast tumor-initiating cell phenotype. Breast Cancer Res Treat 139:691-703.

7. Creighton CJ, Hilger AM, Murthy S, Rae JM, Chinnaiyan AM, El-Ashry D (2006) Activation of mitogen-activated protein kinase in estrogen receptor α-positive breast cancer cells in vitro induces an in vivo molecular phenotype of estrogen receptor α-negative human breast tumors. Cancer Res 66:3903-3911.

8. Bhat-Nakshatri P, Appaiah H, Ballas C, Pick-Franke P, Goulet R, Jr., Badve S, et al (2010) SLUG/SNAI2 and tumor necrosis factor generate breast cells with $CD44^{+}/CD24^{-}$ phenotype. BMC Cancer 10:411.

9. The Cancer Genome Atlas Network (2012) Comprehensive molecular portraits of human breast tumours. Nature 490:61-70.

10. Gao J, Aksoy BA, Dogrusoz U, Dresdner G, Gross B, Sumer SO, et al (2013) Integrative analysis of complex cancer genomics and clinical profiles using the cBioPortal. Sci Signal 6:pl1.

11. Cerami E, Gao J, Dogrusoz U, Gross BE, Sumer SO, Aksoy BA, et al (2012) The cBio cancer genomics portal: an open platform for exploring multidimensional cancer genomics data. Cancer Discov 2:401-404.

Appendix C - Copyright Permissions

This chapter contains information and licenses for the reproduction of material included in this dissertation that was previously published.

American Association for the Advancement of Science (AAAS) Copyright Information

Using AAAS material in a thesis or dissertation

NOTE: If you are the original author of the AAAS article being reproduced, please refer to your License to Publish for rules on reproducing your paper in a dissertation or thesis. AAAS permits the use of content published in its journals *Science, Science Immunology, Science Robotics, Science Signaling, and Science Translational Medicine*, but only provided the following criteria are met:

1. If you are using figure(s)/table(s), permission is granted for use in print and electronic versions of your dissertation or thesis.
2. A full-text article may be used only in print versions of a dissertation or thesis. AAAS does not permit the reproduction of full-text articles in electronic versions of theses or dissertations.
3. The following credit line must be printed along with the AAAS material: "From [Full Reference Citation]. Reprinted with permission from AAAS."
4. All required credit lines and notices must be visible any time a user accesses any part of the AAAS material and must appear on any printed copies that an authorized user might make.
5. The AAAS material may not be modified or altered except that figures and tables may be modified with permission from the author. Author permission for any such changes must be secured prior to your use.
6. AAAS must publish the full paper prior to your use of any of its text or figures.
7. If the AAAS material covered by this permission was published in *Science* during the years 1974–1994, you must also obtain permission from the author, who may grant or withhold permission, and who may or may not charge a fee if permission is granted. See original article for author's address. This condition does not apply to news articles.
8. If you are an original author of the AAAS article being reproduced, please refer to your License to Publish for rules on reproducing your paper in a dissertation or thesis.

Permission covers the distribution of your dissertation or thesis on demand by a third party distributor (e.g. ProQuest / UMI), provided the AAAS material covered by this permission remains in situ and is not distributed by that third party outside of the context of your thesis/dissertation.
Permission does not apply to figures/photos/artwork or any other content or materials included in your work that are credited to non-AAAS sources. If the requested material is sourced to or references non-AAAS sources, you must obtain authorization from that source as well before

using that material. You agree to hold harmless and indemnify AAAS against any claims arising from your use of any content in your work that is credited to non-AAAS sources.
By using the AAAS material identified in your request, you agree to abide by all the terms and conditions herein.
AAAS makes no representations or warranties as to the accuracy of any information contained in the AAAS material covered by this permission, including any warranties of merchantability or fitness for a particular purpose.
Questions about these terms can be directed to the AAAS Permissions Department at permissions@aaas.org**.**

John Wiley and Sons Copyright Information

JOHN WILEY AND SONS LICENSE
TERMS AND CONDITIONS
Oct 12, 2017

This Agreement between Randi Wise ("You") and John Wiley and Sons ("John Wiley and Sons") consists of your license details and the terms and conditions provided by John Wiley and Sons and Copyright Clearance Center.

License Number	4204970596680
License date	Oct 09, 2017
Licensed Content Publisher	John Wiley and Sons
Licensed Content Publication	EMBO Reports
Licensed Content Title	The human protein disulphide isomerase family: substrate interactions and functional properties
Licensed Content Author	Lars Ellgaard,Lloyd W. Ruddock
Licensed Content Date	Jan 1, 2005
Licensed Content Pages	5
Type of use	Dissertation/Thesis
Requestor type	University/Academic
Format	Electronic
Portion	Figure/table
Number of figures/tables	1
Original Wiley figure/table number(s)	Figure 1
Will you be translating?	No
Title of your thesis / dissertation	THE ROLE OF THE SECRETORY PATHWAY AND CELL SURFACE PROTEOLYSIS IN THE REGULATION OF THE AGGRESSIVENESS OF

	BREAST CANCER CELLS
Expected completion date	Nov 2017
Expected size (number of pages)	200
Requestor Location	Randi Wise 141 Chalmers Hall MANHATTAN, KS 66506 United States Attn: Randi Wise
Publisher Tax ID	EU826007151
Billing Type	Invoice
Billing Address	Randi Wise 141 Chalmers Hall MANHATTAN, KS 66506 United States Attn: Randi Wise
Total	0.00 USD

Oxford University Press License and Conditions

OXFORD UNIVERSITY PRESS LICENSE
TERMS AND CONDITIONS
October 12, 2017

This Agreement between Randi Wise ("You") and Oxford University Press ("Oxford University Press") consists of your license details and the terms and conditions provided by Oxford University Press and Copyright Clearance Center.

License Number	4204981397514
License date	Oct 09, 2017
Licensed Content Publisher	Oxford University Press
Licensed Content Publication	Annals of Oncology
Licensed Content Title	Regulation of PD-L1: a novel role of pro-survival signalling in cancer
Licensed Content Author	Chen, J.; Jiang, C. C.
Licensed Content Date	Dec 17, 2015
Type of Use	

Institution name	Thesis/Dissertation
Title of your work	THE ROLE OF THE SECRETORY PATHWAY AND CELL SURFACE PROTEOLYSIS IN THE REGULATION OF THE AGGRESSIVENESS OF BREAST CANCER CELLS
Publisher of your work	n/a
Expected publication date	Nov 2017
Permissions cost	0.00 USD
Value added tax	0.00 USD
Total	0.00 USD
Requestor Location	Randi Wise 141 Chalmers Hall MANHATTAN, KS 66506 United States Attn: Randi Wise
Publisher Tax ID	GB125506730
Billing Type	Invoice
Billing Address	Randi Wise 141 Chalmers Hall MANHATTAN, KS 66506 United States Attn: Randi Wise
Total	0.00 USD

Nature Publishing License

NATURE PUBLISHING GROUP LICENSE
TERMS AND CONDITIONS
Oct 12, 2017

This Agreement between Randi Wise ("You") and Nature Publishing Group ("Nature Publishing Group") consists of your license details and the terms and conditions provided by Nature Publishing Group and Copyright Clearance Center.

License Number	4204981169821
License date	Oct 09, 2017

Licensed Content Publisher	Nature Publishing Group
Licensed Content Publication	Nature Reviews Cancer
Licensed Content Title	The blockade of immune checkpoints in cancer immunotherapy
Licensed Content Author	Drew M. Pardoll
Licensed Content Date	Mar 22, 2012
Licensed Content Volume	12
Licensed Content Issue	4
Type of Use	reuse in a dissertation / thesis
Requestor type	academic/educational
Format	print and electronic
Portion	figures/tables/illustrations
Number of figures/tables/illustrations	1
High-res required	no
Figures	Figure 4
Author of this NPG article	no
Your reference number	
Title of your thesis / dissertation	THE ROLE OF THE SECRETORY PATHWAY AND CELL SURFACE PROTEOLYSIS IN THE REGULATION OF THE AGGRESSIVENESS OF BREAST CANCER CELLS
Expected completion date	Nov 2017
Estimated size (number of pages)	200
Requestor Location	Randi Wise 141 Chalmers Hall MANHATTAN, KS 66506 United States Attn: Randi Wise
Billing Type	Invoice
Billing Address	Randi Wise 141 Chalmers Hall MANHATTAN, KS 66506 United States Attn: Randi Wise
Total	0.00 USD

Springer Copyright Information

Self-archiving policy
We are a 'green' publisher, as we allow self-archiving, but most importantly we are fully transparent about your rights.

Publishing in a subscription-based journal
By signing the Copyright Transfer Statement you still retain substantial rights, such as self-archiving:
"Authors may self-archive the author's accepted manuscript of their articles on their own websites. Authors may also deposit this version of the article in any repository, provided it is only made publicly available 12 months after official publication or later. He/ she may not use the publisher's version (the final article), which is posted on SpringerLink and other Springer websites, for the purpose of self-archiving or deposit. Furthermore, the author may only post his/her version provided acknowledgement is given to the original source of publication and a link is inserted to the published article on Springer's website. The link must be provided by inserting the DOI number of the article in the following sentence: "The final publication is available at link.springer.com via http://dx.doi.org/[insert DOI]"."
Prior versions of the article published on non-commercial pre-print servers like arXiv.org can remain on these servers and/or can be updated with the author's accepted version. The final published version (in PDF or HTML/XML format) cannot be used for this purpose.
Acknowledgement needs to be given to the final publication and a link should be inserted to the published article on Springer's website, by inserting the DOI number of the article in the following sentence: "The final publication is available at Springer via http://dx.doi.org/[insert DOI]".
When publishing an article in a subscription journal, without open access, authors sign the Copyright Transfer Statement (CTS) which also details Springer's self-archiving policy.

SPRINGER LICENSE
TERMS AND CONDITIONS
Oct 12, 2017

This Agreement between Randi Wise ("You") and Springer ("Springer") consists of your license details and the terms and conditions provided by Springer and Copyright Clearance Center.

License Number	4204991097194
License date	Oct 09, 2017
Licensed Content Publisher	Springer
Licensed Content Publication	Breast Cancer Research and Treatment
Licensed Content Title	Protein disulfide isomerases in the endoplasmic reticulum promote anchorage-independent growth of breast cancer cells

Licensed Content Author	Randi Wise, Sara Duhachek-Muggy, Yue Qi et al
Licensed Content Date	Jan 1, 2016
Licensed Content Volume	157
Licensed Content Issue	2
Type of Use	Thesis/Dissertation
Portion	Full text
Number of copies	5
Author of this Springer article	Yes and you are a contributor of the new work
Order reference number	
Title of your thesis / dissertation	THE ROLE OF THE SECRETORY PATHWAY AND CELL SURFACE PROTEOLYSIS IN THE REGULATION OF THE AGGRESSIVENESS OF BREAST CANCER CELLS
Expected completion date	Nov 2017
Estimated size(pages)	200
Requestor Location	Randi Wise 141 Chalmers Hall MANHATTAN, KS 66506 United States Attn: Randi Wise
Billing Type	Invoice
Billing Address	Randi Wise 141 Chalmers Hall MANHATTAN, KS 66506 United States Attn: Randi Wise
Total	0.00 USD

This Agreement between Randi Wise ("You") and Springer ("Springer") consists of your license details and the terms and conditions provided by Springer and Copyright Clearance Center.

License Number	4204991160169
License date	Oct 09, 2017
Licensed Content Publisher	Springer
Licensed Content Publication	Breast Cancer Research and Treatment
Licensed Content Title	Metalloprotease-dependent activation of EGFR modulates CD44+/CD24− populations in triple negative breast cancer cells through the MEK/ERK pathway
Licensed Content Author	Randi Wise, Anna Zolkiewska
Licensed Content Date	Jan 1, 2017
Type of Use	Thesis/Dissertation
Portion	Full text
Number of copies	5
Author of this Springer article	Yes and you are a contributor of the new work
Title of your thesis / dissertation	THE ROLE OF THE SECRETORY PATHWAY AND CELL SURFACE PROTEOLYSIS IN THE REGULATION OF THE AGGRESSIVENESS OF BREAST CANCER CELLS
Expected completion date	Nov 2017
Estimated size(pages)	200
Requestor Location	Randi Wise 141 Chalmers Hall MANHATTAN, KS 66506 United States Attn: Randi Wise
Billing Type	Invoice
Billing Address	Randi Wise 141 Chalmers Hall MANHATTAN, KS 66506 United States Attn: Randi Wise
Total	0.00 USD